Springer Tracts in Modern Physics
Volume 230

Springer Tracts in Modern Physics

Springer Tracts in Modern Physics provides comprehensive and critical reviews of topics of current interest in physics. The following fields are emphasized: elementary particle physics, solid-state physics, complex systems, and fundamental astrophysics.
Suitable reviews of other fields can also be accepted. The editors encourage prospective authors to correspond with them in advance of submitting an article. For reviews of topics belonging to the above mentioned fields, they should address the responsible editor, otherwise the managing editor.
See also springer.com

A. Frank
J. Jolie
P. Van Isacker

Symmetries in Atomic Nuclei

From Isospin to Supersymmetry

Springer

A. Frank
University of Mexico
Mexico
frank@nuclecu.unam.mx

J. Jolie
University zu Köln
Köln, Germany
jolie@ikp.uni-koeln.de

P. Van Isacker
GANIL
Caen, France
isacker@ganil.fr

ISSN 0081-3869 e-ISSN 1615-0430
ISBN 978-0-387-87494-4 e-ISBN 978-0-387-87495-1
DOI 10.1007/978-0-387-87495-1

Library of Congress Control Number: 2008941102

Foreword

One of the main objectives of research in physics is to find simple laws that give rise to a deeper understanding and unification of diverse phenomena. A less ambitious goal is to construct models which, in a more or less restricted range, permit an understanding of the physical processes involved and lead to a systematic analysis of the available experimental data while providing insights into the complex systems being studied. A necessary condition to reach these goals is the development of experimental instruments and methods that give access to the relevant information needed to test these models and guide the introduction of new concepts.

The problem of understanding and predicting the behavior of nuclei is one of the most difficult tasks encountered by scientists of the past and present century. From the beginning of the twentieth century until today startling discoveries have been made in nuclear physics, new elements have been synthesized, novel phenomena have been eludicated and important applications have been established. The history of nuclear physics has been characterized by a steady increase toward today's understanding of the atomic nucleus, starting from Rutherford's famed experiment, passing through the discovery of the neutron by Chadwick and culminating in the formulation of the liquid-drop and shell models, among the most important benchmarks. In spite of the impressive advances that have been made over a period of nearly one century, the field of nuclear physics is currently at a cross roads: the advent of radioactive-ion beams will vastly expand our observational capabilities and first results of this new generation of experiments already indicate that our current understanding of nuclei, which is mainly based on experiments along the line of stability, is in need of modification. The field has always been fertilized through the very strong interaction between experimental observations and theoretical modelling. Indeed, in very few fields of physics the development of experiment and theory is so closely intertwined. This interconnection of experiment and theory is a significant part of what is fascinating in nuclear physics: new ideas can be often proposed and verified or falsified in short succession and experimental observations can quickly lead to new theoretical concepts. A historic example of the latter is Heisenberg's introduction of isospin only a few months after the discovery of the neutron by Chadwick.

The nature of the strong force among nucleons that binds nuclei together, which is still not fully understood, coupled to the many-body characteristics of these systems, has given rise to a rich and complex field of scientific inquiry,

bringing forth a very creative research area. The fact that nuclei contain many particles but not nearly enough to treat them statistically, explains why they can be alternatively described both as a collection of individual nucleons and as a single object akin to a charged, dense liquid drop. These two representations of the nucleus reflect its collective and single-particle features, both of which are prominently displayed by nuclei. The following questions then arise: How do collective effects arise from individual particle behavior? How can we reconcile these properties that seemingly exclude each other? The solution of this paradox was outlined by Elliott in 1958 who indicated how nuclear collective deformation may arise from single-particle excitations using symmetry arguments based on SU(3).

In 1975 Arima and Iachello followed a similar line of argument again using symmetry methods by proposing the Interacting Boson Model (IBM). This model and its extensions have proved remarkably successful in providing a bridge between single-particle and collective behavior, based on the approximately bosonic nature of nucleon-pair superpositions that dominate the dynamics of valence nucleons and that arise from the underlying nuclear forces. This is in close analogy to the Bardeen–Cooper–Schrieffer (BCS) theory of semi-conductors with its coupling of electrons to spin-zero Cooper pairs which gives rise to collective behavior we know as superconductivity. From this conceptual basis a unified framework for even–even and odd-mass nuclei has resulted. One of the most attractive features of the IBM is that it gives rise to a simple algebraic description, where so-called dynamical symmetries play a central role, both as a way to improve our basic understanding of the role of symmetry in nuclear dynamics and as starting points from which more precise calculations can be carried out. More specifically, this approach has, in a first stage, produced a unified description of the properties of medium-mass and heavy even–even nuclei, which are pictured in this framework as belonging (in general) to transitional regions between the various dynamical symmetries. Later, odd-mass nuclei were also analyzed from this point of view, by including the degrees of freedom of a single fermion of the nuclear shell model. The bold suggestion was then made by Iachello in 1980 that a simultaneous description of even–even and odd-mass nuclei was possible through the introduction of a superalgebra, with energy levels in both nuclei belonging to the same (super)multiplet. In essence, this proposal was based on the fact that even–even nuclei behave as (composite) bosons while odd-mass ones behave as (approximate) fermions. At the appropriate energy scales their states can then be viewed as elementary. The simple but far-reaching idea was then put forward that both these nuclei can be embedded into a single conceptual framework, relating boson–boson and boson–fermion interactions in a precise way. These concepts were subsequently tested in several regions of the nuclear table. The final step of including odd–odd nuclei into this unifying framework was then made by extending these ideas to the neutron–proton boson model, thus formulating a supersymmetric theory for quartets of nuclei.

Symmetry and its mathematical framework—group theory—play an increasingly important role in physics. Both classical and quantum many-body systems usually display great complexity but the analysis of their symmetry properties often gives rise to simplifications and new insights which can lead to a deeper understanding. In addition, symmetries themselves can point the way toward the formulation of a correct physical theory by providing constraints and guidelines in an otherwise intractable situation. It is remarkable that, in spite of the wide variety of systems one may consider, all the way from classical ones to molecules, nuclei, and elementary particles, group theory applies the same basic principles and extracts the same kind of useful information from all of them. This universality in the applicability of symmetry considerations is one of the most attractive features of group theory.

Most people have an intuitive understanding of symmetry, particularly in its most obvious manifestation in terms of geometric transformations that leave a body or system invariant. This interpretation, however, is not enough to grasp its deep connections with physics, and it thus becomes necessary to generalize the notion of symmetry transformations to encompass more abstract ideas. The mathematical theory of these transformations is the subject matter of group theory.

Over the years many monographs have been written discussing the mathematical theory of groups and their applications in physics [1, 2, 3, 4, 5, 6, 7, 8]. The present book attempts to give a pedagogical view of symmetry methods as applied to the field of nuclear-structure physics. The authors have collaborated for many years in this field but have also independently studied diverse aspects of nuclei and molecules from a symmetry point of view. Two of us have written a previous text on algebraic methods [7]. The present volume has a different focus as it concentrates on the theory and applications of symmetries in nuclear physics, stressing the underlying physical concepts rather than the mastery of methods in group theory. The discussion starts from the concept of isospin, used to this day in the elucidation of nuclear properties, to arrive at the ideas and methods that underlie the discovery of supersymmetry in the atomic nucleus. We emphasize here crucial experimental verification of these symmetries, explaining some of the experimental methods and adopt a more intuitive physical approach, dispensing of mathematical rigor and attempting to focus on the physical arguments that are at the core of new discoveries and breakthroughs. We also have aimed to give a modern account of the current state of this exciting field of research. This we hope has been achieved through the many boxes and examples with which we have illustrated the ideas explained in the main text.

We apologize for the amount of references to our own work, which we can only attempt to justify by stating our belief that we needed to rely on our own experience in order to have an inside look on the way symmetries can be a guide to study nuclear structure.

It should be clear that a book of this kind has not been written in isolation. We will not embark on the perilous exercise of mentioning physicists with

whom we have collaborated or discussed in the course of writing for fear of leaving out some deserving colleague. Nevertheless, we would like to thank Richard Casten and Stefan Heinze, for their careful reading of a draft of this text and their many constructive comments on it. Finally, we wish to dedicate this book to our wives: Annelies (Jolie) and Vera (Van Isacker), and to our children: Dan (Frank), David (Van Isacker), Joke (Jolie), Marieke (Jolie), Pablo (Frank), Thomas (Van Isacker) and Wouter (Jolie), who have lovingly tolerated us (and our physics) for so long.

Contents

List of Boxes

1 Symmetry and Supersymmetry in Quantal Many-Body Systems

Symmetry, together with its mathematical formulation in terms of group theory, has played an increasingly pivotal role in quantum mechanics. Although symmetry ideas can be applied to classical physics, they have become of central importance in quantum mechanics. To illustrate the generic nature of the idea of symmetry, suppose one has an isolated physical system which does not interact with the outside world. It is then natural to assume that the physical laws governing the system are independent of the choice of the origin, the orientation of the coordinate system and the origin of the time coordinate. The laws of (quantum) physics should thus be invariant with respect to certain transformations of our reference frame. This simple statement leads to three fundamental conservation laws which greatly simplify our description of nature: conservation of energy, linear momentum and angular momentum. On these three conservation laws much of classical mechanics is built. These quantities are also conserved in isolated quantal systems. In some cases an additional space-inversion symmetry applies, yielding another conserved quantity called parity. In a relativistic framework the above transformations on space and time cannot be considered separately but become intertwined. The laws of nature are then invariant under the set of Lorentz transformations which operate in four-dimensional space–time.

The above transformations and their associated invariances can be called 'geometric' in the sense that they are defined in space–time. In quantum mechanics, an important extension of these concepts is obtained by also considering transformations that act in abstract spaces associated with intrinsic variables such as spin, isospin (in atomic nuclei), color (of quarks), etc. It is precisely these 'intrinsic' invariances which have led to the preponderance of symmetry applications in quantal systems.

We start this chapter with a brief review of symmetry in quantum mechanics and present a discussion of the role of symmetry and group theory in quantum mechanics. We then focus in Sect. 1.2 on quantal many-body systems and their analysis in terms of dynamical symmetries. While the material of this chapter is of a general nature and can thus be applied to any quantal system, the remainder of the book is essentially devoted to nuclear physics. Some parts of this chapter are also found in more detail in Ref. [7].

A. Frank et al., *Symmetries in Atomic Nuclei*,
Springer Tracts in Modern Physics 230, DOI 10.1007/978-0-387-87495-1_1,

1.1 Symmetry in Quantum Mechanics

In this section it is shown how the mathematical machinery of group theory can be applied to quantum mechanics. The starting point is to consider transformation acting on a physical system, that is, operations that transform the coordinates $\boldsymbol{r}_i$ and the impulse momenta $\boldsymbol{p}_i$ of the particles that constitute the system. Such transformations are of a geometric nature.For a discussion of symmetry in quantum-mechanical systems this definition is too restrictive because it does not include, for example, the spin degrees of freedom.The appropriate way of dealing with this generalization is to consider, instead of the geometric transformations themselves, the corresponding transformations in the Hilbert space of quantum-mechanical states of the system.The action of the geometric transformation on spin variables (i.e., components of the spin vector) is assumed to be identical to its action on the components of the angular momentum vector $\boldsymbol{l} = \boldsymbol{r} \wedge \boldsymbol{p}$. Furthermore, it can then be shown that a correspondence exists between the geometric transformations in physical space and the transformations induced by it in the Hilbert space of quantum-mechanical states [9].

No distinction is made in the following between geometric and quantum-mechanical transformations, and the elements of the groups and algebras that are defined below are operators acting on the Hilbert space of quantum-mechanical states.

1.1.1 Some Definitions

We begin with a very brief reminder of group-theoretical concepts that will be used throughout this book. An abstract **group** $\mathcal{G}$ is defined by a set of elements $\{G_1, G_2, \ldots, G_n\}$ for which a 'multiplication' rule combining these elements exists and which satisfies the following conditions:

1. **Closure.** If G_i and G_j are elements of the set, so is their product G_iG_j.
2. **Associativity.** The following property is always valid:

$$G_i(G_jG_k) = (G_iG_j)G_k. \tag{1.1}$$

3. **Identity.** There exists an element E of G satisfying

$$EG_i = G_iE = G_i. \tag{1.2}$$

4. **Inverse.** For every G_i there exists an element G_i^{-1} such that

$$G_iG_i^{-1} = G_i^{-1}G_i = E. \tag{1.3}$$

The number n of elements is called the **order** of the group. If n is finite, the group is said to be **finite**; it then is necessarily also discrete. Discrete groups constitute an important class of groups since they classify the point

symmetries of quantum-mechanical systems such as crystals and molecules. To understand the degeneracies brought about by these symmetries, it is necessary to study discrete groups.

A group is said to be **continuous** if its elements form a continuum in a topological sense and if, in addition, the multiplication operation has the appropriate continuity conditions. This leads to the definition of a **Lie group**. The essential idea is that all its elements may be obtained by exponentiation in terms of a basic set of elements $\{g_k, k = 1, 2, \ldots, s\}$, called **generators**, which together form the **Lie algebra** associated with the Lie group.

A simple example is provided by the SO(2) group of rotations in two-dimensional space, with elements that may be realized as

$$G(\alpha) = e^{-i\alpha l_z}, \tag{1.4}$$

where α is the angle of rotation and

$$l_z = -i\left(x\frac{\partial}{\partial y} - y\frac{\partial}{\partial x}\right) \tag{1.5}$$

is the generator of these transformations in the x–y plane.

Three-dimensional rotations require the introduction of two additional generators, associated with rotations in the z–x and y–z planes,

$$l_y = -i\left(z\frac{\partial}{\partial x} - x\frac{\partial}{\partial y}\right), \qquad l_x = -i\left(y\frac{\partial}{\partial z} - z\frac{\partial}{\partial y}\right). \tag{1.6}$$

Finite rotations can then be parametrized by three angles (which may be the Euler angles) and expressed as a product of exponentials of SO(3) generators (1.5) and (1.6) [10]. Evaluating the commutators of these operators, we find

$$[l_x, l_y] = il_z, \qquad [l_y, l_z] = il_x, \qquad [l_z, l_x] = il_y. \tag{1.7}$$

In general, the s operators $\{g_k, k = 1, 2, \ldots, s\}$ define a Lie algebra if they close under commutation,

$$[g_k, g_l] = \sum_m c_{kl}^m g_m, \tag{1.8}$$

and satisfy the **Jacobi identity** [4]

$$[g_k, [g_l, g_m]] + [g_m, [g_k, g_l]] + [g_l, [g_m, g_k]] = 0. \tag{1.9}$$

The set of constants c_{kl}^m are called **structure constants** and their values determine the properties of the Lie algebra. All Lie algebras have been classified by Killing and Cartan and a rich literature on their mathematical properties and their application in physics exists (see, for example, Refs. [4, 8]).

For any Lie algebra $\mathcal{G}$, operators can be defined which are constructed out of the generators with the condition that they commute with all generators of the algebra:

$$\forall g_k \in \mathcal{G} : [C_m[\mathcal{G}], g_k] = 0, \tag{1.10}$$

where m denotes the order in the generators g_k. The operator $C_m[\mathcal{G}]$ is called the **Casimir operator** of order m. There exists a mathematical procedure based on the theory of (semi-simple) Lie algebras for the construction of all such operators in terms of the structure constants c_{kl}^m [8].

1.1.2 Symmetry Transformations

From a general point of view symmetry transformations of a physical system may be defined in terms of the equations of motion for the system [11]. Suppose we consider the equations

$$\mathcal{O}_k \psi_k = 0, \qquad k = 1, 2, \ldots, \tag{1.11}$$

where the functions $\psi_k(\boldsymbol{x})$ denote a vector column with a finite or infinite number of components, or a more general structure such as a matrix depending on the variables x_i. The operators $\mathcal{O}_k$ are quite arbitrary and (1.11) may correspond, for example, to Maxwell, Schrödinger or Dirac equations. The operators g_{kl} defined as

$$\mathcal{O}_k \left(\sum_l g_{kl} \psi_l \right) = 0, \qquad k = 1, 2, \ldots, \tag{1.12}$$

are called **symmetry transformations**, since they transform the solutions ψ_k to other solutions $\sum_l g_{kl}\psi_l$ of the Eq. (1.11). As a particular example we consider the time-dependent Schrödinger equation (with $\hbar = 1$)

$$\left(H(\boldsymbol{x}, \boldsymbol{p}) - i\frac{\partial}{\partial t} \right) \psi(\boldsymbol{x}, t) = 0. \tag{1.13}$$

One can verify that $g(\boldsymbol{x}, \boldsymbol{p}, t)\psi(\boldsymbol{x}, t)$ is also a solution of (1.13) as long as g satisfies the equation

$$[H, g] - i\frac{\partial g}{\partial t} = 0, \tag{1.14}$$

which means that g is an operator associated with a conserved quantity. The last statement follows from the definition of the total derivative of an operator g

$$\frac{dg}{dt} = \frac{\partial g}{\partial t} + i[H, g], \tag{1.15}$$

where H is the quantum-mechanical hamiltonian [12]. If g_1 and g_2 satisfy (1.14), their commutator is again a constant of the motion since

$$\frac{d}{dt}[g_1, g_2] = \frac{\partial}{\partial t}[g_1, g_2] + i[H, [g_1, g_2]]$$
$$= \frac{\partial}{\partial t}[g_1, g_2] - [\frac{\partial g_1}{\partial t}, g_2] - [g_1, \frac{\partial g_2}{\partial t}] = 0, \tag{1.16}$$

where use is made of (1.14) and the Jacobi identity (1.9). A particularly interesting situation arises when the set $\{g_k\}$ is such that $[g_k, g_l]$ closes under commutation to form a Lie algebra as in (1.8). In this case we refer to $\{g_k\}$ as the generators of the **symmetry (Lie) algebra** of the time-dependent quantum system (1.13) [13]. Note that in general these operators do not commute with the hamiltonian but rather satisfy (1.14),

$$[H - i\frac{\partial}{\partial t}, g_k] = 0. \tag{1.17}$$

What about the time-independent Schrödinger equation? This case corresponds to substituting $\psi(\boldsymbol{x}, t)$ by $\psi_n(\boldsymbol{x})e^{-iE_n t}$ in (1.13), leading to

$$[H(\boldsymbol{x}, \boldsymbol{p}) - E_n]\psi_n(\boldsymbol{x}) = 0. \tag{1.18}$$

The set $g_k(\boldsymbol{x}, \boldsymbol{p}, t = 0)$ still satisfies the same commutation relations as before but due to (1.14) does not in general correspond to integrals of the motion anymore. These operators constitute the **dynamical algebra** for the time-independent Schrödinger equation (1.18) and connect all solutions $\psi_n(\boldsymbol{x})$ with each other, including states at different energies. Due again to (1.14), only those g_k generators that are time independent satisfy

$$[H, g_k] = 0, \tag{1.19}$$

which implies that they are constants of the motion for the system (1.18). Equation (1.19) (together with the closure of the g_k operators) constitutes the familiar definition of the symmetry algebra for a time-independent system. The connection between the dynamical algebra $\{g_k(0)\}$ and the symmetry algebra of the corresponding time-dependent system $\{g_k(t)\}$ allows a unique definition of the dynamical algebra [13].

1.1.3 Symmetry

The discussion in the preceding section leads in a natural way to the following definition of symmetry, valid for a time-independent system. A hamiltonian H which commutes with the generators g_k that form a Lie algebra $\mathcal{G}$,

$$\forall g_k \in \mathcal{G} : [H, g_k] = 0, \tag{1.20}$$

is said to have a **symmetry** $\mathcal{G}$ or, alternatively, to be **invariant under** $\mathcal{G}$. According to the theory of classical Lie algebras [4], the construction and enumeration of all operators that satisfy the commutation property (1.20) is entirely determined by the structure constants c_{kl}^m of the algebra.

The determination of operators g_k that leave invariant the hamiltonian of a given physical system is central to any quantum-mechanical description. The reasons for this are profound and can be understood from the correspondence between geometrical and quantum-mechanical transformations mentioned at the beginning of this section. It can be shown [9] that the transformations g_k with the symmetry property (1.20) are induced by geometrical transformations that leave unchanged the corresponding classical hamiltonian. In this way the classical notion of a conserved quantity is transcribed in quantum mechanics in the form of the symmetry property (1.20) of the hamiltonian.

1.1.4 Degeneracy and State Labeling

A well-known consequence of a symmetry is the occurrence of degeneracies in the eigenspectrum of H. Given an eigenstate $|\gamma\rangle$ of H with energy E, the condition (1.20) implies that the states $g_k|\gamma\rangle$ all have the same energy:

$$Hg_k|\gamma\rangle = g_kH|\gamma\rangle = Eg_k|\gamma\rangle. \tag{1.21}$$

An arbitrary eigenstate of H shall be written as $|\Gamma\gamma\rangle$, where the first quantum number Γ is different for states with different energies and the second quantum number γ is needed to label degenerate eigenstates. The eigenvalues of a hamiltonian that satisfies (1.20) depend on Γ only,

$$H|\Gamma\gamma\rangle = E(\Gamma)|\Gamma\gamma\rangle, \tag{1.22}$$

and, furthermore, the transformations g_k do not admix states with different Γ,

$$g_k|\Gamma\gamma\rangle = \sum_{\gamma'} a^{\Gamma}_{\gamma'\gamma}(k)|\Gamma\gamma'\rangle. \tag{1.23}$$

With each element g_k is associated a matrix $\mathbf{a}^{\Gamma}(k)$ which defines the transformation among the degenerate states $|\Gamma\gamma\rangle$ under the action of the operator g_k. The matrices $\{\mathbf{a}^{\Gamma}(k), k = 1, 2, \ldots, s\}$ satisfy exactly the same commutation rules as the operators $\{g_k, k = 1, 2, \ldots, s\}$ and are therefore said to provide a (matrix) **representation** of the Lie algebra $\mathcal{G}$. If *all* matrices $\{\mathbf{a}^{\Gamma}(k), k = 1, 2, \ldots, s\}$ can be brought into a common block-diagonal form through a single unitary transformation, the representation is said to be **reducible**; if not, it is **irreducible**.

This discussion of the consequences of a hamiltonian symmetry illustrates at once the relevance of group theory in quantum mechanics. *Symmetry implies degeneracy and eigenstates that are degenerate in energy provide a space in which representations of the symmetry group are constructed. Consequently, the (irreducible) representations of a given group directly determine the degeneracy structure of a hamiltonian with the symmetry associated to that group.*

The fact that degenerate eigenstates correspond to *irreducible* representations shall be taken for granted here and is known as Wigner's principle [9]. The principle states that the space of degenerate eigenstates provides an irreducible representation of the *complete* symmetry of the hamiltonian. As a consequence of Wigner's principle, an observed degeneracy is either accidental in which case it would disappear by increasing the precision of measurement, or it is the result of a (possibly hidden) symmetry of the hamiltonian.

Because of Wigner's principle, eigenstates of H can be denoted as $|\Gamma\gamma\rangle$ where the symbol Γ labels the irreducible representations of $\mathcal{G}$. Note that the same irreducible representation might occur more than once in the eigenspectrum of H and, therefore, an additional multiplicity label η should be introduced to define a complete labeling of eigenstates as $|\eta\Gamma\gamma\rangle$. This label shall be omitted in the subsequent discussion.

A sufficient condition for a hamiltonian to have the symmetry property (1.20) is that it can be expressed in terms of Casimir operators of various orders. The eigenequation (1.22) then becomes

$$\left(\sum_m \kappa_m C_m[\mathcal{G}]\right)|\Gamma\gamma\rangle = \left(\sum_m \kappa_m E_m(\Gamma)\right)|\Gamma\gamma\rangle. \tag{1.24}$$

In fact, the following discussion is valid for any analytic function of the various Casimir operators but mostly a linear combination is taken, as in (1.24). The energy eigenvalues $E_m(\Gamma)$ are functions of the labels that specify the irreducible representation Γ and are known for all classical Lie algebras [4].

1.1.5 Dynamical Symmetry Breaking

The concept of a dynamical symmetry for which (at least) two algebras $\mathcal{G}_1$ and $\mathcal{G}_2$ with $\mathcal{G}_1 \supset \mathcal{G}_2$ are needed can now be introduced. The eigenstates of a hamiltonian H with symmetry $\mathcal{G}_1$ are labeled as $|\Gamma_1\gamma_1\rangle$. But, since $\mathcal{G}_1 \supset \mathcal{G}_2$, a hamiltonian with $\mathcal{G}_1$ symmetry necessarily must also have a symmetry $\mathcal{G}_2$ and, consequently, its eigenstates can also be labeled as $|\Gamma_2\gamma_2\rangle$. Combination of the two properties leads to the eigenequation

$$H|\Gamma_1\eta_{12}\Gamma_2\gamma_2\rangle = E(\Gamma_1)|\Gamma_1\eta_{12}\Gamma_2\gamma_2\rangle, \tag{1.25}$$

where the role of γ_1 is played by $\eta_{12}\Gamma_2\gamma_2$. In (1.25) the irreducible representation Γ_2 may occur more than once in Γ_1, and hence an additional quantum number η_{12} (also known as a missing label) is needed to characterize the states completely. Because of $\mathcal{G}_1$ symmetry, eigenvalues of H depend on Γ_1 only.

In many examples in physics (one is discussed below), the condition of $\mathcal{G}_1$ symmetry is too strong and a *possible* breaking of the $\mathcal{G}_1$ symmetry can be imposed via the hamiltonian

$$H' = \sum_m \kappa_{1m} C_m[\mathcal{G}_1] + \sum_m \kappa_{2m} C_m[\mathcal{G}_2], \tag{1.26}$$

which consists of a combination of Casimir operators of $\mathcal{G}_1$ and $\mathcal{G}_2$. The symmetry properties of the hamiltonian H' are now as follows. Since $[H', g_k] = 0$ for $g_k \in \mathcal{G}_2$, H' is invariant under $\mathcal{G}_2$. The hamiltonian H', since it contains $C_m[\mathcal{G}_2]$, does not commute, in general, with all elements of $\mathcal{G}_1$ and for this reason the $\mathcal{G}_1$ symmetry is broken. Nevertheless, because H' is a combination of Casimir operators of $\mathcal{G}_1$ and $\mathcal{G}_2$, its eigenvalues can be obtained in closed form:

$$\begin{aligned}\left(\sum_m \kappa_{1m} C_m[\mathcal{G}_1] + \sum_m \kappa_{2m} C_m[\mathcal{G}_2]\right) |\Gamma_1 \eta_{12} \Gamma_2 \gamma_2\rangle \\ = \left(\sum_m \kappa_{1m} E_m(\Gamma_1) + \sum_m \kappa_{2m} E_m(\Gamma_2)\right) |\Gamma_1 \eta_{12} \Gamma_2 \gamma_2\rangle.\end{aligned} \tag{1.27}$$

The conclusion is thus that, although H' is not invariant under $\mathcal{G}_1$, its eigenstates are the same as those of H in (1.25). The hamiltonian H' is said to have $\mathcal{G}_1$ as a **dynamical symmetry**. The essential feature is that, although the eigenvalues of H' depend on Γ_1 *and* Γ_2 (and hence $\mathcal{G}_1$ is not a symmetry), the eigenstates do not change during the breaking of the $\mathcal{G}_1$ symmetry. As the generators of $\mathcal{G}_2$ are a subset of those of $\mathcal{G}_1$, *the dynamical symmetry breaking splits but does not admix the eigenstates.* A convenient way of summarizing the symmetry character of H' and the ensuing classification of its eigenstates is in terms of two **nested algebras**

$$\begin{array}{ccc} \mathcal{G}_1 & \supset & \mathcal{G}_2 \\ \downarrow & & \downarrow \\ \Gamma_1 & & \eta_{12}\Gamma_2 \end{array} . \tag{1.28}$$

This equation indicates the larger algebra $\mathcal{G}_1$ (sometimes referred to as the **dynamical algebra** or **spectrum generating algebra**) and the symmetry algebra $\mathcal{G}_2$, together with their associated labels with possible multiplicities.

Many concrete examples exist in physics of the abstract idea of dynamical symmetry. Perhaps the best known in nuclear physics concerns **isospin** symmetry and its breaking by the Coulomb interaction.

1.1.6 Isospin in Nuclei

After the discovery of the neutron by Chadwick, Heisenberg realized that the mathematical apparatus of the Pauli spin matrices could be applied to the labeling of the two nucleonic charge states, the neutron and the proton [14]. In this way he laid the foundation of an important development in physics, namely the use of symmetry transformations in abstract spaces. The starting point is the observation that the masses of the neutron and proton are very

similar [15], $m_{\rm n}c^2 = 939.56536(8)$ MeV and $m_{\rm p}c^2 = 938.27203(8)$ MeV, and that both have a spin of 1/2. Furthermore, experiment shows that, if one neglects the contribution of the electromagnetic interaction, the forces between two neutrons are about the same as those between two protons. More precisely, the strong nuclear force between two nucleons with antiparallel spins is found to be (approximately) independent of whether they are neutrons or protons. This indicates the existence of a symmetry of the strong interaction, and isospin is the appropriate formalism to explore the consequences of that symmetry in nuclei. We stress that the equality of the masses and the spins of the nucleons are not sufficient for isospin symmetry to be valid and that the charge independence of the nuclear force is equally important. This point was emphasized by Wigner [16] who defined isospin for complex nuclei as we know it today and who also coined the name of 'isotopic spin'.

Because of the near equality of the masses and of the interactions between nucleons, the hamiltonian of the nucleus is (approximately) invariant with respect to transformations between neutron and proton states. For one nucleon, these can be defined by introducing the abstract space spanned by the two vectors

$$|{\rm n}\rangle = \begin{bmatrix} 1 \\ 0 \end{bmatrix}, \qquad |{\rm p}\rangle = \begin{bmatrix} 0 \\ 1 \end{bmatrix}. \tag{1.29}$$

The most general transformation among these states (which conserves their normalization) is a unitary 2×2 matrix. If we represent a matrix close to the identity as

$$\begin{bmatrix} 1+\epsilon_{11} & \epsilon_{12} \\ \epsilon_{21} & 1+\epsilon_{22} \end{bmatrix}, \tag{1.30}$$

where the ϵ_{ij} are infinitesimal complex numbers, unitarity imposes the relations

$$\epsilon_{11} + \epsilon_{11}^* = \epsilon_{22} + \epsilon_{22}^* = \epsilon_{12} + \epsilon_{21}^* = 0. \tag{1.31}$$

An additional condition is found by requiring the determinant of the unitary matrix to be equal to $+1$,

$$\epsilon_{11} + \epsilon_{22} = 0, \tag{1.32}$$

which removes the freedom to make a simultaneous and identical change of phase for the neutron and the proton. We conclude that an infinitesimal, physical tranformation between a neutron and a proton can be parametrized as

$$\begin{bmatrix} 1 - \frac{1}{2}i\epsilon_z & -\frac{1}{2}i(\epsilon_x - i\epsilon_y) \\ -\frac{1}{2}i(\epsilon_x + i\epsilon_y) & 1 + \frac{1}{2}i\epsilon_z \end{bmatrix}, \tag{1.33}$$

which includes a conventional factor $-i/2$ and where the $\{\epsilon_x, \epsilon_y, \epsilon_z\}$ now are infinitesimal real numbers. This can be rewritten in terms of the Pauli spin matrices as

$$\begin{bmatrix} 1 & 0 \\ 0 & 1 \end{bmatrix} - \frac{1}{2}i\epsilon_x \begin{bmatrix} 0 & 1 \\ 1 & 0 \end{bmatrix} - \frac{1}{2}i\epsilon_y \begin{bmatrix} 0 & -i \\ i & 0 \end{bmatrix} - \frac{1}{2}i\epsilon_z \begin{bmatrix} 1 & 0 \\ 0 & -1 \end{bmatrix}. \tag{1.34}$$

The infinitesimal transformations between a neutron and a proton can thus be written in terms of the three operators

$$t_x \equiv \frac{1}{2}\begin{bmatrix} 0 & 1 \\ 1 & 0 \end{bmatrix}, \qquad t_y \equiv \frac{1}{2}\begin{bmatrix} 0 & -i \\ i & 0 \end{bmatrix}, \qquad t_z \equiv \frac{1}{2}\begin{bmatrix} 1 & 0 \\ 0 & -1 \end{bmatrix}, \tag{1.35}$$

which satisfy *exactly* the same commutation relations as those in (1.7), valid for the angular momentum operators. The action of the t_μ operators on a nucleon state is easily found from its matrix represenation. For example,

$$t_z|\mathrm{n}\rangle \equiv \frac{1}{2}\begin{bmatrix} 1 & 0 \\ 0 & -1 \end{bmatrix}\begin{bmatrix} 1 \\ 0 \end{bmatrix} = \frac{1}{2}|\mathrm{n}\rangle, \qquad t_z|\mathrm{p}\rangle \equiv \frac{1}{2}\begin{bmatrix} 1 & 0 \\ 0 & -1 \end{bmatrix}\begin{bmatrix} 0 \\ 1 \end{bmatrix} = -\frac{1}{2}|\mathrm{p}\rangle, \tag{1.36}$$

which shows that $e(1-2t_z)/2$ is the charge operator. Also, the combinations $t_\pm \equiv t_x \pm i t_y$ can be introduced, which satisfy the commutation relations

$$[t_z, t_\pm] = \pm t_\pm, \qquad [t_+, t_-] = 2t_z, \tag{1.37}$$

and play the role of raising and lowering operators since

$$t_-|\mathrm{n}\rangle = |\mathrm{p}\rangle, \qquad t_+|\mathrm{n}\rangle = 0, \qquad t_-|\mathrm{p}\rangle = 0, \qquad t_+|\mathrm{p}\rangle = |\mathrm{n}\rangle. \tag{1.38}$$

Note that we have associated a neutron (proton) with isospin up (down), and that we could have made the opposite association, which is the usual convention of particle physics.

This proves the formal equivalence between spin and isospin, and all results familiar from angular momentum can now be readily transposed to the isospin algebra. For a many-nucleon system (such as a nucleus) a total isospin T and its z projection M_T can be defined which results from the coupling of the individual isospins, just as this can be done for the nucleon spins. The appropriate isospin operators are

$$T_\mu = \sum_k t_\mu(k), \tag{1.39}$$

where the sum is over all the nucleons in the nucleus.

The assumption of isospin invariance can be studied with the isobaric multiplet mass equation. If, in first approximation, the Coulomb interaction between the protons is neglected and, furthermore, if it is assumed that the strong interaction does not distinguish between neutrons and protons, the resulting nuclear hamiltonian H is isospin invariant. Explicitly, invariance under the isospin algebra $\mathrm{SU}(2) \equiv \{T_z, T_\pm\}$ follows from

$$[H, T_z] = [H, T_\pm] = 0. \tag{1.40}$$

As a consequence of these commutation relations, the many-particle eigenstates of H have good isospin symmetry. They can be classified as $|\eta T M_T\rangle$

where T is the total isospin of the nucleus obtained from the coupling of the individual isospins 1/2 of all nucleons, M_T is its projection on the z axis in isospin space, $M_T = (N - Z)/2$ and η denotes all additional quantum numbers. If isospin were a true symmetry, all states $|\eta T M_T\rangle$ with $M_T = -T, -T+1, \ldots, +T$, and with the same T (and identical other quantum numbers η), would be degenerate in energy; for example, neutron and proton would have exactly the same mass.

The Coulomb interaction between the protons destroys the equivalence between the nucleons and hence breaks isospin symmetry. The main effect of the Coulomb interaction is a *dynamical* breaking of isospin symmetry. This can be shown by rewriting the Coulomb interaction,

$$V = \sum_{k<l} \left(\frac{1}{2} - t_z(k)\right)\left(\frac{1}{2} - t_z(l)\right) \frac{e^2}{|\boldsymbol{r}_k - \boldsymbol{r}_l|}, \tag{1.41}$$

as a sum of isoscalar, isovector and isotensor parts [17]

$$V = \sum_{k<l} \sum_{t=0,1,2} V_0^{(t)}(k,l), \tag{1.42}$$

with

$$\begin{aligned}
V_0^{(0)}(k,l) &= \left(\frac{1}{4} - \sqrt{\frac{1}{3}}\,(\boldsymbol{t}(k) \times \boldsymbol{t}(l))_0^{(0)}\right) \frac{e^2}{|\boldsymbol{r}_k - \boldsymbol{r}_l|}, \\
V_0^{(1)}(k,l) &= -\frac{1}{2}\,(\boldsymbol{t}_z(k) + \boldsymbol{t}_z(l))\, \frac{e^2}{|\boldsymbol{r}_k - \boldsymbol{r}_l|}, \\
V_0^{(2)}(k,l) &= \sqrt{\frac{2}{3}}\,(\boldsymbol{t}(k) \times \boldsymbol{t}(l))_0^{(2)}\, \frac{e^2}{|\boldsymbol{r}_k - \boldsymbol{r}_l|},
\end{aligned} \tag{1.43}$$

where the coupling is carried out in isospin. The effect of the Coulomb interaction on a given state $|\eta T M_T\rangle$ can be estimated from first-order perturbation theory, with the energy shift of this state due to the Coulomb interaction V corresponding to the diagonal matrix element $\langle \eta T M_T | V | \eta T M_T \rangle$. To calculate this matrix element, the Wigner–Eckart theorem in isospin space can be applied (see Box on Isoscalar factors and the Wigner–Eckart theorem) and allows to factor out the M_T dependence according to

$$\langle \eta T M_T | \sum_{k<l} V_0^{(t)}(k,l) | \eta T M_T \rangle = \langle T M_T\ t0 | T M_T \rangle \langle \eta T \| \sum_{k<l} V^{(t)}(k,l) \| \eta T \rangle. \tag{1.44}$$

The coupling coefficient here is the usual Clebsch–Gordan coefficient associated with SU(2) $\supset$ SO(2). From the explicit expressions for these coefficients,

$$\langle T M_T\ 00 | T M_T \rangle = 1, \qquad \langle T M_T\ 10 | T M_T \rangle = \frac{M_T}{\sqrt{T(T+1)}},$$

$$\langle TM_T\ 20|TM_T\rangle = \frac{3M_T^2 - T(T+1)}{\sqrt{T(T+1)(2T-1)(2T+3)}}, \tag{1.45}$$

we conclude that the M_T dependence of the diagonal matrix elements of the Coulomb interaction is at most quadratic. If the off-diagonal, isospin mixing matrix elements of the Coulomb interaction V are neglected, it can then be represented as

$$V \simeq \tilde{V} \equiv \kappa_0 + \kappa_1 T_z + \kappa_2 T_z^2, \tag{1.46}$$

for some particular coefficients κ_0, κ_1 and κ_2 which, according to the preceding discussion, depend on the isospin T and other quantum numbers η. In the notation introduced in Sect. 1.1.5, this can be viewed as a dynamical symmetry breaking of the type

$$\begin{array}{ccc} \mathrm{SU}(2) & \supset & \mathrm{SO}(2) \equiv \{T_z\} \\ \downarrow & & \downarrow \\ T & & M_T \end{array} . \tag{1.47}$$

The hamiltonian $\tilde{V}$ splits but does not admix the eigenstates $|\eta T M_T\rangle$ with $M_T = -T, -T+1, \ldots, +T$ and has the eigenspectrum

$$\tilde{E}(M_T) = \kappa_0 + \kappa_1 M_T + \kappa_2 M_T^2. \tag{1.48}$$

Isoscalar factors and the Wigner–Eckart theorem. The Wigner–Eckart theorem is well known [10] for the case $\mathrm{SU}(2) \supset \mathrm{SO}(2)$ with associated labels of angular momentum J and its projection M_J. The generalization involves an arbitrary labeling of the type

$$\begin{array}{ccc} \mathcal{G}_1 & \supset & \mathcal{G}_2 \\ \downarrow & & \downarrow \\ \Gamma & & \gamma \end{array} .$$

Suppose the calculation is required of the matrix element of an operator T^{Γ}_{γ}. This can be obtained from the generalized Wigner–Eckart theorem [4] which states that

$$\langle \Gamma_{\mathrm{f}}\gamma_{\mathrm{f}}|T^{\Gamma}_{\gamma}|\Gamma_{\mathrm{i}}\gamma_{\mathrm{i}}\rangle = \langle \Gamma_{\mathrm{i}}\gamma_{\mathrm{i}}\ \Gamma\gamma|\Gamma_{\mathrm{f}}\gamma_{\mathrm{f}}\rangle\langle \Gamma_{\mathrm{f}}\|T^{\Gamma}\|\Gamma_{\mathrm{i}}\rangle.$$

The matrix element can be written as the product of a generalized coupling coefficient (denoted as $\langle \cdots\ \cdots|\cdots\rangle$) and a reduced matrix element (written as $\langle \cdot\|\cdot\|\cdot\rangle$). The essential point is that all dependence on the quantum numbers associated with the subalgebra $\mathcal{G}_2$ is contained in the generalized coupling coefficient. This coefficient can be calculated with standard algebraic techniques which have been detailed in several textbooks (e.g., Refs. [4, 7]) and which are not of concern here. The generalized Wigner–Eckart theorem considerably facilitates the calculation of matrix elements of tensor operators. Typically, it proceeds by evaluating a simple matrix element

and subsequently obtaining others from ratios of generalized coupling coefficients. In addition to this simplification, selection rules follow from the generalized Wigner–Eckart theorem: if Γ_f is not contained in the product $\Gamma_\mathrm{i} \times \Gamma$, the generalized coupling coefficient is zero and the matrix element vanishes. Selection rules can thus be derived from the multiplication rules of irreducible representations.

The expansion in T_z is but an approximation to the true Coulomb interaction; it represents the diagonal part of it, with the T-mixing isovector and isotensor parts being neglected. In that approximation isospin remains a good quantum number and the expression (1.48) represents the Coulomb energy. To find the total energy of a specific state, we need to include the nuclear interaction and the energy shifts due to the neutron–proton mass difference. If the nuclear interaction is exactly isoscalar, its contribution to all members of an isospin multiplet is constant; if it is at most of two-body character, the dependence of the energy on M_T can be shown to be quadratic at most, following the same arguments as in the case of the Coulomb interaction. On the other hand, the neutron–proton mass difference gives rise to a term linear in M_T. Therefore, in this approximation, the total energies of the members of an isospin multiplet are related through the formula

$$B(A, M_T) = c_0 + c_1 M_T + c_2 M_T^2, \tag{1.49}$$

where the coefficients c_i now include effects of the nuclear interaction and of the neutron–proton mass difference. The quantity $B(A, M_T)$ is the (positive) binding energy of an A-nucleon state with $M_T = (N - Z)/2$ and is related to its mass $M(N, Z)$ by

$$B(A, M_T) = N m_\mathrm{n} c^2 + Z m_\mathrm{p} c^2 - M(N, Z) c^2. \tag{1.50}$$

The summary of this discussion is that the excitation spectra of the different nuclei belonging to the same isospin multiplet (with the same T but different M_T) are identical but that corresponding states (also known as isobaric analog states) do not have the same binding energy. The formula (1.49) implies a relation between the absolute energies of isobaric analog states and is known as the **isobaric-multiplet mass equation** or IMME.

The IMME was proposed by Wigner [18], while expressions for the coefficients κ_i in (1.48) based on perturbation theory of the electromagnetic hamiltonian density were given in Ref. [19]. For $T \geq 3/2$ a test is possible since the parameters c_i can be fixed from the isobaric analog states in three nuclei and thus a prediction follows for the other members of the multiplet. Early applications of the IMME were considered by Wilkinson [20] and since then many more nuclear isospin multiplets have been established [21]. The following example discusses a case of recent interest.

Example: Isobaric multiplets in $A = 32$ and 33 nuclei. With recent advances in experimental techniques the validity of the isobaric-multiplet mass equation

can be put to increasingly stringent tests. Progress has been made in two key areas. First, it has become possible to produce and transport nuclides of ever shorter half-lives. Second, due to a variety of trapping techniques [22] experimenters are able to determine atomic masses with increasing precision, achieving relative uncertainties down to 10^{-8}. As a result, many more isobaric multiplets have become accessible in recent years for which the validity of the IMME (1.49) can be tested.

The measurement of a $T = 2$ quintet and a $T = 3/2$ quartet in the mass $A = 32$ and 33 nuclei illustrates these two experimental improvements. The shortest-lived members of these multiplets are the ^{32}Ar and ^{33}Ar nuclides with half-lives of $T_{1/2} = 98$ ms and $T_{1/2} = 173$ ms, respectively. In spite of the difficulties associated with the production of such short-lived isotopes, an impressively accurate mass measurement was carried out, with uncertainties of only 1.8 and 0.44 keV in the masses of ^{32}Ar and ^{33}Ar, respectively [23]. An additional complication in the test of the IMME is that several members of the multiplets are not the ground state of a nucleus but correspond to an excited state, possibly an unbound one. For example, one member of the $T = 3/2$ quartet is an unbound state in ^{33}Cl, the energy of which needed to be determined from the resonances in the ^{32}S(p,p) reaction [24]. The results as obtained in Ref. [23] are summarized in Fig. 1.1. The figure shows the

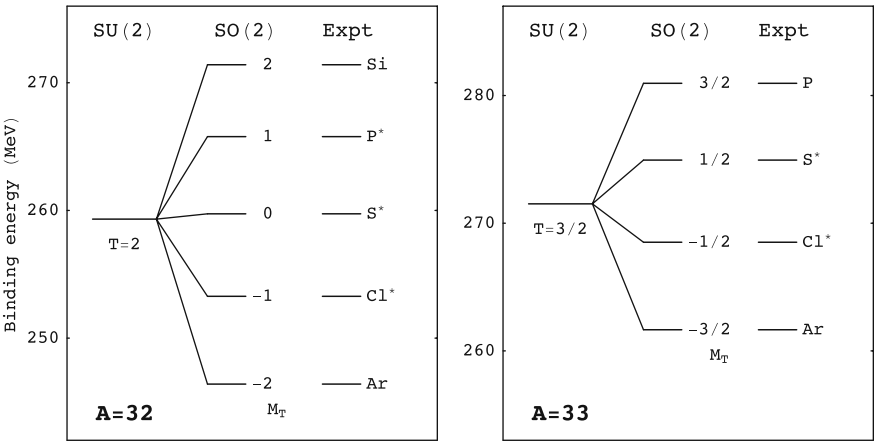

Fig. 1.1. Binding energies of the isobaric members of a $T = 2$ quintet and of a $T = 3/2$ quartet in nuclei with mass $A = 32$ and $A = 33$. The quintet contains states with angular momentum $J^\pi = 0^+$ (ground states of silicon and argon, excited states in phosphor, sulphur and chlorine); the quartet comprises states with $J^\pi = 1/2^+$ (ground states of phosphor and argon, excited states in sulphur and chlorine). In each case the column on the *left* is obtained for an exact SU(2) symmetry, which predicts states with different M_T to be degenerate. The *middle* column is obtained with the IMME with coefficients $c_0 = 259.735$ (271.779), $c_1 = 6.25261$ (6.43351) and $c_2 = -0.207439$ (-0.210090), in MeV, for the quintet (quartet). The column on the *right* gives the experimental binding energies

binding energies of the quartet nuclei ^{33}Ar and ^{33}P which have $T = |M_T| = 3/2$ in their ground state. The isobaric analogue states in ^{33}Cl and ^{33}S are $J^\pi = 1/2^+$ states at excitation energies of 3.375 and 5.480 MeV, respectively; these energies are subtracted from the ground-state binding energies of ^{33}Cl and ^{33}S to give the energies plotted in Fig. 1.1. Similarly, for the quintet nuclei ^{32}Ar and ^{32}Si the ground-state binding energies are shown which have $J^\pi = 0^+$ and $T = |M_T| = 2$ in their ground state; other members of the quintet are excited $J^\pi = 0^+$ states in ^{32}Cl, ^{32}S and ^{32}P. For an exact SU(2) symmetry the members of an isobaric multiplet are degenerate in energy. This degeneracy is lifted by the lowering of the symmetry to SO(2) and the energy splitting is well accounted for by the IMME. In fact, deviations from IMME are less than ~ 1 keV, much less than the splitting between the members of the multiplet which are of the order of 10 MeV.

Deviations from the IMME cannot be revealed through plots of the type of the Fig. 1.1. A convenient way of gauging the precision of the IMME is to increase the expansion in M_T to third order,

$$B(A, M_T) = c_0 + c_1 M_T + c_2 M_T^2 + c_3 M_T^3,$$

and to investigate to what extent the data require the coefficient c_3 to deviate from zero. A non-zero coefficient may be the result of isospin mixing or signals the existence of isospin violating three- or higher-body interactions between the nucleons. Figure 1.2 shows a compilation of values of c_3, taken from Ref. [21]. In total there are six complete quintets (even A) and 26 complete quartets (odd A), in some cases several for the same A. Most c_3 coefficients are consistent with zero and in particular the value found in the $A = 32$ quintet and $A = 33$ quartet deviates less than 1 keV from zero. We stress

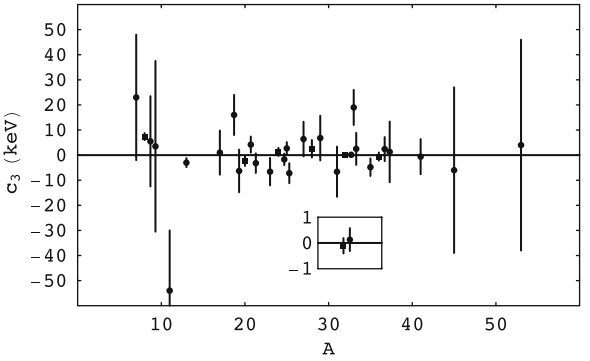

Fig. 1.2. The coefficient c_3 for all known complete isobaric quartets (*circles*) and quintets (*squares*). In some cases there are several quartets for the same A. The inset shows c_3 for the $A = 32$ quintet and $A = 33$ quartet discussed in the text and illustrates the increase in precision achieved over recent years

nevertheless that the quality of fits such as the one in Fig. 1.1 is not the most important aspect of dynamical symmetries, but rather the existence of good quantum numbers (isospin T in this case).

1.1.7 Selection Rules

The most important consequence of a symmetry, which remains valid under the process of a dynamical symmetry breaking, is the existence of conserved quantum numbers. Frequently, these quantum numbers give rise to selection rules in radiative transition, particle-transfer or decay processes. The measurement of transition, transfer or decay probabilities is thus the method to establish the goodness of labels needed to characterize a quantum state and this in turn indicates to what extent a given (dynamical) symmetry is valid.

The link between symmetries and selection rules can be given a precise quantitative formulation via the generalized Wigner–Eckart theorem. Suppose the calculation is required of a transition or transfer matrix element between an initial state $|\Gamma_\mathrm{i}\gamma_\mathrm{i}\rangle$ and a final state $|\Gamma_\mathrm{f}\gamma_\mathrm{f}\rangle$, where the labeling of Sect. 1.1.5 is adopted. To compute the matrix element, it is first necessary to determine the tensor character of the operator associated with the transition or transfer which generally is achieved by writing the operator as $\sum_{\Gamma\gamma} a_{\Gamma\gamma} T^\Gamma_\gamma$. Each piece T^Γ_γ can now be dealt with separately through the generalized Wigner–Eckart theorem. The essential point is that all dependence on the quantum numbers associated with the subalgebra $\mathcal{G}_2$ is contained in a generalized coupling coefficient which can be calculated from algebraic methods (see Box on Isoscalar factors and the Wigner–Eckart theorem). In addition, selection rules now follow from the multiplication rules for irreducible representations of the algebra $\mathcal{G}_1$: if Γ_f is not contained in the product $\Gamma_\mathrm{i} \times \Gamma$, the generalized coupling coefficient is zero and the matrix element of T^Γ_γ vanishes.

A concrete example illustrates the emergence of selection rules as a result of a (dynamical) symmetry.

Example: E1 transitions in self-conjugate nuclei and isospin symmetry breaking. A well-known example of the idea of selection rules concerns electric dipole transitions in self-conjugate nuclei [25, 26], that is, nuclei with an equal number of neutrons and protons ($N = Z$). The E1 operator is, in lowest order of the long-wave approximation, given by

$$T_\mu(\mathrm{E1}) = \sum_{k=1}^{A} e_k r_\mu(k),$$

where the sum runs over all nucleons in the nucleus. Since the charge e_k of the kth nucleon is zero for a neutron and e for a proton, the E1 operator can be rewritten as

$$T_\mu(\mathrm{E1}) = \frac{e}{2}\sum_{k=1}^{A}[1-2t_z(k)]r_\mu(k) = \frac{e}{2}\left[R_\mu - 2\sum_{k=1}^{A} t_z(k) r_\mu(k)\right],$$

where $2t_z$ gives $+1$ for a neutron and -1 for a proton. The first term R_μ in the E1 operator is the center-of-mass coordinate of the total nucleus and does not contribute to an internal E1 transition. (It is responsible for Thomson scattering off a nucleus.) The conclusion is that the electric dipole operator is, in lowest order of the long-wave approximation, of pure isovector character $T^{(T=1)}_{M_T=0}$. The application of the Wigner–Eckart theorem (see Box on Isoscalar factors and the Wigner–Eckart theorem) in isospin space gives

$$\langle \eta_\mathrm{f} T_\mathrm{f} M_{T_\mathrm{f}} | T^{(1)}_0 | \eta_\mathrm{i} T_\mathrm{i} M_{T_\mathrm{i}} \rangle = \langle T_\mathrm{i} M_{T_\mathrm{i}}\ 10 | T_\mathrm{f} M_{T_\mathrm{f}} \rangle \langle \eta_\mathrm{f} T_\mathrm{f} \| T^{(1)} \| \eta_\mathrm{i} T_\mathrm{i} \rangle,$$

where the coupling coefficient is associated with SU(2) $\supset$ SO(2). Self-conjugate nuclei have $M_{T_\mathrm{i}} = M_{T_\mathrm{f}} = 0$ and exhibit as a consequence a simple selection rule: E1 transitions are forbidden between levels with the same isospin $T_\mathrm{i} = T_\mathrm{f} = T$ because of the vanishing Clebsch–Gordan coefficient, $\langle T0\ 10 | T0 \rangle = 0$.

This selection rule has been verified to hold approximately in light self-conjugate nuclei [27] (see also Chap. 1 of Ref. [28]). Deviations occur because of higher-order terms in the E1 operator but also, and more importantly, because isospin is not an exactly conserved quantum number. Isospin mixing can be estimated in a variety of nuclear models. They all show that the mixing (i.e., the non-dynamical breaking of isospin symmetry) is maximal in $N = Z$ nuclei. Isospin mixing effects, caused mainly by the Coulomb interaction, should thus be looked for in heavy $N = Z$ nuclei where they are largest. Such nuclei will be created in abundance and accelerated for study at the newly planned radioactive-ion beam facilities. The spectrum of the heaviest $N = Z$ nucleus studied so far in this respect, ^{64}Ge, is shown in Fig. 1.3. The crucial transition is the E1 between the 5^- and the 4^+ levels with $T = 0$ (indicated by the down arrow) which should be strictly forbidden if the isospin (dynamical) symmetry were exact. A small $B(\mathrm{E1}; 5^- \to 4^+)$ value is measured nevertheless and this is explained through the mixing with higher-lying 5^- and 4^+ levels with $T = 1$ in ^{64}Ge, which are not observed but inferred from their isospin analog states in ^{64}Ga. Although an estimate of the isospin mixing can be made in this way, the procedure is difficult as it requires the measurement of the lifetime, the δ(E2/M1) mixing ratio and the relative intensities of the transitions de-exciting the 5^- level [29]. In addition, to arrive at the isospin-mixing estimate of $P \approx 2.5$ %, the analysis involves some simplifying assumptions such as equal mixing in the initial and final states of the E1 transition. Given these uncertainties, a reliable measurement of isospin admixtures in nuclei, as a function of N and Z, is still very much a declared goal of the current experimental efforts with radioactive-ion beams.

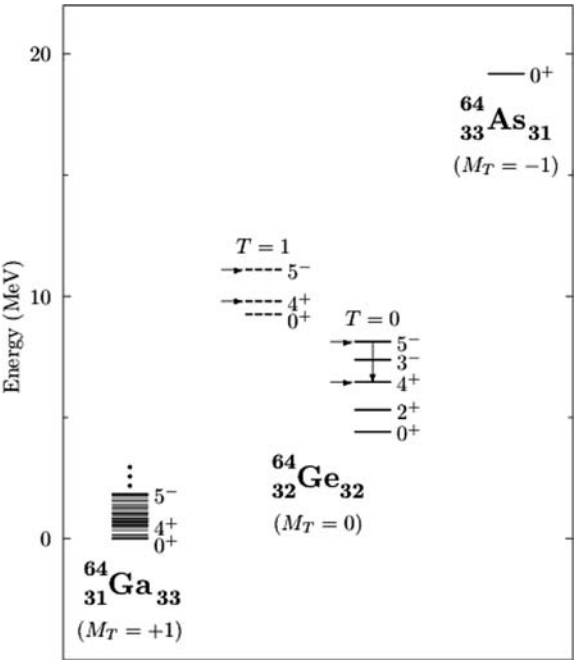

Fig. 1.3. Energy spectra of the nuclei in the $A = 64$ isospin triplet ^{64}Ga, ^{64}Ge and ^{64}As relative to the ground state of the first nucleus. Levels are labeled by their angular momentum and parity J^π. The observed $5^- \rightarrow 4^+$ E1 transition between $T = 0$ states in ^{64}Ge is explained through mixing with the $T = 1$ states, indicated by the *arrows*. The levels in *broken lines* are inferred from the isospin analog levels in ^{64}Ga

1.2 Dynamical Symmetries in Quantal Many-Body Systems

So far the discussion of symmetries has been couched in general terms leading to results that are applicable to any quantum-mechanical system. We shall be somewhat more specific now and show how the concept of dynamical symmetry can be applied systematically to find analytic eigensolutions for a system of interacting bosons and/or fermions. As the results are most conveniently discussed in a second-quantization formalism, first a brief reminder of some essential formulas is given.

1.2.1 Many-Particle States in Second Quantization

In general, particle creation and annihilation operators shall be denoted as $c_i^\dagger$ and c_i, respectively. The index i comprises the complete quantum-mechanical labeling of a single-particle state. In many applications i coincides with the

labels of a stationary quantum state for a single particle in which case $c_i^\dagger$ creates a particle in that stationary state. The index i may include intrinsic quantum numbers such as spin, isospin, color, etc.

The particles are either fermions or bosons, for which the notations $c \equiv a$ and $c \equiv b$, respectively, shall be reserved. They obey different statistics, of Fermi–Dirac and of Bose–Einstein, respectively, which in second quantization is imposed through the (anti-)commutation properties of creation and annihilation operators:

$$\{a_i, a_j^\dagger\} = \delta_{ij}, \qquad \{a_i^\dagger, a_j^\dagger\} = \{a_i, a_j\} = 0, \tag{1.51}$$

and

$$[b_i, b_j^\dagger] = \delta_{ij}, \qquad [b_i^\dagger, b_j^\dagger] = [b_i, b_j] = 0. \tag{1.52}$$

While interactions are carried by bosons (such as photons or gluons), matter consists of fermions. The anti-commutation properties (1.51) ensure that two fermions cannot occupy the same quantum state, which is known as the **Pauli principle**. Introducing the notation

$$[u, v\}_q \equiv uv - (-)^q vu, \tag{1.53}$$

with $q = 0$ for bosons and $q = 1$ for fermions, one can express the relations (1.51) and (1.52) as

$$[c_i, c_j^\dagger\}_q = \delta_{ij}, \qquad [c_i^\dagger, c_j^\dagger\}_q = [c_i, c_j\}_q = 0. \tag{1.54}$$

A many-particle state can be written as

$$|\bar{n}\rangle \equiv \prod_i \frac{(c_i^\dagger)^{n_i}}{\sqrt{n_i!}} |\mathrm{o}\rangle, \tag{1.55}$$

where $|\mathrm{o}\rangle$ is the vacuum state which satisfies

$$\forall i : c_i |\mathrm{o}\rangle = 0. \tag{1.56}$$

A many-particle state is thus completely determined by the number of particles n_i in each quantum state i; the (possibly infinite) set of numbers n_i is collectively denoted as $\bar{n}$. For fermions only $n_i = 0$ and $n_i = 1$ are allowed (since $a_i^\dagger a_i^\dagger |\mathrm{o}\rangle = -a_i^\dagger a_i^\dagger |\mathrm{o}\rangle = 0$) but for bosons no restrictions on n_i exist.

1.2.2 Particle-Number Conserving Dynamical Algebras

The determination of the properties of a quantal system of N interacting particles requires the solution of the eigenvalue equation associated with the hamiltonian

$$H = \sum_i \epsilon_i c_i^\dagger c_i + \sum_{ijkl} v_{ijkl} c_i^\dagger c_j^\dagger c_k c_l + \cdots, \tag{1.57}$$

containing one-body terms ϵ_i, two-body interactions v_{ijkl} and so on; higher-order interactions can be included in the expansion, if needed. The hamiltonian (1.57) satisfies the requirement of particle-number conservation; the particle-number non-conserving case is discussed in the next subsection.

With use of the property [see (1.53) and (1.54)] $c_j^\dagger c_k = (-)^q c_k c_j^\dagger - (-)^q \delta_{jk}$, the hamiltonian (1.57) can be written in a different form as

$$H = \sum_{il} \left(\epsilon_i \delta_{il} - (-)^q \sum_j v_{ijkl} \right) u_{il} + (-)^q \sum_{ijkl} v_{ijkl} u_{ik} u_{jl} + \cdots, \qquad (1.58)$$

where the notation $u_{ij} \equiv c_i^\dagger c_j$ is introduced. The reason for doing so becomes clear when the commutator of the u_{ij} operators is considered,

$$[u_{ij}, u_{kl}] = c_i^\dagger c_k^\dagger [c_j, c_l] + c_i^\dagger [c_j, c_k^\dagger] c_l - c_k^\dagger [c_l, c_i^\dagger] c_j + [c_i^\dagger, c_k^\dagger] c_l c_j,$$

which, because of the identity $[u, v] = [u, v\} - (1 - (-)^q)\, vu$, can be brought into the form

$$[u_{ij}, u_{kl}] = u_{il}\delta_{jk} - u_{kj}\delta_{il} - (1 - (-)^q) \left[c_i^\dagger c_k^\dagger c_l c_j + c_i^\dagger c_k^\dagger c_j c_l \right].$$

The last term on the right-hand side of this equation is zero for bosons (when $q = 0$) as it is for fermions since in that case the expression between square brackets vanishes. This shows that

$$[u_{ij}, u_{kl}] = u_{il}\delta_{jk} - u_{kj}\delta_{il} \qquad (1.59)$$

is valid for a boson as well as a fermion realization of the u_{ij} and that these operators in both cases satisfy the commutation relations of the unitary algebra U(n) where n is the dimensionality of the single-particle space.

The equivalent form (1.58) shows that the solution of the eigenvalue problem for N particles associated with (1.57) requires the diagonalization of H in the symmetric representation $[N]$ of U(n) in case of bosons or in its anti-symmetric representation $[1^N]$ in case of fermions. This, for a general hamiltonian, is a numerical problem which quickly becomes intractable with increasing numbers of particles N or increasing single-particle space n.

A strategy for solving *particular classes* of the many-body hamiltonian (1.57) can be obtained by considering the algebra U(n) as a dynamical algebra $\mathcal{G}_{\rm dyn}$ on which a dynamical symmetry breaking is applied. The generalization of the procedure of Sect. 1.1.5 is straightforward and starts not from two but from a *chain* of nested algebras

$$\mathcal{G}_1 \equiv \mathcal{G}_{\rm dyn} \supset \mathcal{G}_2 \supset \cdots \supset \mathcal{G}_s \equiv \mathcal{G}_{\rm sym}, \qquad (1.60)$$

where the last algebra $\mathcal{G}_{\rm sym}$ in the chain is the symmetry algebra of the problem. To appreciate the relevance of this classification in connection with the

many-body problem (1.57), we note that to a chain of nested algebras (1.60) corresponds a class of hamiltonians that can be written as a linear combination of Casimir operators associated with the algebras in the chain,

$$H = \sum_{r=1}^{s} \sum_{m} \kappa_{rm} C_m[\mathcal{G}_r], \tag{1.61}$$

where κ_{rm} are arbitrary coefficients. This is a generalization of (1.26). The operators in (1.61) satisfy

$$\forall m, m', r, r' : [C_m[\mathcal{G}_r], C_{m'}[\mathcal{G}_{r'}]] = 0. \tag{1.62}$$

This property is evident from the fact that for a chain of nested algebras all elements of $\mathcal{G}_r$ are in $\mathcal{G}_{r'}$ or vice versa. Hence, the hamiltonian (1.61) is written as a sum of commuting operators and as a result its eigenstates are labeled by the quantum numbers associated with these operators. Note that the condition of the *nesting* of the algebras in (1.60) is crucial for constructing a set of commuting operators and hence for obtaining an analytic solution. Casimir operators can be expressed in terms of the operators u_{ij} so that the expansion (1.61) can, in principle, be rewritten in the form (1.58) with the order of the interactions determined by the maximal order m of the invariants.

To summarize these results, the hamiltonian (1.61)—which can be obtained from the general hamiltonian (1.57) for specific coefficients $\epsilon_i, \upsilon_{ijkl} \ldots$—can be solved analytically. Its eigenstates do not depend on the coefficients κ_{rm} and are labeled by

$$\begin{array}{ccccccc} \mathcal{G}_1 & \supset & \mathcal{G}_2 & \supset \cdots \supset & & \mathcal{G}_s & \\ \downarrow & & \downarrow & & & \downarrow & . \\ \Gamma_1 & & \eta_{12}\Gamma_2 & & & \eta_{s-1,s}\Gamma_s & \end{array} \tag{1.63}$$

Its eigenvalues are given in closed form as

$$H|\Gamma_1 \eta_{12} \Gamma_2 \ldots \eta_{s-1,s}\Gamma_s\rangle = \sum_{r=1}^{s} \sum_{m} \kappa_{rm} E_m(\Gamma_r) |\Gamma_1 \eta_{12} \Gamma_2 \ldots \eta_{s-1,s}\Gamma_s\rangle, \tag{1.64}$$

where $E_m(\Gamma_r)$ are known functions introduced in Sect. 1.1.4.

Thus a generic scheme is established for finding analytically solvable hamiltonians (1.57). It requires the enumeration of nested chains of the type (1.60) which is a purely algebraic problem. The symmetry $\mathcal{G}_{\rm dyn}$ is broken dynamically and the only remaining symmetry is $\mathcal{G}_{\rm sym}$ which is the true symmetry of the problem. This idea has found repeated and fruitful application in many branches of physics, as illustrated with the following example.

Example: The Gell-Mann–Okubo mass formula. This example is taken from particle physics and concerns the classification of 'elementary' particles into SU(3) multiplets. In this case the relevant symmetry groups and their associated quantum numbers are

$$\begin{array}{ccccc} \mathrm{SU}(3) & \supset & \mathrm{U}(1) \otimes \Big(& \mathrm{SU}(2) & \supset \mathrm{SO}(2) \Big) \\ \downarrow & & \downarrow & \downarrow & \downarrow \\ (\lambda, \mu) & & Y & T & M_T \end{array},$$

where T and M_T are the isospin and its projection on the z axis and Y is the hypercharge. Instead of the notation (λ, μ), which is followed here, SU(3) representations often are denoted by their dimension, that is, the number of independent basis vectors in the representation [i.e., the number of particles in the corresponding SU(3) multiplet]. Under the assumption of SU(3) invariance all particles belonging to one multiplet are predicted to have the same mass. Since the observed masses differ by hundreds of MeV, they clearly must contain SU(3) symmetry breaking terms. However, SU(3) can be broken while maintaining good quantum numbers Y, T and M_T, that is, it can be broken dynamically. Allowing only up to quadratic terms, we find a mass operator of the form

$$\begin{aligned} M = {} & \kappa_0 + \kappa_1 C_1[\mathrm{U}(1)] + \kappa_2 C_2[\mathrm{U}(1)] + \kappa_3 C_2[\mathrm{SU}(2)] + \kappa_4 C_1[\mathrm{SO}(2)] \\ & + \kappa_5 C_2[\mathrm{SO}(2)], \end{aligned}$$

with the eigenvalues

$$E(Y, T, M_T) = \kappa_0 + \kappa_1 Y + \kappa_2 Y^2 + \kappa_3 T(T+1) + \kappa_4 M_T + \kappa_5 M_T^2.$$

Due to the electromagnetic interaction, discussed previously, M is not scalar in isospin, but contains also isospin vector and tensor terms. Similarly, one assumes the strong interaction to have a certain tensor character under SU(3) and this leads to a relation between the coefficients κ_2 and κ_3 and results in the Gell-Mann–Okubo mass-splitting formula [30, 31, 32],

$$E'(Y, T, M_T) = \kappa_0 + \kappa_1 Y + \kappa_3 \left(T(T+1) - \frac{1}{4} \right) + \kappa_4 M_T + \kappa_5 M_T^2.$$

The process of successive symmetry breakings is illustrated in Fig. 1.4 with the example of the SU(3) octet $(\lambda, \mu) = (1, 1)$, containing the neutron, the proton and the Λ, Σ and Ξ baryons.

1.2.3 Particle-Number Non-conserving Dynamical Algebras

The hamiltonians constructed from the unitary generators u_{ij} necessarily conserve particle number since that is so for the generators themselves. In many cases (involving, e.g., virtual particles, effective phonon-like excitations...) no particle-number conservation can be imposed and a more general formalism is required. Another justification for such generalizations is that the strategy outlined in Sect. 1.2.2 has the drawback that the dynamical algebra $\mathcal{G}_{\mathrm{dyn}}$ can become very large (due a large single-particle space

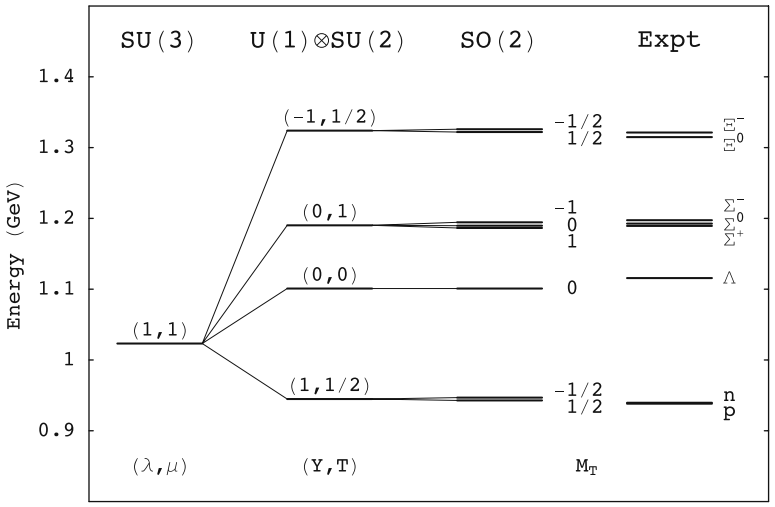

Fig. 1.4. Mass spectrum of the SU(3) octet $(\lambda, \mu) = (1, 1)$. The column on the *left* is obtained for an exact SU(3) symmetry, which predicts all masses to be the same, while the next two columns represent successive breakings of this symmetry in a dynamical manner. The column under SO(2) is obtained with the Gell-Mann–Okubo mass formula with $\kappa_0 = 1112.02$, $\kappa_1 = -189.576$, $\kappa_3 = 44.385$, $\kappa_4 = -3.989$ and $\kappa_5 = 0.768$, in MeV

combined with possible intrinsic quantum numbers such as spin and isospin) which makes the analysis of the group-theoretical reduction (1.60), and the associated labeling (1.63) in particular, too difficult to be of practical use. In some cases the following, more economical, procedure is called for.

In addition to the unitary generators u_{ij}, also the operators $s_{ij} \equiv c_i c_j$ and $s^\dagger_{ij} \equiv c^\dagger_i c^\dagger_j$ are considered. [Note that this notation implies $s^\dagger_{ij} = (s_{ji})^\dagger$.] We now show that the set of operators s_{ij} and $s^\dagger_{ij}$, added to $u'_{ij} \equiv u_{ij} + \frac{1}{2}(-)^q \delta_{ij}$, forms a closed algebraic structure. Since the operators u_{ij} and u'_{ij} differ by a constant only, they satisfy the same commutation relations (1.59), and in the same way it can be shown that

$$[u'_{ij}, s_{kl}] = -s_{kj}\delta_{il} - s_{jl}\delta_{ik}, \qquad [u'_{ij}, s^\dagger_{kl}] = s^\dagger_{il}\delta_{jk} + s^\dagger_{ki}\delta_{jl}. \tag{1.65}$$

The commutator of s_{ij} with $s^\dagger_{kl}$ is more complicated and leads to the following result, valid for both fermions and bosons:

$$[s_{ij}, s^\dagger_{kl}] = (-)^q u'_{li}\delta_{jk} + (-)^q u'_{kj}\delta_{il} + u'_{ki}\delta_{jl} + u'_{lj}\delta_{ik}. \tag{1.66}$$

The modification $u_{ij} \to u'_{ij}$ is thus necessary to ensure closure of the commutator (1.66). The set $\{u'_{ij}, s_{ij}, s^\dagger_{ij}\}$ contains $n(2n+1)$ or $n(2n-1)$ independent generators for bosons or fermions, respectively. From dimensionality (but also from the commutation relations) it can be inferred that the respective Lie algebras are Sp($2n$) and SO($2n$).

It is clear that these algebras can be used to construct number non-conserving hamiltonians. However, the addition of the pair creation and annihilation operators enlarges rather than diminishes the dimension of the dynamical algebra and does not lead to a simplification of the algebraic structure of the problem. The latter can be achieved by considering specific linear combinations

$$U(\bar{\alpha}) \equiv \sum_{ij} \alpha_{ij} u_{ij}, \quad S_+(\bar{\beta}) \equiv \sum_{ij} \beta_{ij} s^\dagger_{ij}, \quad S_-(\bar{\beta}) \equiv \left(S_+(\bar{\beta})\right)^\dagger, \tag{1.67}$$

where the coefficients α_{ij} and β_{ij} are chosen to ensure closure to a *subalgebra* of either Sp($2n$) or SO($2n$).

This procedure will not be formally developed further here. We note that, among the nuclear models, several examples are encountered that illustrate the approach, such as the SU(2) quasi-spin algebra (Sect. 2.1.1) or the SO(8) algebra of neutron–proton pairing (Sect. 4.1).

1.2.4 Superalgebras

To conclude the mathematical methods discussed in this chapter, we now introduce the concept of superalgebra, which generalizes the algebras discussed in the previous sections and which is intimately related to supersymmetry.

In Sect. 1.2.2 it is shown that classical Lie algebras can be realized in terms of either bosons or fermions. Although they obey different statistics with different (anti-)commutation properties (1.51) and (1.52) for the particle creation and annihilation operators, the bilinear products of these operators have the same closure property (1.59). If we introduce the notation $u^{\rm bb}_{ij} \equiv b^\dagger_i b_j$ for bosons and $u^{\rm ff}_{ij} \equiv a^\dagger_i a_j$ for fermions, the closure property can be written as

$$[u^{\rm bb}_{ij}, u^{\rm bb}_{kl}] = u^{\rm bb}_{il}\delta_{jk} - u^{\rm bb}_{kj}\delta_{il}, \qquad [u^{\rm ff}_{ij}, u^{\rm ff}_{kl}] = u^{\rm ff}_{il}\delta_{jk} - u^{\rm ff}_{kj}\delta_{il}. \tag{1.68}$$

This shows that the bosons (fermions) define the unitary Lie algebra $\mathrm{U}^{\rm B}(n)$ [$\mathrm{U}^{\rm F}(m)$] where n (m) is the number of single-particle states that can be occupied by the bosons (fermions). Note that we have added a superscript B or F to indicate the bosonic or fermionic origin of the algebras. Since the boson and fermion operators commute,

$$[u^{\rm bb}_{ij}, u^{\rm ff}_{kl}] = 0, \tag{1.69}$$

the set of operators $\{u^{\rm bb}_{ij}, u^{\rm ff}_{kl}\}$ define the direct product algebra

$$\mathrm{U}^{\rm B}(n) \otimes \mathrm{U}^{\rm F}(m), \tag{1.70}$$

which is the dynamical algebra for the combined boson–fermion system.

As shown in Sect. 1.2.2, the hamiltonian (1.57) of a boson, fermion or boson–fermion system can be built from the bilinear products or generators

of the corresponding dynamical algebras and separately conserves the boson and fermion numbers. The question arises as to whether one may define a generalized dynamical algebra where cross terms of the type $b_i^\dagger a_j$ or $a_j^\dagger b_i$ are included and, if so, what are the consequences of this generalization. From the standpoint of fundamental processes, where bosons correspond to forces (i.e., photons, gluons,...) and fermions to matter (i.e., electrons, nucleons, quarks,...), it may seem strange at first sight to consider symmetries that mix such intrinsically different particles. However, there have been numerous applications of these ideas over the last decades. These symmetries—known as supersymmetries—have given rise to schemes which hold promise in quantum field theory in regards to the unification of the fundamental interactions [33, 34, 35, 36]. In a different context, the consideration of such 'higher' symmetries in nuclear structure physics has provided a unification of the spectroscopic properties of neighboring nuclei [37], as we shall explain in the subsequent chapters of this book. We emphasize that, although similarities exist between these applications of supersymmetry, an important difference is that the bosons in particle physics are elementary, while they are composite in nuclear physics. With this in mind, we consider the effects on the $\mathrm{U^B}(n) \otimes \mathrm{U^F}(m)$ model arising from embedding its dynamical algebra into a superalgebra.

To illustrate the concept of a superalgebra, we consider a schematic example, consisting of a system formed by a single boson and a single ('spinless') fermion, denoted by $b^\dagger$ and $a^\dagger$, respectively. In this case the bilinear products $b^\dagger b$ and $a^\dagger a$ each generate a U(1) algebra. Taken together, these generators conform the

$$\mathrm{U^B}(1) \otimes \mathrm{U^F}(1) \tag{1.71}$$

dynamical algebra. Let us now consider the introduction of the mixed terms $b^\dagger a$ and $a^\dagger b$. Computing the commutator of these operators, we find

$$[a^\dagger b, b^\dagger a] = a^\dagger b b^\dagger a - b^\dagger a a^\dagger b = a^\dagger a - b^\dagger b + 2 b^\dagger b a^\dagger a,$$

which does not close into the original set $\{a^\dagger a, b^\dagger b, a^\dagger b, b^\dagger a\}$. This means that the inclusion of the cross terms does not lead to a Lie algebra. We note, however, that the bilinear operators $b^\dagger a$ and $a^\dagger b$ do not behave like bosons but rather as fermions, in contrast to $a^\dagger a$ and $b^\dagger b$, both of which have bosonic character (in the sense that, e.g., $a_i^\dagger a_j$ *commutes* with $a_k^\dagger a_l$). This suggests the separation of the generators in two sectors, the **bosonic sector** $a^\dagger a$ and $b^\dagger b$ and the **fermionic sector** $a^\dagger b$ and $b^\dagger a$. Computing the *anti*-commutators of the latter, we find

$$\{a^\dagger b, a^\dagger b\} = 0, \qquad \{b^\dagger a, b^\dagger a\} = 0, \qquad \{a^\dagger b, b^\dagger a\} = a^\dagger a + b^\dagger b, \tag{1.72}$$

which indeed close into the same set. The commutators between the bosonic and the fermionic sectors give

$$\begin{aligned} [a^\dagger b, a^\dagger a] &= -a^\dagger b, & [b^\dagger a, a^\dagger a] &= b^\dagger a, \\ [a^\dagger b, b^\dagger b] &= a^\dagger b, & [b^\dagger a, b^\dagger b] &= -b^\dagger a. \end{aligned} \tag{1.73}$$

The operations defined in (1.72) and (1.73), together with the (in this case) trivial $\mathrm{U}^{\mathrm{B}}(1) \otimes \mathrm{U}^{\mathrm{F}}(1)$ commutators

$$[a^\dagger a, a^\dagger a] = [b^\dagger b, b^\dagger b] = [a^\dagger a, b^\dagger b] = 0, \tag{1.74}$$

define the **graded** or **superalgebra** U(1/1). To maintain the closure property for the enlarged set of generators belonging to the boson and fermion sectors, we are thus forced to include both commutators and anti-commutators in the definition of a superalgebra.

In general, superalgebras then involve boson sector generators u_i^{b} and fermion sector generators u_j^{f}, satisfying the generalized relations

$$[u_i^{\mathrm{b}}, u_j^{\mathrm{b}}] = \sum_k c_{ij}^k u_k^{\mathrm{b}}, \quad [u_i^{\mathrm{b}}, u_j^{\mathrm{f}}] = \sum_k d_{ij}^k u_k^{\mathrm{f}}, \quad \{u_i^{\mathrm{f}}, u_j^{\mathrm{f}}\} = \sum_k e_{ij}^k u_k^{\mathrm{b}}, \tag{1.75}$$

where c_{ij}^k, d_{ij}^k and e_{ij}^k are complex constants defining the structure of the superalgebra, hence their denomination as the structure constants of the superalgebra [38]. We shall only be concerned in this book with superalgebras of the form $\mathrm{U}(n/m)$, where n and m denote the dimensions of the boson and fermion subalgebras $\mathrm{U}^{\mathrm{B}}(n)$ and $\mathrm{U}^{\mathrm{F}}(m)$.

1.3 The Algebraic Approach

We have seen in this chapter how the invariance of the hamiltonian of a given system leads to the labeling of its quantum-mechanical states. As was illustrated with several examples, the existence of a symmetry or, equivalently, the goodness of its associated quantum numbers can be tested experimentally via selection rules in various processes.

This methodology to make use of symmetries to solve or simplify quantal many-body problems is also known as the **algebraic approach**. It makes use of dynamical symmetries to compute energy eigenvalues but it goes further in order to describe all relevant aspects of a system in purely algebraic terms. We conclude this chapter by indicating the steps that are typically followed in an algebraic solution:

1. A given system is described in terms of a dynamical algebra $\mathcal{G}_1$ which spans all possible states in the system within a fixed irreducible representation. The choice of this algebra is often dictated by physical considerations (such as the quadrupole nature of collective nuclear excitations).
2. The hamiltonian and all other operators in the system (e.g., for electromagnetic transitions) should be expressed in terms of the generators of the dynamical algebra. Since the matrix elements of the generators can be evaluated from the commutation properties of the dynamical algebra, this implies that all observables of the system can be calculated algebraically.

3. The appropriate bases for the computation of matrix elements are supplied by the dynamical symmetries of the system. The enumeration of all dynamical symmetries proceeds through the construction of chains of nested algebras $\mathcal{G}_1 \supset \mathcal{G}_2 \supset \cdots$ starting from the dynamical algebra.
4. Branching rules for the different algebra chains as well as eigenvalues of their Casimir operators need to be evaluated to determine the character of the dynamical symmetries and their associated energy eigenvalues. All results thus obtained are analytic but for the occurrence of missing labels in the branching rules.
5. In a dynamical symmetry the wave function of an eigenstate does not depend on its energy. This leads to stringent selection rules and analytic predictions for transition matrix elements between eigenstates that can be experimentally verified.
6. When several algebra chains containing the symmetry algebra are present in the system, the hamiltonian will in general not be diagonal in any given chain but rather include invariant operators of all possible subalgebras. In that case the hamiltonian should be diagonalized in one of the bases. Dynamical symmetries are still useful as limiting cases where all observables can be analytically determined.

2 Symmetry in Nuclear Physics

While in the previous chapter symmetry techniques were presented from a general perspective with potential applications in all fields of quantum physics, in this chapter we turn our attention to atomic nuclei. Symmetry considerations have played an important role in nuclear physics, starting from the birth of the discipline, and have continued to do so throughout its development. A comprehensive overview of all such applications would be a gargantuan task and no attempt at that is made here. Our aim is rather to present in this chapter some of the most important developments of symmetry-based models in nuclear physics (including early ones) from a modern and coherent perspective. The early models are due to Wigner, Racah and Elliott and can be considered as precursors to the more modern ones such as the interacting boson model of Arima and Iachello.

Nuclear models based on symmetry concepts can be separated rather naturally into two groups. In the first, a nucleus is considered as a system of interacting neutrons and protons, that is, fermions. This is nothing but the nuclear shell model which is taken here as the starting point for the description of a nucleus. In the first part of this chapter we discuss the two types of shell-model hamiltonian that can be solved analytically with the techniques of Chap. 1, namely those with pairing and those with quadrupole interactions. In the second group of symmetry-based models, a nucleus is treated as a system of interacting bosons which are of composite character and represent correlated pairs of nucleons. The choice of the different bosons is dictated by the nature of the nucleonic interactions and also depends on the particular nucleus that is considered, as is discussed in Sect. 2.2. Throughout this chapter we pay particular attention to the connections that can be established via symmetry techniques between the nuclear shell model and the interacting boson model. We close the chapter with a detailed study of the nucleus ^{112}Cd in Sect. 2.3 which illustrates how such symmetries are studied experimentally.

2.1 The Nuclear Shell Model

The structure of the atomic nucleus is determined, in first approximation, by the nuclear **mean field**, the average potential felt by one nucleon through

A. Frank et al., *Symmetries in Atomic Nuclei*,
Springer Tracts in Modern Physics 230, DOI 10.1007/978-0-387-87495-1_2,

the interactions exerted by all others. This average potential is responsible for the shell structure of the nucleus. For a description that goes beyond this most basic level, the **residual interaction** between nucleons must be taken into account and what usually matters most for nuclear structure at low energies is the residual interaction between nucleons in the valence shell. This interaction depends in a complex fashion on the numbers of valence neutrons and protons and the valence orbits available.

Many of the basic features of the structure of nuclei can be derived from a few essential characteristics of the nuclear mean field and the residual interaction. A schematic nuclear hamiltonian that grasps these essential features is of the form

$$H = \sum_{k=1}^{A} \left(\frac{p_k^2}{2m_\mathrm{n}} + \frac{1}{2} m_\mathrm{n} \omega^2 r_k^2 + \zeta_{ll} l_k^2 + \zeta_{ls} \boldsymbol{l}_k \cdot \boldsymbol{s}_k \right) + \sum_{1 \le k < l}^{A} V_\mathrm{ri}(\xi_k, \xi_l), \quad (2.1)$$

where k, l run from 1 to A, the number of nucleons in the nucleus, ξ_k is a short-hand notation for the spatial coordinates, spin and isospin variables of nucleon k, $\xi_k \equiv \{\boldsymbol{r}_k, \boldsymbol{s}_k, \boldsymbol{t}_k\}$ and m_n is the nucleon mass. The first term in (2.1) is the kinetic energy of the A nucleons. The second term is a harmonic-oscillator potential with frequency ω which is a first-order approximation to the nuclear mean field [28]. The choice of a more realistic nuclear mean field (e.g., a Woods–Saxon potential) leads to a different radial dependence of the single-particle wave functions and, in particular, it does not display the degeneracy of states with different orbital angular momentum l in the same major shell, characteristic of a harmonic oscillator. This deficiency of the harmonic-oscillator potential can be softened by adding an l^2 orbit–orbit term which lifts this degeneracy. The last one-body term in (2.1) corresponds to a spin–orbit coupling in the nucleonic motion. The assumption of its existence provided the decisive step in the development of the nuclear shell model [39, 40] since it led to a natural explanation of the observed shell structure of nuclei and their 'magic' numbers and to concept of core and **valence** nucleons (i.e., nucleons that occupy the outer most shells). The last term in (2.1) is the residual two-body interaction which, in principle, depends in a complicated way on the average one-body potential as well as on the valence space available to the nucleons. In this sense it is an *effective* interaction. Very often either a *realistic* or a *schematic* interaction is taken; for the former one adopts matrix elements adjusted to the data, while for the latter the interaction is assumed to have a simple spatial form and one calculates its matrix elements in a harmonic-oscillator basis.

If the single-particle energy spacings are large in comparison with a typical matrix element of the residual interaction, nucleonic motion is independent and the shell model of independent particles results. In this case the hamiltonian (2.1) has uncorrelated many-particle eigenstates that are Slater determinants constructed from the single-particle wave functions of the harmonic oscillator. If the residual interaction cannot be neglected, a genuine

many-body problem results which is much harder to solve. Interestingly, two types of residual interaction exist—pairing and quadrupole—which allow an analytic solution and which have found fruitful application in nuclear physics.

The attractive, short-range nature of the residual interaction has far-reaching consequences. In the extreme short-range limit of a delta interaction $\delta(\boldsymbol{r}_1 - \boldsymbol{r}_2)$, the many-body nuclear wave function conserves total orbital angular momentum L and total spin S, besides total angular momentum J associated with rotational invariance. This classification (LS or Russell–Saunders coupling) is badly broken by the **spin–orbit** term in the nuclear mean field. The conflicting tendency between the short-range character of the residual interaction, which favors LS coupling, and the spin–orbit term in the average potential, which leads to a jj-coupled classification, is a crucial element in the structural determination of the nucleus. This conflict was recognized and studied in the early days of the nuclear shell model [41]. The generally accepted conclusion is that, while the LS classification is appropriate for very light nuclei, with increasing mass it is gradually replaced by jj coupling which is relevant for the vast majority of nuclei [42].

The second important feature that determines the structure of the nucleus is the number of neutrons and protons in the valence shell. The residual interaction between identical nucleons has a pairing character which favors the formation of pairs of nucleons in time-reversed orbits. This is no longer true when the valence shell contains both neutrons and protons, in which case the interaction acquires an important quadrupole component. Hence, nuclei display a wide variety of spectra, from pairing-type toward rotational like. The evolution from one type to the other is governed by the product $n_\mathrm{n} n_\mathrm{p}$ of neutron and proton numbers in the valence shell [43].

In summary, the gross structure of nuclei is determined by (i) the competition between residual interaction and shell structure, (ii) the strength of the short-range interaction versus the spin–orbit term in the mean field and (iii) the balance between pairing and quadrupole interactions.

2.1.1 The SU(2) Pairing Model

The residual interaction among the valence nucleons is assumed to have a **pairing** character. Thus, for example, in a single j shell one considers an interaction which is attractive for two particles coupled to angular momentum $J = 0$ and zero otherwise,

$$\langle j^2 J M_J | V_\mathrm{pairing} | j^2 J M_J \rangle = -\frac{1}{2}(2j+1) g_0 \delta_{J0}, \tag{2.2}$$

where g_0 is a (positive) strength parameter. This is a reasonable, albeit schematic, approximation to the residual interaction between *identical* nucleons and hence can only be appropriate in semi-magic nuclei. The pairing interaction is illustrated in Fig. 2.1 for the nucleus ^{210}Pb which can be

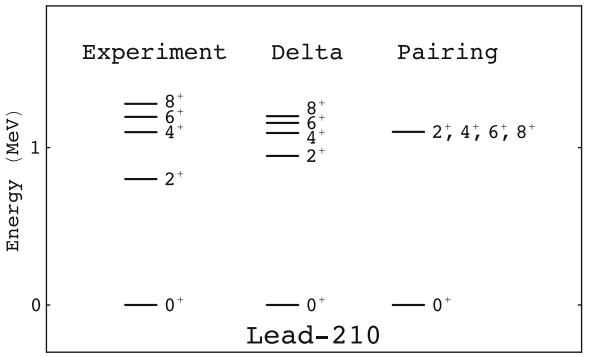

Fig. 2.1. Observed [44] energy spectrum of ^{210}Pb (*left*), and the corresponding spectra for a delta (*middle*) and for a pairing interaction (*right*). Levels are labeled by their angular momentum and parity J^π

described as two neutrons in a $1g_{9/2}$ orbit outside the doubly magic ^{208}Pb inert core.

The shell-model hamiltonian with a two-body pairing interaction can be diagonalized analytically in a space of n identical fermions in a single j shell. This can be shown in a variety of ways but one elegant derivation relies on the existence of an SU(2) symmetry of the pairing hamiltonian [45]. In second quantization, the pairing interaction is written as

$$V_{\text{pairing}} = -g_0 S^j_+ S^j_- \tag{2.3}$$

with

$$S^j_+ = \frac{1}{2}\sqrt{2j+1}\,(a^\dagger_j \times a^\dagger_j)^{(0)}_0, \qquad S^j_- = \left(S^j_+\right)^\dagger, \tag{2.4}$$

where $a^\dagger_{jm}$ creates a particle in orbit j with projection m. The commutator of S^j_+ and S^j_- leads to the operator

$$S^j_z = \frac{1}{4}\left(\sum_{m=-j}^{j} 2a^\dagger_{jm}a_{jm} - 2j - 1\right) = \frac{1}{4}(2n_j - 2j - 1). \tag{2.5}$$

The operator S^j_z equals, up to a constant, n_j which counts the number of particles in orbit j. The resulting three operators close under commutation:

$$[S^j_z, S^j_\pm] = \pm S^j_\pm, \qquad [S^j_+, S^j_-] = 2S^j_z. \tag{2.6}$$

This shows that the set of operators $\{S^j_z, S^j_\pm\}$ forms an **SU(2)** algebra, which is referred to as the **quasi-spin** algebra. Because of this relation with the quasi-spin SU(2) algebra, the pairing hamiltonian can be solved analytically. From the commutation relations (2.6) it follows that

$$S^j_+ S^j_- = \left(S^j\right)^2 - \left(S^j_z\right)^2 + S^j_z, \tag{2.7}$$

which shows that the pairing hamiltonian can be written as a combination of Casimir operators belonging to

$$\begin{array}{ccc} \mathrm{SU}(2) & \supset & \mathrm{SO}(2) \equiv \{S_z\} \\ \downarrow & & \downarrow \\ S & & M_S \end{array} . \tag{2.8}$$

The associated eigenvalue problem can be solved instantly with the techniques of Chap. 1 which yield the energy expression

$$E(S, M_S) = -g_0 \left[S(S+1) - M_S(M_S - 1) \right] . \tag{2.9}$$

The quantum numbers S and M_S can be put in relation to the more usual ones of **seniority** v, introduced by Racah [46], and (valence) particle number n,

$$S = \frac{1}{4}(2j - 2v + 1), \qquad M_S = \frac{1}{4}(2n - 2j - 1), \tag{2.10}$$

leading to the well-known energy expression of the seniority model [47],

$$E(n, v) = -\frac{g_0}{4}(n - v)(2j - n - v + 3). \tag{2.11}$$

By repeated action of S_+^j on a state with $n = v$, it can be shown that the seniority quantum number v corresponds to the *number of nucleons not in pairs coupled to angular momentum zero.*

A generalization of these concepts concerns that toward several orbits. In case of degenerate orbits this can be achieved by making the substitution $S_+^j \mapsto S_+ \equiv \sum_j S_+^j$ which leaves all previous results such as the algebraic structure (2.6) unchanged. The ensuing formalism can then be applied to semi-magic nuclei but, since it requires the assumption of a pairing interaction with degenerate orbits, its applicability is limited.

A more generally valid model is obtained if one imposes the following condition on the shell-model hamiltonian:

$$[[H, S_+^0], S_+^0] = \Delta \left(S_+^0 \right)^2 , \tag{2.12}$$

where S_+^0 creates the lowest two-particle eigenstate of H and Δ is a constant. This condition of generalized seniority, derived by Talmi [48], is much weaker than the assumption of a pairing interaction and, in particular, it does not require that the commutator $[S_+^0, S_-^0]$ yields (up to a constant) the number operator which is central to the quasi-spin formalism. In spite of the absence of a closed algebraic structure, it is still possible to compute the exact ground-state eigenvalue of hamiltonians satisfying 2.12.

The concepts of seniority and quasi-spin have found repeated application in nuclear physics and have been the subject of fruitful generalizations. An important extension concerns the seniority classification of neutron–proton systems which is presented in Sect. 4.1.

The discussion of pairing correlations in nuclei traditionally has been inspired by the treatment of superfluidity in condensed matter. The superfluid

phase in the latter systems is characterized by the presence of a large number of identical bosons in a single quantum state. In superconductors the bosons are pairs of electrons with opposite momenta that form at the Fermi surface. The character of the bosons in nuclei can be understood from the structure of the ground state of a pairing hamiltonian which, for even–even nuclei, is given by $(S_+)^{n/2}|\mathrm{o}\rangle$, where $|\mathrm{o}\rangle$ is the vacuum state for the S pairs. In nuclei the bosons are thus pairs of valence nucleons with opposite angular momenta.

Condensed-matter superfluidity (and associated superconductivity) was explained by Bardeen, Cooper and Schrieffer [49] and the resulting BCS theory has strongly influenced the discussion of pairing in nuclei [50], in particular as regards the problem of pairing of nucleons in non-degenerate orbits. Nevertheless, the approximations made in BCS theory are less appropriate for nuclei since the number of nucleons is comparatively small. An exact method to solve the problem of particles distributed over non-degenerate levels interacting through a pairing force was proposed a long-time ago by Richardson [51] based on the Bethe *ansatz* [52]. Surprisingly, this method passed almost unnoticed despite its potential impact. Only recently Richardson's work has been properly recognized as well as generalized to other classes of integrable pairing models [53].

As an illustration of Richardson's approach, we supplement the pairing interaction (2.3) with single-particle energies to obtain the following hamiltonian:

$$H = \sum_j \epsilon_j n_j - g_0 S_+ S_- = \sum_j \epsilon_j n_j - g_0 \sum_j S_+^j \sum_{j'} S_-^{j'}, \tag{2.13}$$

where n_j is the number operator for orbit j, ϵ_j is its single-particle energy and $S_+ = \sum_j S_+^j$. The solvability of the hamiltonian (2.13) arises as a result of the symmetry $\mathrm{SU}(2) \otimes \mathrm{SU}(2) \otimes \cdots$ where each SU(2) algebra pertains to a specific j. Whether the solution of (2.13) can be called superfluid depends on the differences $\epsilon_j - \epsilon_{j'}$ in relation to the strength g_0. In all cases the solution is known in closed form for all possible choices of ϵ_j.

Solution of the Richardson model. An exact solution of the eigenvalue problem associated with the pairing hamiltonian in non-degenerate orbits, $H = \sum_j \epsilon_j n_j - g_0 S_+ S_-$, is known in general. It is instructive to analyze first the case of $n = 2$ particles because it gives insight into the structure of the general problem. The two-particle, $J = 0$ eigenstates can be written as

$$\mathcal{S}_+^{\boldsymbol{x}}|\mathrm{o}\rangle = \sum_j x_j S_+^j |\mathrm{o}\rangle,$$

with x_j coefficients that are to be determined from the eigenequation

$$H\mathcal{S}_+^{\boldsymbol{x}}|\mathrm{o}\rangle = E\mathcal{S}_+^{\boldsymbol{x}}|\mathrm{o}\rangle,$$

where E is the unknown eigenenergy. With some elementary manipulations this can be converted into the secular equation

$$2\epsilon_j x_j - g_0 \sum_{j'} \Omega_{j'} x_{j'} = E x_j,$$

from which the following expression for the coefficients x_j can be deduced:

$$x_j = \left(\sum_{j'} \Omega_{j'} x_{j'} \right) \frac{g_0}{2\epsilon_j - E},$$

with $\Omega_j = j + 1/2$. This is still not an explicit solution since x_j occurs at both sides of the equation. However, since we are interested in x_j up to a normalization constant $\mathcal{N}$ only, we can write

$$x_j = \mathcal{N} \frac{g_0}{2\epsilon_j - E}.$$

If the eigenenergy E is known, one thus finds the corresponding eigenstate (up to a normalization factor)

$$\left(\sum_j \frac{1}{2\epsilon_j - E} S_+^j \right) |\mathrm{o}\rangle.$$

The eigenenergy E can be found by substituting the solution for x_j into the secular equation, leading to

$$\sum_j \frac{\Omega_j}{2\epsilon_j - E} = \frac{1}{g_0}.$$

This equation can be solved graphically which is done in Fig. 2.2 for a particular choice of single-particle energies ϵ_j, degeneracies Ω_j and pairing strength g_0. The single-particle orbits and their energies are given in

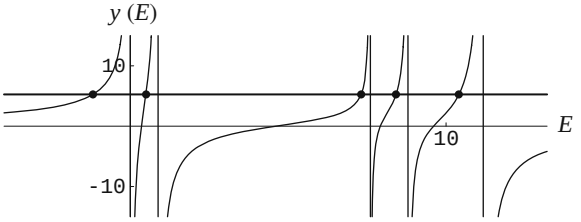

Fig. 2.2. Graphical solution of the Richardson equation for $n = 2$ fermions distributed over $s = 5$ single-particle orbits. The sum $\sum_j \Omega_j/(2\epsilon_j - E) \equiv y(E)$ is plotted as a function of E; the intersections of this curve with the line $y = 1/g_0$ (*dots*) then correspond to the solutions of the Richardson equation

Table 2.1. Single-neutron energies (in MeV) in the tin isotopes

	$2d_{5/2}$	$1g_{7/2}$	$3s_{1/2}$	$2d_{3/2}$	$1h_{11/2}$
ϵ_j	0.00	0.44	3.80	4.40	5.60
Ω_j	3	4	1	2	6

Table 2.1 and the pairing strength is $g_0 = 0.19$ MeV. This is an appropriate set of values for the tin isotopes with $Z = 50$ protons and neutrons distributed over the 50–82 shell. In the case of two particles coupled to angular momentum $J = 0$ there are as many eigenstates as there are single-particle orbits. This property is, of course, not generally valid for $n \neq 2$. In the limit $g_0 \to \pm 0$ of weak pairing interaction, the solutions $E \to 2\epsilon_j$ are obtained, as should be. Of more interest is the limit of strong pairing, $g_0 \to +\infty$. From the graphical solution we see that in this limit there is one eigenstate of the pairing hamiltonian which lies well below the other eigenstates with approximately constant amplitudes x_j since for that eigenstate $|E| \gg 2|\epsilon_j|$. Hence, in the limit of strong pairing one finds a low-lying $J = 0$ two-particle ground state which can be approximated as

$$\mathcal{S}_+^{\mathrm{c}}|\mathrm{o}\rangle \approx \sqrt{\frac{1}{\Omega}} \sum_j S_+^j |\mathrm{o}\rangle,$$

where $\Omega = \sum_j \Omega_j$. Because of this property this state is often referred to as the collective S state, in the sense that all single-particle orbits contribute equally to its structure.

This result can be generalized to n particles, albeit that the general solution is more complex. On the basis of the two-particle problem one may propose, for an even number of particles n, a ground state of the hamiltonian (2.13) of the form (up to a normalization factor)

$$\prod_{\alpha=1}^{n/2} \left(\sum_j \frac{1}{2\epsilon_j - E_\alpha} S_+^j \right) |\mathrm{o}\rangle,$$

which is known as the Bethe *ansatz* [52]. Each pair in the product is defined through coefficients $x_j = (2\epsilon_j - E_\alpha)^{-1}$ in terms of an energy E_α depending on α which labels the $n/2$ pairs. This product indeed turns out to be the ground state provided the E_α are solutions of $n/2$ coupled, non-linear equations

$$\sum_j \frac{\Omega_j}{2\epsilon_j - E_\alpha} - \sum_{\beta(\neq\alpha)}^{n/2} \frac{2}{E_\beta - E_\alpha} = \frac{1}{g_0}, \qquad \alpha = 1, \ldots, n/2,$$

known as the Richardson equations [51]. Note the presence of a second term on the left-hand side with differences of the unknowns $E_\beta - E_\alpha$ in the denominator, which is absent in the two-particle case. In addition, the energy of the corresponding state is given by

$$\sum_{\alpha=1}^{n/2} E_\alpha .$$

The Richardson equations can be derived from the Bethe *ansatz* for any eigenstate of the hamiltonian (2.13). A characteristic feature of the Bethe *ansatz* is that it no longer consists of a superposition of *identical* pairs since the coefficients $(2\epsilon_j - E_\alpha)^{-1}$ vary as α runs from 1 to $n/2$. Richardson's model thus provides a solution that covers all possible hamiltonians (2.13), ranging from those with superfluid character to those with little or no pairing correlations [54].

The Box on the Solution of the Richardson model presents a discussion of the generalized pairing hamiltonian (2.13) with an explicit solution in the two-particle case with elementary methods which is then generalized to $n \neq 2$.

Example: Two-nucleon separation energies in the tin isotopes. Evidence for pairing correlations among identical nucleons has several aspects and is well documented [47]. Good pairing indicators are nucleon separation energies. The two-neutron separation energy, for example, is defined as

$$S_{2\mathrm{n}}(N,Z) = B(N,Z) - B(N-2,Z),$$

where $B(N,Z)$ denotes the ground-state binding energy of a nucleus with N neutrons and Z protons. In some simple approximation the binding energy of the ground state of a semi-magic nucleus can be related to the pairing interaction energy among its valence nucleons. For the exact superfluid case of several degenerate orbits, this leads to the following result for the difference of two-nucleon separation energies:

$$S_{2\mathrm{n}}(N,Z) - S_{2\mathrm{n}}(N-1,Z) = -g_0,$$

that is, the two-nucleon separation energy varies linearly as a function of nucleon number. For a system of identical nucleons occupying a set of non-degenerate single-particle levels as shown on the left of Fig. 2.3, the complete absence of pairing correlations ($g_0 = 0$) would lead to a staircase behavior of $S_{2\mathrm{n}}$ as a function of N (see Fig. 2.3a). The other extreme, strong pairing correlations among nucleons distributed over closely spaced single-particle levels, is represented in Fig. 2.3b which shows a smooth decrease of $S_{2\mathrm{n}}$ as the nucleon number increases. Figure 2.3c shows the two-neutron separation energies measured in the tin isotopes, as a function of neutron number. As far as the 50–82 shell is concerned, the data are consistent with the superfluid

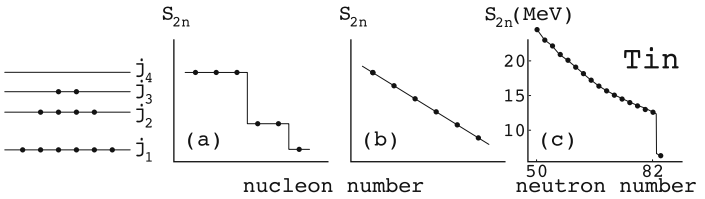

Fig. 2.3. The two-nucleon separation energy S_{2n} as an indicator of pairing. If there are no pairing correlations among the nucleons occupying the levels shown on the *left*, the separation energy, as a function of nucleon number, behaves as in (**a**). Superfluidity leads to the behavior shown in (**b**). The observed [55] two-neutron separation energies in (**c**) show that the superfluid solution is appropriate for the tin isotopes with active neutrons in the 50–82 shell

solution. At $N = 82$ a large jump in S_{2n} is observed. This indicates that pairing correlations are confined to the 50–82 shell.

In addition to the applications discussed so far (all related to pairing), SU(2) has been repeatedly used as a quasi-spin algebra but in different contexts. The most noteworthy example in nuclear physics is the Lipkin–Meshkov–Glick (LMG) model [56] which considers two levels (assigned $\sigma = -$ and $\sigma = +$) each with degeneracy Ω over which n particles are distributed. In terms of the creation and annihilation operators $a^\dagger_{m\sigma}$ and $a_{m\sigma}$, $m = 1, \ldots, \Omega, \sigma = \pm$, it can be shown that the operators

$$K_+ = \sum_m a^\dagger_{m+} a_{m-}, \qquad K_- = (K_+)^\dagger, \qquad K_z = \frac{1}{2}(n_+ - n_-), \tag{2.14}$$

form an SU(2) algebra. The hamiltonian

$$H = \epsilon K_z + \frac{1}{2}\upsilon(K_+K_- + K_-K_+) + \frac{1}{2}\omega(K_+^2 + K_-^2), \tag{2.15}$$

can, with use of the underlying SU(2) algebra, be solved analytically for certain values of the parameters ϵ, υ and ω. These have a simple physical meaning: ϵ is the energy needed to promote a particle from the $-$ to the $+$ level, υ is the strength of the interaction that mixes configurations with the same numbers of particles n_- and n_+, and ω is the strength of the interaction that mixes configurations differing by two in these numbers. The LMG model has thus three ingredients (albeit in schematic form) that are of importance in determining the structure of nuclei: an interaction υ between the nucleons in a valence shell, the possibility to excite nucleons from the valence shell into a higher shell at the cost of an energy ϵ and an interaction ω that mixes these particle–hole excitations with the valence configurations. With these ingredients the LMG model has played an important role as a testing ground of various approximations proposed in nuclear physics.

2.1.2 The SU(3) Rotation Model

In the early days of nuclear physics, nuclei with a rotational-like spectrum were interpreted either with the liquid drop model of Bohr and Mottelson [57] (see Box on The collective model of nuclei) or with a *deformed* single-particle shell model of Nilsson [58]. An understanding of rotational phenomena in terms of the spherical shell model, however, was lacking. Elliott's SU(3) model [59] provides such an understanding from a symmetry perspective. Since SU(3) is based on Wigner's supermultiplet model, we begin with a discussion of the latter.

The collective model of nuclei. Among the historically most important models of nuclear structure is the collective model developed by Bohr and Mottelson [57], which complements the shell model by including motions of the whole nucleus such as rotations and vibrations. The origin of the collective model goes back to the liquid drop model (LDM), which considers the nucleus as a very dense quantum liquid in which fundamental nuclear properties—such as its binding energy—are described in terms of volume and surface energy, or compressibility, which are macroscopic concepts usually associated with a liquid. This model has been useful in describing how a nucleus deforms and undergoes fission [60].

The collective model emphasizes the coherent behavior of many nucleons, including quadrupole and higher-multipole deformations, as well as rotations and vibrations that involve the entire nucleus. It can be viewed as an extension of the LDM and has been shown also to be an appropriate starting point for the analysis of fission. Very generally, the nuclear surface can be expressed as a sum over spherical harmonics [61, 62]

$$R = R_0 \left[1 + \sum_{\mu} \alpha_{\lambda\mu} Y^*_{\lambda\mu}(\theta, \phi) \right],$$

where the $\alpha_{\lambda\mu}$ can be considered as (time dependent) variables that determine the shape of the nuclear surface. For particular choices of λ different shapes are obtained. This is illustrated in Fig. 2.4 where the quadrupole case ($\lambda = 2$) is shown with or without axial symmetry (prolate, oblate and triaxial) as well as an example of octupole ($\lambda = 3$) and hexadecapole ($\lambda = 4$) deformation. For the dominant quadrupole deformations with $\lambda = 2$ a corresponding hamiltonian can be written as

$$H = T + V = \frac{1}{2B} \sum_{\mu} (\pi_{2\mu})^2 + \frac{1}{2} C \sum_{\mu} (\alpha_{2\mu})^2 ,$$

where $\pi_{2\mu}$ is the momentum variable associated with $\alpha_{2\mu}$, $\pi_{2\mu} = B\dot{\alpha}_{2\mu}$, with B the mass parameter and C the restoring force. This represents a

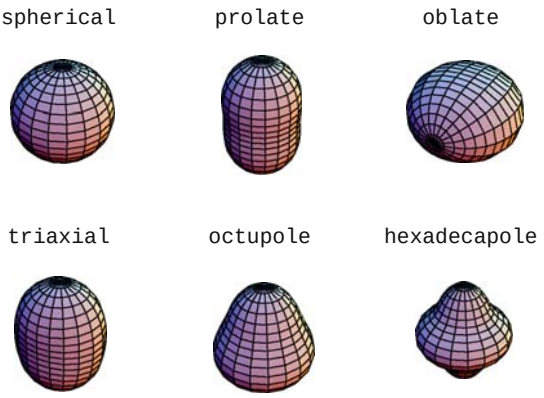

Fig. 2.4. Surfaces and their dependence on the variables $\alpha_{\lambda\mu}$. The cases shown are (i) spherical (all $\alpha_{\lambda\mu}$ are zero); (ii) prolate ($\alpha_{20} > 0$); (iii) oblate ($\alpha_{20} < 0$); (iv) triaxial ($\alpha_{20} \neq 0$ and $\alpha_{2\pm2} \neq 0$); (v) octupole ($\alpha_{30} \neq 0$) and (vi) hexadecapole ($\alpha_{40} \neq 0$)

five-dimensional harmonic oscillator in the collective variables $\alpha_{2\mu}$ as can be seen by differentiating H with respect to time,

$$B\frac{d^2\alpha_{2\mu}}{dt^2} + C\alpha_{2\mu} = 0.$$

This is indeed the differential equation for a harmonic oscillator and, for each $\alpha_{2\mu}$, the oscillations have the frequency $\omega = \sqrt{C/B}$ and its vibrational energy is $\hbar\omega$. The quantization of this hamiltonian and the introduction of intrinsic coordinates (β, γ) and the Euler angles $(\vartheta_i, i = 1, 2, 3)$ lead to the well-known form of the Bohr–Mottelson hamiltonian:

$$H = -\frac{\hbar^2}{2B}\left[\frac{1}{\beta^4}\frac{\partial}{\partial\beta}\beta^4\frac{\partial}{\partial\beta} + \frac{1}{\beta^2}\left(\frac{1}{\sin 3\gamma}\frac{\partial}{\partial\gamma}\sin 3\gamma\frac{\partial}{\partial\gamma} - \frac{1}{4}\sum_{\kappa}\frac{{L'_\kappa}^2}{\sin^2(\gamma - 2\pi\kappa/3)}\right)\right] + \beta^2,$$

where L'_κ are the components of the angular momentum in the intrinsic frame of reference. The general solutions of this equation were found by Chacón et al. [63] and by Chacón and Moshinsky [64]. These eigenfunctions can be used as a complete basis for the diagonalization of general potentials of the form $V(\beta, \gamma)$ [65]. The rotational part transforms this solution to the laboratory frame and is associated with Wigner's D-functions [10]. The potential $V(\beta, \gamma)$ can be displayed in the (β, γ) plane as contour plots, and an illustration is shown in Fig. 2.5.

The collective model and its extensions have been very successful in describing a wide variety of nuclear properties, especially energy levels

in nuclei with an even number of protons and neutrons. These energy levels show the characteristics of rotating or vibrating systems expected from quantum mechanics. Commonly measured properties of these nuclei,

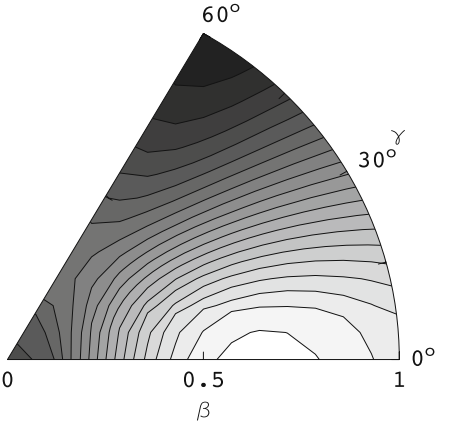

Fig. 2.5. Illustration of a $V(\beta, \gamma)$ potential in the (β, γ) plane. Symmetry considerations require that the entire potential is specified by the domain $0 \leq \gamma \leq \pi/3$

including broad systematics of excited state energies, angular momentum, magnetic moments and nuclear shapes, can be understood from the collective model.

Recently, symmetry arguments were introduced in the collective model leading to so-called critical-point symmetries [66, 67]. These symmetries are outside the scope of this book and the interested reader may consult Ref. [68] for a review.

The nuclear shell model and the collective model represent extreme forms of behavior of nucleons in a nucleus, where the former stresses the single-particle character of the nucleons, while the latter idealizes their coherent motion. A great deal of work has been accomplished in nuclear physics (such as Elliott's SU(3) scheme or Arima and Iachello's boson model) with the purpose to reconcile these seemingly conflicting views of the nucleus.

Wigner's **supermultiplet** model [16] assumes nuclear forces to be invariant under rotations in *spin* as well as *isospin* space. This invariance is expressed by the following commutation relations:

$$[H, S_\mu] = [H, T_\mu] = [H, Y_{\mu\nu}] = 0, \tag{2.16}$$

where

$$S_\mu = \sum_{k=1}^{A} s_\mu(k), \qquad T_\mu = \sum_{k=1}^{A} t_\mu(k), \qquad Y_{\mu\nu} = \sum_{k=1}^{A} s_\mu(k) t_\nu(k), \tag{2.17}$$

are the spin, isospin and spin–isospin operators, in terms of $s_\mu(k)$ and $t_\mu(k)$, the spin and isospin components of nucleon k. The 15 operators (2.17) generate the Lie algebra **SU(4)**. According to the discussion in Chap. 1, any hamiltonian satisfying the conditions (2.16) has SU(4) symmetry, and this in addition to symmetries associated with the conservation of total spin S and total isospin T.

To obtain a qualitative understanding of SU(4) symmetry, it is instructive to analyze the case of two nucleons in an oscillator shell. Total anti-symmetry of the wave function requires that the spatial part is symmetric and the spin–isospin part anti-symmetric or vice versa. Both cases correspond to a different symmetry under SU(4), the first being anti-symmetric and the second symmetric. The symmetry under a given algebra can characterized by the so-called **Young diagram** (see Box on Permutation symmetry and Young diagrams). For two particles the anti-symmetric configuration is denoted as $[1,1]$, while the symmetric one is written as $[2,0]$.

Permutation symmetry and Young diagrams. Systems of A identical particles are invariant with respect to the permutations P_{ij} that exchange *all* coordinates of the two particles i and j. As a consequence the hamiltonian is invariant under the permutation group $\mathcal{S}_A$ and its eigenstates can be classified according to the irreducible representations of that group. If the constituent particles are fermions, such as is the case for the atomic nucleus, any physical state must be completely anti-symmetric. If nothing else is known of the system's hamiltonian than its invariance with respect to P_{ij}, not much further can be learned from permutation symmetry. In many cases, however, a quantum-mechanical system may exhibit an invariance, albeit approximate, under the exchange of *part* of the coordinates of two particles i and j. For example, the nuclear interaction is to a good approximation charge independent. As a result, and if furthermore the effects of the Coulomb interaction are neglected, the nuclear hamiltonian can be assumed invariant under the exchange P^t_{ij} of only the isobaric coordinates of particles i and j (see the discussion of isospin in Sect. 1.1.6). Likewise, although this is a much more questionable hypothesis, one may impose invariance under the exchange P^s_{ij} of only the spin coordinates of particles i and j. The additional symmetries, associated with the invariance with respect to permutations that act on a partial set of the nucleons' coordinates, can be used to devise additional quantum numbers. The central idea is that while all eigenstates must be completely anti-symmetric or completely symmetric under P_{ij}, for fermions or bosons, respectively, this is not necessarily the case for permutations such as P^t_{ij} or P^s_{ij} and their symmetry character under such partial permutations can be exploited to yield additional labels.

The symmetry type under (total or partial) permutations is specified by n integers $\lambda_1 \geq \lambda_2 \geq \cdots \geq \lambda_n \geq 0$ which sum to A and where n is the

number of single-particle states (see Sect. 1.2.1). The symmetry pattern associated with this series of integers is denoted as $[\lambda_1, \lambda_2, \ldots, \lambda_n]$ and can be given a pictorial representation which is referred to as a Young pattern or diagram. It corresponds to rows of boxes with length λ_1, λ_2, etc. which are placed on top of each other, beginning with λ_1. For a permutational symmetry associated with a certain Young diagram basis states can be specified by placing each of the A particles in a box according to the following rule. To each particle we associate a label from 1 to A and we distribute them over the boxes such that for each row of boxes the particle index increases from left to right and that for each column of boxes it increases from top to bottom. The configurations obtained in this way are named Young tableaux and each of them corresponds to a different state with a given mixed symmetry, which has been obtained by anti-symmetrizing in the particles belonging to the same column after having symmetrized in the particles belonging to the same row (or vice versa).

For complete symmetry the Young diagram reduces to a single row of A boxes and there is only one Young tableau possible, namely the one with increasing particle index from left to right. Similarly for complete anti-symmetry when the Young diagram is a single column of A boxes (which must be smaller than n because of the Pauli principle) with a single associated Young tableau. This illustrates that in the case of overall (anti-)symmetry all states have an identical permutational character which cannot therefore be used to distinguish between them. Only when states have a mixed-symmetry character (i.e., neither completely symmetric nor anti-symmetric) under a partial permutational symmetry is it possible to use this feature to label wave functions.

A full and detailed description of the irreducible representations of the permutation group $\mathcal{S}_A$ is given by Hamermesh [1]. A particularly clear and succinct account of the use of Young diagrams in many-particle quantum physics is given by Lipas (Chap. 2 of Ref. [69]).

This argument can be generalized to an arbitrary number of nucleons and the result emerges that the SU(4) quantum numbers specify the way in which the overall anti-symmetry is distributed over the spatial and spin–isospin parts of the wave function. More formally, the orbital/spin–isospin decomposition is equivalent to the algebraic reduction

$$\begin{array}{ccccc} \mathrm{U}(4\Omega) & \supset & \mathrm{U}(\Omega) & \otimes & \mathrm{U}(4) \\ \downarrow & & \downarrow & & \downarrow \\ [1^n] & & [f_1, f_2, f_3, f_4] & & [\bar{f}_1, \bar{f}_2, \bar{f}_3, \bar{f}_4] \end{array} , \tag{2.18}$$

where Ω denotes the orbital shell size (i.e., $\Omega = 1, 3, 6, \ldots$ for the s, p, sd,... shells). The U(4) algebra consists of the SU(4) generators (2.17) supplemented with the particle number operator n. The overall anti-symmetry $[1^n]$ of the wave function requires conjugate symmetry under U(Ω) and

Table 2.2. Classification of one and two particle(s) in the *sd* shell

n	$[f_1, f_2, f_3, f_4]$	L	$[\bar{f}_1, \bar{f}_2, \bar{f}_3, \bar{f}_4]$	(λ, μ, ν)	(S, T)
1	[1]	0, 2	[1]	(1, 0, 0)	(1/2, 1/2)
2	[2, 0]	$0^2, 2^2, 4$	[1, 1]	(0, 1, 0)	(0, 1), (1, 0)
	[1, 1]	1, 2, 3	[2, 0]	(2, 0, 0)	(0, 0), (1, 1)

U(4), which defines the relation between $[f_1, f_2, f_3, f_4]$ and $[\bar{f}_1, \bar{f}_2, \bar{f}_3, \bar{f}_4]$: they have *conjugate* Young diagrams [1]. As an example, the symmetry classification of one and two particles in the *sd* shell is summarized in Table 2.2. The table also gives the more commonly used SU(4) labels which are related to those of U(4) through

$$\lambda = \bar{f}_1 - \bar{f}_2, \qquad \mu = \bar{f}_2 - \bar{f}_3, \qquad \nu = \bar{f}_3 - \bar{f}_4. \tag{2.19}$$

The physical relevance of Wigner's supermultiplet classification is connected with the short-range attractive nature of the residual interaction as a result of which states with spatial symmetry are favored energetically. To see this point, consider an extreme form of a short-range interaction, namely a delta interaction. It has a vanishing matrix element in a spatially antisymmetric two-nucleon state since in that case the wave function has zero probability of having $\boldsymbol{r}_1 = \boldsymbol{r}_2$. In contrast, the matrix element is attractive in the spatially symmetric case with [1, 1] U(4) symmetry. Again, this result can be generalized to many nucleons, leading to the conclusion that the energy of a state depends on its SU(4) labels.

Wigner's supermultiplet model is a nuclear LS-coupling scheme. With the advent of the nuclear shell model the importance of the spin–orbit coupling became clear and, as a result, the SU(4) model was largely abandoned. In spite of its limited applicability, Wigner's idea remains important because it demonstrates the connection between the short-range character of the residual interaction and the spatial symmetry of the many-body wave function. The break down of SU(4) symmetry is a consequence of the spin–orbit term in the nuclear mean field (2.1) which does not satisfy the second and third commutator in (2.16). The spin–orbit term breaks SU(4) symmetry [SU(4) representations are admixed by it] and does so increasingly in heavier nuclei since the energy splitting of the spin doublets $l - 1/2$ and $l + 1/2$ increases with nucleon number A. In addition, SU(4) symmetry is also broken by the Coulomb interaction—an effect that also increases with A—and by spin-dependent residual interactions.

Example: Wigner's mass anomaly in $N = Z$ nuclei. The break down of SU(4) symmetry with increasing nuclear mass number A can be illustrated with Gamow–Teller β decay [70] and with nuclear binding energies [71]. A simple way to represent the latter effect involves the double differences of nuclear

binding energies [72, 73],

$$\delta V_{\rm np}(N,Z) = \frac{1}{4}[B(N,Z) - B(N-2,Z) - B(N,Z-2) + B(N-2,Z-2)],$$

where $B(N,Z)$ is the binding energy of a nucleus with N neutrons and Z protons and where N and Z are assumed even. The quantity $\delta V_{\rm np}(N,Z)$ acts as a filter to isolate the interaction between neutrons and protons and was recently shown to be correlated with the growth of collectivity in nuclei [74]. Particularly large values of $\delta V_{\rm np}(N,Z)$ are found for $N = Z$ [75]. The erosion of this $N = Z$ enhancement with mass number A provides a proof of the breaking of SU(4) symmetry. An example is shown in Fig. 2.6 which shows on the left the measured double binding energy $\delta V_{\rm np}(N,Z)$ for even–even nuclei in the *sd* shell. The SU(4) result of Fig. 2.6b is obtained by assuming a nuclear binding energy of the form $a + b\langle C_2[{\rm SU}(4)]\rangle$ where a and b are coefficients depending smoothly on mass number and $\langle C_2[{\rm SU}(4)]\rangle$ is the eigenvalue of the quadratic Casimir of SU(4) in the favored SU(4) representation [76]. As long as the departure from SU(4) symmetry is not too important, its breaking can be investigated by assuming a nuclear ground state which does not correspond entirely to the favored SU(4) representation but contains an admixture of the next-favored SU(4) representation. These admixtures will modify the behavior of $\delta V_{\rm np}(N,Z)$ at $N \sim Z$. This is illustrated in Fig. 2.6c where $\delta V_{\rm np}(N,Z)$ is plotted by taking a varying mixture of first- and second-favored SU(4) representations. As the mass of the nucleus increases, one notes indeed a decrease of the $N = Z$ enhancement effect for $\delta V_{\rm np}(N,Z)$, roughly consistent with the experimental observations. An exceptional point occurs for $N = Z = 20$ where the calculation is unrealistic since ^{40}Ca is taken as doubly closed and hence corresponds to a unique SU(4) representation with no possible admixtures.

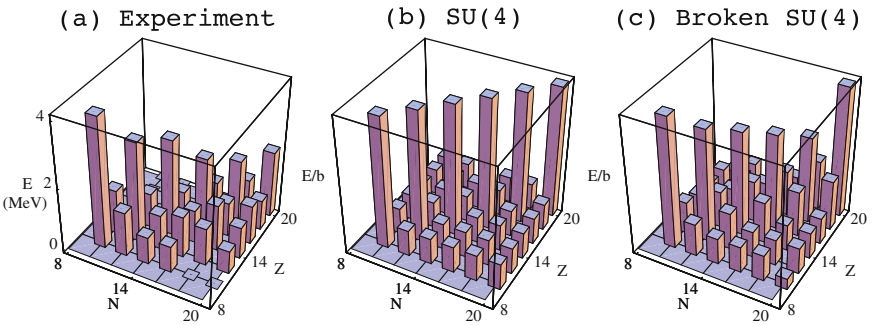

Fig. 2.6. Barchart representation of double binding energy differences (**a**) as observed in even–even *sd* shell nuclei [55], (**b**) as predicted by Wigner's unbroken SU(4) symmetry and (**c**) as obtained by taking a mixture of first- and second-favored SU(4) representations. The x and y coordinates of the center of a cuboid define N and Z and its height z defines $\delta V_{\rm np}(N,Z)$. An empty square indicates that the data are lacking

In Wigner's supermultiplet model the spatial part of the wave function is left unspecified. It is only assumed that the total orbital angular momentum L is a good quantum number. The main feature of Elliott's model [59] is that it provides an orbital classification which incorporates *rotational* characteristics. Elliott's model of rotation presupposes Wigner's SU(4) classification and assumes in addition that the residual interaction has a **quadrupole** character, a reasonable hypothesis if the valence shell contains neutrons and protons. With reference to the schematic hamiltonian (2.1), one requires that it reduces to

$$H = \sum_{k=1}^{A} \left(\frac{p_k^2}{2m_\mathrm{n}} + \frac{1}{2} m_\mathrm{n} \omega^2 r_k^2 \right) + V_\mathrm{quadrupole}, \tag{2.20}$$

where $V_\mathrm{quadrupole} = -g_2 Q \cdot Q$ contains a quadrupole operator

$$Q_\mu = \sqrt{\frac{3}{2}} \left[\sum_{k=1}^{A} \frac{1}{b^2} (\boldsymbol{r}_k \times \boldsymbol{r}_k)_\mu^{(2)} + \frac{b^2}{\hbar^2} \sum_{k=1}^{A} (\boldsymbol{p}_k \times \boldsymbol{p}_k)_\mu^{(2)} \right], \tag{2.21}$$

in terms of coordinates $\boldsymbol{r}_k$ and momenta $\boldsymbol{p}_k$, and where b is the oscillator length parameter, $b = \sqrt{\hbar/m_\mathrm{n}\omega}$. Note that $Q \cdot Q$ contains one-body ($k = l$) as well as two-body ($k \neq l$) terms.

To recognize that the shell-model hamiltonian (2.20) is analytically solvable, it is best to write it in second-quantized form. Because of its symmetric structure in $\boldsymbol{r}$ and $\boldsymbol{p}$, the quadrupole operator Q_μ does not couple to states outside a given valence shell and particle creation operators $a^\dagger_{lm_l sm_s tm_t}$ can be assigned l quantum numbers of that shell, together with spin and isospin labels. The quadrupole operator (2.21) can then be rewritten as (see Chap. 30 of Ref. [47])

$$Q_\mu = \sum_l \sqrt{8(2l+1)}\, (a^\dagger_{lst} \times \tilde{a}_{lst})^{(200)}_{\mu 00}, \tag{2.22}$$

where $\tilde{a}_{lm_l sm_s tm_t} = (-)^{l-m_l+s-m_s+t-m_t} a_{l-m_l s-m_s t-m_t}$. By construction, the quadrupole operator (2.21) is a scalar in spin and isospin, as it does not change either of them, and a tensor in orbital angular momentum. Likewise, the orbital angular momentum operator, $L_\mu = \sum_k (\boldsymbol{r}_k \wedge \boldsymbol{p}_k)_\mu/\hbar$, reads in second quantization

$$L_\mu = \sum_l \sqrt{4l(l+1)(2l+1)/3}\, (a^\dagger_{lst} \times \tilde{a}_{lst})^{(100)}_{\mu 00}. \tag{2.23}$$

In summary of the preceding discussion, the hamiltonian (2.20) can be rewritten as

$$H = \hbar\omega \left(\mathcal{N} + \frac{3}{2} \right) - g_2 Q \cdot Q, \tag{2.24}$$

where $\mathcal{N}$ is an operator that counts the number of oscillator quanta. For a given number of nucleons in the valence shell the first term in (2.24) reduces

to a constant; the second term, however, generates a spectrum as can be seen as follows. The hamiltonian (2.20) satisfies the commutation relations (2.16) and hence has SU(4) symmetry. Its additional symmetry character depends on the orbital space available to the valence nucleons. With reference to the classification (2.18), the operators L_μ and Q_μ are scalar in spin and isospin and hence are generators of U(Ω). Furthermore, from their explicit expressions (2.22) and (2.23) one derives the commutation relations

$$\begin{aligned}
[Q_\mu, Q_\nu] &= 3\sqrt{10}\,\langle 2\mu\; 2\nu|1\mu+\nu\rangle L_{\mu+\nu}, \\
[L_\mu, Q_\nu] &= -\sqrt{6}\,\langle 1\mu\; 2\nu|2\mu+\nu\rangle Q_{\mu+\nu}, \\
[L_\mu, L_\nu] &= -\sqrt{2}\,\langle 1\mu\; 1\nu|1\mu+\nu\rangle L_{\mu+\nu},
\end{aligned} \tag{2.25}$$

which show that they generate an **SU(3)** Lie algebra that must then be a subalgebra of U(Ω). With the commutation relations (2.25) it can also be shown that the quadratic combination $Q \cdot Q + 3L \cdot L$ commutes with all generators of SU(3). The quadrupole interaction is thus a combination of Casimir operators,

$$Q \cdot Q = 4C_2[\mathrm{SU}(3)] - 3L \cdot L = 4C_2[\mathrm{SU}(3)] - 3C_2[\mathrm{SO}(3)], \tag{2.26}$$

and it follows that the hamiltonian (2.20) has the eigenvalues

$$E(\lambda, \mu, L) = E_0 - g_2 \left[4(\lambda^2 + \mu^2 + \lambda\mu + 3\lambda + 3\mu) - 3L(L+1)\right], \tag{2.27}$$

where E_0 is a constant energy associated with the first term in the hamiltonian (2.24). The quadrupole interaction implies the orbital reduction

$$\begin{array}{ccccc}
\mathrm{U}(\Omega) & \supset & \mathrm{SU}(3) & \supset & \mathrm{SO}(3) \\
\downarrow & & \downarrow & & \downarrow \\
[f_1, f_2, f_3, f_4] & & (\lambda, \mu) & & K_L L
\end{array}, \tag{2.28}$$

and represents an example of dynamical symmetry breaking. The degeneracy within a given Wigner supermultiplet is lifted (dynamically) by the quadrupole interaction.

Example: The rotational spectrum of ^{20}Ne. A simple illustration of SU(3) dynamical symmetry is shown in Fig. 2.7. The nucleus ^{20}Ne contains two neutrons and two protons in the *sd* shell ($\Omega = 6$) above the ^{16}O closed-shell configuration. These four nucleons can acquire a spatially symmetric configuration, leading to $[f_1, f_2, f_3, f_4] = [4, 0, 0, 0] \equiv [4]$ in U(6). All states in this symmetric configuration correspond to a single supermultiplet with labels $[\bar{f}_1, \bar{f}_2, \bar{f}_3, \bar{f}_4] = [1, 1, 1, 1] \equiv [1^4]$ in U(4) and with $S = T = 0$. The degeneracy of this supermultiplet is lifted by the residual quadrupole interaction which gives rise to the SU(3) spectrum shown in Fig. 2.7. This interaction separates the different SU(3) multiplets (or representations) which can be $(\lambda, \mu) = (8, 0)$, (4,2), (0,4) or (2,0). The allowed values of the total orbital

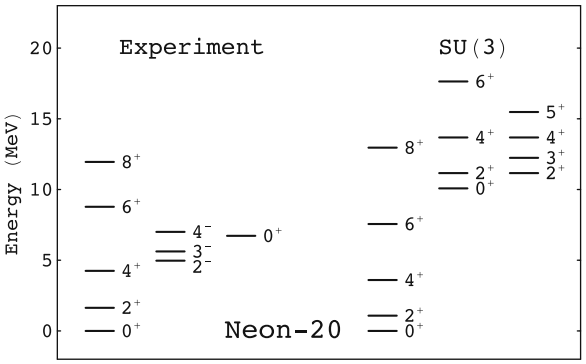

Fig. 2.7. Observed [44] low-energy spectrum of ^{20}Ne (*left*) compared with the lowest SU(3) rotational bands (*right*). Levels are labeled by their angular momentum and parity J^π. The SU(3) spectrum is generated with a quadrupole interaction $-g_2 Q \cdot Q$ with strength $g_2 = 0.06$ MeV

angular momentum L (and, since $S = 0$, of the total angular momentum J) follow from the SU(3) $\supset$ SO(3) reduction rule [59]. For the lowest SU(3) multiplet with $(\lambda, \mu) = (8, 0)$ they are $L = 0, 2, 4, 6, 8$. The observed angular momenta J of the states and their excitation energies as a function of J are approximately consistent with those of a rotational band with $K = 0$ projection of the total angular momentum on the axis of symmetry. The SU(3) model predicts this band to terminate at $J^\pi = 8^+$ which is consistent with the observations since the lowest $J^\pi = 10^+$ occurs at 27.5 MeV [44], well above the energy expected from a rotational behavior. The experimental spectrum of ^{20}Ne contains many more levels than those in the $K^\pi = 0^+$ band, the lowest of which are shown in Fig. 2.7. States of four nucleons in the *sd* shell have positive parity and, consequently, the observed negative-parity levels necessarily must involve a (particle–hole) excitation outside this shell. The first-excited 0^+ level possibly belongs to the next SU(3) multiplet with $(\lambda, \mu) = (4, 2)$, also shown in Fig. 2.7, containing the levels $L = 0, 2^2, 3, 4^2, 5, 6$. Alternatively, it may correspond to a two-particle–two-hole excitation outside the *sd* shell.

The importance of Elliott's idea is that it gives rise to a rotational classification of states through mixing of spherical configurations. With the SU(3) model it was shown, for the first time, how deformed nuclear shapes may arise out of the spherical shell model. As a consequence, Elliott's work bridged the gap between the nuclear shell model and the liquid drop model which up to that time (1958) existed as separate views of the nucleus.

At this point we can summarize the situation as follows. Elliott's SU(3) model provides a natural explanation of rotational phenomena, ubiquitous in nuclei, but it does so by assuming Wigner's SU(4) symmetry which is known to be badly broken in most nuclei. This puzzle has motivated much work since Elliott: How can rotational phenomena in nuclei be understood

starting from a jj-coupling scheme induced by the spin–orbit term in the nuclear mean field? Arguably the most successful way to do so and to extend the applications of the SU(3) model to heavy nuclei is based on the concept of **pseudo-spin** symmetry. The starting point for the explanation of this symmetry is the single-particle part of the hamiltonian (2.1),

$$H_{\rm sp} = \sum_{k=1}^{A} \left(\frac{p_k^2}{2m_{\rm n}} + \frac{1}{2} m_{\rm n} \omega^2 r_k^2 + \zeta_{ll} l_k^2 + \zeta_{ls} \boldsymbol{l}_k \cdot \boldsymbol{s}_k \right). \tag{2.29}$$

For $\zeta_{ll} = \zeta_{ls} = 0$ a three-dimensional isotropic harmonic oscillator is obtained which exhibits degeneracies associated with U(3) symmetry. For arbitrary non-zero values of ζ_{ll} and ζ_{ls} this symmetry is broken. However, for the particular combination $4\zeta_{ll} = \zeta_{ls}$ some degree of degeneracy, associated with a so-called pseudo-spin symmetry, is restored in the spectrum of $H_{\rm sp}$. To understand the nature of pseudo-spin symmetry, consider the unitary transformation

$$U = \sum_{k=1}^{A} u_k, \qquad u_k = 2i \frac{\boldsymbol{s}_k \cdot \boldsymbol{r}_k}{r_k}, \tag{2.30}$$

and apply this transformation to the hamiltonian (2.29). One finds

$$U^{-1} H_{\rm sp} U = \sum_{k=1}^{A} \left(\frac{p_k^2}{2m_{\rm n}} + \frac{1}{2} m_{\rm n} \omega^2 r_k^2 + \zeta_{ll} l_k^2 + (4\zeta_{ll} - \zeta_{ls}) \boldsymbol{l}_k \cdot \boldsymbol{s}_k \right) + C, \tag{2.31}$$

where $C = A(\hbar\omega + 2\zeta_{ll} - \zeta_{ls})$ is a constant. The original and transformed hamiltonians have the same eigenspectrum since they are related, up to the constant, by a unitary transformation. This shows that for $4\zeta_{ll} = \zeta_{ls}$ the spectrum of $H_{\rm sp}$ is identical (up to a constant) to that of a single-particle hamiltonian with only an orbit–orbit and no spin–orbit term. This results in single-particle orbits with $j = l + 1/2$ and $j = (l+2) - 1/2$ being degenerate for *all* values of l. These single-particle orbits can be considered as originating from a pseudo-orbital angular momentum $\tilde{l} = l + 1$, in the presence of zero pseudo-spin–orbit splitting $\tilde{l} \cdot \tilde{s}$.

Pseudo-spin symmetry has a long history in nuclear physics. The existence of nearly degenerate pseudo-spin doublets in the nuclear mean-field potential was pointed out 40 years ago by Hecht and Adler [77] and by Arima et al. [78] who noted that, because of the small pseudo-spin–orbit splitting, pseudo-LS (or $\tilde{L}\tilde{S}$) coupling should be a reasonable starting point in medium-mass and heavy nuclei where LS coupling becomes unacceptable. With $\tilde{L}\tilde{S}$ coupling as a premise, an **pseudo-SU(3)** model can be constructed [79] in much the same way as Elliott's SU(3) model can be defined in LS coupling. The formal definition of the pseudo-spin transformation (2.30) in terms of a helicity operator was given in Refs. et al. [80, 81]. Finally, it is only many years after its original suggestion that Ginocchio showed pseudo-spin to be a symmetry of

the Dirac equation which occurs if the scalar and vector potentials are equal in size but opposite in sign [82].

The models discussed so far all share the property of being confined to a single shell, either an oscillator or a pseudo-oscillator shell. A full description of nuclear collective motion requires correlations that involve configurations outside a single shell. The proper framework for such correlations invokes the concept of a non-compact algebra which, in contrast to a compact one, can have infinite-dimensional unitary representations. The latter condition is necessary since the excitations into higher shells can be infinite in number unless they are artificially restricted as is the case, for example, in the LMG model. The inclusion of excitations into higher shells of the harmonic oscillator was achieved by Rosensteel and Rowe by embedding the SU(3) algebra into the symplectic algebra Sp(3,R) [83].

2.1.3 A Symmetry Triangle for the Shell Model

The overview of symmetries of the nuclear shell model given in the preceding sections can be summarized as in Fig. 2.8. The top vertex corresponds to a mean-field hamiltonian with no residual interactions and with uncorrelated Hartree–Fock type eigenstates. This limit is reached if the single-particle energy spacings are large in comparison with a typical matrix element of the residual interaction. The two bottom vertices correspond to genuine many-body hamiltonians with correlated eigensolutions that involve a superposition of several, possibly many, Slater determinants. They differ through the residual interaction, which is either of pairing or of quadrupole nature. Both interactions allow an analytic solution of the many-body problem, which is rather fortunate since pairing and quadrupole are the dominant components of nucleonic interactions in nuclei. Pairing models have an underlying

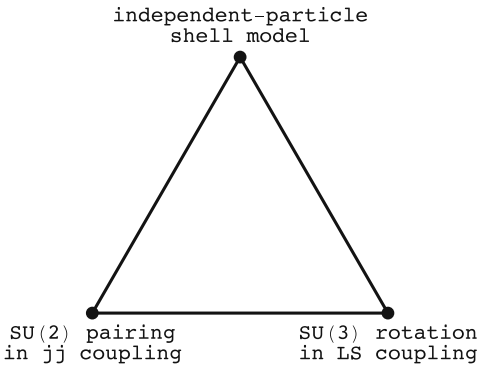

Fig. 2.8. Schematic representation of the shell-model parameter space with its two main classes of analytically solvable models of pairing and quadrupole type, respectively

quasi-spin SU(2) symmetry or its appropriate extension to include isospin and are usually (though not exclusively) applied in a jj-coupling regime. The underlying symmetry of quadrupole models is SU(3); this symmetry presupposes LS coupling and its extension into the jj-coupling regime is much more problematic. Figure 2.8, of course, in no way gives a realistic representation of the entire shell-model parameter space nor does it account for all analytic solutions of the nuclear shell model. A systematic procedure for constructing analytically solvable shell-model hamiltonians was devised by Ginocchio [84] and was later developed as the fermion dynamical symmetry model [85].

2.2 The Interacting Boson Model

We have seen in the previous section that seniority-type as well as rotational-like spectra find a natural explanation in the nuclear shell model. A third, vibrational type of spectrum is frequently exhibited by nuclei, and its shell-model explanation is more problematic. Evidence for a so-called tri-partite classification of nuclei [86] can be obtained, for example, from the energies of the first-excited 2^+ and 4^+ states in even–even nuclei (see Fig. 2.9). The inset shows $E_{\rm x}(4_1^+)$ as a function of $E_{\rm x}(2_1^+)$ for all even–even nuclei where both energies are known. There is a considerable scatter of points, especially at the high-energy range. This is not surprising since many nuclei with a high-lying 2_1^+ level have seniority characteristics and the ratio $E_{\rm x}(4_1^+)/E_{\rm x}(2_1^+)$ in such nuclei depends on the details of the residual interaction which can vary strongly from shell to shell. At low energies, however, $E_{\rm x}(2_1^+)$ is correlated

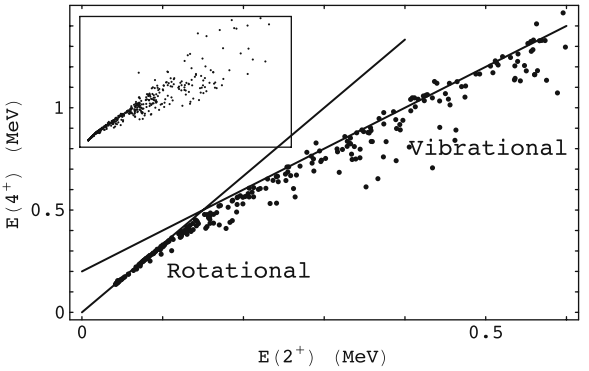

Fig. 2.9. Energies $E_{\rm x}(4_1^+)$ versus $E_{\rm x}(2_1^+)$. The inset shows the correlation for all even–even nuclei where both energies are known experimentally [44]. The full figure shows the correlation for all nuclei with $E_{\rm x}(2_1^+) < 0.6$ MeV. The two lines with slopes 3.33 and 2 indicate the rotational and vibrational regions of nuclei, respectively

with $E_{\rm x}(4_1^+)$ as is clear from Fig. 2.9, which shows a subset of nuclei with $E_{\rm x}(2_1^+) < 0.6$ MeV. The correlation is particularly strong for very low energies, $E_{\rm x}(2_1^+) < 0.1$ MeV, where all nuclei fall on a straight line with slope 10/3. This is the rotational regime of nuclei. In addition, there seems evidence for another nuclear behavior where the slope of the $E_{\rm x}(4_1^+)/E_{\rm x}(2_1^+)$ line is close to 2. This is the vibrational regime of nuclei.

Vibrational nuclei find an interpretation in terms of the geometric model of Bohr and Mottelson [57] where the vibrations are associated with (mainly quadrupole) oscillations of the nuclear surface. The disadvantage of such interpretation is that a transparent connection with the nuclear shell model is lacking. In this respect the interacting boson model (IBM) of Arima and Iachello [87] plays a crucial role: The model contains a vibrational and a rotational limit (as well as one which can be considered as intermediate)—which connects well with the phenomenology of nuclei—and it can be brought into relation with the shell model.

In this section we give a brief outline of the basic features of the simplest version of the IBM. There are two extensions of this elementary version which are of particular relevance: the inclusion of fermion degrees of freedom for a description of odd-mass nuclei and of the neutron–proton degree of freedom. These developments are presented separately in Chapts. 4 and 5, respectively.

In the original version of the IBM, applicable to even–even nuclei, the basic building blocks are s and d bosons [88]. Unitary transformations among the six states $s^\dagger|{\rm o}\rangle$ and $d_m^\dagger|{\rm o}\rangle, m = 0, \pm 1, \pm 2$, generate the Lie algebra $\mathbf{U(6)}$. The s and d bosons can be interpreted as correlated or **Cooper pairs** formed by two nucleons in the valence shell coupled to angular momenta $J = 0$ and $J = 2$. This interpretation constitutes the basis of the connection between the boson and the shell model [89]. Given the microscopic interpretation of the bosons, a low-lying collective state of an even–even nucleus with $2N$ valence nucleons is approximated as an N-boson state. Although the separate boson numbers n_s and n_d are not necessarily conserved, their sum $n_s + n_d = N$ is. This implies a total-boson-number conserving hamiltonian of the generic form

$$H = H_0 + H_1 + H_2 + H_3 + \cdots, \tag{2.32}$$

where the index refers to the order of the interaction in the generators of U(6). The first term is a constant which represents the nuclear binding energy of the core. The second term is the one-body part

$$H_1 = \epsilon_s n_s + \epsilon_d n_d, \tag{2.33}$$

where ϵ_s and ϵ_d are the single-boson energies of the s and d bosons. The third term in the hamiltonian (2.32) represents the two-body interaction

$$H_2 = \sum_{l_1 \le l_2, l_1' \le l_2', L} v^L_{l_1 l_2 l_1' l_2'} \left((b^\dagger_{l_1} \times b^\dagger_{l_2})^{(L)} \times (\tilde{b}_{l_2'} \times \tilde{b}_{l_1'})^{(L)} \right)^{(0)}_0 , \tag{2.34}$$

where the v coefficients are related to the interaction matrix elements between normalized two-boson states,

$$\langle l_1 l_2; LM_L|H_2|l_1' l_2'; LM_L\rangle = \sqrt{\frac{(1+\delta_{l_1 l_2})(1+\delta_{l_1' l_2'})}{2L+1}} v^L_{l_1 l_2 l_1' l_2'}. \tag{2.35}$$

Since the bosons are necessarily symmetrically coupled, the allowed two-boson states are s^2 ($L = 0$), sd ($L = 2$) and d^2 ($L = 0, 2, 4$). Since for n states with a given spin one has $n(n+1)/2$ interactions, seven independent two-body interactions v are found: three for $L = 0$, three for $L = 2$ and one for $L = 4$.

This analysis can be extended to higher-order interactions. Specifically, one may consider the three-body interactions $\langle l_1 l_2 l_3; LM_L|H_3|l_1' l_2' l_3'; LM_L\rangle$. The allowed three-boson states are s^3 ($L = 0$), $s^2 d$ ($L = 2$), sd^2 ($L = 0, 2, 4$) and d^3 ($L = 0, 2, 3, 4, 6$), leading to $6 + 6 + 1 + 3 + 1 = 17$ independent three-body interactions for $L = 0, 2, 3, 4, 6$, respectively. The number of possible interactions at each order n is summarized in Table 2.3 for up to $n = 3$. Some of these interactions exclusively contribute to the binding energy and do not influence the excitation spectrum of a single nucleus. To determine the number of such interactions, one notes that the hamiltonian NH_{n-1} for constant boson number (i.e., a single nucleus) essentially reduces to the $(n-1)$-body hamiltonian H_{n-1}. Consequently, of the $\mathcal{N}_n$ independent interactions of order n contained in H_n, $\mathcal{N}_{n-1}$ terms of the type NH_{n-1} must be discarded if one wishes to retain only those that influence the excitation energies. For example, given that there is one term of order zero (i.e., a constant), one of the two first-order terms (i.e., the combination N) does not influence the excitation spectrum. This means that the eigenspectrum of the hamiltonian remains unchanged if both ϵ_s and ϵ_d are modified by the same amount. Likewise, there are two first-order terms (i.e., n_s and n_d) and hence two of the seven two-body interactions do not influence the excitation spectrum. This argument leads to the numbers quoted in Table 2.3.

Table 2.3. Enumeration of n-body interactions in IBM for $n \leq 3$

Order	Number of interactions		
	total	constant[a]	variable[b]
$n = 0$	1	1	0
$n = 1$	2	1	1
$n = 2$	7	2	5
$n = 3$	17	7	10

[a] Interaction energy is constant for all states with the same N.
[b] Interaction energy varies from state to state.

2.2.1 Dynamical Symmetries

The characteristics of the most general IBM hamiltonian which includes up to two-body interactions and its group-theoretical properties are by now well understood [90]. Numerical procedures exist to obtain its eigensolutions but, as in the nuclear shell model, this many-body problem can be solved analytically for particular choices of boson energies and boson–boson interactions. For an IBM hamiltonian with up to two-body interactions between the bosons, three different analytical solutions or limits exist: the **vibrational U(5)** [91], the **rotational SU(3)** [92] and the **γ-unstable SO(6)** limit [93]. They are associated with the algebraic reductions

$$\mathrm{U}(6) \supset \left\{ \begin{array}{c} \mathrm{U}(5) \supset \mathrm{SO}(5) \\ \mathrm{SU}(3) \\ \mathrm{SO}(6) \supset \mathrm{SO}(5) \end{array} \right\} \supset \mathrm{SO}(3). \tag{2.36}$$

The algebras appearing in (2.36) are subalgebras of U(6) generated by operators of the type $b^\dagger_{lm} b_{l'm'}$, the explicit form of which is listed, for example, in Ref. [88]. With the subalgebras U(5), SU(3), SO(6), SO(5) and SO(3) there are associated one linear [of U(5)] and five quadratic Casimir operators. This matches the number of one- and two-body interactions quoted in the last column of Table 2.3. The total of all one- and two-body interactions can be represented by including in addition the operators $C_1[\mathrm{U}(6)]$, $C_2[\mathrm{U}(6)]$ and $C_1[\mathrm{U}(6)]C_1[\mathrm{U}(5)]$. The most general IBM hamiltonian with up to two-body interactions can thus be written in an *exactly* equivalent way with Casimir operators. Specifically, the hamiltonian reads

$$\begin{aligned} H_{1+2} = {} & \kappa_1 C_1[\mathrm{U}(5)] + \kappa_1' C_2[\mathrm{U}(5)] + \kappa_2 C_2[\mathrm{SU}(3)] \\ & + \kappa_3 C_2[\mathrm{SO}(6)] + \kappa_4 C_2[\mathrm{SO}(5)] + \kappa_5 C_2[\mathrm{SO}(3)], \end{aligned} \tag{2.37}$$

which is just an alternative way of writing $H_1 + H_2$ of (2.33) and (2.34) if interactions are omitted that contribute to the binding energy only.

The representation (2.37) is much more telling when it comes to the symmetry properties of the IBM hamiltonian. If some of the coefficients κ_i vanish such that H_{1+2} contains Casimir operators of subalgebras belonging to a *single* reduction in (2.36), then, according to the discussion of Chap. 1, the eigenvalue problem can be solved analytically. Three classes of spectrum generating hamiltonians can thus be constructed of the form

$$\begin{aligned} \mathrm{U}(5) &: H_{1+2} = \kappa_1 C_1[\mathrm{U}(5)] + \kappa_1' C_2[\mathrm{U}(5)] + \kappa_4 C_2[\mathrm{SO}(5)] + \kappa_5 C_2[\mathrm{SO}(3)], \\ \mathrm{SU}(3) &: H_{1+2} = \kappa_2 C_2[\mathrm{SU}(3)] + \kappa_5 C_2[\mathrm{SO}(3)], \\ \mathrm{SO}(6) &: H_{1+2} = \kappa_3 C_2[\mathrm{SO}(6)] + \kappa_4 C_2[\mathrm{SO}(5)] + \kappa_5 C_2[\mathrm{SO}(3)]. \end{aligned} \tag{2.38}$$

In each of these limits the hamiltonian is written as a sum of commuting operators and, as a consequence, the quantum numbers associated with the different Casimir operators are conserved. They can be summarized as follows:

$$\begin{array}{ccccccc} \mathrm{U}(6) & \supset & \mathrm{U}(5) & \supset & \mathrm{SO}(5) & \supset & \mathrm{SO}(3) \supset \mathrm{SO}(2) \\ \downarrow & & \downarrow & & \downarrow & & \downarrow \quad \downarrow \\ [N] & & n_d & & \tau & & \nu_\Delta L \quad M_L \end{array},$$

$$\begin{array}{ccccccc} \mathrm{U}(6) & \supset & \mathrm{SU}(3) & \supset & \mathrm{SO}(3) & \supset & \mathrm{SO}(2) \\ \downarrow & & \downarrow & & \downarrow & & \downarrow \\ [N] & & (\lambda,\mu) & & K_L L & & M_L \end{array},$$

$$\begin{array}{ccccccccc} \mathrm{U}(6) & \supset & \mathrm{SO}(6) & \supset & \mathrm{SO}(5) & \supset & \mathrm{SO}(3) & \supset & \mathrm{SO}(2) \\ \downarrow & & \downarrow & & \downarrow & & \downarrow & & \downarrow \\ [N] & & \sigma & & \tau & & \nu_\Delta L & & M_L \end{array}. \tag{2.39}$$

Furthermore, for each of the three hamiltonians in (2.38) an analytic eigenvalue expression is available,

$$\begin{aligned} \mathrm{U}(5) &: E(n_d, v, L) = \kappa_1 n_d + \kappa_1' n_d(n_d+4) + \kappa_4 \tau(\tau+3) + \kappa_5 L(L+1), \\ \mathrm{SU}(3) &: E(\lambda,\mu,L) = \kappa_2(\lambda^2+\mu^2+\lambda\mu+3\lambda+3\mu) + \kappa_5 L(L+1), \\ \mathrm{SO}(6) &: E(\sigma,\tau,L) = \kappa_3\sigma(\sigma+4) + \kappa_4\tau(\tau+3) + \kappa_5 L(L+1). \end{aligned} \tag{2.40}$$

One can add Casimir operators of U(6) to the hamiltonians in (2.37) without breaking any of the symmetries. For a given nucleus they reduce to a constant contribution. They can be omitted if one is only interested in the spectrum of a single nucleus but they should be introduced if one calculates binding energies. Note that none of the hamiltonians in (2.38) contains a Casimir operator of SO(2). This interaction breaks the SO(3) symmetry (lifts the M_L degeneracy) and would only be appropriate if the nucleus is placed in an external electric or magnetic field.

Example: Gamma-soft platinum isotopes. The suggestion in 1978 by Arima and Iachello that SO(6) is a third possible limit of the IBM [94] and the subsequent discovery by Cizewski et al. [95] that ^{196}Pt represents an excellent example of this limit has had a major impact on the use of the model. First, it gave a solid basis to the introduction of the s boson in the IBM which was needed to describe vibrational U(5) as well as rotational SU(3) nuclei and which gave rise to the new SO(6) limit. Second, as was soon demonstrated, only a small departure from the SO(6) limit gave a description of the complex transitional region in between γ-unstable and well-deformed prolate rotors [96]. As the third benchmark to which nuclei can be compared, the SO(6) limit was also at the origin of the Casten triangle which allows the classification of a large fraction of all observed nuclei [97].

The SO(6) limit of the IBM is special in several respects. Its generic features are best understood from the IBM hamiltonian (2.37). The SO(6) limit

is obtained if the parameters κ_1, κ_1' and κ_2 are zero. The conserved quantum numbers and the energy eigenvalues in that case are given in Eqs. (2.39) and (2.40), respectively. The lowest states have the maximum allowed value of σ, $\sigma = N$. States at higher energies have $\sigma = N-2, N-4, \ldots, 1$ or 0. For a given σ, τ takes the values $\tau = 0, 1, \ldots, \sigma$. Since the SO(5) quantum number τ turns out to play an important role in many aspects of the IBM, it deserves a more detailed discussion. Note that any hamiltonian (2.37) with $\kappa_2 = 0$ conserves the SO(5) quantum number [98, 99]. If in addition $\kappa_3 = 0$, one obtains the U(5) limit with the solution given in Eqs. (2.39) and (2.40). We have deliberately used the same quantum number τ (instead of the more common v) in (2.39) for labeling SO(5) representations in the U(5) and SO(6) limits to emphasize that this algebra is common to both limits. The SO(5) symmetry leads to a peculiar structure of the wave functions which will be a superposition of components with either an even or an odd number of d bosons. This is trivially the case in the U(5) limit where the number of d bosons, n_d, is a conserved quantum number. This property can also be proven analytically in the SO(6) limit [93]. In fact, it holds for all solutions of the hamiltonian (2.37) with $\kappa_2 = 0$. The expansion is in terms of an even (odd) number of d bosons when τ is even (odd).

Because the SO(5) properties are often similar in the SO(6) and U(5) limits, detailed information on the structure of the lowest $\sigma = N-2$ states is needed to establish the validity of the SO(6) classification in a nucleus. To this end, also electric quadrupole properties must be considered which in the IBM are described with the operator

$$T_\mu(\mathrm{E2}) = e_\mathrm{b} Q_\mu \equiv e_\mathrm{b}[(s^\dagger \times \tilde{d} + d^\dagger \times s)^{(2)}_\mu + \chi(d^\dagger \times \tilde{d})^{(2)}_\mu], \tag{2.41}$$

where e_b is a boson effective charge. The quadrupole operator contains a parameter χ, the value of which is normally chosen consistently in the E2 and hamiltonian operators (consistent Q-formalism of Warner and Casten [100]). In this formalism, a nucleus corresponds to the SO(6) limit if characterized by $\chi = 0$ in both operators. The most prominent consequences are (i) vanishing quadrupole moments, because for $\chi = 0$ the quadrupole operator changes the d-boson number by one which leads to a $|\Delta\tau| = 1$ selection rule and (ii) vanishing transitions between states with different σ because for $\chi = 0$ the quadrupole operator is a generator of SO(6). Property (ii) was clearly established for ^{196}Pt [101]. This nucleus has, however, a first-excited state with a non-vanishing quadrupole moment, $Q(2_1^+) = +0.62(8)$ eb [102]. This deviation can be related to the very rapid structural change occurring for the γ-soft Pt nuclei [103].

The dynamical symmetries of the IBM arise if combinations of certain coefficients κ_i in the hamiltonian (2.37) vanish. The converse, however, cannot be said: Even if all parameters κ_i are non-zero, in some cases the hamiltonian H_{1+2} still may exhibit a dynamical symmetry and be analytically solvable. This is a consequence of the existence of unitary transformations which preserve the eigenspectrum of the hamiltonian H_{1+2} (and hence its analyticity

properties) and which can be represented as transformations in the parameter space $\{\kappa_i\}$. A *systematic* procedure exists for finding such transformations or parameter symmetries [104] which can, in fact, be applied to any hamiltonian describing a system of interacting bosons and/or fermions.

The enumeration of all symmetries of a hamiltonian system [which includes symmetries obvious from reductions such as (2.36) but also hidden symmetries revealed through parameter transformations] is important for a proper understanding of its chaoticity character [105, 106]. Since they correspond to a sum of mutually commuting operators, hamiltonians with a dynamical symmetry are integrable and their spectrum is regular. The three classifications (2.39) and their parameter-transformed analogues do indeed correspond to integrable hamiltonians but they do not necessarily define *all* such hamiltonians. In fact, the U(5) and SO(6) vertices are connected by a *integrable* path in terms of the product algebra $\mathrm{SU}_s(1,1) \otimes \mathrm{SU}_d(1,1)$ [107]. Along this edge the IBM hamiltonian reduces to a pairing interaction between s and d bosons distributed over two non-degenerate levels and can be solved with Richardson's technique outlined in Sect. 2.1.1.

While a numerical solution of the shell-model eigenvalue problem in general rapidly becomes impossible with increasing particle number, the corresponding problem in the IBM with s and d bosons remains tractable at all times, requiring the diagonalization of matrices with dimension of the order of $\sim 10^2$. One of the main reasons for the success of the IBM is that it provides a workable, albeit approximate, scheme which allows a description of transitional nuclei with a few relevant parameters. Numerous papers have been published on such transitional calculations. We limit ourselves here to citing those that first treated the transitions between the three limits of the IBM: from U(5) to SU(3) [108], from SO(6) to SU(3) [109] and from U(5) to SO(6) [110]. Another attractive aspect of the IBM is that it can easily be extended to include new interactions or degrees of freedom of which also numerous examples can be found in the literature [111]. Notably, the inclusion of the hexadecapole degree of freedom can be achieved through the g boson leading to a U(15) algebraic structure which has been investigated extensively (for a review, see Ref. [112]). Likewise, negative-parity dipole and octupole states can be described by the inclusion of p and f bosons [92, 113].

2.2.2 Geometry

An important aspect of the IBM is its geometric interpretation. As was demonstrated by several groups simultaneously [114, 115, 116], geometry can be derived from an algebraic description by means of **coherent** (or intrinsic) states. The ones used for the IBM are of the form

$$|N;\alpha_\mu\rangle \propto \left(s^\dagger + \sum_\mu \alpha_\mu d^\dagger_\mu\right)^N |\mathrm{o}\rangle, \tag{2.42}$$

where $|\mathrm{o}\rangle$ is the boson vacuum and α_μ are five complex variables. These have the interpretation of (quadrupole) shape variables and their associated

conjugate momenta. If one limits oneself to static problems, the α_μ can be taken as real; they specify a shape and are analogous to the shape variables of the liquid drop model of the nucleus [62]. In the same way as in that model, the α_μ can be related to three Euler angles $\{\theta_1, \theta_2, \theta_3\}$ which define the orientation of an intrinsic frame of reference, and two intrinsic shape variables, β and γ, that parametrize quadrupole vibrations of the nuclear surface around an equilibrium shape. In terms of the latter variables, the coherent state (2.42) is rewritten as

$$|N;\beta\gamma\rangle \propto \left(s^\dagger + \beta\left[\cos\gamma d_0^\dagger + \sqrt{\frac{1}{2}}\sin\gamma(d_{-2}^\dagger + d_{+2}^\dagger)\right]\right)^N |\mathrm{o}\rangle. \tag{2.43}$$

The calculation of the expectation value of a quantum-mechanical operator in this state leads to a functional expression in N, β and γ. In this way, the most general IBM hamiltonian (even with higher-order interactions) can be converted in a potential surface in (β, γ), familiar from the geometric model (see Fig. 2.5). An analysis of this type shows that the three limits of the IBM have simple geometric counterparts that are frequently encountered in nuclei. They correspond to vibrations around a spherical shape [U(5)], around a spheroidal shape, either prolate or oblate, [SU(3)] and around a spheroidal shape which is flat against triaxial deformation [SO(6)]. In the SU(3) and SO(6) limits, vibrational excitations are combined with rotations. Hence, for each of the three limits of the IBM it is possible to construct its equivalent geometric model. First, the geometric equivalent of the U(5) limit is the anharmonic-vibrator model of Brink et al. [117]. Second, the SU(3) limit generates the spectrum of a deformed nucleus that exhibits quadrupole oscillations around an axially symmetric equilibrium shape which is a well-established description of the nucleus since the work of Bohr and Mottelson [57]. Third, the SO(6) limit yields a γ-unstable rotor known as the Wilets–Jean model [118]. Finally, the entire SU(1,1) limit [or U(5)–SO(6) transition] has a geometric counterpart with the γ-unstable model of Ref. [119].

A catastrophe analysis [120] of the potential surfaces in (β, γ) as a function of the hamiltonian parameters determines the stability properties of these shapes. This analysis was carried out for the general IBM hamiltonian with up to two-body interactions by López-Moreno and Castaños [121]. The results of this study were confirmed in Ref. [122] where a simplified IBM hamiltonian is considered of the form

$$H = \epsilon n_d + \kappa Q \cdot Q. \tag{2.44}$$

This hamiltonian provides a simple parametrization of the essential features of nuclear structural evolution in terms of a vibrational term n_d (the number of d bosons) and a quadrupole interaction $Q \cdot Q$ with

$$Q_\mu = (s^\dagger \times \tilde{d} + d^\dagger \times s)_\mu^{(2)} + \chi(d^\dagger \times \tilde{d})_\mu^{(2)}. \tag{2.45}$$

Besides an overall energy scale, the spectrum of the hamiltonian (2.44) is determined by two parameters: the ratio ϵ/κ and χ. The three limits of the IBM are obtained with an appropriate choice of parameters: U(5) if $\kappa = 0$, $\mathrm{SU}_{\pm}(3)$ if $\epsilon = 0$ and $\chi = \pm\sqrt{7}/2$ and SO(6) if $\epsilon = 0$ and $\chi = 0$. One may thus represent the parameter space of the simplified IBM hamiltonian (2.44) on a triangle with vertices that correspond to the three limits U(5), SU(3) and SO(6), and where arbitrary points correspond to specific values of ϵ/κ and χ. Since there are two possible choices for SU(3), $\chi = -\sqrt{7}/2$ and $\chi = +\sqrt{7}/2$, the triangle can be extended to cover both cases by allowing χ to take negative as well as positive values.

The geometric interpretation of any IBM hamiltonian on the triangle can now be found from its expectation value in the coherent state (2.43) which for the particular hamiltonian (2.44) gives

$$V(\beta,\gamma) = \frac{N\epsilon\beta^2}{1+\beta^2} + \kappa\left[\frac{N(5+(1+\chi^2)\beta^2)}{1+\beta^2} + \frac{N(N-1)}{(1+\beta^2)^2}\left(\frac{2}{7}\chi^2\beta^4 - 4\sqrt{\frac{2}{7}}\chi\beta^3\cos 3\gamma + 4\beta^2\right)\right]. \quad (2.46)$$

The catastrophe analysis of this surface is summarized with the phase diagram shown in Fig. 2.10. Analytically solvable limits are indicated by the

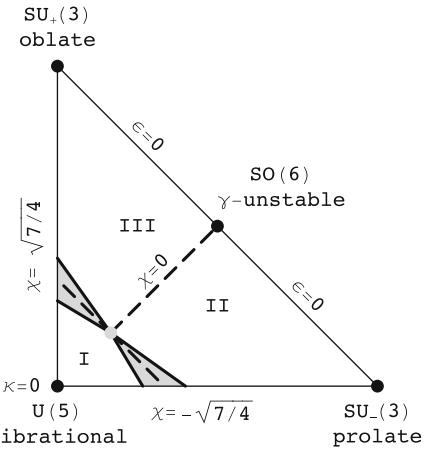

Fig. 2.10. Phase diagram of the hamiltonian (2.44) and the associated geometric interpretation. The parameter space is divided into three regions depending on whether the corresponding potential has (I) a spherical, (II) a prolate deformed or (III) an oblate deformed absolute minimum. These regions are separated by *dashed lines* and meet in a triple point (*gray dot*). The *shaded area* corresponds to a region of coexistence of a spherical and a deformed minimum. Also indicated are the points on the triangle (*black dots*) which correspond to the dynamical-symmetry limits of the hamiltonian (2.44) and the choice of parameters ϵ, κ and χ for specific points or lines of the diagram

dots. Two different SU(3) limits occur corresponding to two possible choices of the quadrupole operator, $\chi = \pm\sqrt{7}/2$. Close to the U(5) vertex, the IBM hamiltonian has a vibrational-like spectrum. Toward the SU(3) and SO(6) vertices, it acquires rotational-like characteristics. This is confirmed by a study of the character of the potential surface in β and γ associated with each point of the triangle. In the region around U(5), corresponding to large ϵ/κ ratios, the minimum of the potential is at $\beta = 0$. On the other hand, close to the $\mathrm{SU}_+(3)$–SO(6)–$\mathrm{SU}_-(3)$ axis the IBM hamiltonian corresponds to a potential with a deformed minimum between $\beta = 0$ and $\beta = \sqrt{2}$. Furthermore, in the region around prolate $\mathrm{SU}_-(3)$ ($\chi < 0$) the minimum occurs for $\gamma = 0^\mathrm{o}$, while around oblate $\mathrm{SU}_+(3)$ ($\chi > 0$) it does for $\gamma = 60^\mathrm{o}$. In this way the picture emerges that the IBM parameter space can be divided into three regions according to the character of the associated potential having (I) a spherical minimum, (II) a prolate deformed minimum or (III) an oblate deformed minimum. The boundaries between the different regions (the so-called Maxwell set) are indicated by the dashed lines in Fig. 2.10 and meet in a triple point. The spherical–deformed border region displays another interesting phenomenon. Since the *absolute* minimum of the potential must be either spherical, or prolate or oblate deformed, its character uniquely determines the three regions and the dividing Maxwell lines. Nevertheless, this does not exclude the possibility that, in passing from one region to another, the potential may display a second *local* minimum. This indeed happens for the U(5)–SU(3) transition [123] where there is a narrow region of coexistence of a spherical and a deformed minimum, indicated by the shaded area in Fig. 2.10. Since, at the borders of this region of coexistence, the potential undergoes a *qualitative* change of character, the boundaries are genuine critical lines of the potential surface [120].

Although these geometric results have been obtained with reference to the simplified hamiltonian (2.44) and its associated 'triangular' parameter space, it must be emphasized that they remain valid for the general IBM hamiltonian with up to two-body interactions [121].

Shape phase transitions and Landau theory. The hamiltonian (2.44) can be rewritten as

$$H = \alpha \left(\eta\, n_d + \frac{\eta - 1}{N} Q \cdot Q \right),$$

and contains two essential parameters: η, describing the transition between spherical and deformed shapes, and χ which occurs in the quadrupole operator (2.45) and describes the transition between prolate, γ-soft and oblate deformed shapes. The parameter α is an overall energy scaling factor. Because n_d is a one-body term while $Q \cdot Q$ is of two-body character, the latter term in the hamiltonian is scaled down by a factor N. This ensures that the contributions of both terms remain of the same order in the large-N limit. Furthermore, the hamiltonian is written such that the full range of structures

is described by values of η between 0 and 1. The equilibrium shape of the potential surface (2.46) is spherical for η values ranging down from unity, changes from spherical to deformed at some critical value $\eta = \eta_c$ and is deformed for $\eta < \eta_c$. The critical value η_c at which the absolute minimum turns from spherical to deformed depends on the parameter χ. This additional parameter, related to axial asymmetry, markedly increases the richness of the structures possible with the hamiltonian (2.44). For $\chi < 0$ ($\chi > 0$) and $\eta < \eta_c$ a prolate (oblate) axially symmetric minimum is found, while $\chi = 0$ corresponds to a completely γ-independent potential.

To understand the evolution of structure with (η, χ) [124, 125], it is useful to turn to the classical Landau theory of phase transitions [126]. The energy surface (2.46) can be written as an expansion in powers of β [124, 125, 127],

$$\Phi(\beta, \gamma) = \Phi_0 + A\beta^2 + B\beta^3 \cos 3\gamma + C\beta^4 + \mathcal{O}(\beta^5).$$

Equilibrium conditions occur when $\Phi(\beta, \gamma)$ has a minimum for some value(s) (β_0, γ_0). A minimum at $\beta_0 = 0$ corresponds to the highest (spherical) symmetry, while for $\beta_0 \neq 0$ a lower (deformed) symmetry is obtained. The coefficients A, B and C are parametric functions of some control variables. In Landau theory these are often pressure and temperature. In the nuclear case they depend, for example, on the number of nucleons, the orbits they occupy or the interactions between these nucleons. All such effects are assumed to be parametrized in terms of η and χ.

We now present a simplified analysis which largely ignores the parameter γ because its influence is trivial. Only terms up to β^4 are kept in $\Phi(\beta, \gamma)$. The equilibrium values of γ are either $\gamma_0 = 0^o$ for $B < 0$ or $\gamma_0 = 60^o$ for $B > 0$ and, as a result, the effect of γ can be absorbed in the sign of β. This analysis, though oversimplified, captures the essence of the physics.

To obtain a stable equilibrium state, the first derivative of $\Phi(\beta, \gamma)$ with respect to β must be zero and the second derivative must be positive, leading to the conditions

$$\beta(2A + 3B\beta \cos 3\gamma + 4C\beta^2) = 0, \qquad 2A + 6B\beta \cos 3\gamma + 12C\beta^2 > 0.$$

For the potential to be well behaved at $\beta \to \infty$ the coefficient C must be positive. Furthermore, there are two possible solutions. One is spherical, $\beta_0 = 0$; this is a minimum of $\Phi(\beta, \gamma)$ only if $A > 0$, which is required for the second derivative to be positive. The second solution occurs for $\beta_0 \neq 0$ and is obtained by solving the quadratic equation in β. For $B = 0$ the two solutions are

$$\beta_0 = \pm\sqrt{\frac{-A}{2C}}.$$

This requires A and C to be of opposite sign and hence $A < 0$ since $C > 0$. The nuclear phase diagram has thus three phases: spherical ($\beta_0 = 0$),

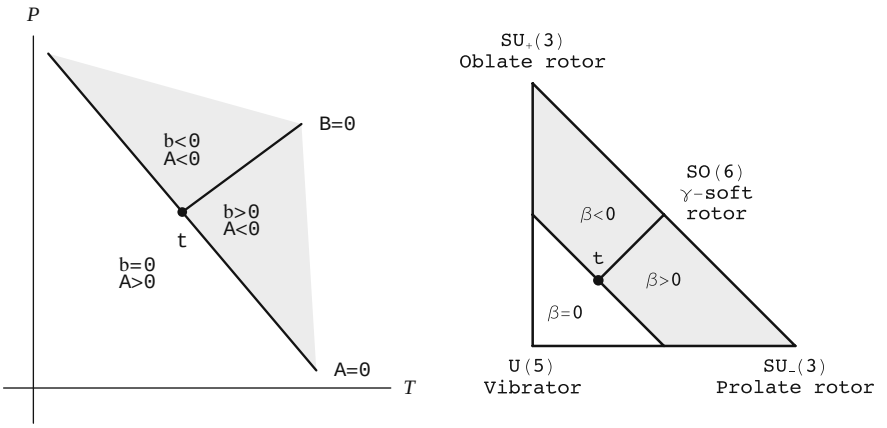

Fig. 2.11. Landau analysis of nuclear phase transitions. The *left-hand side* shows a simplified representation of the phases and first-order phase transition lines corresponding to $A = 0$ and $B = 0$. The axes are labeled by the pressure P and temperature T. The *right-hand side* shows the application of this analysis to the equilibrium phases of nuclei where (P, T) is replaced by the parameters (η, χ). The symbol t denotes a nuclear triple point where the two first-order phase transition lines meet. The *white area* denotes the region with the highest, spherical symmetry, while the *gray area* has lower, ellipsoidal symmetry

prolate ($\beta_0 > 0$) and oblate ($\beta_0 < 0$). The spherical–deformed phase transition occurs when A changes from positive to negative, that is, at $A = 0$. The prolate–oblate phase transition occurs when B changes from negative to positive, that is, at $B = 0$ (and in addition $A < 0$ and $C > 0$). As illustrated in Fig. 2.11 (left), if we interpret the (η, χ) diagram in analogy with the (P, T) phase diagram of Landau theory, the first-order phase transition conditions, $A = 0$ or $B = 0$, each corresponds to a curve in the phase diagram. These two first-order phase-transition trajectories meet in an isolated point defined by $A = B = 0$. This is a nuclear triple point that corresponds to a second-order phase transition. On the right-hand side of Fig. 2.11 these ideas are transposed in the context of the extended symmetry triangle of the IBM [127].

The hamiltonian (2.44) can also be analyzed in terms of Landau theory (see Box on Shape phase transitions and Landau theory) by which it is possible to identify the nature and order of the transitions between the different phases of the nucleus. It is also of interest to study how the eigensolutions of the hamiltonian (2.44) behave across these first-order phase transitions. To do so, we show in Fig. 2.12 the characteristic ratio of excitation energies $R_{4/2} \equiv E_{\rm x}(4_1^+)/E_{\rm x}(2_1^+)$ for the U(5)–SU(3) transition and the quadrupole moment $Q(2_1^+)$ for the SU$_-$(3)–SO(6)–SU$_+$(3) prolate–oblate transition. The ratio $R_{4/2}$ increases from 2.0 in U(5) to 3.33 in SU(3) and the phase transition

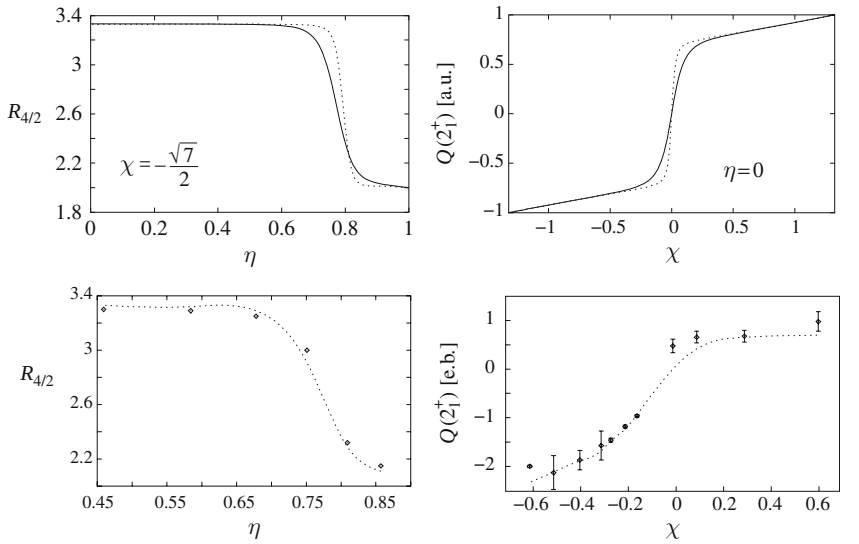

Fig. 2.12. Behavior of observables across the two first-order phase transitions discussed in the text, from spherical to deformed and from prolate to oblate. *Top*: Calculated values of $R_{4/2}$ as a function of $\eta \equiv \epsilon/(\epsilon - N\kappa)$ for $\chi = -\sqrt{7}/2$ for the spherical–deformed transition (*left*) and of $Q(2_1^+)$ as a function of χ for $\eta = 0$ for the prolate–oblate transition (*right*). In the latter case $\chi = 0$ corresponds to the phase transitional point (analogous to $B = 0$ in Landau theory) as well as to the SO(6) dynamical symmetry. The calculations are for $N = 10$ (*full line*) and $N = 20$ (*dashed line*). *Bottom*: Experimental values for $R_{4/2}$ in the Sm isotopes and for $Q(2_1^+)$ in the Hf–Hg region. The line gives the theoretical values obtained with the appropriate boson number N and the fitted η and χ values [103, 108], with a constant effective charge $e_\mathrm{b} = 0.15\ e\mathrm{b}$

occurs at the point of sharpest increase (maximum of $dR_{4/2}/d\eta$) where $\eta \equiv \epsilon/(\epsilon - N\kappa)$. This feature immediately discloses an important aspect of structural evolution of the hamiltonian (2.44), namely, the highly non-linear way in which structure changes from the U(5) vertex to the deformed SU$_-$(3)–SO(6)–SU$_+$(3) leg. It implies, for example, that well-deformed nuclei (with, say, $R_{4/2} \sim 3.31$) may actually be situated rather far from the SU(3) vertex. Along the SU$_-$(3)–SO(6)–SU$_+$(3) transition, $Q(2_1^+)$ changes from negative (prolate) to positive (oblate) at SO(6). The critical point of the phase transition coincides with SO(6) and marks the point where $Q(2_1^+)$ changes sign and $dQ(2_1^+)/d\chi$ peaks. For both transitions the comparison of results for the boson numbers $N = 10$ and $N = 20$ shows that there is an increase in sharpness with increasing N, as expected for a classical phase transition [125, 128, 129]. Figure 2.12 includes examples of empirical behavior for each of these transitions [the Sm isotopes for U(5)–SU(3) and the Hf–Hg isotopes for SU$_-$(3)–SO(6)–SU$_+$(3)]. The observed behavior nicely mimics the

calculations. (Detailed comparisons are shown in the original literature [103, 108].) While data for a prolate–oblate transition are scarce and do not reach fruition on the oblate side because of the impending double shell closure at ^{208}Pb, there is a moderate increase in $Q(2_1^+)$ in going from Pt to Hg. Clearly, a fascinating quest in exotic nuclei would be to search for a full prolate–oblate transitional region. With the altered single-particle level sequences thought possible in weakly bound, very neutron-rich nuclei there are grounds for speculating that the regions of deformation there might be more compact in N and Z and more prolate–oblate symmetric.

2.2.3 Partial Dynamical Symmetries

As argued in Chap. 1, a dynamical symmetry can be viewed as a generalization and refinement of the concept of symmetry. Its basic paradigm is to write a hamiltonian in terms of Casimir operators of a set of nested algebras. Its hallmarks are (i) solvability of the complete spectrum, (ii) existence of exact quantum numbers for all eigenstates and (iii) pre-determined structure of the eigenfunctions, independent of the parameters in the hamiltonian. A further enlargement of these ideas is obtained by means of the concept of **partial dynamical symmetry**. The essential idea is to relax the stringent conditions of *complete* solvability so that the properties (i–iii) are only partially satisfied.

Partiality comes in three different guises:

1. *Some of the eigenstates keep all of the quantum numbers.* In this case the properties of solvability, good quantum numbers and symmetry-dictated structure are fulfilled exactly, but only by a subset of eigenstates [130]. This is possible, for example, in the SU(3) limit of the IBM where a hamiltonian can be constructed which is not scalar in SU(3), of which a subset of eigenstates is solvable with conserved SU(3) symmetry, while all others are mixed [131].
2. *All eigenstates keep some of the quantum numbers.* In this case none of the eigenstates is solvable, yet some quantum numbers (of the conserved symmetries) are retained. This occurs, for example, if the hamiltonian contains interaction terms from two different chains with a common subalgebra, such as SO(5) which occurs in the U(5) and SO(6) classifications. As a consequence, the SO(5) label τ is conserved even if U(5) and SO(6) Casimir operators simultaneously occur in the hamiltonian [98]. In general, this type of partial dynamical symmetry arises if the hamiltonian preserves some of the quantum numbers in a dynamical-symmetry classification while breaking others. Such a scenario is possible, for example, in the SO(6) limit of the IBM by constructing a hamiltonian which preserves the U(6), SO(6) and SO(3) symmetries (and the associated quantum numbers N, σ and L) but not the SO(5) symmetry, leading to τ admixtures [132]. To obtain this type of partial dynamical symmetry, it might be necessary to include higher-order (three- or more-body) interactions in the hamiltonian.

3. *Some of the eigenstates keep some of the quantum numbers.* This is a combination of the previous cases and represents the weakest form of partial dynamical symmetry. For example, in the IBM it is possible to construct a hamiltonian which is not invariant under SO(6) but with a subset of solvable eigenstates with good SO(6) symmetry, while other states are mixed and no state conserves the SO(5) symmetry [133].

We emphasize that dynamical symmetry, be it partial or not, are notions that are not restricted to a specific model but can be applied to any quantal system consisting of interacting particles. Quantum hamiltonians with a partial dynamical symmetry can be constructed with general techniques and their existence is closely related to the order of the interaction among the particles. We first discuss the procedure in general terms and subsequently illustrate it with an application to the nucleus ^{196}Pt.

The analysis starts from the chain of nested algebras

$$\begin{array}{ccccc} \mathcal{G}_{\rm dyn} & \supset \cdots \supset & \mathcal{G} & \supset \cdots \supset & \mathcal{G}_{\rm sym} \\ \downarrow & & \downarrow & & \downarrow \\ [h] & & \Gamma & & \Lambda \end{array} . \tag{2.47}$$

As discussed in Chap. 1, $\mathcal{G}_{\rm dyn}$ is the dynamical algebra such that operators of all physical observables can be written in terms of its generators; each of its representations contains all states of relevance in the problem. In contrast, $\mathcal{G}_{\rm sym}$ is the symmetry algebra and a single of its representations contains states that are degenerate in energy. A frequently encountered example of a symmetry algebra is SO(3), the algebra of rotations in three dimensions, with its associated quantum number of total angular momentum J. Other examples of conserved quantum numbers can be the total spin S in atoms or total isospin T in atomic nuclei.

The classification (2.47) is generally valid and does not require conservation of particle number. Although the generalization to partial dynamical symmetry can be formulated under such general conditions, for simplicity of notation it is assumed in the following that particle number is conserved. All states, and hence the representation $[h]$, can then be assigned a definite particle number N. For N identical particles the representation $[h]$ of the dynamical algebra $\mathcal{G}_{\rm dyn}$ is either symmetric $[N]$ (bosons) or anti-symmetric $[1^N]$ (fermions) and shall be denoted as $[h_N]$. For particles that are non-identical under a given dynamical algebra $\mathcal{G}_{\rm dyn}$, a larger algebra can be chosen such that they become identical under this larger algebra. (For mixed systems of bosons and fermions the appropriate representation is a supersymmetric representation $[N\}$ of a superalgebra as will be introduced in Chap. 3.) The classification (2.47) implies that eigenstates can be labeled as $|[h_N]\Gamma \ldots \Lambda\rangle$; additional labels (indicated by $\ldots$) shall be suppressed in the following. Likewise, operators can be classified according to their tensor character under (2.47) as $T_{[h_n]\gamma\lambda}$. Of specific interest in the construction of a partial dynamical symmetry associated with the classification (2.47) are the n-particle annihilation operators T which satisfy the property

$$T_{[h_n]\gamma\lambda}|[h_N]\Gamma_0\Lambda\rangle = 0, \tag{2.48}$$

for all possible values of Λ contained in a given representation Γ_0. Any interaction that can be written in terms of these annihilation operators (and their hermitian conjugates) can be added to the hamiltonian with the dynamical symmetry (2.47) while still preserving the solvability of states with $\Gamma = \Gamma_0$. The annihilation condition (2.48) is satisfied if none of the $\mathcal{G}$ representations Γ contained in the $\mathcal{G}_{\rm dyn}$ representation $[h_{N-n}]$ belongs to the Kronecker product $\Gamma_0 \times \gamma$. So the problem of finding interactions that preserve solvability for part of the states (2.47) is reduced to carrying out a Kronecker product.

Partial dynamical symmetries have been applied in the context of the IBM, notably in its SU(3) limit [131]. We illustrate here the procedure outlined above with a different example where the classification (2.47) is that of the SO(6) limit of the IBM.

Example: Partial dynamical symmetries in the SO(6) limit. The classification in the SO(6) limit of the IBM is given in Eq. (2.39); the dynamical algebra $\mathcal{G}_{\rm dyn}$ is U(6), while $\mathcal{G}$ is SO(6) in this case. The eigenstates $|[N]\Sigma\tau LM_L\rangle$ are obtained with a hamiltonian which is a combination of Casimir operators of the algebras SO(6), SO(5) and SO(3), as in Eq. (2.38). Hamiltonians with an SO(6) partial dynamical symmetry preserve the analyticity of a *subset* of all eigenstates. The construction of interactions with this property requires boson creation and annihilation operators with definite tensor character in the SO(6) basis:

$$B^\dagger_{[n]\sigma vlm_l}, \qquad \tilde{B}_{[n]\sigma vlm_l} \equiv (-1)^{l-m} B_{[n]\sigma vl-m_l}.$$

Of particular interest are tensor operators with $\sigma < n$. They have the property

$$\tilde{B}_{[n]\sigma vlm_l}|[N]\Sigma = N\tau LM_L\rangle = 0, \qquad \sigma < n.$$

This is so because the action of $B_{[n]\sigma vlm_l}$ leads to an $(N-n)$-boson state that contains the SO(6) representations with $\Sigma = N - n - 2i, i = 0, 1, \ldots$, which cannot be coupled with σ to yield the SO(6) representation with $\Sigma = N$ since $\sigma < n$. Interactions that are constructed out of such tensors with $\sigma < n$ (and their hermitian conjugates) thus have $|[N]\Sigma = N\tau LM_L\rangle$ as eigenstates with eigenvalue 0.

A systematic enumeration of all interactions with this property is a simple matter of SO(6) coupling. For *one-body* operators one has

$$B^\dagger_{[1]1000} = s^\dagger \equiv b^\dagger_0, \qquad B^\dagger_{[1]112m_l} = d^\dagger_{m_l} \equiv b^\dagger_{2m_l},$$

and no annihilation operator has the property (2.48).

Coupled *two-body* operators are of the form

$$B^\dagger_{[2]\sigma vlm_l} \propto \sum_{v_k v_{k'}} \sum_{kk'} C^{\sigma vl}_{v_k k, v'_k k'} (b^\dagger_k \times b^\dagger_{k'})^{(l)}_{m_l},$$

Table 2.4. Normalized two- and three-boson SO(6) tensors $B^{\dagger}_{[n]\sigma v l m_l}$

n	σ	v	l	$B^{\dagger}_{[n]\sigma v l m_l}$
2	2	2	4	$\sqrt{\frac{1}{2}}\,(d^{\dagger}\times d^{\dagger})^{(4)}_{m_l}$
2	2	2	2	$\sqrt{\frac{1}{2}}\,(d^{\dagger}\times d^{\dagger})^{(2)}_{m_l}$
2	2	1	2	$(s^{\dagger}\times d^{\dagger})^{(2)}_{m_l}$
2	2	0	0	$\sqrt{\frac{5}{12}}\,(s^{\dagger}\times s^{\dagger})^{(0)}_{0}+\sqrt{\frac{1}{12}}\,(d^{\dagger}\times d^{\dagger})^{(0)}_{0}$
2	0	0	0	$-\sqrt{\frac{1}{12}}\,(s^{\dagger}\times s^{\dagger})^{(0)}_{0}+\sqrt{\frac{5}{12}}\,(d^{\dagger}\times d^{\dagger})^{(0)}_{0}$
3	3	3	6	$\sqrt{\frac{1}{6}}\,((d^{\dagger}\times d^{\dagger})^{(4)}\times d^{\dagger})^{(6)}_{m_l}$
3	3	3	4	$\sqrt{\frac{7}{22}}\,((d^{\dagger}\times d^{\dagger})^{(2)}\times d^{\dagger})^{(4)}_{m_l}$
3	3	3	3	$\sqrt{\frac{7}{30}}\,((d^{\dagger}\times d^{\dagger})^{(2)}\times d^{\dagger})^{(3)}_{m_l}$
3	3	3	0	$\sqrt{\frac{1}{6}}\,((d^{\dagger}\times d^{\dagger})^{(2)}\times d^{\dagger})^{(0)}_{0}$
3	3	2	4	$\sqrt{\frac{1}{2}}\,((s^{\dagger}\times d^{\dagger})^{(2)}\times d^{\dagger})^{(4)}_{m_l}$
3	3	2	2	$\sqrt{\frac{1}{2}}\,((s^{\dagger}\times d^{\dagger})^{(2)}\times d^{\dagger})^{(2)}_{m_l}$
3	3	1	2	$\sqrt{\frac{7}{16}}\,((s^{\dagger}\times s^{\dagger})^{(0)}\times d^{\dagger})^{(2)}_{m_l}+\sqrt{\frac{5}{112}}\,((d^{\dagger}\times d^{\dagger})^{(0)}\times d^{\dagger})^{(2)}_{m_l}$
3	3	0	0	$\sqrt{\frac{5}{48}}\,((s^{\dagger}\times s^{\dagger})^{(0)}\times s^{\dagger})^{(0)}_{0}+\sqrt{\frac{3}{16}}\,((s^{\dagger}\times d^{\dagger})^{(2)}\times d^{\dagger})^{(0)}_{0}$
3	1	1	2	$-\sqrt{\frac{1}{16}}\,((s^{\dagger}\times s^{\dagger})^{(0)}\times d^{\dagger})^{(2)}_{m_l}+\sqrt{\frac{5}{16}}\,((d^{\dagger}\times d^{\dagger})^{(0)}\times d^{\dagger})^{(2)}_{m_l}$
3	1	0	0	$-\sqrt{\frac{1}{16}}\,((s^{\dagger}\times s^{\dagger})^{(0)}\times s^{\dagger})^{(0)}_{0}+\sqrt{\frac{5}{16}}\,((s^{\dagger}\times d^{\dagger})^{(2)}\times d^{\dagger})^{(0)}_{0}$

where $C^{\sigma v l}_{v_k k, v'_{k'} k'}$ is a U(6) $\supset$ SO(6) $\supset$ SO(5) $\supset$ SO(3) isoscalar factor (see Box on Isoscalar factors and the Wigner–Eckart theorem), which is known in the specific cases needed in the sum. This leads to the normalized two-boson SO(6) tensors shown in Table 2.4. There is one operator with $\sigma < n = 2$ and it gives rise to the interaction

$$B^{\dagger}_{[2]0000}\tilde{B}_{[2]0000}=\frac{1}{3}P_{+}P_{-}=\frac{1}{12}\left\{N(N+4)-C_2[\mathrm{SO}(6)]\right\},$$

where $P_{+}\equiv(s^{\dagger}s^{\dagger}-d^{\dagger}\cdot d^{\dagger})/2$ is the boson-pairing operator. This proves that a two-body interaction which is diagonal in $|[N]\Sigma=N\tau LM_L\rangle$ is diagonal in all states $|[N]\Sigma\tau LM_L\rangle$. This result is valid in the SO(6) limit but not in general. For example, from a tensor decomposition of two-boson operators in SU(3) one concludes that the SU(3) limit of the IBM *does* allow a partial dynamical symmetry with two-body interactions.

Three-body operators with good SO(6) labels can be obtained from a similar expansion and this leads to the normalized three-boson SO(6) tensors shown in Table 2.4. In terms of the boson pair operator introduced above, the two operators with $\sigma < n = 3$ are

$$B^\dagger_{[3]1000} = \frac{1}{2} P_+ s^\dagger, \qquad B^\dagger_{[3]112m_l} = \frac{1}{2} P_+ d^\dagger_{m_l},$$

and from these one can construct the interactions with an SO(6) partial dynamical symmetry. The only three-body interactions that are partially solvable in SO(6) are thus $P_+ n_s P_-$ and $P_+ n_d P_-$. Since the combination $P_+(n_s + n_d)P_-$ is completely solvable in SO(6), there is only one genuine partially solvable three-body interaction which can be chosen as $P_+ n_s P_-$.

The generalization to higher orders now suggests itself. For example, *four-body* interactions with SO(6) partial dynamical symmetry are written in terms of $B^\dagger_{[4]2vlm_l}$ and $B^\dagger_{[4]0000}$, and hermitian conjugate operators. Without loss of generality, these operators can be written as

$$B^\dagger_{[4]2vlm_l} \propto P_+ B^\dagger_{[2]2vlm_l}, \quad B^\dagger_{[4]0000} \propto P^2_+.$$

A four-body interaction with SO(6) partial dynamical symmetry is thus of the form $P_+ V_2 P_-$ where V_2 is an arbitrary two-body interaction. This interaction leaves solvable all states with $\Sigma = N$ but in general admixes those with $\Sigma < N$. The conclusion is that we can construct a hierarchy of interactions of the form $P^k_+ n_s P^k_-$ and $P^k_+ V_2 P^k_-$, of order $2k+1$ and $2k+2$, respectively, that leave all states with $\Sigma > N - 2k$ solvable.

The advantage of the use of higher-order interactions with a partial dynamical symmetry is that they can be introduced without destroying results previously obtained with a dynamical symmetry. This is illustrated in Fig. 2.13, the middle panel of which shows the experimental energy spectrum of ^{196}Pt [134]. One of the problems in the comparison with the SO(6) limit of the IBM (left-hand panel) is that the lowest 0^+–2^+–2^+ levels belonging to

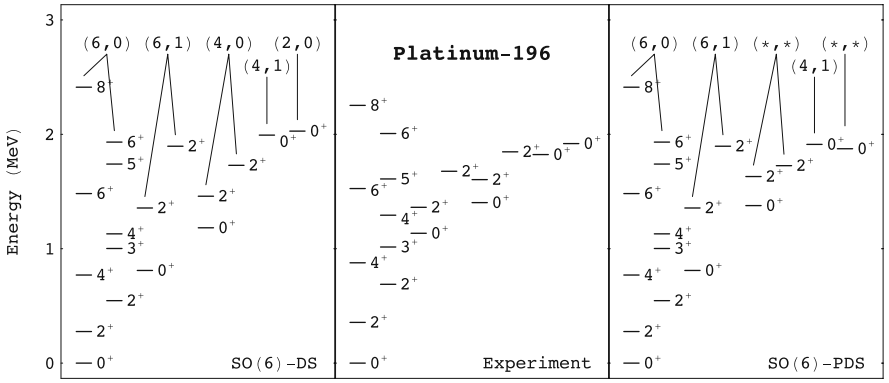

Fig. 2.13. Observed spectrum of ^{196}Pt compared with the theoretical spectra with SO(6) dynamical symmetry (DS) and partial dynamical symmetry (PDS). Levels are labeled by their angular momentum and parity J^π and by (Σ, ν_Δ) where Σ pertains to SO(6) and ν_Δ is the label missing between SO(5) and SO(3). The notation $(*,*)$ indicates that these labels are mixed

Table 2.5. Parameters (in keV) for the nucleus ^{196}Pt

	κ_3	κ_4	κ_5	κ_3'
dynamical symmetry	−42.25	45.0	25.0	—
partial dynamical symmetry	−29.50	45.0	25.0	34.9

the $\Sigma = N-2$ multiplet are not at the correct excitation energy. Three-body d-boson interactions have been proposed in the past that remedy this problem [135] but this is a delicate matter since the interaction used also changes the low-lying states of the $\Sigma = N$ multiplet. On the basis of the preceding discussion one may propose to use instead the hamiltonian [136]

$$H = \kappa_3 C_2[\mathrm{SO}(6)] + \kappa_4 C_2[\mathrm{SO}(5)] + \kappa_5 C_2[\mathrm{SO}(3)] + \kappa_3' P_+ n_s P_-.$$

The spectrum of this hamiltonian is shown in the right-hand panel of Fig. 2.13 and its parameters without and with the higher-order interaction are given in Table 2.5. The states belonging to the $\Sigma = N = 6$ multiplet remain solvable and do not change from the dynamical-symmetry calculation. States with $\Sigma \neq 6$ are generally admixed (not-solvable) but agree better with the data than in the exact SO(6) limit. Note that also a partial dynamical symmetry of type 2 in the classification discussed above occurs since τ is a conserved quantum number for *all* states of the eigenspectrum. As a consequence, some of the states with $\Sigma \neq 6$ remain completely solvable. For example, the 0^+ level with $(\Sigma, \nu_\Delta) = (4, 1)$ is solvable because its value $\tau = 4$ is unique among the levels with $\Sigma \neq 6$. As far as electric quadrupole probabilities are concerned, these are reasonably well described both in DS and in PDS [136] but, unfortunately, most of the data concern transitions between $\Sigma = 6$ levels and hence do not distinguish between the two. The crucial selection rule forbidding E2 transitions (for $\chi = 0$) between $\Sigma = 6$ and the other states is, however, conserved.

2.2.4 Core Excitations

The microscopic interpretation of the bosons of the IBM is one of correlated pairs of nucleons in the valence shell of the nucleus. Consequently, the elementary version of the model provides a description only of (collective) excitations of particles in the valence shell and assumes a totally inert core. In many nuclei this assumption is not justified and core excitations occur at low energies comparable to those of valence excitations. This situation arises in particular in nuclei where one type of nucleon has a closed or almost closed-shell configuration, while the other type is at mid-shell [137].

Consider as an example ^{116}Sn. This nucleus is magic in the protons ($Z = 50$) and is exactly in between the neutron closed-shell configurations $N = 50$ and $N = 82$. With ^{100}Sn as inert core, valence excitations correspond to rearrangements of the neutrons in the 50–82 shell. It is, however,

well established [138] that this nucleus exhibits a two-particle–two-hole (2p–2h) $J^\pi = 0^+$ excitation of the *protons* at $E_x = 1.757$ MeV (the second-excited state above the $J^\pi = 2^+$ level at 1.294 MeV), which corresponds to a core-excited or **intruder** configuration. The characteristic feature of this nucleus—rather typical for nuclei in which one type of nucleon has a closed or almost closed-shell configuration—is that the core-excited states occur at energies comparable to those of the usual valence excitations.

A complete description of the low-energy states of such nuclei should thus include both particle excitations in the valence shells and hole excitations in the core shells. In even–even nuclei these predominantly occur as pair excitations and, as a result, the situation can be described neatly in the IBM through the introduction of two types of bosons [139]: particle bosons (particle pairs in the valence shells) and hole bosons (hole pairs in the core shells), which may or may not be treated differently, depending on the degree of sophistication of the approach. If a distinction is made, one is confronted with a system of interacting bosons of two different types and one may consider them as one type of boson in two different intrinsic states. In analogy with the isospin formalism of Sect. 1.1.6, one assigns an I**-spin** quantum number to the bosons, $I = 1/2$, with $I_z = -1/2$ for a particle boson and $I_z = +1/2$ for a hole boson [140]. We close this section by showing an example of an I-spin multiplet with $I = 3/2$ (Fig. 2.14). It is seen that a (dynamical) I-spin

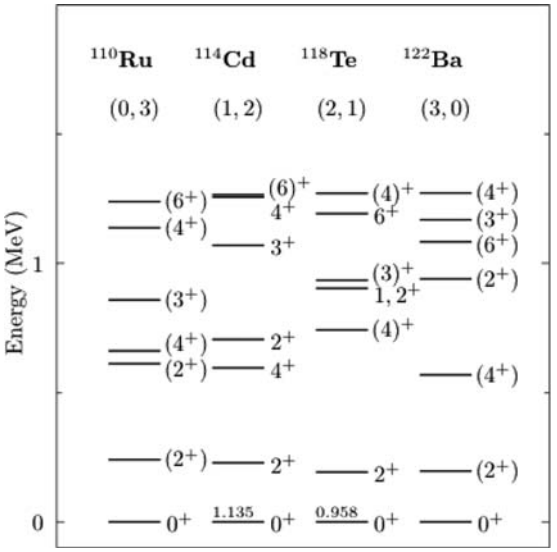

Fig. 2.14. Observed [44] spectra of nuclei belonging to an I-spin multiplet with $N_\nu^{\rm p} + N_\pi^{\rm h} = 3$, where $N_\nu^{\rm p}$ ($N_\nu^{\rm h}$) is the number of proton particle (hole) bosons. Levels are labeled by their angular momentum and parity J^π. Underneath each isotope are given the boson numbers $(N_{\rm p}^\pi, N_{\rm h}^\pi)$. The levels are drawn relative to the lowest $I = 3/2$ state; in the $I_z = \pm 1/2$ nuclei ^{114}Cd and ^{118}Te these are excited states with an energy as indicated on top of the level

symmetry (which gives rise to identical excitation spectra) is only approximately valid. Deviations arise due to the difference in microscopic structure between the particle and the hole pairs that correspond to the bosons.

2.3 A Case Study: ^{112}Cd

The $Z = 50$ mass region is very favorable for nuclear structure studies due to the large abundance of stable isotopes combined with the interesting features of the nearby $Z = 50$ proton shell closure and with the occurrence of neutrons in the middle of the $N = 50$–82 shell. This theoretical interest coupled with the possibility of detailed experimental studies makes the cadmium ($Z = 48$), tin ($Z = 50$) and tellurium ($Z = 52$) isotopes ideal for testing the influence of symmetries in their structure. This is illustrated here with the example of ^{112}Cd, one of the best known nuclei.

2.3.1 Early Evidence for Vibrational Structures and Intruder Configurations

The earliest work started with the observation by Schraff-Goldhaber and Wesener [141] that the Cd isotopes exhibit low-lying states that resemble the quadrupole-vibrational excitations of a surface with spherical equilibrium as predicted by the collective model of Bohr and Mottelson [57]. Besides the one-phonon quadrupole state, candidates for two-phonon quadrupole states were observed around 1.2 MeV, twice the energy of the first-excited 2^+ state. The two-phonon states were found non-degenerate, indicating the need to include anharmonic effects in the phonon–phonon interactions. Furthermore, additional 0^+ and 2^+ states were observed in transfer studies [142]. Attempts by Bes and Dussel to explain these as strongly anharmonic three-phonon states failed [143]. The explanation of the additional states was then related to two-particle–two-hole (2p–2h) excitations of the protons across the $Z = 50$ closed shell. Evidence that the extra 0^+ and 2^+ states were indeed 2p–4h states was obtained from (^{3}He,n) two-proton-transfer experiments [144]. By the early 1990s intruder bands were identified in most even–even Cd isotopes [145]. Strong support for the intruder interpretation came from the systematic behavior of these states as a function of the number of valence neutrons. Due to the increase in neutron–proton quadrupole interaction, intruder states decrease in energy proportional to the number of neutrons, reaching a lowest value near mid-shell [146]. In the Cd isotopes this mechanism gives rise to intruder and two-phonon states close in energy, resulting in complex spectra but also in interesting symmetry effects.

2.3.2 The ^{110}Pd(α,2nγ)^{112}Cd Reaction and its Interpretation

At the end of the 1980s an important reorientation of nuclear structure research occurred. Major investments were turned to the study of the structure of the nucleus at high rotational frequencies, following the

discovery of superdeformation by Twin and collaborators [147]. Somewhat later the first radioactive-ion beam experiments were performed at Louvain-la-Neuve [148] opening the access to a largely unexploited degree of freedom, the neutron-to-proton ratio. Both fields attracted most of the resources and changed the *modus operandi* of the nuclear structure community considerably. Many stable-beam facilities were closed, and the classical approach of complete spectroscopy remained possible at a limited number of research centers only. Theoretical nuclear physicists turned to these new fields or applied nuclear physics techniques to other domains of physics, such as molecular and condensed-matter physics. Those who remained active in low-energy nuclear structure profited from the improvements in instrumentation and especially from the ever increasing computer power for the analysis of ever more complex data sets.

It was in this context that an extensive study of ^{112}Cd was performed at the PSI Philips Cyclotron by Délèze et al. using the ^{110}Pd(α,2nγ)^{112}Cd reaction and an array of Compton suppressed Ge detectors [149, 150]. Light-ion-induced fusion–evaporation reactions provided a very complete population of low-to-medium spin states [151] and the use of anti-Compton shields improved the quality of the data significantly. From the excitation functions to assign the spins and from the angular distributions to determine mixing ratios, a comprehensive level scheme up to spins of $14\hbar$ could be obtained. The data can be interpreted with the interacting boson model with intruder states in its simplest form [150], in contrast to the standard intruder description which is based on the interacting boson model with neutron and proton bosons (see Sect. 4.3). The analysis relies very strongly on symmetry concepts. The known normal states in ^{112}Cd are fitted with the U(5) energy expression in Eq. (2.40) with $\kappa_1' = 0$. The three-parameter fit yields an excellent description of the energies of the vibrational states and can be extended to higher-lying high-spin states up to the six-phonon level (see left-hand side of Fig. 2.15). Because in this approach many states are not described, in a second step all fitted normal states are removed from the spectrum. The remaining states starting with the 0^+ level at 1,224.4 keV form a second collective structure which can be fitted with the SO(6) energy expression in Eq. (2.40) with the assumption that κ_3 is large and negative as no $\sigma = N-2$ states could be identified. This is shown on the right-hand side of Fig. 2.15.

In a third step a configuration-mixing procedure is applied. To lowest order this can be done with a mixing hamiltonian of the form

$$H_{\rm mix} = \alpha(s^\dagger \times s^\dagger + s \times s)^{(0)} + \beta(d^\dagger \times d^\dagger + \tilde{d} \times \tilde{d})^{(0)}. \qquad (2.49)$$

This form fulfils the necessary conditions of scalar invariance and hermiticity. Before mixing an energy shift Δ is applied to the intruder states. With $\Delta = 1,230$ keV, $\alpha = 30$ keV and $\beta = 20$ keV the energies of the one- and two-phonon as well as the two lowest intruder states are well described. In addition, Table 2.6 shows that the model can account for the observed electric quadrupole properties (except for the $0_3^+ \rightarrow 2_1^+$ transition) which are

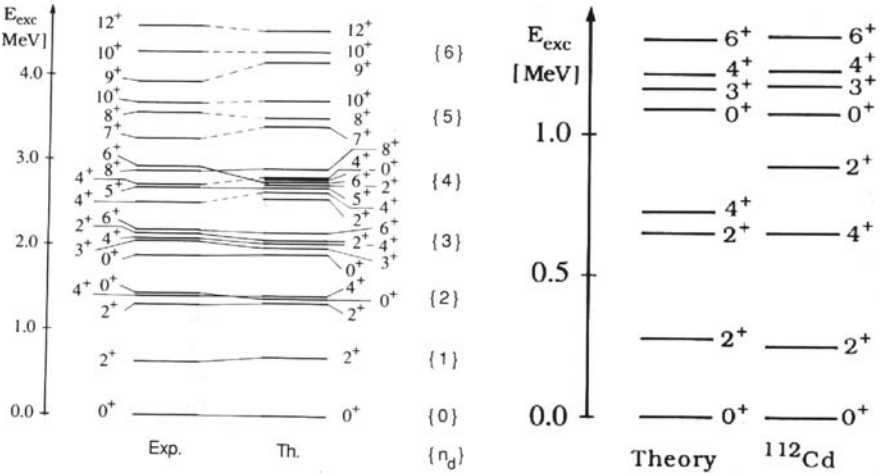

Fig. 2.15. Classification of the positive-parity states in ^{112}Cd in the U(5)–O(6) approach described in the text. The *left-hand side* shows the normal states calculated in the U(5) limit with parameters $\kappa_1 = 697$, $\kappa_4 = -9.8$ and $\kappa_5 = 5.51$ (in keV). The *right-hand side* shows the intruder states calculated in the SO(6) limit with parameters $\kappa_4 = -60.6$, $\kappa_5 = 6.0$ (in keV) and κ_3 large and negative (based on ref [149])

Table 2.6. Observed E2 transition rates involving normal and intruder states in ^{112}Cd compared with the predictions of a U(5)–SO(6) mixing calculation

	$B(\mathrm{E2}; J_\mathrm{i} \to J_\mathrm{f})^a$	Experiment	U(5)–SO(6)
normal → normal	$B(\mathrm{E2}; 2_1^+ \to 0_1^+)$	98(2)	99
	$B(\mathrm{E2}; 2_2^+ \to 0_1^+)$	2.8(3)	0.001
	$B(\mathrm{E2}; 2_2^+ \to 2_1^+)$	180(80)	177
	$B(\mathrm{E2}; 4_1^+ \to 2_1^+)$	197(25)	177
	$B(\mathrm{E2}; 0_3^+ \to 2_1^+)$	0.039(3)	98
	$B(\mathrm{E2}; 0_3^+ \to 2_2^+)$	317(26)	140
intruder → normal	$B(\mathrm{E2}; 0_2^+ \to 2_1^+)$	130(30)	87
	$B(\mathrm{E2}; 2_3^+ \to 0_1^+)$	1.0(3)	0.034
	$B(\mathrm{E2}; 2_3^+ \to 0_2^+)$	190(50)	276
	$B(\mathrm{E2}; 2_3^+ \to 0_3^+)$	128(64)	50
	$B(\mathrm{E2}; 2_3^+ \to 2_1^+)$	1.0(5)	0.5

[a] In units of $10^{-3}\ e^2\mathrm{b}^2$.

obtained with a quadrupole operator of the form (2.41) with a boson effective charge $e_\mathrm{b} = 0.111\ e\mathrm{b}$ and with $\chi = -1.969$ and $\chi = 0$, for normal and intruder states, respectively. Finally, the negative-parity states of octupole character can also be well described through the inclusion of p and f bosons with the help of the computer code OCTUPOLE which also incorporates intruder states [152].

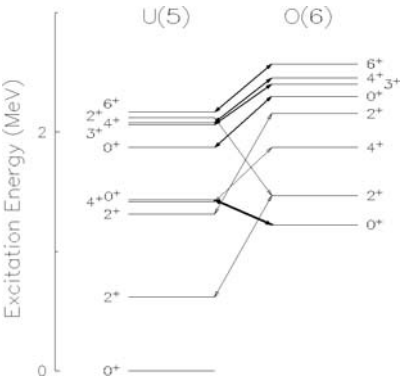

Fig. 2.16. Selective mixing between normal (*left*) and intruder (*right*) positive-parity states in ^{112}Cd in the U(5)–SO(6) model. The mixing is indicated by the thickness of the arrows connecting states with the same angular momentum. (Reprinted from H. Lehmann et al., Phys. Lett. B387 (1996) 259 © Elsevier Science NL, with kind permission.)

Because of the success of this simple U(5)–SO(6) description, the model was studied in more detail in Ref. [99] and, specifically, the influence of the common SO(5) group was investigated and it was found that the resulting symmetry constraints are very important. Since the mixing hamiltonian (2.49) is an SO(5) scalar, it can only mix states with the same seniority in the U(5) and SO(6) limit, as indicated in Fig. 2.16. One notices in particular that the 2_2^+ and 2_3^+ states remain pure despite their small energy difference, while the 0_2^+ and 0_3^+ levels are strongly admixed. Interestingly, experiments using high-resolution inelastic scattering of polarized protons on ^{112}Cd performed at the Q3D in Munich came exactly to this conclusion, finding pure 2^+ states and maximally admixed 0^+ states [153].

Another major consequence is related to the SO(6) character of the mixing hamiltonian [99]. It is possible to rewrite the hamiltonian (2.49) such that its tensor character in the SO(6) limit becomes apparent,

$$H_{\rm mix} = \frac{1}{6}\left(\alpha - \sqrt{5}\beta\right) T_{[2]000} + \frac{5}{6}\left(\alpha + \frac{1}{\sqrt{5}}\beta\right) T_{[2]200}, \tag{2.50}$$

where the subscripts refer to the labels $[N]\sigma\tau L$ and the tensors are $T_{[N]\sigma\tau L} = B^\dagger_{[N]\sigma\tau L} + \tilde{B}_{[N]\sigma\tau L}$ in terms of the operators defined in Table 2.4. Because the lowest intruder states are characterized by an SO(6) quantum number $\sigma = N + 2$ while the normal states have at most $\sigma = N$, they cannot be coupled by the first term in (2.50). Therefore only the second term mixes the two configurations and instead of two free parameters α and β only the sum $(\alpha + \beta/\sqrt{5})$ counts. This holds not only for the U(5)–SO(6) model but also for any hamiltonian describing normal and intruder states which conserves the SO(5) symmetry or which has a partial SO(5) dynamical symmetry.

2.3.3 Studies of ^{112}Cd Using the (n,n′γ) Reaction

The Kentucky facility is unique for the study of low-spin yrare states because it delivers a quasi mono-energetic tunable neutron beam. This is achieved with the ^{3}H(p,n)^{3}He reaction on a tritium gas target. The absence of excited states in ^{3}He and the slightly negative Q value for this reaction leads after collimation to a low-energy mono-energetic neutron beam in forward direction with a typical energy spread of 60 keV. This energy can be tuned by varying the energies of the proton beam. After collimation the neutrons are incident on a massive target (5–50 g) containing the isotope to be studied. The large quantity of mono-isotopic material needed is the main limitation of the method. To measure the γ rays emitted in the (n,n′γ) reaction, neutron time-of-flight measurements are used, which also provide a proper normalization.

The main advantage of inelastic neutron scattering is the absence of the Coulomb barrier. Therefore the neutrons interact with the atomic nucleus without energy loss. Thus the maximal excitation energy is given by the incident neutron energy which can be varied. This is a paramount advantage compared to fusion–evaporation reactions in which the nucleus is excited in a loosely defined and broad energy range. In contrast to the similar situation in inelastic photon scattering, inelastic neutron scattering does not only make dipole and quadrupole excitations but also populates all states with spins up to about $6\hbar$. The typical dependence of the excitation cross-section on neutron energy and transferred spin allows the determination of the spin values. The excitation energies can, of course, also be extracted from these excitation functions. Multipolarities of transitions are obtained from the angular distributions with respect to the incident neutron beam. While the intensities measured in the angular distributions yield the mixing ratios, the observed Doppler shift can be used to extract the lifetimes using the DSA method [154]. A major advantage is the possibility to avoid side feeding by tuning the neutron energies such that the excited states under investigation are populated but no higher-lying levels. If it were not for the delicate use of a tritium target and the need of huge quantities of enriched material, inelastic neutron scattering would be the ideal way to perform low-spin spectroscopy.

For the (n,n′γ) study of ^{112}Cd at the Kentucky facility the scattering sample consisted of 50 g of ^{112}CdO with an enrichment of 98.17%. Several experiments were performed and the final data analysis was finished in 2007. The results were analyzed in steps by going up in excitation energy. The first analysis concerned the three-phonon states for which absolute transition rates were obtained. Therefore the lifetimes were extracted by analyzing the angular distribution for Doppler shift using mono-energetic neutrons of 2.5 MeV. This choice of energy avoided the population of higher-lying states which would have affected the lifetimes due to time delays from the feeding of higher-excited states. In addition, the clean spectra allowed the observation of several new transitions depopulating the 2_4^+ state at 2,121.6 keV.

This new decay pattern showed large deviations from the expected decay, indicating a strongly fragmented state. Therefore it was concluded that there was no evidence for a 2^+ three-phonon state. Other candidates such as the 2_5^+ and 2_6^+ states were studied [155] and it was found that they decay with strong M1 transitions making them candidates for mixed-symmetry states but not for a three-phonon state (see Sect. 4.3). The lifetimes of the 3^+ and 4^+ states lifetimes were measured, yielding strong collective decay patterns as expected. The precise order of the intruder and three-phonon states could never be reproduced and also remained problematic in detailed numerical calculations [149] using the more sophisticated neutron–proton IBM.

Already in Ref. [149] it was observed that the intruder states in ^{112}Cd resemble the normal states in ^{108}Ru, as expected on the basis of I spin (see Sect. 2.2.4). This was investigated in detail in Ref. [156] where the complete $I = 3/2$ multiplet is described by separating the hamiltonian in its I-spin scalar, vector and tensor parts, leading to [157]

$$E(M_I) = \kappa_0 + \kappa_1 M_I + \kappa_2 M_I^2. \tag{2.51}$$

For each level of the $I = 3/2$ multiplet it is possible to fit a quadratic function of M_I allowing the prediction of excited intruder states in ^{116}Te as shown in Fig. 2.17.

To extend the study to even higher energies, a much more extended data set was needed, involving further angular distribution measurements with 3.4 and 4.2 MeV neutrons, an excitation function using neutron energies

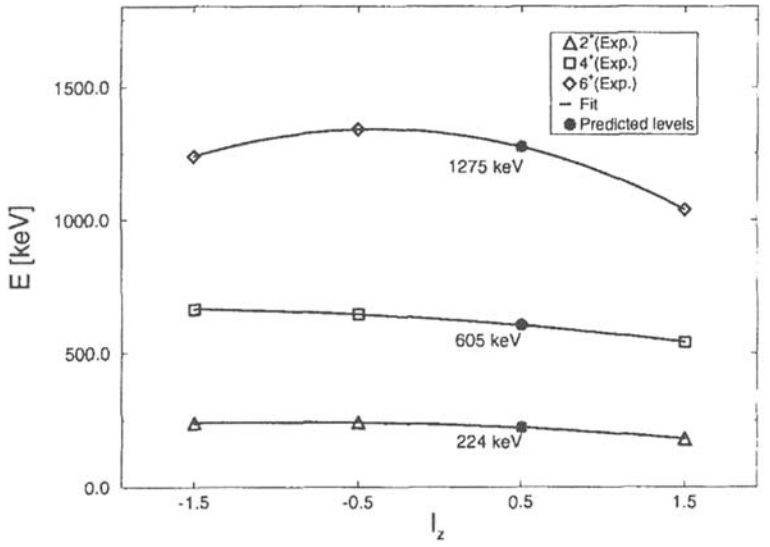

Fig. 2.17. Quadratic fit of observed states in ^{108}Ru, ^{112}Cd and ^{120}Ba, allowing the prediction of excited intruder states in ^{116}Te. (Reprinted from H. Lehmann et al., Nucl. Phys. A621 (1997) 767 © Elsevier Science NL, with kind permission.)

between 1.8 and 4.2 MeV and γ–γ coincidences using collimated 4.2 MeV neutrons. This makes the study of ^{112}Cd the most detailed ever performed with inelastic neutron scattering. In a first step negative-parity states situated around 2.5 MeV were investigated [158]. They are candidates for the quintuplet of states with $J^\pi = 1^-$, 2^-, 3^-, 4^- and 5^- formed by the coupling of a quadrupole and an octupole boson. Based on the collective E2 decay of most states, candidates for such quadrupole–octupole coupled states could be clearly identified in agreement with an *spdf* calculation. Figure 2.18 illustrates the agreement obtained with this description of ^{112}Cd in the *spdf* IBM.

The full data analysis was performed in two steps. In Ref. [159] the newly observed levels and their spin and parities are deduced and compared to level-density formulas. In a second step the deduced lifetimes and multipolarities allowed the determination of hundreds of new absolute transition rates [160] up to 4 MeV excitation energy. The results combined with those of transfer reactions were compared to detailed IBM-2 configuration-mixing calculations [149], shown in Fig. 2.19. This very detailed and difficult study illustrates the limit of what can be understood using symmetry arguments. While some evidence for three-phonon states was obtained in earlier studies, it turned out to be impossible to identify clearly the low-spin members of this quintuplet as well as low-spin members of the higher multi-phonon states using absolute decay properties. The origin of this failure is the complex mixing with other excitations such as hexadecapole (g boson) and quasiparticle excitations in the high-level-density regime occurring around 2 MeV.

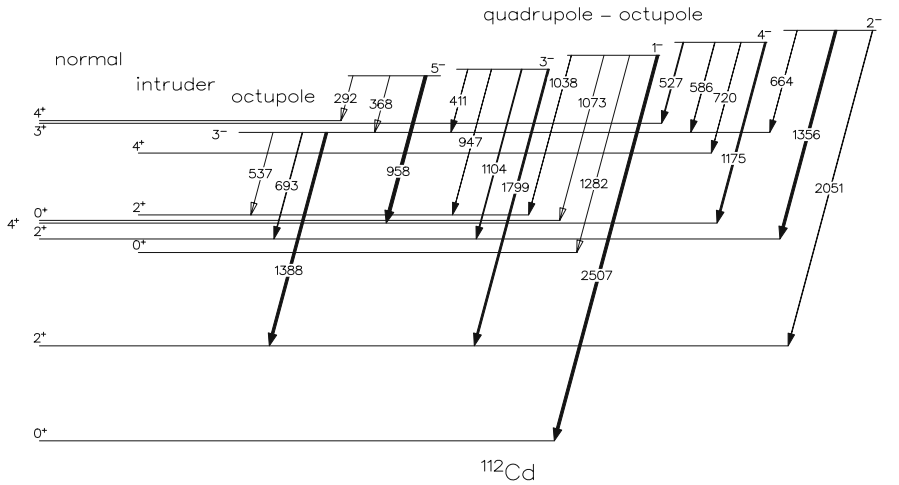

Fig. 2.18. Quadrupole–octupole states in ^{112}Cd as identified by their electric dipole de-excitation to states with positive parity. (Reprinted from P.E. Garrett et al., Phys. Rev. C59 (1999) 2455 ©1999 by the American Physical Society, with kind permission.)

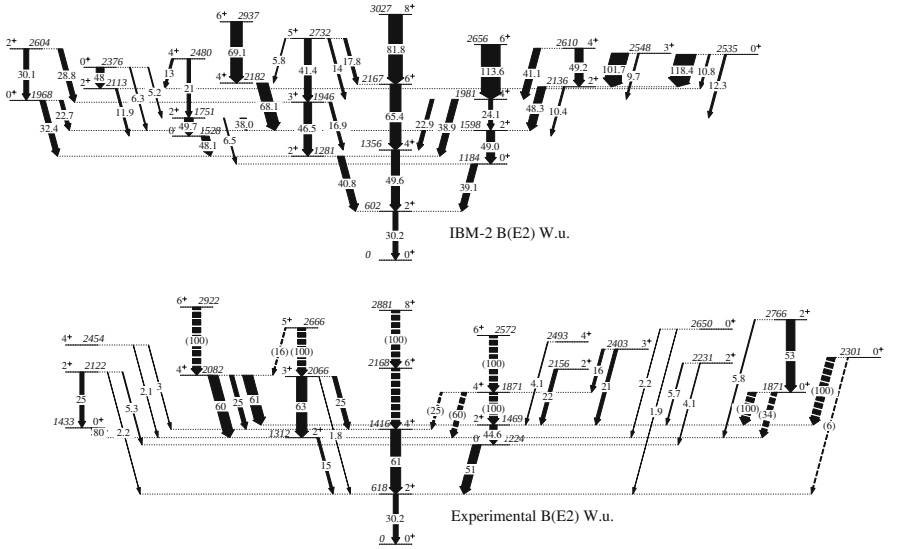

Fig. 2.19. Comparison between observed E2 rates between positive-parity states in ^{112}Cd (*bottom*) and those calculated with IBM-2 (*top*). *Dashed arrows* present those values where only upper limits are known. (Reprinted from P.E. Garrett et al., Phys. Rev. C75 (2007) 054310 ©2007 by the American Physical Society, with kind permission.)

The example of ^{112}Cd clearly underlines the importance of symmetry principles in nuclear physics as well as their limitations. At low excitation energy they lead to clear predictions which can be tested. They also allow to tackle more difficult situations as was shown with the example of the U(5)–SO(6) model of shape coexistence. At higher excitation energies quadrupole–octupole states still allow for a model description since they are rather isolated negative-parity states. However, once the density of states of a given spin and parity increases drastically due to quasi-particle or other excitations, it becomes very difficult, if not impossible, to get a detailed agreement with the data, especially for the electromagnetic decay properties. Here statistical approaches such as presented in Ref. [159] seem more appropriate. It should be mentioned that several other even–even Cd isotopes were recently studied with very high precision such that these nuclei form one of the most detailed testing grounds of the role of symmetries in nuclear structure.

3 Supersymmetry in Nuclear Physics

One particularly important extension of the interacting boson model (IBM) concerns odd-mass nuclei, achieved by considering, in addition to the bosons, a fermion coupled to the core with an appropriate boson–fermion interaction. The resulting interacting boson–fermion model (IBFM) is thus a specific version of the particle–core coupling model which has been widely used in nuclear physics to describe odd-mass nuclei [62]. The characteristic feature of the IBFM is that it lends itself very well to a study based on symmetry considerations whereby certain classes of boson–fermion hamiltonians can be solved analytically. Essential features of the IBFM are recalled in Sect. 3.1, while its symmetry structure is outlined in Sect. 3.2. Since the IBFM is described in detail in Ref. [161], no comprehensive review is given here. Two dynamical-symmetry limits of the IBFM which are of relevance in this and the remaining chapters, are discussed in Sect. 3.3.

A particularly attractive feature is the similarity in the description of even–even and odd-mass nuclei which has given rise to the development of a supersymmetric model, discussed in Sect. 3.4.

Nuclear supersymmetry is a composite-particle phenomenon, linking the properties of boson and fermion systems, framed here in the context of the IBM and IBFM. Composite particles, such as the α particle, are known to behave as approximate bosons. In fact, our knowledge of boson systems is largely derived from cases where the bosons have a composite character. For example, He atoms become superfluid at low temperatures and under certain conditions can also form Bose–Einstein condensates. At higher densities (or temperatures) the constituent fermions begin to be felt and the Pauli principle sets in. Odd-particle composite systems, on the other hand, behave as approximate fermions and are, in the context of the IBFM, treated as a combination of bosons and an (ideal) fermion. In contrast to the theoretical construct of supersymmetry in particle physics, where it is postulated as a generalization of the Lorentz–Poincaré invariance at a fundamental level, experimental evidence has been found for nuclear dynamical supersymmetry, and one particular case is presented in detail in Sect. 3.5.

Although supersymmetries in nuclei traditionally have been associated with dynamical symmetries (i.e., algebraic classification schemes), it is important to make a distinction between the two concepts. In fact, both exist separately: It is possible to find evidence for supersymmetry without dynamical

A. Frank et al., *Symmetries in Atomic Nuclei*,
Springer Tracts in Modern Physics 230, DOI 10.1007/978-0-387-87495-1_3,

symmetry or vice versa. This point, as well as its significance in the analysis of data, is explained in the final section of this chapter.

3.1 The Interacting Boson–Fermion Model

As mentioned in the introduction to this chapter, the IBFM can be thought of, on one level, as a core–particle coupling model with the advantage of a versatile IBM description of the collective core states. However, there are two aspects of the approach which go further. First, as for the IBM in even–even nuclei, it is possible to forge a link between the collective hamiltonian and the underlying single-particle shell structure. Second, symmetries play a central role in the IBFM, just as they do in the boson case. The three symmetries which emerge from the algebraic treatment of the boson problem reappear in the odd-mass formalism although their existence and structure now depend on the single-particle space available to the odd fermion.

The IBFM of odd-mass nuclei was introduced by Iachello and Scholten [162]. Different versions of the model can be constructed depending on the realization of the algebra in terms of creation and annihilation operators. One such realization, called Holstein–Primakoff, leads to a somewhat different version of the IBFM, which is known as the truncated quadrupole phonon–fermion model [163]. The discussion here shall be limited to a brief outline of the basic features of the simplest version of the IBFM.

The basic building blocks of the IBFM are N s and d bosons, in terms of which the even–even core states are modeled, and fermions which occupy a set of single-particle orbits $\{j, j', \ldots\}$. Low-lying collective states of an odd-mass nucleus with $2N + 1$ valence nucleons are approximated as N-boson states coupled to a single fermion. The creation and annihilation operators are $b^\dagger_{lm}$ and b_{lm} for the bosons and $a^\dagger_{jm}$ and a_{jm} for the fermions, and satisfy the (anti-)commutation relations

$$\{a_{jm}, a^\dagger_{j'm'}\} = \delta_{jj'}\delta_{mm'}, \qquad \{a^\dagger_{jm}, a^\dagger_{j'm'}\} = \{a_{jm}, a_{j'm'}\} = 0, \tag{3.1}$$

and

$$[b_{lm}, b^\dagger_{l'm'}] = \delta_{ll'}\delta_{mm'}, \qquad [b^\dagger_{lm}, b^\dagger_{l'm'}] = [b_{lm}, b_{l'm'}] = 0. \tag{3.2}$$

Furthermore, it is assumed that boson and fermion operators commute,

$$[b_{lm}, a_{j'm'}] = [b_{lm}, a^\dagger_{j'm'}] = [b^\dagger_{lm}, a_{j'm'}] = [b^\dagger_{lm}, a^\dagger_{j'm'}] = 0. \tag{3.3}$$

To the extent that nucleons are ideal fermions (which, in fact, they are not since they consist of three quarks), the anti-commutation relations (3.1) are valid exactly. The bosons are composite objects with an internal structure and only approximately satisfy the commutation relations (3.2) and (3.3). The approach followed in the IB(F)M is to impose particle statistics rigorously and to correct for the neglect of the Pauli principle by including additional correlations in the hamiltonian. Such Pauli corrections are particularly important for the boson–fermion interaction.

The hamiltonian of the IBFM consists of a boson and a fermion part, and a boson–fermion interaction, and can be written as

$$H = H^{\mathrm{B}} + H^{\mathrm{F}} + V^{\mathrm{BF}}. \tag{3.4}$$

The boson hamiltonian can be taken directly from the IBM, see Sect. 2.2. As in the boson case, the fermion hamiltonian can be expanded in the order of the interaction. In general, for odd-mass nuclei, only one fermion is coupled to the boson core and this implies that only the one-body part of the fermion hamiltonian matters, which then can be written as

$$H^{\mathrm{F}} = \sum_j \epsilon_j n_j, \tag{3.5}$$

where n_j is the number of fermions in orbit j and ϵ_j its single-particle energy. We note that the simplication of the fermion hamiltonian is a consequence of the assumption of coupling one fermion to the bosons. If several fermions are coupled to the core, their mutual interaction should be included in H^{F}. Notably, this is important in odd–odd nuclei where a neutron *and* a proton are coupled to the even–even core, as will be discussed in Chap. 5. The need for a fermion–fermion interaction also arises if two-particle or two-quasi-particle states are coupled to a boson core which is required for the description of high-spin phenomena such as band crossing and back bending [164, 165, 166]. This approach has even been extended to the coupling of four-quasi-particle states to a boson core [167, 168]. The third term in the hamiltonian (3.4) is the interaction between bosons and fermion which, in lowest order, is of two-body character,

$$V^{\mathrm{BF}} = \sum_{ljl'j'J} v^J_{ljl'j'} \left((b^\dagger_l \times a^\dagger_j)^{(J)} \times (\tilde{b}_{l'} \times \tilde{a}_{j'})^{(J)} \right)^{(0)}_0, \tag{3.6}$$

where the v coefficients are related to the interaction matrix elements between normalized boson–fermion states,

$$\langle lj; JM_J | V^{\mathrm{BF}} | l'j'; JM_J \rangle = \sqrt{\frac{1}{2J+1}} v^J_{ljl'j'}. \tag{3.7}$$

The boson–fermion interaction (3.6) is too general to be of use in a phenomenological analysis. On the basis of shell-model considerations, a simplied form of this interaction can be proposed [162] which contains a monopole, a quadrupole and an exchange term,

$$\begin{aligned}
V^{\mathrm{BF}}_{\mathrm{monopole}} &= \sum_j \kappa_j \left((d^\dagger \times \tilde{d})^{(0)} \times (a^\dagger_j \times \tilde{a}_j)^{(0)} \right)^{(0)}_0, \\
V^{\mathrm{BF}}_{\mathrm{quadrupole}} &= \sum_{jj'} \kappa_{jj'} \left(Q^{\mathrm{B}} \times (a^\dagger_j \times \tilde{a}_{j'})^{(2)} \right)^{(0)}_0, \\
V^{\mathrm{BF}}_{\mathrm{exchange}} &= \sum_{jj'j''} \kappa^{j''}_{jj'} : \left((d^\dagger \times \tilde{a}_j)^{(j'')} \times (\tilde{d} \times a^\dagger_{j'})^{(j'')} \right)^{(0)}_0 :,
\end{aligned} \tag{3.8}$$

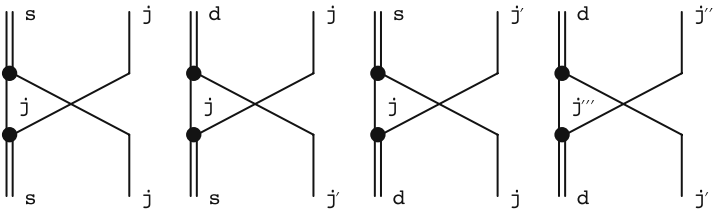

Fig. 3.1. Schematic representation of different boson–fermion exchange interactions

where the notation $: \cdots :$ indicates normal order and Q^{B}_{μ} is the quadrupole operator (2.45) with an additional index B to indicate its boson character. The monopole and quadrupole interactions are the most important components in a multipole expansion of the interaction and should be included as such. The exchange interaction [169, 170] takes account of the fact that the bosons have an internal structure, and this leads to the exchange effects illustrated in Fig. 3.1. Since the bosons are fermion pairs, they are represented by a double line, while a fermion corresponds to a single line; the vertices denote (two-nucleon) interactions. Microscopic considerations suggest [171] that the d-to-d exchange interaction is its most important component.

3.2 Bose–Fermi Symmetries

The Lie algebras associated with the IBFM are $\mathrm{U}^{\mathrm{B}}(6)$ and $\mathrm{U}^{\mathrm{F}}(\Omega)$ where $\Omega = \sum_j (2j+1)$ denotes the size of the single-particle space available to the fermion. The usual boson algebra $\mathrm{U}^{\mathrm{B}}(6)$ describes the collective core excitations, while $\mathrm{U}^{\mathrm{F}}(\Omega)$ corresponds to the unitary transformations among the available single-particle states $a^{\dagger}_{jm}|\mathrm{o}\rangle$. The dynamical algebra for an odd-mass nucleus is then the product algebra

$$\mathrm{U}^{\mathrm{B}}(6) \otimes \mathrm{U}^{\mathrm{F}}(\Omega). \tag{3.9}$$

It contains two sets of generators, in terms of bosons $b^{\dagger}_{lm}\tilde{b}_{l'm'}$ and in terms of fermions $a^{\dagger}_{jm}\tilde{a}_{j'm'}$. Note that the IBFM hamiltonian conserves the number of bosons as well as fermions; it can be expressed in terms of the generators of the algebra (3.9) which therefore can be considered as the dynamical algebra.

The existence of analytically solvable IBFM hamiltonians relies on **isomorphisms** between boson and fermion algebras. A simple example of two isomorphic algebras is provided by the angular momentum algebras which can be defined for bosons and for fermions. The former consists of the angular momentum operators L^{B}_{μ} which generate the boson algebra $\mathrm{SO}^{\mathrm{B}}(3)$ and

occurs in the lattice (2.36). The fermion angular momentum operators L^{F}_{μ} have commutation properties which are identical to those of L^{B}_{μ} and thus are generators of an identical Lie algebra which shall be denoted as $\mathrm{SU}^{\mathrm{F}}(2)$. Although the elements of both Lie algebras can be put into one-to-one correspondence, expressed by the isomorphism $\mathrm{SO}^{\mathrm{B}}(3) \simeq \mathrm{SU}^{\mathrm{F}}(2)$, the difference in notation refers to the fact that the bosons can couple to integer angular momenta only, while for the fermions they can also be half-integer. Because of the property (3.3), L^{B}_{μ} and L^{F}_{μ} commute, and the summed operators $L^{\mathrm{B}}_{\mu} + L^{\mathrm{F}}_{\mu}$ close under commutation and generate the boson–fermion algebra $\mathrm{SU}^{\mathrm{B+F}}(2)$. This is the algebra of the total angular momentum, which can be integer or half-integer, depending on whether the number of fermions is even or odd. Since $\mathrm{SO}^{\mathrm{B}}(3)$ is a subalgebra of $\mathrm{U}^{\mathrm{B}}(6)$ and $\mathrm{SU}^{\mathrm{F}}(2)$ is one of $\mathrm{U}^{\mathrm{F}}(\Omega)$, it follows that $\mathrm{SU}^{\mathrm{B+F}}(2)$ is a subalgebra of $\mathrm{U}^{\mathrm{B}}(6) \otimes \mathrm{U}^{\mathrm{F}}(\Omega)$,

$$\mathrm{U}^{\mathrm{B}}(6) \otimes \mathrm{U}^{\mathrm{F}}(\Omega) \supset \cdots \supset \mathrm{SU}^{\mathrm{B+F}}(2). \tag{3.10}$$

In the following, we shall omit the superscripts B+F in the total angular momentum algebra which then shall be denoted as SO(3), Spin(3) or SU(2), depending on whether the angular momenta are only integer or only half-integer or both integer and half-integer.

The classification of all analytically solvable, rotationally invariant IBFM hamiltonians amounts to finding the subalgebras of $\mathrm{U}^{\mathrm{B}}(6) \otimes \mathrm{U}^{\mathrm{F}}(\Omega)$ which contain SU(2). It is clear that this classification depends on Ω and the specific single-particle orbits $\{j, j', \ldots\}$ available to the fermion. The subalgebra structure of $\mathrm{U}^{\mathrm{B}}(6) \otimes \mathrm{U}^{\mathrm{F}}(\Omega)$ depends on the existence of isomorphisms between boson and fermion algebras: Whenever an isomorphism is established between $\mathcal{G}^{\mathrm{B}}$ and $\mathcal{G}^{\mathrm{F}}$, $\mathcal{G}^{\mathrm{B}} \simeq \mathcal{G}^{\mathrm{F}}$, a boson–fermion algebra $\mathcal{G}^{\mathrm{B+F}}$ can be defined (by adding the corresponding generators) and incorporated into the lattice (3.10).

The algebraic structure of the boson part of the problem is well known and contained in lattice (2.36), although careful consideration should be given to the parameter symmetries mentioned in Sect. 2.2. On the fermion side, since Ω can be large, the algebraic substructure of $\mathrm{U}^{\mathrm{F}}(\Omega)$ may be complex and not known a priori. A powerful method to determine subalgebras is based on the separation of the nucleon angular momentum $\boldsymbol{j} = \tilde{\boldsymbol{l}} + \tilde{\boldsymbol{s}}$ into a pseudo-orbital part $\tilde{\boldsymbol{l}}$ and a pseudo-spin part $\tilde{\boldsymbol{s}}$ [84]. For $\tilde{s} \neq 1/2$ this is a generalization of the pseudo-spin scheme of Sect. 2.1. This separation carries with it the definition of the particle creation operators

$$a^{\dagger}_{\tilde{l}\tilde{s},jm_j} = \sum_{\tilde{m}_l \tilde{m}_s} \langle \tilde{l}\tilde{m}_l \; \tilde{s}\tilde{m}_s | jm_j \rangle a^{\dagger}_{\tilde{l}\tilde{m}_l \tilde{s}\tilde{m}_s}, \tag{3.11}$$

where $a^{\dagger}_{\tilde{l}\tilde{m}_l \tilde{s}\tilde{m}_s}$ is related as follows to the usual $(ls)j$-coupled creation operators:

$$a^{\dagger}_{\tilde{l}\tilde{m}_l\tilde{s}\tilde{m}_s} = \sum_{jm_j} \langle \tilde{l}\tilde{m}_l\ \tilde{s}\tilde{m}_s | jm_j \rangle a^{\dagger}_{jm_j} \tag{3.12}$$

The separation $\boldsymbol{j} = \tilde{\boldsymbol{l}} + \tilde{\boldsymbol{s}}$, is equivalent to the reduction $\mathrm{U}^{\mathrm{F}}(\Omega) \supset \mathrm{U}^{\mathrm{F}}\ (2\tilde{l}+1) \otimes \mathrm{U}^{\mathrm{F}}(2\tilde{s}+1)$, where the generators of $\mathrm{U}^{\mathrm{F}}(2\tilde{l}+1)$ are scalars in $\tilde{s}$, while the generators of $\mathrm{U}^{\mathrm{F}}(2\tilde{s}+1)$ are scalars in $\tilde{l}$.

These techniques define a large class of subalgebras of $\mathrm{U}^{\mathrm{F}}(\Omega)$, which subsequently may be combined with $\mathrm{U}^{\mathrm{B}}(6)$ or one of its subalgebras by virtue of isomorphism. In this way the classification of analytically solvable IBFM hamiltonians is reduced to a group-theoretical problem concerning the subalgebra structure of $\mathrm{U}^{\mathrm{B}}(6) \otimes \mathrm{U}^{\mathrm{F}}(\Omega)$. A comprehensive review of the dynamical symmetries of IBFM, which includes results up to 1991, was given in Ref. [161]; experimental examples were reviewed in Ref. [172]. We refer to these reports for details on specific cases. In the next section we present the two cases which have been most studied and which are of importance for the subsequent discussion of supersymmetry and its extension.

3.3 Examples of Bose–Fermi Symmetries

The first example of a dynamical-symmetry limit of the IBFM was proposed by Iachello [37] who worked out its details in collaboration with Kuyucak [173, 174]. It concerns the case where the bosons are classified according to the SO(6) limit of U(6) and where the fermion occupies a single orbit with $j = 3/2$. Accordingly, the dynamical algebra is $\mathrm{U}^{\mathrm{B}}(6) \otimes \mathrm{U}^{\mathrm{F}}(4)$ and, because of the isomorphism $\mathrm{SO}^{\mathrm{B}}(6) \simeq \mathrm{SU}^{\mathrm{F}}(4)$, it allows the classification

$$\begin{array}{ccccccc}
\mathrm{U}^{\mathrm{B}}(6) & \otimes & \mathrm{U}^{\mathrm{F}}(4) & \supset & \mathrm{SO}^{\mathrm{B}}(6) & \otimes & \mathrm{SU}^{\mathrm{F}}(4) \quad \supset \mathrm{Spin}^{\mathrm{B+F}}(6) \supset \\
\downarrow & & \downarrow & & \downarrow & & \downarrow \qquad\qquad\ \downarrow \\
[N] & & [1] & & \langle\sigma\rangle & & \langle 1/2,1/2,1/2\rangle \quad \langle\sigma_1,\sigma_2,\sigma_3\rangle
\end{array}$$

$$\begin{array}{ccc}
\mathrm{Spin}^{\mathrm{B+F}}(5) & \supset & \mathrm{Spin}(3) \\
\downarrow & & \downarrow \\
(\tau_1,\tau_2) & & J
\end{array} . \tag{3.13}$$

Since the fundamental representation [1] of SU(4) corresponds to the representation $\langle 1/2,1/2,1/2\rangle$ of SO(6), the allowed labels $\langle\sigma_1,\sigma_2,\sigma_3\rangle$ are obtained from the multiplication $\langle\sigma\rangle \times \langle 1/2,1/2,1/2\rangle$ and given by $\langle\sigma+1/2,1/2,1/2\rangle$ and $\langle\sigma-1/2,1/2,-1/2\rangle$, where σ takes the values known from IBM, $\sigma = N, N-2,\ldots,1$ or 0. If a single fermion is coupled to the N bosons, all representations thus obtained are labeled by half-integer numbers and these are known as *spinor* representations. This is also the reason that spinor algebras appear in the reduction (3.13). Note also that the third $\mathrm{Spin}^{\mathrm{B+F}}(6)$ label σ_3 can be either $-1/2$ or $+1/2$; it can be shown that both choices are equivalent and in the following only the absolute value $|\sigma_3|$ will be given. The $\mathrm{Spin}^{\mathrm{B+F}}(5)$

labels (τ_1, τ_2) are determined from the Spin(6) $\supset$ Spin(5) reduction which, for $\langle \sigma_1, 1/2, 1/2 \rangle$, is given by $(\tau_1, \tau_2) = (\sigma_1, 1/2), (\sigma_1 - 1, 1/2), \ldots, (1/2, 1/2)$. Finally, the allowed values of the angular momentum J are found from the Spin(5) $\supset$ Spin(3) reduction and this gives that $(\tau_1, 1/2)$ contains $J = 2v+1/2, 2v-1/2, \ldots, v+1-\frac{1}{4}[1-(-)^{2(\tau-v)/3}]$ with $v = \tau_1, \tau_1-3, \tau_1-6, \ldots$ and $v > 0$. This also shows that for $\tau_1 \geq 7/2$ some J values may occur more than once.

We can now follow the procedure as outlined in Sect. 1.2 and write the hamiltonian in terms of Casimir operators of algebras in the nested chain (3.13). If operators are omitted that give a constant contribution to all states of a given odd-mass nucleus, this leads to a hamiltonian with four Casimir operators,

$$H = \kappa_3 C_2[\mathrm{SO^B}(6)] + \kappa_3' C_2[\mathrm{Spin^{B+F}}(6)] + \kappa_4 C_2[\mathrm{Spin^{B+F}}(5)] + \kappa_5 C_2[\mathrm{Spin}(3)], \tag{3.14}$$

with eigenvalues that are known in terms of the quantum numbers appearing in (3.13),

$$E(\sigma, \sigma_i, \tau_i, J) = \kappa_3 \sigma(\sigma+4) + \kappa_3'[\sigma_1(\sigma_1+4) + \sigma_2(\sigma_2+2) + \sigma_3^2] + \kappa_4[\tau_1(\tau_1+3) + \tau_2(\tau_2+1)] + \kappa_5 J(J+1). \tag{3.15}$$

Furthermore, the eigenstates of the hamiltonian (3.14) have fixed wave functions, that is, they are independent of the parameters κ_i and can be expressed in terms of known isoscalar factors associated with the reductions in (3.13). This, in turn, allows the calculation of many other nuclear properties such as electromagnetic-transition rates and moments or particle-transfer probabilities, extensively discussed in Refs. [173, 174]. Empirical evidence for this dynamical-symmetry limit of the IBFM is found in the Ir–Au region, as reviewed in Ref. [172].

As a second example of a dynamical-symmetry limit of the IBFM, we consider the case with a fermion in orbits with angular momenta $j = 1/2$, $3/2$ and $5/2$. This scheme was first considered by Balantekin et al. [175]. It is particularly attractive because, for all three boson symmetries, U(5), SU(3) and SO(6), it is possible to construct analytically solvable limits. For this reason, this case has been the subject of several detailed studies [176, 177]. Of special relevance is the SO(6) limit [178, 179] which has been applied extensively in the platinum isotopes (see Sect. 3.5). For an account of the U(5) and SU(3) limits we refer to the original papers [178, 180, 181].

The relevant dynamical algebra is $\mathrm{U^B}(6) \otimes \mathrm{U^F}(12)$ and an isomorphism between the boson and the fermion algebras is established by introducing a pseudo-spin $\tilde{s} = 1/2$ and the pseudo-orbital angular momenta $\tilde{l} = 0$ and 2 for the fermion. The classification in the SO(6) limit then becomes

$$
\begin{array}{ccccccc}
\mathrm{U^B}(6) & \otimes & \mathrm{U^F}(12) & \supset & \mathrm{U^B}(6) \otimes \mathrm{U^F}(6) & \otimes & \mathrm{U^F}(2) \supset \\
\downarrow & & \downarrow & & \downarrow \quad \downarrow & & \downarrow \\
[N] & & [1] & & [N] \quad [1] & & [1]
\end{array}
$$

$$
\begin{array}{ccccccc}
\mathrm{U^{B+F}}(6) & \otimes & \mathrm{SU^F}(2) & \supset & \mathrm{SO^{B+F}}(6) & \otimes & \mathrm{SU^F}(2) \supset \\
\downarrow & & \downarrow & & \downarrow & & \downarrow \\
[N_1, N_2] & & \tilde{s} = 1/2 & & \langle \sigma_1, \sigma_2 \rangle & & \tilde{s}
\end{array}
$$

$$
\begin{array}{ccccccccc}
\mathrm{SO^{B+F}}(5) & \otimes & \mathrm{SU^F}(2) & \supset & \mathrm{SO^{B+F}}(3) & \otimes & \mathrm{SU^F}(2) & \supset & \mathrm{Spin}(3) \\
\downarrow & & \downarrow & & \downarrow & & \downarrow & & \downarrow \\
(\tau_1, \tau_2) & & \tilde{s} & & \tilde{L} & & \tilde{s} & & J
\end{array} \quad . \tag{3.16}
$$

One obtains two classes of U(6) representations: $[N_1, N_2]$ follows from the multiplication $[N] \times [1]$ which gives $[N+1, 0]$ and $[N, 1]$. The two-rowed representations of $\mathrm{U^{B+F}}(6)$ reflect a mixed-symmetry character which is allowed for a system consisting of two sets of distinguishable quantum objects, in this case bosons and fermions. For $[N+1, 0]$ the $\mathrm{U}(6) \supset \mathrm{SO}(6)$ reduction is known from even–even nuclei and gives $\langle \sigma_1, \sigma_2 \rangle = \langle N+1, 0 \rangle, \langle N-1, 0 \rangle, \ldots, \langle 1, 0 \rangle$ or $\langle 0, 0 \rangle$. For $[N, 1]$ one obtains $\langle \sigma_1, \sigma_2 \rangle = \langle N-1, 0 \rangle, \langle N-3, 0 \rangle, \ldots, \langle 1, 0 \rangle$ or $\langle 0, 0 \rangle$ and $\langle \sigma_1, \sigma_2 \rangle = \langle N, 1 \rangle, \langle N-2, 1 \rangle, \ldots, \langle 2, 1 \rangle$ or $\langle 1, 1 \rangle$. The SO(5) representations contained in $\langle \sigma_1, 0 \rangle$ are $(\tau_1, \tau_2) = (\sigma_1, 0), (\sigma_1 - 1, 0), \ldots, (0, 0)$ and those contained in $\langle \sigma_1, 1 \rangle$ are $(\tau_1, \tau_2) = (\sigma_1, 0), (\sigma_1 - 1, 0), \ldots, (0, 0)$ and $(\tau_1, \tau_2) = (\sigma_1, 1), (\sigma_1 - 1, 1), \ldots, (1, 1)$. Also for the $\mathrm{SO}(5) \supset \mathrm{SO}(3)$ reduction we have two cases: $(\tau_1, 0)$ contains the angular momenta $\tilde{L} = 2v, 2v-2, 2v-3, \ldots, v$ with $v = \tau_1, \tau_1 - 3, \tau_1 - 6, \ldots$ and $v \geq 0$, and $(\tau_1, 1)$ contains $\tilde{L} = 2v+1, 2v, \ldots, v+1+\delta_{v\tau_1}$ with $v = \tau_1, \tau_1 - 1, \ldots, 0$. Finally, the pseudo-spin value $\tilde{s}$ is coupled with $\tilde{L}$ to give the total angular momentum J. This coupling causes the typical doublet structure with $J = \tilde{L} \pm 1/2$ for odd-mass states with $\tilde{L} \neq 0$.

If one neglects Casimir operators which contribute to the nuclear binding energy only, five second-order operators remain, and the hamiltonian reads

$$
\begin{aligned}
H = {} & \kappa_0 C_2[\mathrm{U^{B+F}}(6)] + \kappa_3 C_2[\mathrm{SO^{B+F}}(6)] + \kappa_4 C_2[\mathrm{SO^{B+F}}(5)] \\
& + \kappa_5 C_2[\mathrm{SO^{B+F}}(3)] + \kappa_5' C_2[\mathrm{Spin}(3)].
\end{aligned} \tag{3.17}
$$

The energy E of the eigenstates is, then, an analytic expression in terms of the relevant quantum numbers:

$$
\begin{aligned}
& E(N_i, \sigma_i, \tau_i, \tilde{L}, J) \\
& \quad = \kappa_0 [N_1(N_1+5) + N_2(N_2+3)] + \kappa_3 [\sigma_1(\sigma_1+4) + \sigma_2(\sigma_2+2)] \\
& \qquad + \kappa_4 [\tau_1(\tau_1+3) + \tau_2(\tau_2+1)] + \kappa_5 \tilde{L}(\tilde{L}+1) + \kappa_5' J(J+1).
\end{aligned} \tag{3.18}
$$

Again, the eigenstates of the hamiltonian (3.14) are independent of the parameters κ_i and known in terms of isoscalar factors which enables the calculation of many nuclear properties, as discussed in Refs. [178, 179]. The application of this dynamical-symmetry limit to the nucleus ^{195}Pt is presented in detail in Sect. 3.5.

3.4 Nuclear Supersymmetry

In the previous section we showed how dynamical-symmetry limits arise in the IBFM and we illustrated them with two examples. In each of these examples it is clear that, if the no-fermion case is considered, the odd-mass classification in IBFM reduces to one of the three IBM classifications valid for even–even nuclei. This, in fact, is a generic property and it forms the basis of a supersymmetric model that allows a simultaneous description of even–even and odd-mass nuclei. Note, however, that such a unified description is not achieved with the formalism of the previous section since the dynamical algebra $\mathrm{U^B}(6) \otimes \mathrm{U^F}(\Omega)$ does not contain even–even and odd-mass nuclei in a single of its representations. The search is thus on for a larger dynamical algebra which necessarily must be supersymmetric in nature.

Nuclear supersymmetry should not be confused with fundamental supersymmetry which predicts the existence of supersymmetric particles, such as the photino and the selectron, for which, up to now, no evidence has been found. If such particles exist, however, supersymmetry must be strongly broken since large mass differences must exist among superpartners, or otherwise they would have been already detected. Competing supersymmetry models give rise to diverse mass predictions and are the basis for current superstring and brane theories [36, 182]. Nuclear supersymmetry, on the other hand, is a theory that establishes precise links among the spectroscopic properties of certain neighboring nuclei. Even-mass nuclei are composite bosonic systems, while odd-mass nuclei are fermionic. It is in this context that nuclear supersymmetry provides a theoretical framework where bosonic and fermionic systems are treated as members of the same supermultiplet. Nuclear supersymmetry treats the excitation spectra and transition intensities of the different nuclei as arising from a single hamiltonian and a single set of transition operators. A necessary condition for such an approach to be successful is that the energy scale for bosonic and fermionic excitations is comparable which is indeed the case in nuclei. Nuclear supersymmetry was originally postulated by Iachello and co-workers [37, 183] as a symmetry among pairs of nuclei. Subsequently, it was extended to quartets of nuclei, where odd–odd nuclei could be incorporated in a natural way, as discussed in Chapt. 5.

Building on the concepts developed in the preceding sections, we now show that even–even and odd-mass nuclei can be treated in a unified framework based on symmetry ideas of IBM and IBFM. Schematically, states in such nuclei are connected by the generators

$$\left(\begin{array}{c|c} b^\dagger b & 0 \\ \hline 0 & a^\dagger a \end{array}\right), \tag{3.19}$$

where indices are omitted for simplicity. States in an even–even nucleus are connected by the operators in the upper left-hand corner of (3.19), while

those in odd-mass nuclei require both sets of generators. The operators (3.19) provide a *separate* description of even–even and odd-mass nuclei; although the treatment is similar in both cases, no operator exists that *connects* even–even and odd-mass states.

An extension of the algebraic structure (3.19) considers in addition operators that transform a boson into a fermion or vice versa:

$$\left(\begin{array}{c|c} b^\dagger b & b^\dagger a \\ \hline a^\dagger b & a^\dagger a \end{array}\right). \tag{3.20}$$

This set does not any longer form a classical Lie algebra which is defined in terms of commutation relations. Instead, to define a closed algebraic structure, one needs to introduce an internal operation that corresponds to a mixture of commutation and anti-commutation, as explained in Sect. 1.2.4. The resulting graded or superalgebra is $\mathrm{U}(6/\Omega)$, where 6 and Ω are the dimensions of the boson and fermion algebras.

By embedding $\mathrm{U^B}(6)\otimes\mathrm{U^F}(\Omega)$ into a superalgebra $\mathrm{U}(6/\Omega)$, the unification of the description of even–even and odd-mass nuclei is achieved. From a mathematical point of view this can be seen from the reduction

$$\begin{array}{ccccc} \mathrm{U}(6/\Omega) & \supset & \mathrm{U^B}(6) & \otimes & \mathrm{U^F}(\Omega) \\ \downarrow & & \downarrow & & \downarrow \\ [\mathcal{N}\} & & [N] & & [1^M] \end{array}. \tag{3.21}$$

The supersymmetric representation $[\mathcal{N}\}$ of $\mathrm{U}(6/\Omega)$ imposes symmetry in the bosons and anti-symmetry in the fermions and contains the $\mathrm{U^B}(6)\otimes\mathrm{U^F}(\Omega)$ representations $[N]\times[1^M]$ with $\mathcal{N}=N+M$ [183]. Thus, a single supersymmetric representation contains states in even–even ($M=0$) as well as odd-mass ($M=1$) nuclei.

To understand better the purpose of the introduction of the supersymmetric generators $a^\dagger b$ or $b^\dagger a$, one may inspect their action on an even–even nucleus, say ^{194}Pt, which appears in the example discussed in the next section,

$$a^\dagger b\ {}^{194}_{78}\mathrm{Pt}_{116} \longrightarrow a^\dagger\ {}^{196}_{78}\mathrm{Pt}_{118} \longrightarrow {}^{195}_{78}\mathrm{Pt}_{117}, \tag{3.22}$$

where bosons and fermions are assumed to have a neutron-hole character. The supersymmetric generators thus induce a connection between even–even and odd-mass nuclei with the same total number of bosons plus fermions. A description with the superalgebra $\mathrm{U}(6/\Omega)$ leads to a *simultaneous* treatment of such pairs of nuclei.

This idea is illustrated schematically in Fig. 3.2 for the case of a particular U(6/12) supermultiplet. The supermultiplet containing ^{194}Pt also contains ^{195}Pt, since the two nuclei are connected by the supersymmetric generator (3.22). Further action of $a^\dagger b$ on ^{195}Pt leads to configurations whereby two neutron-holes are coupled to a ^{198}Pt core, that is, to two-quasiparticle excitations in ^{196}Pt. This action of $a^\dagger b$ may continue indefinitely until no more

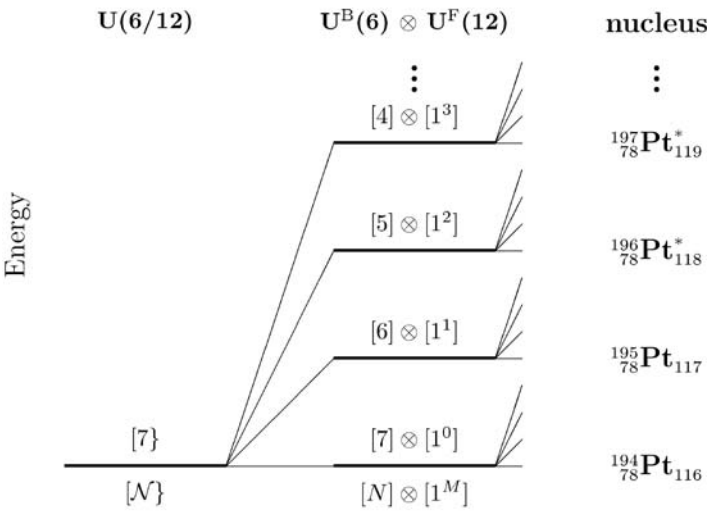

Fig. 3.2. Schematic illustration of part of a U(6/12) supermultiplet in the platinum region. The supermultiplet is characterized by the supersymmetric representation $[\mathcal{N}\}$ with $\mathcal{N} = N + M = 7$. A breaking of the U(6/12) supersymmetry leads to a splitting in the binding energies of the different nuclei

bosons are available. A U(6/12) symmetry predicts all states of all nuclei belonging to the supermultiplet to be degenerate in energy; this degeneracy is first lifted by including $\mathrm{U^B}(6) \otimes \mathrm{U^F}(12)$ invariants which correspond to nuclear binding energy terms. The analysis then proceeds with the inclusion of Casimir operators of the lower algebras, as schematically indicated in Fig. 3.2.

3.5 A Case Study: Detailed Spectroscopy of ^{195}Pt

The nucleus ^{195}Pt is situated in a spherical-to-deformed transitional region. Its core, ^{196}Pt, can be reasonably well described as an SO(6) nucleus (see Sect. 2.2.1). The dominant natural-parity orbits for the neutrons are $3p_{1/2}$, $3p_{3/2}$ and $2f_{5/2}$, which can be decomposed into pseudo-orbital angular momenta $\tilde{l} = 0$ and $\tilde{l} = 2$, and pseudo-spin $\tilde{s} = 1/2$. Therefore, the nucleus ^{195}Pt presents itself as the ideal test of the SO(6) limit of $\mathrm{U^B}(6) \otimes \mathrm{U^F}(12)$ and U(6/12). The analysis of the empirical evidence for this claim is naturally divided into two parts. In the first the validity of the IBFM classification (4.16) in ^{195}Pt is studied. In the second part the validity of U(6/12) supersymmetry for the pair ^{194}Pt–^{195}Pt is analyzed. This section is mainly concerned with the first question and the analysis of supersymmetry in this region is largely deferred to the discussion of quartet supersymmetry in Sect. 5.4.

3.5.1 Early Studies of ^{195}Pt

An essential question in the evaluation of Bose–Fermi symmetries is how to assign quantum numbers to observed levels. This is closely related to the goodness of these quantum numbers. These issues were studied in the 1980s by means of selection rules in electromagnetic transitions and particle-transfer reactions. An example of the former is given in Table 3.1 where 25 measured $B(\mathrm{E2})$ values in ^{195}Pt [184, 185] are compared with the predictions of the symmetry classification for this nucleus, obtained with the E2 operator

$$T_\mu(\mathrm{E2}) = e_\mathrm{b} Q^\mathrm{B}_\mu + e_\mathrm{f} Q^\mathrm{F}_\mu, \tag{3.23}$$

where Q^B_μ and Q^F_μ are the boson and fermion quadrupole operators, and e_b and e_f the effective boson and fermion charges, which have the values $e_\mathrm{b} = -e_\mathrm{f} = 0.15\ e\mathrm{b}$. The description is good as large $B(\mathrm{E2})$ values are observed where they are predicted to be non-zero and small values are found when they are forbidden, with the exception of the transition from the level at 420 keV to that at 99 keV.

The structure of the levels of ^{195}Pt can also be probed by magnetic dipole properties and, specifically, by magnetic dipole moments μ which are particularly sensitive to the single-particle structure. The magnetic moment operator

Table 3.1. Observed E2 transition rates between negative-parity states in ^{195}Pt compared with the predictions of the SO(6) limit of U(6/12)

				$B(\mathrm{E2}; J_\mathrm{i} \to J_\mathrm{f})^b$						$B(\mathrm{E2}; J_\mathrm{i} \to J_\mathrm{f})^b$	
$E_\mathrm{i}{}^a$	J^π_i	$E_\mathrm{f}{}^a$	J^π_f	Expt	Th	$E_\mathrm{i}{}^a$	J^π_i	$E_\mathrm{f}{}^a$	J^π_f	Expt	Th
211	$3/2^-$	0	$1/2^-$	190(10)	179	667	$9/2^-$	239	$5/2^-$	200(40)	239
239	$5/2^-$	0	$1/2^-$	170(10)	179	563	$9/2^-$	239	$5/2^-$	91(22)	22
525	$3/2^-$	0	$1/2^-$	17(1)	0	239	$5/2^-$	99	$3/2^-$	60(20)	0
544	$5/2^-$	0	$1/2^-$	8(4)	0	525	$3/2^-$	99	$3/2^-$	≤ 33	7
99	$3/2^-$	0	$1/2^-$	38(6)	35	613	$7/2^-$	99	$3/2^-$	5(3)	9
130	$5/2^-$	0	$1/2^-$	66(4)	35	420	$3/2^-$	99	$3/2^-$	5(4)	177
420	$3/2^-$	0	$1/2^-$	15(1)	0	508	$7/2^-$	99	$3/2^-$	240(50)	228
455	$5/2^-$	0	$1/2^-$	≤ 0.04	0	389	$5/2^-$	99	$3/2^-$	200(70)	219
199	$3/2^-$	0	$1/2^-$	25(2)	0	525	$3/2^-$	130	$5/2^-$	9(5)	3
389	$5/2^-$	0	$1/2^-$	7(1)	0	667	$9/2^-$	130	$5/2^-$	12(3)	10
613	$7/2^-$	211	$3/2^-$	170(70)	215	563	$9/2^-$	130	$5/2^-$	240(40)	253
508	$7/2^-$	211	$3/2^-$	55(17)	20	389	$5/2^-$	130	$5/2^-$	≤ 14	55
525	$3/2^-$	239	$5/2^-$	≤ 19	72						

[a] Energy in units of keV.
[b] In units of $10^{-3}\ e^2\mathrm{b}^2$.

is proportional to the angular momentum operator and consists of a collective (boson) and a single-particle (fermion) part,

$$T_\mu(\mathrm{M1}) = \sqrt{\frac{3}{4\pi}} \left(g_\mathrm{b} L^\mathrm{B}_\mu + \sum_j g_j L^\mathrm{F}_\mu(j) \right), \tag{3.24}$$

where L^B_μ and $L^\mathrm{F}_\mu(j)$ are the angular momentum operators for the d bosons and for fermions in orbit j. The effective boson gyromagnetic ratio is determined from the magnetic dipole moment $\mu(2^+_1)$ of the neighboring even–even Pt isotopes to be $g_\mathrm{b} = 0.3\ \mu_\mathrm{N}$, while for the g_j factors Schmidt values are taken with an appropriate quenching (60%) of the spin part. Magnetic dipole moments of states in the odd-mass nucleus ^{195}Pt are then entirely determined and, in fact, closed expressions can be derived for them [186]. Results for the moments of yrast symmetric and non-symmetric states are shown in Fig. 3.3. Given that no free parameters are involved in this calculation, the level of agreement can be regarded as remarkable.

Results of similar quality were also obtained [187, 188] for intensities of one-neutron-transfer reactions starting from and leading to ^{195}Pt and confirmed the proposed assignment of quantum numbers.

All data on ^{195}Pt existing at that time (1989) can be combined and reproduced [189] through an extended fit shown in Fig. 3.4 which includes 22 levels in ^{195}Pt and eight levels in ^{194}Pt. The levels at 99, 130, 212, 239, 508,

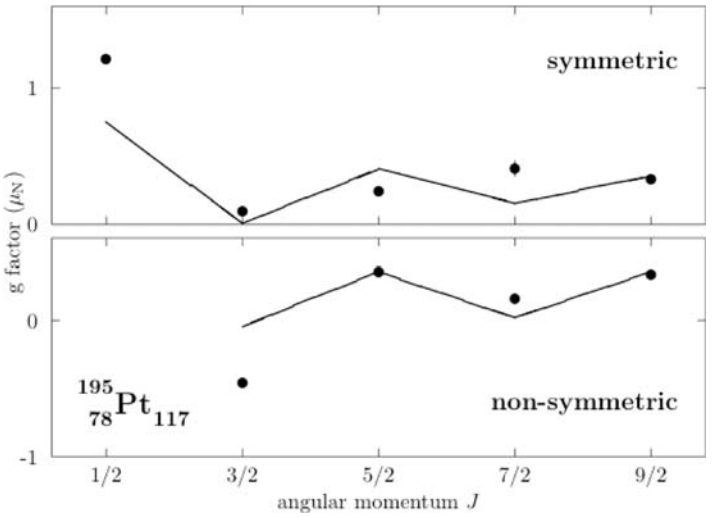

Fig. 3.3. Observed g factors (*dots*) of the yrast symmetric $[7, 0]$ and non-symmetric $[6, 1]$ levels in ^{195}Pt compared with the prediction of the SO(6) limit of U(6/12) (*line*). The g factor of a state is defined as its magnetic dipole moment divided by its angular momentum J

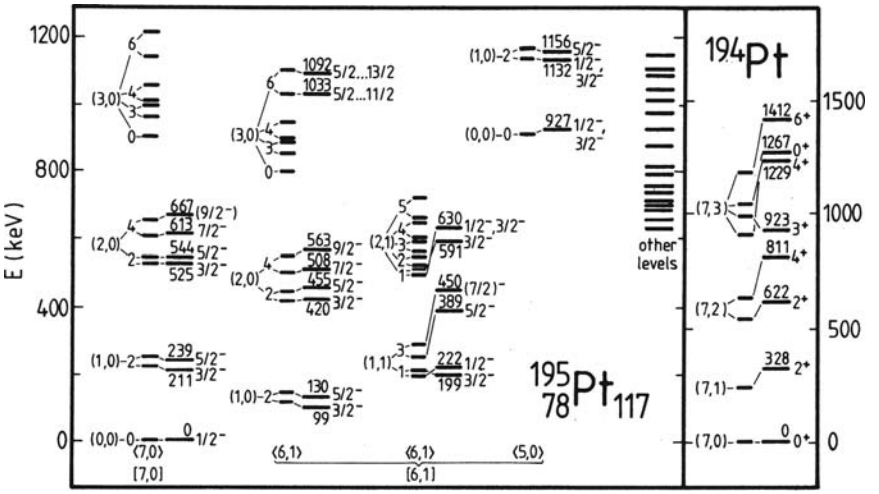

Fig. 3.4. Observed and calculated negative-parity spectrum of ^{195}Pt (*left*) and positive-parity spectrum of ^{194}Pt (*right*). Levels are labeled by their angular momentum and parity J^π and by the other quantum numbers in the classification (3.16). Levels with unassigned J^π are shown as other levels.(Reprinted from A. Mauthofer et al., Phys. Rev. C39 (1989) 1111 ©1989 by the American Physical Society, with kind permission.)

563, 612 and 667 keV are classified by taking account of their E2 branching ratios. Because this classification does not allow the determination of all parameters in the hamiltonian (4.17), Mauthofer et al. additionally proposed that the levels at 927, 1,132 and 1,156 keV are the three lowest states of the $[6,1]\langle 5,0\rangle$ band. This leads to the parameters in the hamiltonian (3.17) as shown in the first line of Table 3.2. Since all quantum numbers of all states are known, this automatically fixes the spectra of ^{194}Pt and ^{195}Pt which are shown in Fig. 3.4. Levels are labeled by their angular momentum and parity J^π, and also by the quantum number $\tilde{L}$ which results from the coupling of the angular momentum of the bosons to the pseudo-orbital angular momentum of the fermion. Also given are the other quantum numbers occurring in the classification (3.16). As shown in the figure, there were many unassigned states above 600 keV, for which no definite spins and parities were available at that time. Also some higher-lying levels, such as the one at 927 keV, had no uniquely determined spin values.

Table 3.2. Parameters (in keV) for the nuclei ^{194}Pt and ^{195}Pt

	κ_0	κ_3	κ_4	κ_5	κ_5'
Mauthofer et al. [189]	64.4	−56.7	49.8	1.2	6.0
Metz et al. [190]	48.7	−42.2	49.8	5.6	3.4

3.5.2 High-Resolution Transfer Studies Using (p,d) and (d,t) Reactions

The question of the validity of supersymmetry formed the focus of a new collaboration between groups at the Universities of Fribourg and Bonn, and the Ludwig-Maximillian University in Munich, aiming at a complete spectroscopy of ^{196}Au (see Sect. 5.4). One of the most important spin-offs of this study concerns the spectroscopy of ^{195}Pt which shall now be presented.

In this study the high-resolution magnetic spectrometer Q3D at the accelerator laboratory of the Ludwig-Maximillians Universität and Technische Universität in Munich was used. This remarkable instrument is able to deliver data with a high-energy resolution for angular distributions of the emitted particles. Today it achieves an energy resolution of 4 keV in the ^{196}Pt(p,d)^{195}Pt reaction for particles having an energy of about 20 MeV (in the earlier measurements [188] on ^{195}Pt the resolution for this reaction was 16 keV). This is achieved using the optics provided by one dipole and three quadrupole magnets [191] and a detector which allows one to reconstruct the focal plane off-line [192]. For comparison, normal semiconductor γ-ray detectors achieve a resolution of 2 keV at only 1 MeV. In addition, the Q3D spectrometer is able to identify the particle emitted in the reaction.

Originally considered as a calibration run for the spectrometer, the results of the ^{196}Pt(p,d)^{195}Pt and polarized ^{196}Pt($\mathbf{d}$,t)^{195}Pt reactions [190] turned out to be overwhelmingly rich and enormously extended the knowledge of ^{195}Pt. The (p,d) reaction with an energy resolution of 3 keV allows a direct population of the excited states. The excitation energies of the populated states are observed as the missing energy of the out-coming deuteron. The experiment established 22 new states in the energy region 1.0–1.6 MeV. To extract information on quantum numbers and excitation strength, the ^{196}Pt($\mathbf{d}$,t)^{195}Pt reaction can be used. In contrast to (p,d), the (d,t) reaction is more restricted to the nuclear surface and therefore sensitive to the details of the orbit in which the odd neutron is transferred. By measuring the angular distribution of the outgoing tritons, the l value, as transferred to the excited state, can be determined. Since the transfer reaction starts from the $J^\pi = 0^+$ ground state of ^{196}Pt, the parity of the excited state in ^{195}Pt is uniquely determined from the transferred l value. As regards the total angular momentum, the (d,t) reaction leaves $J = l \pm 1/2$ as possible values for the populated state, with the l value obtained from the angular distribution of the deuterons.

The J value can be determined when polarized deuterons are used in the transfer reaction. Since the deuteron (which is in a $J^\pi = 1^+$ state with parallel spins of proton and neutron) is now oriented in space, the orientation of the spin of the transferred neutron is fixed. Using a 60(3)% vector polarized deuteron beam, for which the vector polarization could be inverted without any effect on the beam position, the difference in angular cross-sections with spin up and spin down gives after proper renormalization the so-called vector

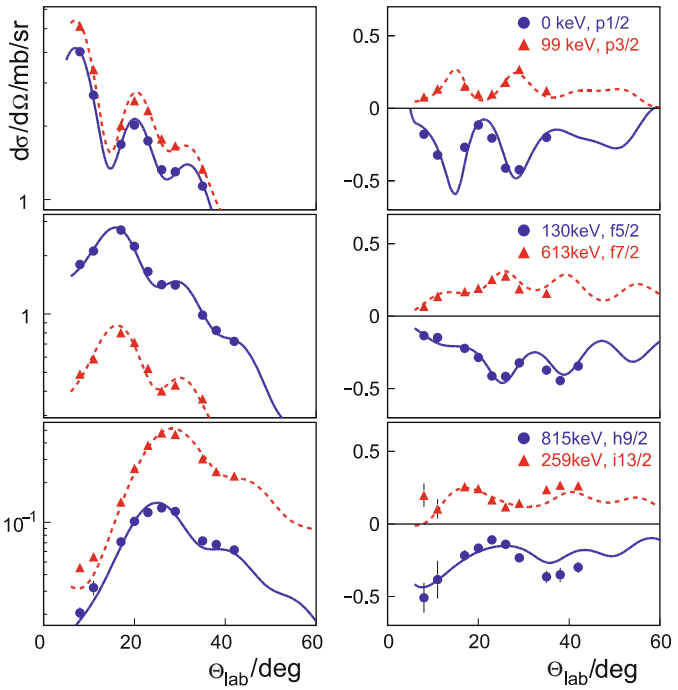

Fig. 3.5. Typical examples of angular distributions (*left*) and analyzing powers (*right*) for excited states in ^{195}Pt populated in the ^{196}Pt(**d**,t)^{195}Pt reaction. (Reprinted from A. Metz et al., Phys. Rev. C61 (2000) 064313 ©2000 by the American Physical Society, with kind permission.)

analyzing power A_y, which is positive for a transferred total angular momentum $j = l + 1/2$ and negative for $j = l - 1/2$ (see Fig. 3.5). Therefore, the use of a polarized deuteron beam for (**d**,t) transfer on an even–even target yields directly the J^π value of the final state. The differential cross-section contains further information about the final states via the spectroscopic strengths G_{lj} or factors S_{lj}:

$$\frac{d\sigma}{d\Omega}(\theta) = G_{lj}\sigma_{lj}(\theta) = v_j^2(2j+1)S_{lj}\sigma_{lj}(\theta), \tag{3.25}$$

where $\sigma_{lj}(\theta)$ contains the kinematical factors described in a distorted wave Born approximation (DWBA) and v_j^2 is the occupation probability of the neutron orbit j. The spectroscopic strengths and factors thus determine the amplitudes of the odd neutron occupying the j orbit in the wave function of an excited state.

With the ^{196}Pt(**d**,t)^{195}Pt reaction [190] it was possible to establish new or unique J^π values for 42 states and to determine the spectroscopic strengths to 62 states. One of those J^π values contradicts the previous assignment of

the lowest $\langle 5,0,0\rangle$ state in ^{195}Pt as shown in Fig. 3.4 since the 927 keV state turned out to have $J^\pi = 3/2^-$. This changes the parameters in the hamiltonian (3.17), the values of which are given in the second line of Table 3.2. The combination of all available spectroscopic information leads to a greatly extended negative-parity level scheme of ^{195}Pt which is compared with U(6/12) in Fig. 3.6. With only five parameters the U(6/12) model is able to describe all 53 negative-parity levels in ^{195}Pt below 1.44 MeV. The same parameters also describe eight states in ^{194}Pt. One should not underestimate the difficulty of obtaining such level of agreement, even with five parameters: All states are calculated at about the correct energy and for each J^π the correct number of levels is found.

Besides the energy spectrum, the transfer reaction also yields the transfer strengths which can be compared with the theoretical predictions. To calculate transfer strengths, one first needs to determine the transfer operator T_{lj}. Unfortunately, different reactions lead to different operators which are combinations of fermion and boson creation and annihilation operators complicating the description of most reactions. Fortunately however, the ^{196}Pt(**d**,t)^{195}Pt reaction is relatively easy to describe in the model since one starts from ^{196}Pt described by six hole bosons and ends in ^{195}Pt with the same number of bosons and an additional neutron fermion hole. The simplest form for the model's transfer operator is then given by the following linear combination of the fermion creation operators $a_j^\dagger$:

$$T_{lj} = v_{1/2} a^\dagger_{1/2} \delta_{j,1/2} + v_{3/2} a^\dagger_{3/2} \delta_{j,3/2} + v_{5/2} a^\dagger_{5/2} \delta_{j,5/2}, \tag{3.26}$$

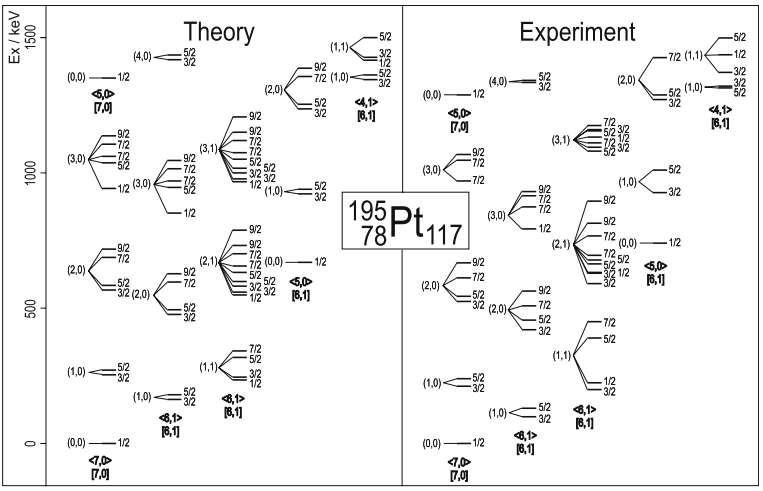

Fig. 3.6. Observed and calculated negative-parity spectrum of ^{195}Pt. Levels are labeled by their angular momentum J (to the *right* of each level) and by the other quantum numbers in the classification (3.16)

with the square root of the occupation probabilities as weighting factors. With this transfer operator the spectroscopic strengths from a state with angular momentum J_i to a state J_f are given by

$$G_{lj} = \frac{1}{2J_\mathrm{i}+1}\langle J_\mathrm{f} \parallel T_{lj} \parallel J_\mathrm{i}\rangle^2. \tag{3.27}$$

As in the case of the E2 transitions, this transfer operator has a definite tensor character which leads to population of only some of the states shown in Fig. 3.6. They necessarily must have the quantum numbers $\langle 7 \text{ or } 5, 0\rangle(0 \text{ or } 1, 0)$ or $\langle 6, 1\rangle(1, 0)$.

To determine the tensor character of the transfer operator, we note that it corresponds to $N = 0$ and $M = 1$. Application of the reduction rules given above leads to the character $|[0][1], [1, 0], \langle 1, 0\rangle, (1, 0), 2, 2 \pm 1/2\rangle$ or $|[0][1], [1, 0], \langle 1, 0\rangle, (0, 0), 0, 1/2\rangle$. The tensor character under U(6), SO(6) and SO(5) leads to the population of states with $\langle N \pm 1, 0\rangle(0, 0)$ or $(1, 0)$ and $\langle N, 1\rangle(1, 0)$ since the initial state is the even–even ground state $|[N]\langle N\rangle, (0), 0\rangle$.

Despite the simplicity of the operator, good agreement with the data is found, as shown in Table 3.3. The table also shows the adopted levels given by the Nuclear Data Sheets (NDS) [44] before the experiment was performed. The spectroscopic strengths are calculated with the U(6/12) wave functions and the transfer operator (3.26) with $v^2_{1/2} = 0.56$, $v^2_{3/2} = 0.44$ and $v^2_{5/2} = 0.50$. Except for one $3/2^-$ state at 1,095 keV all observed strength predicted to be forbidden is found to be small. Also, the predicted non-forbidden strength agrees very well with the experimental values. More complicated transfer operators can be constructed. However, the next term to be included is a three-body operator consisting of two creation operators and one annihilation operator, and thus becomes very complicated. A possible way to fix the operator without increasing the number of parameters is to use its form as obtained from the fermion operator of the shell model, $c^\dagger_{lj}$, mapped onto the boson–fermion space of the IBFM. This is reported and extensively discussed in Refs. [190, 193].

One of the results obtained from the transfer data concerns the effect of the limited model space. The U(6/12) model describes only excitations in which the odd neutron occupies the $3p_{1/2}$, $3p_{3/2}$ or $2f_{5/2}$ orbits but it neglects the $2f_{7/2}$ orbit. The polarized-deuteron data do provide information on the spectroscopic strength of the $2f_{7/2}$ orbit. From the observed strengths given in Table 3.3 one notes the different behavior of the $2f_{7/2}$ strength which increases slowly with energy and becomes important only at energies well above the centroids for the $3p_{1/2}$, $3p_{3/2}$ and $2f_{5/2}$ strengths. One can thus conclude that the U(6/12) model space is appropriate for the lower-lying states but less so for states above ~ 1 MeV.

In conclusion, the doublet of atomic nuclei ^{194}Pt and ^{195}Pt represents an excellent example of a dynamical U(6/12) supersymmetry, with 61 excited states in the two nuclei that are described by a single algebraic hamiltonian

Table 3.3. Observed (d,t) transfer strength to negative-parity states in ^{195}Pt compared with the predictions of the SO(6) limit of U(6/12)

NDS		Experiment			Theory		
E^a	J^π	E^a	J^π	${G_{lj}}^b$	E^a	J^π	${G_{lj}}^b$
0.0	$1/2^-$	0.0	$1/2^-$	78.12(22)	0.0	$1/2^-$	69.72
98.882(4)	$3/2^-$	99.5(6)	$3/2^-$	88.72(28)	162.5	$3/2^-$	133.01
129.777(5)	$5/2^-$	129.5(6)	$5/2^-$	209.2(6)	179.6	$5/2^-$	226.97
199.526(12)	$3/2^-$	199.2(6)	$3/2^-$	12.76(12)	244.7	$3/2^-$	0.0
211.398(6)	$3/2^-$	212.4(6)	$3/2^-$	20.60(12)	253.3	$3/2^-$	34.25
222.225(6)	$1/2^-$	223.5(7)	$1/2^-$	14.6(8)	234.4	$1/2^-$	0.0
239.269(6)	$5/2^-$	238.7(6)	$5/2^-$	34.98(24)	270.5	$5/2^-$	58.56
389.16(6)	$5/2^-$	389.5(7)	$5/2^-$	1.44(6)	318.0	$5/2^-$	0.0
419.703(4)	$3/2^-$	419.5(7)	$3/2^-$	0.76(4)	476.5	$3/2^-$	0.0
449.66(5)	$(7/2^-)$	450.0(7)	$7/2^-$	1.52(16)	342.9	$7/2^-$	
455.20(4)	$5/2^-$	455.6(7)	$5/2^-$	1.50(12)	493.7	$5/2^-$	0.0
508.08(6)	$5/2^-, 7/2^-$	507.9(6)	$7/2^-$	51.12(24)	596.3	$7/2^-$	
524.848(4)	$3/2^-$	524.6(6)	$3/2^-$	0.76(4)	567.4	$3/2^-$	0.0
544.2(6)	$5/2^-$	543.9(6)	$5/2^-$	2.76(6)	584.5	$5/2^-$	0.0
562.81(5)	$9/2^-$	562.6(7)	$9/2^-$	31.4(7)	627.2	$9/2^-$	
590.896(5)	$3/2^-$	NR^c			558.8	$3/2^-$	0.0
612.72(8)	$7/2^-$	612.0(6)	$7/2^-$	51.36(24)	687.1	$7/2^-$	
630.138(8)	$1/2^-, 3/2^-$	628.8(7)	$1/2^-$	0.60(4)	548.5	$1/2^-$	0.0
632.1(5)	$1/2^-, 3/2^-$	NR^c			581.2	$3/2^-$	0.0
664.200(10)	$5/2^-, 7/2^-$	664.2(6)	$5/2^-$	10.92(12)	598.4	$5/2^-$	0.0
667.1(5)	$(9/2^-)$	NR^c			718.0	$9/2^-$	
678(1)	$5/2^-, 7/2^-$	678.4(8)	$5/2^-$	0.79(6)	632.0	$5/2^-$	0.0
695.30(6)	$(7/2^-)$	695.3(6)	$7/2^-$	10.64(16)	656.1	$7/2^-$	
739.546(6)	$1/2^-, 3/2^-$	739.5(6)	$1/2^-$	11.04(6)	668.9	$1/2^-$	34.11
765.8(9)	$(7/2^-)$	766.7(6)	$7/2^-$	14.80(16)	700.9	$7/2^-$	
793.0(10)	$3/2^-$	NR^c			851.3	$1/2^-$	0.0
814.52(4)	$9/2^-$	814.9(6)	$9/2^-$	119.3(14)	731.9	$9/2^-$	
875(1)	$5/2^-, 7/2^-$	873.8(6)	$7/2^-$	14.21(16)	970.1	$7/2^-$	
895.42(7)	$9/2^-$	895.0(9)	$9/2^-$	6.10(40)	787.9	$9/2^-$	
915(1)		916.0(6)	$7/2^-$	24.16(16)	1015.0	$7/2^-$	
925.(5)	$5/2^-, 7/2^-$	$\rightarrow$916.0					
926.89(5)	$1/2^-, 3/2^-$	927.9(6)	$3/2^-$	7.92(8)	922.2	$3/2^-$	5.94
930.71	$(9/2^-)$	NR^c			1045.9	$9/2^-$	
971.3	$5/2^-, 7/2^-$	970.6(6)	$7/2^-$	29.76(16)	1060.3	$7/2^-$	
1016(5)	$5/2^-, 7/2^-$	1010.4(7)	$5/2^-$	5.34(12)	939.4	$5/2^-$	10.14
1049.3(7)		1047.1(7)	$7/2^-$	40.80(24)	1105.8	$7/2^-$	
1058(5)	$5/2^-, 7/2^-$						
new		1068.8(7)	$9/2^-$	20.4(8)	1136.7	$9/2^-$	
new		1079.7(7)	$5/2^-$	6.18(12)	1017.1	$5/2^-$	0.0
1091.8(5)	(5/2 to 13/2)	NR^c					
1095.8(4)	$1/2^-, 3/2^-$	1095.5(7)	$3/2^-$	34.44(12)	977.5	$3/2^-$	0.0
new		1111.2(7)	$7/2^-$	2.72(16)	1074.8	$7/2^-$	

Table 3.3. Continued

NDS		Experiment			Theory		
E^a	J^π	E^a	J^π	${G_{lj}}^b$	E^a	J^π	${G_{lj}}^b$
1132.40(2)	$1/2^-, 3/2^-$	1132.3(7)	$1/2^-$	3.30(4)	967.2	$1/2^-$	0.0
1151(6)	$1/2^-, 3/2^-$						
1155.8		1155.7(8)	$5/2^-$	8.58(24)	1050.7	$5/2^-$	0.0
1160.38	$1/2^-, 3/2^-$	NR[c]			999.9	$3/2^-$	0.0
1166.4	$1/2^+, 3/2^+$	NR[c]					
1189(6)	$5/2^-, 7/2^-$	1175.5(8)	$7/2^-$	9.28(16)	1119.7	$7/2^-$	
1271.0(3)	$1/2^-, 3/2^-$	1271.2(9)	$3/2^-$	3.40(4)	1236.3	$3/2^-$	0.06
1287.7(4)	$1/2^-, 3/2^-$	1288.3(9)	$1/2^-$	2.56(8)	1350.7	$1/2^-$	7.68
new		1288.3(9)	$5/2^-$	8.22(30)	1253.5	$5/2^-$	0.0
1294(1)	$1/2^-, 3/2^-$	$\rightarrow$1288.3					
1306(10)							
new		1314.1(10)	$5/2^-$	5.76(12)	1361.5	$5/2^-$	0.0
1320.8(4)	$1/2^-, 3/2^-$	1321.0(10)	$3/2^-$	0.64(4)	1344.3	$3/2^-$	0.0
1334.7(4)	$1/2^-, 3/2^-$	NR[c]			1418.6	$3/2^-$	0.0
new		1342.4(13)	$5/2^-, 7/2^-$	0.96(8)	1435.8	$5/2^-$	0.0
1346.9(6)	$1/2, 3/2$	NR[c]					
1372.7(4)	$1/2^-, 3/2^-$	1371.9(12)	$3/2^-$	1.48(4)	1426.6	$3/2^-$	0.0
1411.1(5)	$1/2^-, 3/2^-$	NR[c]					
1425.0(5)	$1/2^-, 3/2^-$	NR[c]					
new		1426.6(14)	$7/2^-$	1.52(8)	1356.1	$7/2^-$	
1438.3(4)	$1/2, 3/2$	1437.7(14)	$1/2^-$	1.28(4)	1416.3	$1/2^-$	0.0
1445.3(5)	$1/2^-, 3/2^-$	1445.9(14)	$3/2^-$	1.72(4)			
new		1455.9(14)	$7/2^-$	0.56(8)			
new		1464.7(15)	$5/2^-$	1.86(12)	1499.8	$5/2^-$	0.0
new		1473.2(15)	$3/2^-$	0.48(4)			

[a] Energy in units of keV.
[b] Spectroscopic strength in units of 10^{-2}.
[c] Not resolved.

with only five parameters. Not only are all negative-parity states of ^{195}Pt below 1.44 MeV accounted for but also electromagnetic transition probabilities and transfer-reaction amplitudes are well described. The essential ingredient to arrive at the conclusion that the nucleus ^{195}Pt provides a beautiful manifestation of a Bose–Fermi symmetry and dynamical supersymmetry was the use of high-resolution transfer reactions providing a quasi-complete level scheme.

3.6 Supersymmetry without Dynamical Symmetry

The concept of dynamical algebra implies a generalization of that of a symmetry algebra, as explained in Sect. 1.2.2. If $\mathcal{G}_{\rm dyn}$ is the dynamical algebra of a given system, all physical states considered belong to a *single*

irreducible representation of $\mathcal{G}_{\rm dyn}$. For a symmetry algebra, in contrast, each set of degenerate states of the system is associated to one of its irreducible representations. A consequence of the existence of a dynamical algebra is that all states can be reached by acting with the algebra's generators or, equivalently, all physical operators can be expressed in terms of these generators. Rather naturally, the same hamiltonian and the same transition operators are employed for all states. To clarify this point with an example in the framework of IBM, a single hamiltonian and a single set of operators are associated to a given even–even nucleus and can be expressed in terms of the generators of U(6) which thus plays the role of dynamical algebra. It does not matter whether this hamiltonian can be expressed or not in terms of the generators of a single chain of nested algebras. In short, the existence of a dynamical symmetry is not a prerequisite for the existence of a dynamical algebra.

This general statement can be illustrated with the example of U(6/12) supersymmetry. If we consider U(6/12) to be the dynamical algebra for the pair of nuclei ^{194}Pt–^{195}Pt, it follows that the same hamiltonian and operators (including in this case the transfer operators which connect states in the two nuclei) should apply to all states. It also follows that no restriction should be imposed on the form of the hamiltonian or operators, except that they must be a function of the generators of U(6/12) (i.e., belong to its enveloping algebra).

In particular cases this generalization of supersymmetry can be achieved in a straightforward way. With reference to the IBM hamiltonian (2.37) and the IBFM hamiltonian (3.17), the following combination of Casimir operators can be proposed:

$$\begin{aligned} H = {} & \kappa_0 C_2[\mathrm{U}^{\mathrm{B+F}}(6)] + \kappa_1 C_1[\mathrm{U}^{\mathrm{B+F}}(5)] + \kappa_1' C_2[\mathrm{U}^{\mathrm{B+F}}(5)] \\ & + \kappa_2 C_2[\mathrm{SU}^{\mathrm{B+F}}(3)] + \kappa_3 C_2[\mathrm{SO}^{\mathrm{B+F}}(6)] + \kappa_4 C_2[\mathrm{SO}^{\mathrm{B+F}}(5)] \\ & + \kappa_5 C_2[\mathrm{SO}^{\mathrm{B+F}}(3)] + \kappa_5' C_2[\mathrm{SU}(2)]. \end{aligned} \tag{3.28}$$

All Casimir operators belong to U(6/12) which therefore remains the dynamical algebra of this generalized hamiltonian. [In fact, they all are in $\mathrm{U}^{\mathrm{B}}(6) \otimes \mathrm{U}^{\mathrm{F}}(12)$ but the transfer between ^{194}Pt and ^{195}Pt requires operators which belong to U(6/12).] Nuclear supersymmetry imposes the use of an identical hamiltonian for even–even and odd-mass nuclei, and this hypothesis can be equally well tested for the generalized hamiltonian (3.28).

This idea has been applied to the ruthenium and rhodium isotopes [194]. The even–even ruthenium isotopes are situated in a transitional region which falls outside a single IBM limit but requires the combination of the Casimir operators of U(5) and SO(6) [110]. The observed positive-parity levels of $^{102-108}$Ru [195] are consistent with such transitional behavior (see Fig. 3.7). For example, the excitation energy of the first 2^+ state decreases with increasing neutron number and the 4^+–2^+–0^+ two-phonon triplet structure, typical of vibrational U(5) nuclei, is clearly present in ^{102}Ru but gradually disappears in the heavier isotopes as the 0^+ level detaches itself from the triplet.

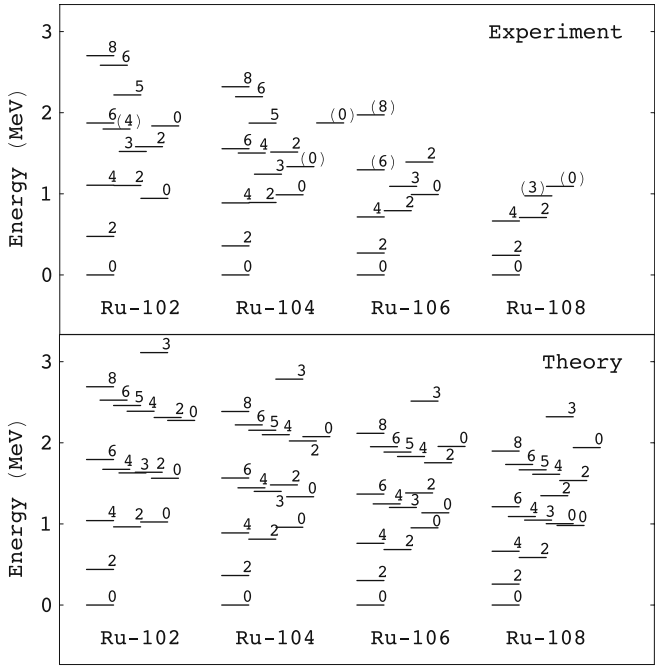

Fig. 3.7. Observed and calculated positive-parity spectra of $^{102-108}$Ru. Levels are labelled by their angular momentum J and grouped into multi-phonon multiplets (see text)

Both features can be reproduced with a U(5)–SO(6) transitional hamiltonian. The transition from U(5) to SO(6) is obtained by varying κ_1, the coefficient of $C_1[\mathrm{U}^{\mathrm{B+F}}(5)]$, linearly with the number of bosons N [196], as shown in Table 3.4. At higher excitation energies the theoretical levels can still be grouped into multiplets (e.g., a three-phonon quintuplet or a four-phonon septuplet) but it is clear from the figure that it becomes difficult to establish an unambiguous correspondence with observed levels.

In the odd-mass rhodium isotopes the dominant negative-parity orbits for the protons are $2p_{1/2}$, $2p_{3/2}$ and $1f_{5/2}$. This matches the angular momenta required for U(6/12) but it cannot be expected that a single of its limits describes the series of rhodium isotopes since we know this is not the case for the even–even ruthenium isotopes. The supersymmetry idea, however, still applies to the hamiltonian (3.28) and, specifically, we may use the values

Table 3.4. Parameters (in keV) for the ruthenium and rhodium nuclei

κ_0	κ_1	κ_1'	κ_2	κ_3	κ_4	κ_5	κ_5'
$7N-42$	$841-54N$	0.0	0.0	-23.3	30.8	-9.5	15.0

for κ_i obtained from the ruthenium spectra to predict levels in the rhodium isotopes. This prediction is not entirely free of ambiguity since the coefficient κ_0 cannot be fixed from the even–even energy spectra nor can the separate coefficients κ_5 and κ_5' be obtained from it but only the combination $\kappa_5 + \kappa_5'$. Additional information from the odd-mass spectra such as, for example, the doublet splitting in the odd-mass spectra is thus needed to fix all parameters. The result of this (partial) supersymmetric prediction for the rhodium isotopes, with the parameters of Table 3.4, is shown in Fig. 3.8. The figure shows the negative-parity levels relative to the lowest $1/2^-$ which is the ground state only in ^{103}Rh.

An important aspect of the hamiltonian (3.28) is that, although it does not consist of Casimir operators of a single nested chain of algebras and hence is not analytically solvable, it still defines a number of exact quantum numbers besides the total angular momentum J. For example, the algebra $\mathrm{SO}^{\mathrm{B+F}}(3)$ is common to *all* limits of U(6/12) and hence the associated label [$\tilde{L}$ in the classification (3.16)] is a good quantum number of the generalized

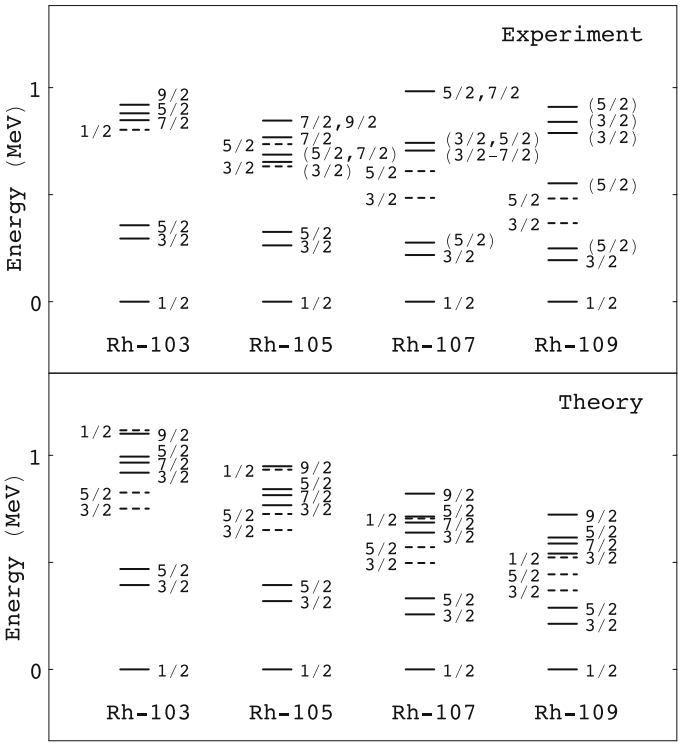

Fig. 3.8. Observed [44] and calculated negative-parity spectra of $^{103-109}$Rh, plotted relative to the lowest $1/2^-$ level. Symmetric states $[N+1, 0]$ are shown as full lines with the angular momentum J on the *right* and non-symmetric states $[N, 1]$ as dashed lines with J on the *left*

hamiltonian (3.28). The same property is valid for $\mathrm{U}^{\mathrm{B+F}}(6)$ and its labels $[N_1, N_2]$. Finally, the algebra $\mathrm{SO}^{\mathrm{B+F}}(5)$ is common to both the $\mathrm{U}^{\mathrm{B+F}}(5)$ and the $\mathrm{SO}^{\mathrm{B+F}}(6)$ limits of U(6/12), and its labels (τ_1, τ_2) are thus good quantum numbers of the hamiltonian (3.28) as long as $\kappa_2 = 0$, that is, as long as the hamiltonian is transitional between $\mathrm{U}^{\mathrm{B+F}}(5)$ and $\mathrm{SO}^{\mathrm{B+F}}(6)$. This is the generalization to odd-mass nuclei of the conservation of SO(5) in the U(5)–SO(6) transition in even–even nuclei, discussed in Sect. 2.2.

On the basis of this argument, all calculated states in Fig. 3.8 can be assigned the quantum numbers $[N_1, N_2]$, (τ_1, τ_2) and $\tilde{L}$, and, in particular, they are either symmetric under U(6), $[N_1, N_2] = [N + 1, 0]$, or non-symmetric, $[N_1, N_2] = [N, 1]$. The structure of the negative-parity levels in the rhodium isotopes above the lowest $1/2^-$ state is essentially determined by two $3/2^-$–$5/2^-$ doublets. The excitation energies of both the symmetric and the non-symmetric doublets are decreasing with increasing neutron number but at a rate that depends on the symmetry character. These features are reproduced by the supersymmetric calculation. Many more levels are observed at or above the excitation energy of the second $3/2^-$–$5/2^-$ doublet but, given the uncertain spin assignments, their theoretical identification is more problematic.

The supersymmetric analysis can also be applied to other nuclear properties such as for instance one-proton transfer strengths. Ideally, to test U(6/12) supersymmetry, the transfer should be between supersymmetric partners. However, in that case a complicated transfer operator must be used, of the form $a^\dagger \tilde{b}$ or $b^\dagger \tilde{a}$, which is poorly known microscopically. A simpler transfer operator is T_{lj} in (3.26) which in the case at hand describes proton pick-up on the palladium toward the rhodium isotopes. The coefficients v_j in the

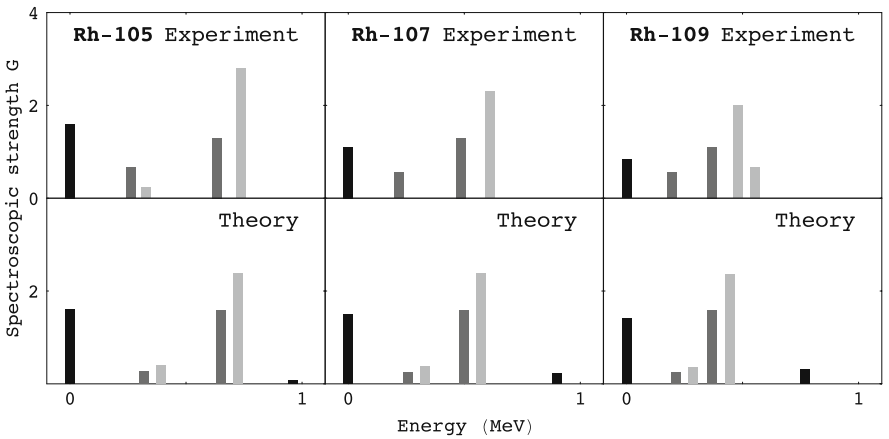

Fig. 3.9. Observed [44] and calculated spectroscopic strengths for the proton pick-up reactions ${}^{A+1}\mathrm{Pd} \rightarrow {}^{A}\mathrm{Rh}$ for $A = 105$, 107 and 109. The spectoscopic strength to the $1/2^-$ (*black*), $3/2^-$ (*dark gray*) and $5/2^-$ (*light gray*) states is shown

operator are the square roots of the occupation probabilities of the different orbits and these are taken as $v^2_{1/2} = 0.90$ and $v^2_{3/2} = v^2_{5/2} = 0.46$. The results of a calculation of this transfer are summarized in Fig. 3.9. A characteristic feature of the data is the concentration of most of the $j = 1/2, 3/2, 5/2$ strength below 1 MeV in the ground state and the two lowest $3/2^-$–$5/2^-$ doublets. This is reproduced by the supersymmetric calculation.

Recently, the idea of supersymmetry without dynamical symmetry was used to describe shape phase transitions in odd-mass nuclei [197]. The approach is based on the consistent-Q formalism for odd-mass nuclei [198]. (In fact, the consistent-Q formalism as presented in Ref. [198] represents the first studied example of a broken dynamical Bose–Fermi symmetry in $\mathrm{U^B}(6) \otimes \mathrm{U^F}(12)$.) Since the U(6/12) supersymmetry implies a relation between even–even (B) and odd-mass (B+F) operators, the hamiltonian of the consistent-Q formalism for even–even nuclei [100] can be generalized in this way to odd-mass nuclei. This supersymmetric hamiltonian was applied to the Os–Hg region which exhibits a prolate–oblate phase transition [103]. The situation can be summarized with the phase diagram shown in Fig. 3.10 which is similar to the corresponding diagram 2.10 for even–even nuclei.

The study [197] also reveals the existence of partial dynamical symmetries of the consistent-Q IBFM hamiltonian; for example, throughout the entire prolate–oblate transition the pseudo-orbital angular momentum $\tilde{L}$, associated with $\mathrm{SO^{B+F}}(3)$ in (3.16) remains a conserved quantum number. This leads to the occurrence of unavoided crossings of levels with different $\tilde{L}$ and the same J values.

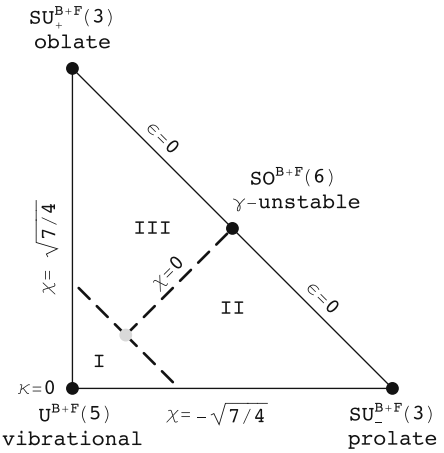

Fig. 3.10. Phase diagram of a schematic consistent-Q IBFM hamiltonian for $\mathrm{U^B}(6) \otimes \mathrm{U^F}(12)$. The *black dots* indicate the location of the Bose–Fermi symmetries and the *gray dot* corresponds to a second-order phase transition between spherical (I) and deformed nuclei with prolate (II) and oblate (III) shapes. The *dashed lines* represent first-order phase transitions

Dynamical symmetries (even approximate ones) do not occur that often in nuclei. If their occurrence is considered as a prerequisite for the existence of a dynamical supersymmetry, examples of the latter will be even more difficult to find. An immediate consequence of the proposal of supersymmetry without dynamical symmetry is that it opens up the possibility of testing supersymmetry in other regions of the nuclear chart.

4 Symmetries with Neutrons and Protons

Atomic nuclei consist of neutrons and protons. This seemingly trivial observation has far-reaching consequences as far as the structure of nuclei is concerned. Neutrons and protons are the elementary building blocks of the nuclear shell model. They are always included in the model, either explicitly or via the formalism of isospin which assigns to each nucleon an intrinsic label $T = 1/2$ with different projections for neutron and proton. While the neutron–proton degree of freedom is an essential part of the shell model, it is not always one of the interacting boson model (IBM). In fact, in the version of the model discussed in Sect. 2.2 no distinction is made between neutrons and protons and all bosons are considered as identical. Nevertheless, to make the model more realistic, it is essential to introduce this distinction. This is the main objective of the present chapter.

In analogy with the isospin of nucleons, the neutron–proton degree of freedom can be introduced in the IBM by assigning an intrinsic label to the bosons. This so-called F spin has, by convention, a projection $M_F = -1/2$ for a neutron boson and $M_F = +1/2$ for a proton boson. This approach gives rise to the simplest version of the boson model that deals with neutrons and protons, the so-called neutron–proton interacting boson model or IBM-2.

Although the IBM-2 is one of the most successful extensions of the boson model, to make contact with the shell model, and, specifically, with the isospin quantum number of that model, more elaborate versions of the IBM are needed. As argued in Sect. 2.2, the s and d bosons of the IBM can be associated with Cooper pairs of nucleons in the valence shell coupled to angular momenta $J = 0$ and $J = 2$. This interpretation constitutes the basis of the connection between the boson and the shell model. A mapping between the two models is rather involved for the *sd* IBM with U(6) dynamical symmetry. A simplified version of the IBM with only s bosons, however, has an immediate connection with the pairing limit of the shell model discussed in Sect. 2.1.1. The s-boson creation and annihilation operators are associated with the operators $S_\pm$ which, together with S_z, form the quasi-spin SU(2) algebra. With use of this correspondence, the pairing interaction between identical nucleons can be mapped *exactly* onto an s-boson hamiltonian.

By analogy, to obtain a better understanding of boson models with neutrons and protons, we should analyze the pairing limit of the shell model with non-identical nucleons. This is done in Sect. 4.1. A shell-model analysis

A. Frank et al., *Symmetries in Atomic Nuclei*,
Springer Tracts in Modern Physics 230, DOI 10.1007/978-0-387-87495-1_4,

of this type forms the basis for a proper formulation of a neutron–proton version of the boson model. With neutrons and protons, as in the case of identical nucleons, the mapping between the shell and the boson model is exact if limited to s bosons. The inclusion of d bosons leads to the most elaborate version of the boson model, known as IBM-4 and presented in Sect.4.2. The microscopic foundation of IBM-4 then allows us to study under what conditions it reduces to its simpler sibling IBM-2, discussed in Sect. 4.3. We conclude the chapter with a detailed analysis of ^{94}Mo as an illustration of the application of neutron–proton symmetries.

4.1 Pairing Models with Neutrons and Protons

In Sect. 2.1.1 we discussed the quasi-spin solution of the pairing problem of n identical nucleons. We assumed that the nucleons occupy a set of degenerate single-particle states in jj coupling, each orbit being characterized by a total (i.e., orbital plus spin) angular momentum j. We begin this section with a brief derivation of similar results in ls coupling, which is more convenient for the subsequent generalization to neutrons and protons.

If all nucleons are of the same kind (either all neutrons or all protons), a nucleon creation operator in ls coupling can be denoted as $a^\dagger_{lm_l sm_s}$. The identical nucleons are assumed to interact through a pairing force of the form

$$V_{\text{pairing}} = -g_0 S^0_+ S^0_-, \tag{4.1}$$

with

$$S^0_+ = \sqrt{\frac{1}{2}} \sum_l \sqrt{2l+1} (a^\dagger_{ls} \times a^\dagger_{ls})^{(00)}_{00}, \qquad S^0_- = \left(S^0_+\right)^\dagger . \tag{4.2}$$

The notation S indicates that these are nucleon pairs coupled to total orbital angular momentum $L = 0$, while the superscript 0 in $S^0_\pm$ refers to the coupled spin $S = 0$. Since the nucleons are identical, only one pair state is allowed by the Pauli principle, namely, the state with antiparallel spins for either neutrons or protons (see Fig. 4.1). Therefore, this pairing mode is called **spin singlet**. The ls-coupled pair operators (4.2) and their jj-coupled analogs (2.4) satisfy the same commutation relations (2.6) if in the former $S^0_z = (n - \Omega)/2$ is taken where n is the nucleon number operator and Ω is the orbital shell size, $\Omega \equiv \sum_l (2l+1)$. The hamiltonian (4.1) can thus be solved analytically by virtue of an SU(2) dynamical symmetry, of the same type as encountered in Sect. 2.1.1. For an even number of nucleons, the lowest eigenstate of (4.1) with $g_0 > 0$ has a condensate structure of the form

$$\left(S^0_+\right)^{n/2} |\mathrm{o}\rangle, \tag{4.3}$$

where $|\mathrm{o}\rangle$ represents the vacuum. As in the jj-coupled case, a conserved quantum number emerges from this analysis which is seniority [46], the number of nucleons not in pairs coupled to $L = 0$.

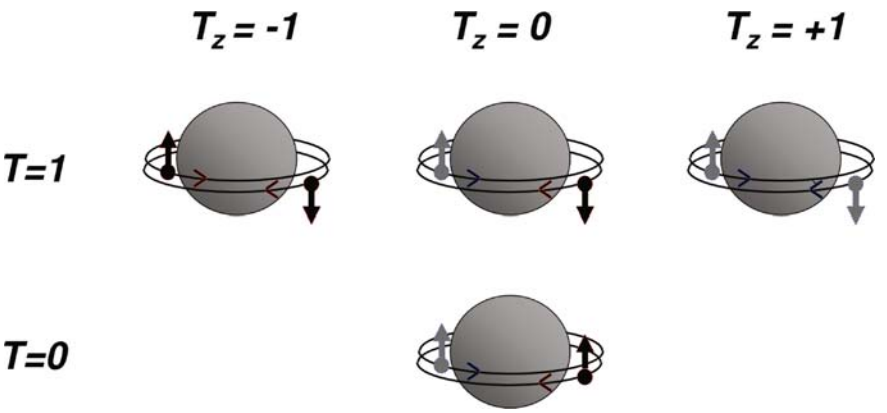

Fig. 4.1. Schematic illustration of the different types of nuclear pairs. The valence neutrons (*grey*) or protons (*black*) that form the pair occupy time-reversed orbits (circling the core of the nucleus in opposite direction). If the nucleons are identical, they must have anti-parallel spins—a configuration which is also allowed for a neutron–proton pair (*top*). The configuration with parallel spin is only allowed for a neutron–proton pair (*bottom*)

Next we consider neutrons and protons. The pairing interaction is assumed to be isospin invariant, which implies that it is the same in the three possible $T = 1$ channels, neutron–neutron, neutron–proton and proton–proton, and that (4.1) can be rewritten as

$$V'_{\text{pairing}} = -g_0 \sum_{\mu} S^{01}_{+,\mu} S^{01}_{-,\mu} \equiv -g_0 S^{01}_{+} \cdot S^{01}_{-}, \tag{4.4}$$

where the dot indicates a scalar product in isospin. In terms of the nucleon operators $a^{\dagger}_{lm_l sm_s tm_t}$, which now carry also isospin indices (with $t = 1/2$), the pair operators are

$$S^{01}_{+,\mu} = \sqrt{\frac{1}{2}} \sum_{l} \sqrt{2l+1} (a^{\dagger}_{lst} \times a^{\dagger}_{lst})^{(001)}_{00\mu}, \qquad S^{01}_{-,\mu} = \left(S^{01}_{+,\mu}\right)^{\dagger}, \tag{4.5}$$

where the superscripts 0 and 1 in $S^{01}_{\pm,\mu}$ refer to the pair's spin $S = 0$ and isospin $T = 1$. The index μ (isospin projection) distinguishes neutron–neutron ($\mu = +1$), neutron–proton ($\mu = 0$) and proton–proton ($\mu = -1$) pairs. There are thus three different pairs with $S = 0$ and $T = 1$ (top line in Fig. 4.1) and they are related through the action of the isospin operators $T_{\pm}$. The dynamical symmetry of the hamiltonian (4.4) is **SO(5)** which makes the problem analytically solvable [199, 200, 201], although in a much more laborious way than in the case of SU(2). The quantum number, besides seniority, that emerges from this analysis is **reduced isospin** [199], which is the isospin of the nucleons not in pairs coupled to $L = 0$.

For a neutron and a proton there exists a different paired state with *parallel* spins (bottom line of Fig. 4.1). The most general pairing interaction

for a system of neutrons and protons thus involves, besides the spin-singlet, also a **spin-triplet** term,

$$V''_{\text{pairing}} = -g_0 S^{01}_{+} \cdot S^{01}_{-} - g'_0 S^{10}_{+} \cdot S^{10}_{-}, \tag{4.6}$$

where the $S = 1, T = 0$ pair operators are defined as

$$S^{10}_{+,\mu} = \sqrt{\frac{1}{2}} \sum_{l} \sqrt{2l+1} (a^{\dagger}_{lst} \times a^{\dagger}_{lst})^{(010)}_{0\mu 0}, \qquad S^{10}_{-,\mu} = \left(S^{10}_{+,\mu}\right)^{\dagger}. \tag{4.7}$$

The index μ is the spin projection in this case and distinguishes the three spatial orientations of the $S = 1$ pair. The pairing hamiltonian (4.6) now involves two parameters g_0 and g'_0, the strength of the spin-singlet and spin-triplet interactions, respectively. Alternatively, since they concern the $T = 1$ and $T = 0$ channels of the pairing interaction, they are referred to as the **isovector** and **isoscalar** components of the pairing interaction. While in the previous cases the single strength parameter g_0 just defines an overall scale, this is no longer true for a generalized pairing interaction. Specifically, solutions with an intrinsically different structure are obtained for different ratios g_0/g'_0.

In general, the eigenproblem associated with the interaction (4.6) can only be solved numerically which, given a typical size of a shell-model space, can be a formidable task. However, for specific choices of g_0 and g'_0 the solution of V''_{pairing} can be obtained analytically [202, 203, 204]. The analysis reveals the existence of a dynamical algebra formed by the pair operators (4.5) and (4.7), their commutators, the commutators of these among themselves and so on until a closed algebraic structure is attained. Closure is obtained by introducing the number operator n, the spin and isospin operators S_μ and T_μ and the Gamow–Teller-like operators $Y_{\mu\nu}$ which are defined in (2.17). In summary, the set of 28 operators consisting of $S^{01}_{\pm,\mu}$ and $S^{10}_{\pm,\mu}$, defined in (4.5) and (4.7), together with the operator $(n - \Omega)/2$ and

$$\begin{aligned} S_\mu &= \sum_l \sqrt{2l+1} (a^{\dagger}_{lst} \times \tilde{a}_{lst})^{(010)}_{0\mu 0}, \\ T_\mu &= \sum_l \sqrt{2l+1} (a^{\dagger}_{lst} \times \tilde{a}_{lst})^{(001)}_{00\mu}, \\ Y_{\mu\nu} &= \sum_l \sqrt{2l+1} (a^{\dagger}_{lst} \times \tilde{a}_{lst})^{(011)}_{0\mu\nu}, \end{aligned} \tag{4.8}$$

forms the algebra **SO(8)** which is thus the dynamical algebra of the problem.

The symmetry character of the interaction (4.6) is obtained by studying the subalgebras of SO(8). Of relevance are the subalgebras $\text{SO}_T(5) \equiv \{S^{01}_{\pm,\mu}, n, T_\mu\}$, $\text{SO}_T(3) \equiv \{T_\mu\}$, $\text{SO}_S(5) \equiv \{S^{10}_{\pm,\mu}, n, S_\mu\}$, $\text{SO}_S(3) \equiv \{S_\mu\}$ and $\text{SO}(6) \equiv \{S_\mu, T_\mu, Y_{\mu\nu}\}$, which can be placed in the following lattice of algebras:

$$\text{SO}(8) \supset \left\{ \begin{array}{c} \text{SO}_S(5) \otimes \text{SO}_T(3) \\ \text{SO}(6) \\ \text{SO}_T(5) \otimes \text{SO}_S(3) \end{array} \right\} \supset \text{SO}_S(3) \otimes \text{SO}_T(3). \tag{4.9}$$

The dynamical symmetries of the SO(8) model. By use of the explicit form of the generators of SO(8) and its subalgebras, and their commutation relations [203], the following relations can be shown to hold:

$$S_+^{01}\cdot S_-^{01} = \frac{1}{2}C_2[\mathrm{SO}_T(5)] - \frac{1}{2}C_2[\mathrm{SO}_T(3)] - \frac{1}{8}(2\Omega - n)(2\Omega - n + 6),$$
$$S_+^{01}\cdot S_-^{01} + S_+^{10}\cdot S_-^{10} = \frac{1}{2}C_2[\mathrm{SO}(8)] - \frac{1}{2}C_2[\mathrm{SO}(6)] - \frac{1}{8}(2\Omega - n)(2\Omega - n + 12),$$
$$S_+^{10}\cdot S_-^{10} = \frac{1}{2}C_2[\mathrm{SO}_S(5)] - \frac{1}{2}C_2[\mathrm{SO}_S(3)] - \frac{1}{8}(2\Omega - n)(2\Omega - n + 6).$$

This shows that the interaction (4.6) in the three cases (i) $g_0 = 0$, (ii) $g_0' = 0$ and (iii) $g_0 = g_0'$ can be written as a combination of Casimir operators of algebras belonging to a chain of *nested* algebras of the lattice (4.9). They are thus the dynamical symmetries of the SO(8) model in the sense explained in Chap. 1. As a consequence, in the three cases $g_0 = 0$, $g_0' = 0$ and $g_0 = g_0'$, eigenvalues are known analytically as a sum of those of the different Casimir operators which are given by

$$\langle C_2[\mathrm{SO}(8)]\rangle_{\omega_1,\omega_2,\omega_3,\omega_4} = \omega_1(\omega_1+6) + \omega_2(\omega_2+4) + \omega_3(\omega_3+2) + \omega_4^2,$$
$$\langle C_2[\mathrm{SO}(6)]\rangle_{\sigma_1,\sigma_2,\sigma_3} = \sigma_1(\sigma_1+4) + \sigma_2(\sigma_2+2) + \sigma_3^2,$$
$$\langle C_2[\mathrm{SO}(5)]\rangle_{\upsilon_1,\upsilon_2} = \upsilon_1(\upsilon_1+3) + \upsilon_2(\upsilon_2+1),$$
$$\langle C_2[\mathrm{SO}(3)]\rangle_R = R(R+1) \text{ with } R = S, T.$$

The above discussion has introduced a large number of labels ω_i, σ_i, υ_i, S and T which are conserved quantum numbers for appropriate values of the pairing strengths g_0 and g_0' in the hamiltonian (4.6). The physical meaning of these labels is as follows. The S and T are the total spin and total isospin. The $\mathrm{SO}_T(5)$ labels (υ_1, υ_2) are known from the SO(5) formalism for $T = 1$ pairing [200]: $\upsilon_1 = 2\Omega - v_t/2$ and $\upsilon_2 = t$, where v_t is the usual seniority and t is the reduced isospin. A similar formalism involving the algebra $\mathrm{SO}_S(5)$ can be developed for $T = 0$ pairing by interchanging the role of S and T and leads to an associated seniority v_s and the concept of reduced spin s which is the spin of the nucleons not in pairs coupled to $L = 0$. The SO(6) labels $(\sigma_1, \sigma_2, \sigma_3)$ characterize a supermultiplet [16]. Because of the isomorphism $\mathrm{SO}(6) \simeq \mathrm{SU}(4)$, they are equivalent to SU(4) labels, the correspondence being given by

$$\sigma_1 = \frac{1}{2}(\lambda + 2\mu + \nu), \qquad \sigma_2 = \frac{1}{2}(\lambda + \nu), \qquad \sigma_3 = \frac{1}{2}(\lambda - \nu),$$

where (λ, μ, ν) are defined in Eq. (3.19). Finally, the SO(8) labels $(\omega_1, \omega_2, \omega_3, \omega_4)$ are known from the solution of the full pairing problem [203]. In particular, $\omega_1 = \Omega - v/2$ and the remaining three labels are the reduced supermultiplet labels (i.e., the supermultiplet labels of the nucleons not in pairs coupled to $L = 0$).

The lattice (4.9) permits the determination of the symmetry structure of this model (see Box on The dynamical symmetries of the SO(8) model). The important point to retain from that discussion is that a whole set of quantum numbers exists that are conserved for particular combinations of the pairing strengths in the hamiltonian (4.6). It will be shown in the next section that a boson model can be constructed which has dynamical symmetries with equivalent labels and that in these symmetry limits an *exact* mapping can be established between its boson states and a *subset* of the fermion states of the SO(8) model. Specifically, the subset in question contains only seniority-zero states with all nucleons in pairs coupled to angular momentum zero. (Such states occur in even–even and odd–odd but not in odd-mass nuclei.) It can be shown [205] that for an attractive pairing interaction ($g_0, g_0' > 0$) the lowest-energy states have seniority zero in two of the three limits, namely in the isovector pairing ($g_0' = 0$) and in the equal pairing ($g_0 = g_0'$) limits.

Since a realistic shell-model hamiltonian has values $g_0 \approx g_0'$ [206], the analytic solution obtained for $g_0 = g_0'$ should be the correct starting point for nuclei and we consider this limit to illustrate the connection between the SO(8) model and the IBM. The seniority-zero eigenstates of the pairing hamiltonian (4.6) with $g_0 = g_0'$ carry the following labels:

$$\begin{array}{ccccccc} \mathrm{SO}(8) & \supset & \mathrm{SO}(6) & \supset & \mathrm{SO}_S(3) \otimes \mathrm{SO}_T(3) & & \\ \downarrow & & \downarrow & & \downarrow & \downarrow & \\ (\Omega, 0, 0, 0) & & (\sigma_1, 0, 0) & & S & T & \end{array} , \tag{4.10}$$

where σ_1 is the first of the SO(6) labels, the others being necessarily zero for $v = 0$. The energies of these eigenstates are

$$E(n, \Omega, \sigma_1) = -\frac{g_0}{8}[n(4\Omega - n + 12) - 4\sigma_1(\sigma_1 + 4)]. \tag{4.11}$$

In the next section we will derive the corresponding results in the IBM and in this way establish its connection with the SO(8) model.

We conclude this section with a brief discussion of the nature of SO(8) superfluidity in the specific example of the ground state of $N = Z$ nuclei. In the SO(6) limit of the SO(8) model the exact ground-state solution can be written as [207]

$$\left(S_+^{01} \cdot S_+^{01} - S_+^{10} \cdot S_+^{10}\right)^{n/4} |\mathrm{o}\rangle. \tag{4.12}$$

This shows that the superfluid solution acquires a *quartet* structure in the sense that it reduces to a condensate of bosons each of which corresponds to four nucleons. Since the boson in (4.12) is a scalar in spin and isospin, it can be thought of as an α particle; its orbital character, however, might be different from that of an actual α particle. A quartet structure is also present in the two SO(5) limits of the SO(8) model, which yields a ground-state wave function of the type (4.12) with either the first or the second term suppressed. Thus, a reasonable *ansatz* for the $N = Z$ ground-state wave function of the SO(8) pairing interaction (4.6) with arbitrary strengths g_0 and g_0' is

$$\left(\cos\theta\ S_+^{01}\cdot S_+^{01} - \sin\theta\ S_+^{10}\cdot S_+^{10}\right)^{n/4}|\mathrm{o}\rangle, \tag{4.13}$$

where θ is a parameter that depends on the ratio g_0/g_0'.

The condensate (4.13) of α-like particles provides an excellent approximation to the $N = Z$ ground state of the pairing hamiltonian (4.6) for any combination of g_0 and g_0'. Nevertheless, it should be stressed that, in the presence of both neutrons and protons in the valence shell, the pairing hamiltonian (4.6) is *not* a good approximation to a realistic shell-model hamiltonian which contains an important quadrupole component. Consequently, any model based on $L = 0$ fermion pairs (or s bosons) only, remains necessarily schematic in nature. A realistic model should include also $L \neq 0$ pairs or, equivalently, go beyond an s-boson approximation.

4.2 Interacting Boson Models with Neutrons and Protons

The IBM was originally proposed as a phenomenological model in which the precise relation between the bosons and the actual neutrons and protons in the nucleus was not specified. The recognition that the bosons can be identified with Cooper pairs of valence nucleons coupled to angular momenta $J = 0$ or $J = 2$ made it apparent that a connection between the boson and shell models required an explicit distinction between neutrons and protons. Consequently, an extended version of the model was proposed by Arima et al. [208] in which this distinction was made, referred to as IBM-2, as opposed to the original version of the model, IBM-1.

If neutrons and protons occupy different valence shells, it seems natural to assume correlated neutron–neutron and proton–proton pairs and to include the neutron–proton interaction explicitly between both types of pairs. Since in the nuclear shell model the strongest component of the neutron–proton interaction is of quadrupole character [209], it is natural to make a similar assumption for the interaction between the bosons. If the neutrons and protons occupy the same valence shell, this approach is no longer valid since there is no reason not to include the $T = 1$ neutron–proton pair. This is what Elliott and White proposed in Ref. [210] and the ensuing model was called IBM-3. Because the IBM-3 includes the complete $T = 1$ triplet, it can be made isospin invariant enabling a more direct comparison with the shell model. All bosons included in IBM-3 have $T = 1$ and, in principle, other bosons can be introduced that correspond to $T = 0$ neutron–proton pairs. This further extension (referred to as IBM-4) has indeed been proposed by Elliott and Evans [211]; it can be considered as the most elaborate version of the IBM.

For the purpose of establishing a connection with the shell model, the IBM-4 is the most natural model because it allows the construction of state vectors with many of the labels that are encountered in fermionic systems. However, the full IBM-4 with s and d bosons is a rather complicated model.

Therefore, we begin by investigating the properties of a boson model that only includes bosons which have orbital angular momentum $L = 0$ and have the spin–isospin combinations $(S, T) = (0, 1)$ and (1,0). These are exactly the quantum numbers of the fermion pairs of the SO(8) model discussed in the previous section and our main objective in the first part of this section is to show the connection between both schematic models. Subsequently, in the second part, bosons with orbital angular momentum $L \neq 0$ are introduced.

4.2.1 *s* Bosons Only

The elementary bosons of an $L = 0$ IBM-4 are s^{01} which is scalar in spin and vector in isospin and s^{10} which is vector in spin and scalar in isospin. To simplify notation superscripts are suppressed; instead, the first boson is denoted as s and the second as p. Since both bosons have orbital angular momentum $L = 0$, all states always have $L = 0$ and there is no need to indicate L in this section.

The dynamical algebra of this $L = 0$ IBM-4 consists of the generators

$$\begin{aligned}
&N_s = \sqrt{3}(s^\dagger \times \tilde{s})^{(00)}_{00}, \qquad T_\mu = \sqrt{2}(s^\dagger \times \tilde{s})^{(01)}_{0\mu}, \qquad Q^s_\mu = (s^\dagger \times \tilde{s})^{(02)}_{0\mu}, \\
&N_p = \sqrt{3}(p^\dagger \times \tilde{p})^{(00)}_{00}, \qquad S_\mu = \sqrt{2}(p^\dagger \times \tilde{p})^{(10)}_{\mu 0}, \qquad Q^p_\mu = (p^\dagger \times \tilde{p})^{(20)}_{\mu 0}, \\
&Y^+_{\mu\nu} = (s^\dagger \times \tilde{p} + p^\dagger \times \tilde{s})^{(11)}_{\mu\nu}, \qquad Y^-_{\mu\nu} = (s^\dagger \times \tilde{p} - p^\dagger \times \tilde{s})^{(11)}_{\mu\nu},
\end{aligned} \tag{4.14}$$

where the coupling is in spin and isospin, respectively. The $\tilde{s}$ and $\tilde{p}$ operators transform as vectors in isospin and spin space, respectively, $\tilde{s}_\mu = (-)^{1-\mu} s_{-\mu}$ and $\tilde{p}_\mu = (-)^{1-\mu} p_{-\mu}$. The operators (4.14) are 36 in number and they form the algebra U(6).

Two meaningful limits of U(6) which conserve spin and isospin can be defined with the following lattice:

$$\mathrm{U}(6) \supset \left\{ \begin{array}{c} \mathrm{U}_s(3) \otimes \mathrm{U}_p(3) \\ \mathrm{SU}(4) \end{array} \right\} \supset \mathrm{SO}_s(3) \otimes \mathrm{SO}_p(3), \tag{4.15}$$

where the algebras are defined as $\mathrm{U}_s(3) = \{N_s, T_\mu, Q^s_\mu\}$, $\mathrm{SO}_s(3) = \{T_\mu\}$, $\mathrm{U}_p(3) = \{N_p, S_\mu, Q^p_\mu\}$, $\mathrm{SO}_p(3) = \{S_\mu\}$ and $\mathrm{SU}(4) = \{T_\mu, S_\mu, Y^+_{\mu\nu}\}$. An alternative SU(4) algebra can be defined with $Y^-_{\mu\nu}$ instead of $Y^+_{\mu\nu}$. The hamiltonians associated with these two different choices have the same eigenspectrum but differ through phases in their eigenfunctions. This is yet another example of the parameter symmetries mentioned in Sect. 3.2 and is similar to the existence of the $\mathrm{SO}_+(6)$ and $\mathrm{SO}_-(6)$ limits of IBM-1 [212].

The analysis of this model may now proceed in the usual fashion [213]. This involves constructing the most general hamiltonian with single-boson energies and two-body interactions between the s and the p bosons and showing that it can be rewritten in terms of Casimir operators of the algebras in the lattice (4.15). Furthermore, for certain energies and interactions this hamiltonian can be written in terms of Casimir operators belonging to a chain of

nested algebras in the lattice (4.15) in which case it can be solved analytically with the techniques discussed in Chap. 1.

For the purpose of the present discussion we highlight a few aspects of this model. The first illustrates the relation between IBM-3 which involves isovector bosons only and IBM-4 which is constructed from both isoscalar and isovector bosons. The states of IBM-3 clearly are a subset of those in IBM-4 and a precise relation between them can be established [214] via one of the classifications in the lattice (4.15), namely

$$\begin{array}{ccccccc} \mathrm{U}(6) & \supset & \mathrm{U}_S(3) \otimes \mathrm{U}_T(3) & \supset & \mathrm{SO}_S(3) \otimes \mathrm{SO}_T(3) \\ \downarrow & & \downarrow \quad \downarrow & & \downarrow \quad \downarrow & & \downarrow \quad , \\ [N] & & [N_p] \quad [N_s] & & S & & T \end{array} \tag{4.16}$$

where N is the total number of bosons and N_p and N_s are the separate numbers of p and s bosons with $N = N_p + N_s$. States belonging to IBM-3 have no p bosons, $N_p = 0$. The implication of this statement is that removing all $N_p \neq 0$ states from the spectrum (e.g., through a large positive p-boson energy) essentially reduces IBM-4 to IBM-3. Consequently, the second classification of the lattice (4.15),

$$\begin{array}{ccccc} \mathrm{U}(6) & \supset & \mathrm{SU}(4) & \supset & \mathrm{SO}_S(3) \otimes \mathrm{SO}_T(3) \\ \downarrow & & \downarrow & & \downarrow \quad \downarrow \quad , \\ [N] & & (0, \mu, 0) & & S \quad T \end{array} \tag{4.17}$$

is specific to IBM-4 and cannot be realized in IBM-3 because a state (4.17), written in the basis (4.16), in general can have $N_p \neq 0$ components. Another way of stating the same result is that any boson realization of Wigner's supermultiplet symmetry must necessarily involve $T = 0$ *and* $T = 1$ bosons. In fact, it must do so with both bosons treated on an equal footing.

A second aspect concerns the microscopic foundation of the IBM. In the limit of equal isoscalar and isovector pairing strengths, the link between the shell and the boson models is particularly simple to establish. Comparison of the IBM-4 classification (4.17) and the classification (4.10) of the neutron–proton pairing model provides the connection. The IBM-4 hamiltonian in the SU(4) limit,

$$H = \kappa_0 C_1[\mathrm{U}(6)] + \kappa_0' C_2[\mathrm{U}(6)] + \kappa\, C_2[\mathrm{SU}(4)], \tag{4.18}$$

has the eigenvalues

$$E(N, \mu) = \kappa_0 N + \kappa_0' N(N+5) + \kappa\, \mu(\mu+4). \tag{4.19}$$

Since the boson number N is half the number of nucleons, $N = n/2$, and the SU(4) labels $(0, \mu, 0)$ correspond to the SO(6) labels $(\sigma_1, 0, 0)$, the choice of parameters

$$\kappa_0 = -(2\Omega + 11)\frac{g_0}{2}, \qquad \kappa_0' = \frac{g_0}{2}, \qquad \kappa = \frac{g_0}{2}, \tag{4.20}$$

leads to *exactly* the energy expression (4.11) in the SO(6) limit of the SO(8) model. Similarly, the $U_s(3) \otimes U_p(3)$ limit of U(6) can be mapped onto the two SO(5) limits of SO(8) through two different choices of parameters. This, in fact, is a generic result and we see that, through the use of symmetries, the fermionic shell model can be connected to the bosonic IBM, hence providing a miscroscopic foundation of the latter in terms of the former.

If departures are allowed from the exact symmetry limits, conserved quantum numbers cannot any longer be used to establish a connection, which then must be found with some mapping technique. There exists a rich and varied literature [215] on general procedures to carry out boson mappings in which pairs of fermions are represented as bosons. They fall into two distinct classes. In the first one establishes a correspondence between boson and fermion operators by requiring them to have the same commutation relations. In the second class the correspondence is established between state vectors in both spaces. In each case further subclasses exist that differ in their technicalities (e.g., the nature of the operator expansion or the hierarchy in the state correspondence). In the specific example at hand, namely the mapping from the shell model to the IBM, the most successful procedure is the so-called Otsuka–Arima–Iachello (OAI) mapping [89] which associates state vectors based on a seniority hierarchy in fermion space with state vectors based on a U(5) hierarchy in boson space. It has been used in highly complex situations that go well beyond the simple version of IBM with just identical s and d bosons. Its success has been limited to nuclei close to the U(5) limit which can be understood from the fact that deformation breaks the seniority classification. In the case of the SO(8) model, a Dyson mapping (of the first class mentioned above) has been carried out to connect it to an $L = 0$ IBM-4 [207]. This analysis confirms the results obtained here in the symmetry limits of the SO(8) model and can be applied to any SO(8) hamiltonian [213].

4.2.2 *s* and *d* Bosons

The logical extension of the $L = 0$ boson model discussed in Sect. 4.2.1 is to assume the same spin–isopin structure for the bosons, $(S, T) = (0, 1)$ and (1,0), and to extend the orbital structure to include $L = 2$. The total set of bosons in this *sd* IBM-4 is shown in Table 4.1 where the conventional spectroscopic notation $^{2S+1}L_J$ is also indicated. Note that there is now an unambiguous distinction between the boson orbital angular momentum L and the total angular momentum J. In the simpler versions IBM-1,2,3 the bosons have no intrinsic spin and the total angular momentum J necessarily coincides with L.

There are several reasons for including also $T = 0$ bosons. One justification is found in the LS-coupling limit of the nuclear shell model, where the two-particle states of lowest energy have orbital angular momenta $L = 0$ and $L = 2$ with $(S, T) = (0, 1)$ or (1,0) (see Table 2.2). In addition, the choice of

Table 4.1. Enumeration of bosons in the IBM-4

L	S	J	T	M_T	Operator
0,2	0	0,2	1	-1	$s^\dagger_\nu, d^\dagger_\nu$
0,2	0	0,2	1	0	$s^\dagger_\delta, d^\dagger_\delta$
0,2	0	0,2	1	$+1$	$s^\dagger_\pi, d^\dagger_\pi$
0	1	1	0	0	$\theta'^\dagger_1$ $(^3S_1)$
2	1	1	0	0	$\theta^\dagger_1$ $(^3D_1)$
2	1	2	0	0	$\theta^\dagger_2$ $(^3D_2)$
2	1	3	0	0	$\theta^\dagger_3$ $(^3D_3)$

bosons in IBM-4 allows a boson classification containing Wigner's supermultiplet algebra SU(4). This was explicitly shown in Sect. 4.2.1 for the $L = 0$ IBM-4 and it remains true if d bosons are considered. These qualitative arguments in favor of IBM-4 have been corroborated by quantitative, microscopic studies in even–even [216] and odd–odd [217] *sd*-shell nuclei.

The IBM-4 classification that conserves orbital angular momentum L, intrinsic spin S and isospin T, reads

$$\begin{array}{ccccccc} \mathrm{U}(36) \supset & \Big(\mathrm{U}(6) & \supset \cdots \supset & \mathrm{SO}(3)\Big) & & & \\ \downarrow & \downarrow & & \downarrow & & & \\ [N] & [N_1,\ldots,N_6] & & L & & & \\ & \otimes & \Big(\mathrm{U}(6) & \supset \mathrm{SU}(4) & \supset \mathrm{SO}(3) & \otimes \mathrm{SO}(3)\Big) & \\ & & \downarrow & \downarrow & \downarrow & \downarrow & \\ & & [N_1,\ldots,N_6] & (\lambda,\mu,\nu) & S & T & \end{array} , \tag{4.21}$$

where the dots refer to one of the possible reductions of U(6). To analyze this coupling scheme, it is helpful to compare it to the fermion supermultiplet classification, which is given in Table 2.2 for one and two particles in the *sd* shell. The corresponding problem for *bosons* is worked out in Table 4.2. The essential point to note here is that, of the two SU(4) representations $(0,1,0)$ and $(2,0,0)$ that occur for two fermions, the first one is also the fundamental (or one-boson) representation in the boson classification.

Table 4.2. Classification of one and two boson(s) in IBM-4

N	$[N_1,\ldots,N_6]$	L	(λ,μ,ν)	(S,T)
1	$[1]$	$0,2$	$(0,1,0)$	$(0,1),(1,0)$
2	$[2,0]$	$0^2,2^2,4$	$(0,2,0)$	$(0,0),(0,2),(1,1),(2,0)$
			$(0,0,0)$	$(0,0)$
	$[1,1]$	$1,2,3$	$(1,0,1)$	$(0,1),(1,0),(1,1)$

The starting point of the IBM-4 is thus a truncation of the shell model which preserves the labels (λ, μ, ν), S, L, J and T of an LS-coupling scheme in the shell model. A crucial aspect of the IBM-4 is that it does *not* require the exact validity of such quantum numbers in the shell model for carrying out the mapping to the boson space. An example of this flexibility is provided by the pseudo-LS coupling scheme discussed in Sect. 2.1.2. Neither the orbital angular momentum L nor the spin S are good quantum numbers in this coupling scheme. Nevertheless, the *pseudo*-orbital angular momentum $\tilde{L}$ and the *pseudo*-spin $\tilde{S}$ are conserved and *they* can be mapped onto the corresponding boson classification (4.21). This provides an explicit example in which the labels L and S in (4.21) do *not* correspond to the fermionic orbital angular momentum and intrinsic spin. In particular, the L and S associated with a single boson should *not* be thought of as the orbital angular momentum and the spin of a pair of fermions but rather as effective labels in fermion space which acquire an exact significance in terms of bosons. A similar argument holds for the Wigner supermultiplet labels (λ, μ, ν). In contrast, the label T in (4.21) does correspond to the total isospin, and this is so as long as isospin is an exact dynamical symmetry in the fermion space.

In the IBM-3 there are three kinds of bosons (ν, δ and π) each with six components and, as a result, an N-boson state belongs to the symmetric representation $[N]$ of U(18). It is possible to construct IBM-3 states that have good total angular momentum (denoted by L, as in IBM-1 and IBM-2) and good total isospin T via the classification

$$\begin{array}{ccccccc} \mathrm{U}(18) \supset & \Big(\mathrm{U}(6) & \supset \cdots \supset & \mathrm{SO}(3) \Big) & & & \\ \downarrow & \downarrow & & \downarrow & & & \\ [N] & [N_1, N_2, N_3] & & L & & & \\ \otimes & \Big(\mathrm{U}(3) & \supset & \mathrm{SU}(3) & \supset & \mathrm{SO}(3) \Big) & \\ & \downarrow & & \downarrow & & \downarrow & \\ & [N_1, N_2, N_3] & & (\lambda, \mu) & & T & \end{array} \quad . \tag{4.22}$$

Overall symmetry of the N-boson wavefunction requires the representations of U(6) and U(3) to be identical. Consequently, the allowed U(6) representations can have up to three rows in contrast to IBM-1 where the representations necessarily are symmetric. The SU(3) representations are denoted in Elliott's notation of Sect. 2.1.2, $\lambda = N_1 - N_2, \mu = N_2 - N_3$, and determine the allowed values of the isospin T of the bosons. Thus the choice of a particular spatial boson symmetry $[N_1, N_2, N_3]$ determines the allowed isospin values T.

The classification of dynamical symmetries of IBM-3, of which (4.22) is but an example, is rather complex and as yet their analysis is incomplete. The cases with dynamical SU(3) charge symmetry [corresponding to (4.22)] were studied in detail in Ref. [218]. Other classifications that conserve L and T [but not charge SU(3)] were proposed and analyzed in Refs. [219, 220].

The δ or neutron–proton boson plays an essential role in the construction of states with good isospin. To illustrate this we consider the example of a state consisting of two s bosons coupled to isospin $T = 0$, which is a boson representation of a two-neutron–two-proton state with seniority $v = 0$. If the isospin components of the bosons are written explicitly, $(s^\dagger \times s^\dagger)^{(0)}_0 = \sum_\mu (1\mu\ 1-\mu|00) s^\dagger_\mu s^\dagger_{-\mu}$, the two-boson state can be rewritten as

$$|s^2; T = 0\rangle = \sqrt{\frac{2}{3}}|s_\nu s_\pi\rangle - \sqrt{\frac{1}{3}}|s^2_\delta\rangle, \tag{4.23}$$

which shows that a sizeable fraction (33 %) involves δ bosons. This remains true for many-particle states but with the size of the δ component depending on the number of neutrons and protons [221]. Nuclei with $N \sim Z$ have comparable numbers of neutrons and protons in the valence shell and have important δ admixtures at low energies. These decrease in importance as the neutron excess increases. In fact, if the neutrons are holes (i.e., fill more than half the valence shell) and the protons are particles, the δ admixtures vanish in the limit of large shell size [222]. In this case IBM-2 states approximately have good isospin. In heavier nuclei where neutrons and protons occupy different valence shells, IBM-2 states have isospin $T = (N-Z)/2$ and this result is exact insofar that the assumption of different valence shells for neutrons and protons is valid [223]. The application of the IBM-3 and IBM-4 is thus restricted to nuclei where neutrons and protons occupy the same valence shell and where they are all particles or all holes. In all other situations the simpler IBM-2 approach can be used which is discussed in the next section.

4.3 The Interacting Boson Model-2

In the IBM-2 the total number of bosons N is the sum of the neutron and proton boson numbers, N_ν and N_π, which are conserved separately. The algebraic structure of IBM-2 is a product of U(6) algebras,

$$\mathrm{U}_\nu(6) \otimes \mathrm{U}_\pi(6), \tag{4.24}$$

consisting of neutron $b^\dagger_{\nu lm} b_{\nu l' m'}$ and proton $b^\dagger_{\pi lm} b_{\pi l' m'}$ generators. The model space of IBM-2 is the product of symmetric representations $[N_\nu] \times [N_\pi]$ of $\mathrm{U}_\nu(6) \otimes \mathrm{U}_\pi(6)$. In this model space the most general, (N_ν, N_π)-conserving, rotationally invariant IBM-2 hamiltonian must be diagonalized.

The IBM-2 gives a successful phenomenological description of low-energy collective properties of virtually all medium-mass and heavy nuclei. A comprehensive review of the model and its implications for nuclear structure can be found in Ref. [224]. The classification and analysis of its symmetry limits are considerably more complex than the corresponding problem in IBM-1 but are known for the most important limits which are of relevance in the analysis of nuclei [225].

For the present purpose we highlight the two main features of the IBM-2. The first is that the existence of two kinds of bosons offers the possibility to assign an F**-spin** quantum number to them, $F = 1/2$, the boson being in two possible charge states with $M_F = -1/2$ for neutrons and $M_F = +1/2$ for protons [89]. Formally, F spin is defined by the algebraic reduction

$$\begin{array}{ccccc} \mathrm{U}(12) \supset & \mathrm{U}(6) & \otimes & \mathrm{U}(2) & \\ \downarrow & \downarrow & & \downarrow & , \\ [N] & [N-f,f] & & [N-f,f] & \end{array} \tag{4.25}$$

and with $2F$ the difference between the Young-tableau labels that characterize U(6) or U(2), $F = [(N-f)-f]/2 = (N-2f)/2$. The algebra U(12) consists of the generators $b^\dagger_{\rho lm} b_{\rho' l' m'}$, with $\rho, \rho' = \nu$ or π, which also includes operators that change a neutron boson into a proton boson or vice versa ($\rho \neq \rho'$). Under this algebra U(12) bosons behave symmetrically; as a result the representations of U(6) and U(2) are identical.

The mathematical structure of F spin is entirely similar to that of isospin. An F-spin SU(2) algebra [which is a subalgebra of U(2) in (4.25)] can be defined which consists of the diagonal operator $F_z = (-N_\nu + N_\pi)/2$ and the raising and lowering operators $F_\pm$ that transform neutron bosons into proton bosons or vice versa. These are the direct analogs of the isospin generators T_z and $T_\pm$ and they can be defined in an entirely similar fashion (see Sect. 1.1.6). The physical meaning of F spin and isospin is different, however: the mapping onto the IBM-2 of a shell-model hamiltonian with isospin symmetry does not necessarily yield an F-spin conserving hamiltonian. Conversely, an F-spin conserving IBM-2 hamiltonian may or may not have eigenstates with good isospin. In fact, if the neutrons and protons occupy different shells, so that the bosons are defined in different shells, then *any* IBM-2 hamiltonian has eigenstates that correspond to shell-model states with good isospin, irrespective of its F-spin symmetry character. If, on the other hand, neutrons and protons occupy the same shell, a general IBM-2 hamiltonian does *not* lead to states with good isospin. The isospin symmetry violation is particularly significant in nuclei with approximately equal numbers of neutrons and protons ($N \sim Z$) and requires the consideration of IBM-3, discussed in the previous section. As the difference between the numbers of neutrons and protons in the same shell increases, an approximate equivalence of F spin and isospin is recovered [222] and the need for IBM-3 disappears.

Just as isobaric multiplets of nuclei are defined through the connection implied by the raising and lowering operators $T_\pm$, F-spin multiplets can be defined through the action of $F_\pm$ [226]. The states connected are in nuclei with $N_\nu + N_\pi$ constant; these can be isobaric (constant nuclear mass number A) or may differ by multiples of α particles, depending on whether the neutron and proton bosons are of the same or of a different type (which refers to their particle- or hole-like character).

There exists also a close analogy between F spin and I spin, the particle–hole boson exchange symmetry discussed in Sect. 2.2.4. While the F-spin

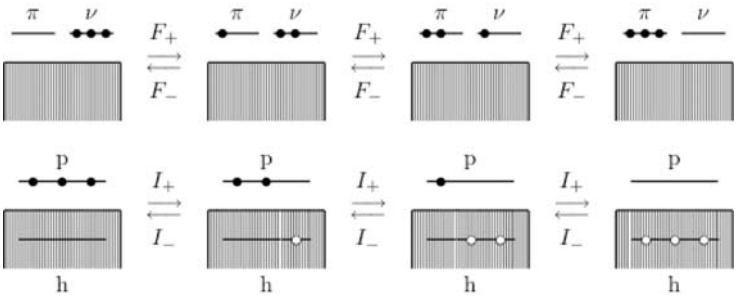

Fig. 4.2. Schematic illustration of the action of the F-spin and I-spin raising and lowering operators on a system of $N = 3$ bosons, where N is either the number of neutron plus proton bosons, $N = N_\nu + N_\pi$, or the number of particle plus hole bosons, $N = N_\mathrm{p} + N_\mathrm{h}$

raising and lowering operators transform neutron into proton bosons and vice versa, the corresponding I-spin operators connect particle and hole bosons. As an example, the action of the F-spin raising and lowering operators $F_\pm$ is illustrated in Fig. 4.2 and compared to the corresponding actions of $I_\pm$. In both cases the total number of bosons is conserved; in an F-spin multiplet this sum is made up from proton and neutron bosons, while in an I-spin multiplet it consists of particle and hole bosons.

In spite of the formal equivalence between F-spin and I-spin multiplets, there is one difference in their application which can be made clear from Fig. 4.2. Action of $F_\pm$ on the ground state of a nucleus in an F-spin multiplet leads to the ground state of another member of the multiplet. This is not necessarily so in an I-spin multiplet: the action of I_+ on the three particle bosons on the left-hand side leads to a 2p–1h boson state which is an excited configuration in a nucleus with a pair of nucleons in the valence shell. In this respect I-spin multiplets are akin to isobaric multiplets.

The empirical evidence for F-spin multiplets of nuclei is illustrated with the following example.

Example: Evidence for F-spin multiplets of nuclei. The relation between levels belonging to an F-spin multiplet depends on the F-spin symmetry character of the hamiltonian which comes down to a question of IBM-2 phenomenology. Specifically, a hamiltonian with an F-spin symmetry satisfies

$$[H, F_z] = [H, F_\pm] = 0.$$

This implies, among other things, that all nuclei in an F-spin multiplet have equal binding energies. This clearly is inappropriate and the condition should be relaxed to one of a *dynamical* F-spin symmetry,

$$[H, F^2] = [H, F_z] = 0,$$

which still implies a classification in terms of F and M_F but now with non-degenerate ground-state energies given by

$$E_{\rm gs}(M_F) = \kappa_0 + \kappa_1 M_F + \kappa_2 M_F^2.$$

This is the direct analog of the isobaric multiplet mass equation discussed in Chap. 1, and therefore can be called an 'F-spin multiplet mass equation' or FMME. (A related approach to predict nuclear binding energies based on F-spin symmetry was proposed in Ref. [227]). In addition, the excitation spectra of the $F = F_{\rm max}$ states of nuclei belonging to an F-spin multiplet are identical for a hamiltonian with a dynamical F-spin symmetry.

Empirical evidence for F-spin multiplets has thus two aspects: (i) To what extent can ground-state binding energies be described by the FMME? (ii) Are low-energy excitation spectra of F-spin multiplet nuclei identical?

The first aspect is illustrated in Table 4.3 where the experimental [55] binding energies of nuclei belonging to an F-spin multiplet with $N_\nu + N_\pi = 12$ are compared to results obtained with the FMME. The table also gives the differences Δ between the measured binding energies and those obtained with the FMME.

The second aspect is illustrated in Fig. 4.3 which shows the observed excitation spectra [44] of the nuclei in the same $N_\nu + N_\pi = 12$ F-spin multiplet [226]. With some exceptions levels are seen to be constant in energy as implied by a dynamical F-spin symmetry. One exception concerns the first-excited 0^+ level; its peculiar behavior, at variance with the ground-band states, may have an interpretation that invokes the concept of a partial

Table 4.3. Observed [55] and calculated binding energies of the ground states of nuclei in an F-spin multiplet with $N_\nu + N_\pi = 12$

				Binding energy[a]			
Nucleus	N_ν	N_π	F_z	Expt	Error	FMME[b]	Δ
^{156}Dy	4	8	2	1278.020	0.007	1278.003	−0.017
^{160}Er	5	7	1	1304.270	0.024	1304.301	+0.031
^{164}Yb	6	6	0	1329.954	0.016	1329.969	+0.015
^{168}Hf	7	5	−1	1355.013	0.028	1355.007	−0.006
^{172}W	8	4	−2	1379.470	0.028	1379.415	−0.055
^{176}Os	9	3	−3	1403.191	0.028	1403.193	+0.002
^{180}Pt	10	2	−4	1426.250	0.011	1426.341	+0.091
^{184}Hg	11	1	−5	1448.884	0.010	1448.859	−0.025

[a] In units of MeV.
[b] With parameters $\kappa_0 = 1329.969$ $\kappa_1 = -25.353$, $\kappa_2 = -0.315$, in MeV.

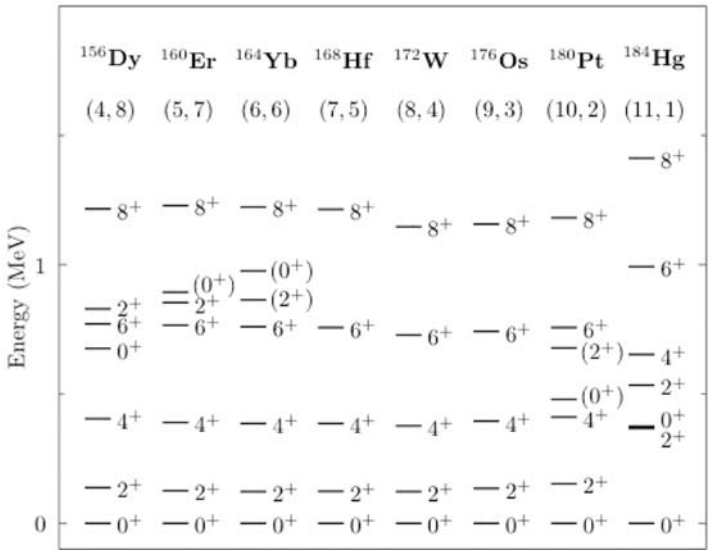

Fig. 4.3. Observed [44] spectra of nuclei belonging to an F-spin multiplet with $N_\nu + N_\pi = 12$. Underneath each isotope label the neutron and proton boson numbers (N_ν, N_π) are given. Levels are labeled by their angular momentum and parity J^π.

dynamical F-spin symmetry. Similarly, it is seen that the spectrum of ^{184}Hg strongly differs from that of all other isotopes in the F-spin multiplet; this is a result of the propinquity of the $Z = 82$ shell closure which makes the excitations of that particular isotope less collective.

The phenomenology of F-spin multiplets is similar to that of isobaric multiplets [21] but for one important difference. The nucleon–nucleon interaction favors spatially symmetric configurations and consequently nuclear excitations at low energy generally have $T = T_{\min} = |(N - Z)/2|$. Boson–boson interactions also favor spatial symmetry but that leads to low-lying levels with $F = F_{\max} = (N_\nu + N_\pi)/2$. As a result, in the case of an F-spin multiplet a relation is implied between the low-lying spectra of the nuclei in the multiplet, while an isobaric multiplet (with $T \geq 1$) involves states at higher excitation energies in some nuclei.

The second important aspect of IBM-2 is that it predicts states which are additional to those found in IBM-1. Their structure can be understood in terms of the F-spin classification (4.25). States with maximal F spin, $F = N/2$, are symmetric in U(6) and are the exact analogs of IBM-1 states. The next class of states has $F = N/2 - 1$ and these are no longer symmetric in U(6) but belong to its representation $[N - 1, 1]$. Such states were studied theoretically in 1984 by Iachello [228] and since then have been observed in many nuclei (see Sect. 4.4).

The existence of these states with **mixed symmetry** (MS), excited in a variety of reactions, is by now well established, at least in even–even nuclei. The pattern of the lowest symmetric and mixed-symmetric states is shown in Fig. 4.4. The spectra are obtained with a reasonable choice of parameters in the three limits of IBM-2 in which F spin is a conserved quantum number [225]. In those limits the correspondence between the symmetric states $[N]$ of IBM-2 and all states of IBM-1 is exact. The figure also shows the lowest $[N-1,1]$ states with angular momentum and parity 1^+, 2^+ and 3^+ and their expected energies in the three limits.

Of particular relevance are 1^+ states, since these are allowed in IBM-2 but not in IBM-1. The characteristic excitation of 1^+ levels is of magnetic dipole type. The IBM-2 prediction for the M1 strength to the 1^+ mixed-symmetry state is [225]

$$B(\mathrm{M1}; 0_1^+ \to 1_{\mathrm{MS}}^+) = \frac{3}{4\pi}(g_\nu - g_\pi)^2 f(N) N_\nu N_\pi, \tag{4.26}$$

where g_ν and g_π are the boson g factors and the subscript 'MS' refers to the mixed-symmetry character of the 1^+ state. The function $f(N)$ is known analytically in the three principal limits of the IBM-2,

$$f(N) = \begin{cases} 0 & \mathrm{U}(5) \\ \dfrac{8}{2N-1} & \mathrm{SU}(3) \\ \dfrac{3}{N+1} & \mathrm{SO}(6) \end{cases} . \tag{4.27}$$

This gives a simple and reasonably accurate estimate of the total M1 strength of orbital nature to 1^+ MS states in even–even nuclei.

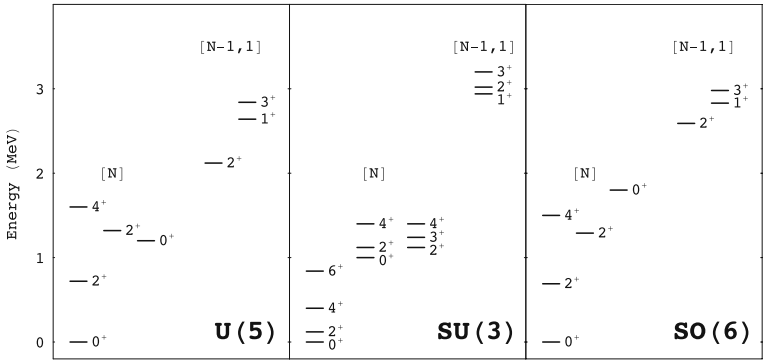

Fig. 4.4. Partial energy spectra in the three limits of IBM-2 in which F spin is a conserved quantum number. Levels are labeled by their angular momentum and parity J^π; the U(6) labels $[N-f, f]$ are also indicated

The geometric interpretation of MS states can be found by taking the limit of large boson number [229]. From this analysis emerges that they correspond to linear or angular displacement oscillations in which the neutrons and protons are out of phase, in contrast to the symmetric IBM-2 states for which such oscillations are in phase. The occurrence of such states was first predicted in the context of geometric two-fluid models in vibrational [230] and deformed [231] nuclei in which they appear as neutron–proton counter oscillations. Because of this geometric interpretation, MS states are often referred to as **scissors** states which is the pictorial image one has in the case of deformed nuclei. The IBM-2 thus confirms these geometric descriptions but at the same time generalizes them to *all* nuclei, not only spherical and deformed, but γ unstable and transitional as well. The empirical evidence for mixed-symmetry states is reviewed in the next section.

4.4 A Case Study: Mixed-Symmetry States in ^{94}Mo

The experimental study of MS states is complicated because the lowest of them occur at relatively high excitation energies (> 2 MeV) and are of low spin. Therefore, they need to be populated and to be distinguished from other levels with the same spin and parity. Population of highly excited low-spin states cannot be achieved using heavy-ion-induced reactions and is often difficult with light-ion fusion–evaporation reactions for very low-spin values. There exist, however, a number of special methods to populate states with low spin up to high energy. They are Coulomb excitation, β decay, nuclear resonance fluorescence (NRF), transfer reactions, the (n,γ) reaction with thermal neutrons and inelastic scattering with fast neutrons, protons, α particles or electrons.

Once populated, the MS state needs to be identified. This is usually achieved by the measurement of a collective magnetic dipole transition to the normal (i.e., symmetric) states. To do so, the multipolarity and parity of the depopulating transition need to be determined as well as the lifetime of the MS state. Its lifetime is obtained either by measuring the natural line width or by observing the Doppler shifts on the depopulating transition. The latter are dependent on the (unknown) lifetime and the known slowing-down mechanism of the atom containing the excited nucleus and moving as a result of the nuclear reaction. In the late 1980s two new experimental techniques were developed and allowed for the first time the measurement of lifetimes of excited states populated by the (n,γ) and (n,n$'$) reactions. They have strongly contributed to the study of collectivity of low-spin states at high energy.

4.4.1 The Discovery of Mixed-Symmetry States in Deformed Nuclei

The first example of a state with MS character was found by Richter and collaborators using inelastic electron scattering on ^{156}Gd [232]. To have a

first idea of properties of MS states in well-deformed nuclei, the appropriate starting point is the F-spin symmetric SU(3) limit [225] of the IBM-2 introduced in the previous section. In this limit, the lowest MS state has spin–parity $J^\pi = 1^+$ and is characterized by a strong M1 transition to the ground state, with a $B(\mathrm{M1})$ value of about 1 μ_N^2 [see Eq. (4.26)]. Since dipole transitions from the even–even ground state are the main excitation mechanism in NRF, this technique is very well suited for the search of 1^+ MS states. Moreover, if the branching ratios are known, the excitation cross-section can be used to determine the lifetime of the populated state. The main experimental problem of NRF is to distinguish between electric dipole excitation, populating 1^- states, and magnetic dipole excitation, populating the 1^+ MS states of interest here. This problem was solved by combining results with those of (e,e′) scattering in the original experiment by Bohle et al. [232]. An essential element of the latter experiment was the detection of inelastically scattered electrons at very backward angles where magnetic excitations are dominant. In ^{156}Gd a 1^+ state was observed at 3.075 MeV excited with a $B(\mathrm{M1}; 0^+ \rightarrow 1^+)$ value of 1.5 μ_N^2. The existence of this state was later confirmed by a NRF experiment [233].

Extensive studies with the (e,e′) [234] and (γ, γ') [235] reactions over the last 20 years led to the systematic discovery of 1^+ MS states in most stable, deformed nuclei [236]. However, only MS states with spin–parity 1^+ could be clearly observed although strongly fragmented in most cases. Other MS states are difficult to identify [237]. The reason is that the excitation probability from the ground state to other excited MS states is small in the reactions used and also because the MS state just above 1^+ has spin–parity 2^+ and typically is the 10th excited 2^+ state. This renders its population with most reactions very unlikely and leads to fragmentation over several states due to the very high level density in deformed nuclei.

Finally, it is worth mentioning that a scissors mode was observed recently in Bose–Einstein condensates [238] which illustrates the general character of this mode in two-component systems.

4.4.2 Mixed-Symmetry States in Near-Spherical Nuclei

While there is ample evidence for 1^+ scissors states in deformed nuclei, only a few MS states have been identified in non-rotational nuclei. For these nuclei the appropriate starting point can be the F-spin symmetric U(5) or SO(6) limit [225] of IBM-2. In both cases the lowest MS state has spin–parity 2^+ and it decays with weak E2 and strong M1 transitions to the normal states. Therefore, there is no clear experimental signature for the excitation of this state from the ground state, like it is the case for the scissors state in deformed nuclei. On the other hand, the advantage of nearly spherical (as compared to deformed) nuclei is their lower level density; as a result, the 2^+ MS state is expected to be the third-to-sixth excited 2^+ state. In the mid-1980s Hamilton *et al.* proposed several candidates based on measured E2/M1 mixing ratios

showing dominant M1 decay to the 2_1^+ state [239]. While this is a necessary condition to establish the MS character of a state, it is not a sufficient one and lifetimes need to be determined to establish the collectivity of the M1 decay to the 2_1^+ state. As an example, the lifetime measurement of Ref. [240] showed that the close-lying second- and third-excited 2^+ states in ^{56}Fe share the MS configuration. With the advent of the γ-ray induced Doppler (GRID) technique [241], which allows to determine lifetimes after thermal neutron capture using ultra-high-resolution γ-ray spectroscopy (with $\Delta E/E = 10^{-6}$), the lifetime of one of the proposed states could be measured and a first pure 2^+ MS state in a vibrational nucleus was established in ^{54}Cr [242]. This then permitted the study of the energy dependence of the MS states in the $N = 30$ isotones [243]. As one might wonder whether the IBM-2 can be applied in these nuclei with only two and three bosons, it is worth mentioning that a large-scale shell-model calculation within the pf shell reached conclusions consistent with IBM-2 [244]. Further examples of 2^+ MS states could be established later in other mass regions [155, 245]. Finally, with the NRF technique 1^+ MS states were found in the SO(6) nuclei ^{196}Pt [246] and ^{134}Ba [247], without, however, the identification of the expected lowest 2^+ MS state.

4.4.3 Mixed-Symmetry States in ^{94}Mo

During the past years extended MS structures have been established in ^{94}Mo by Pietralla, Fransen and their collaborators. As a result, this atomic nucleus has become the best-established case to test the IBM-2 predictions for these excitations. In a first set of experiments, NRF on ^{94}Mo at the Dynamitron accelerator of the University of Stuttgart was combined with β decay at the FN Tandem accelerator of the University of Cologne. In NRF only 1^+, 1^- and 2^+ states are populated. To study the β decay, the ^{94}Mo(p,n)^{94}Tc reaction at 13 MeV was used to produce the $J^\pi = (2)^+$ low-spin isomer of ^{94}Tc which has a half-life of 52 minutes [248]. This (p,n) reaction favors the population of the low-spin isomer compared to the 7^+ ground state, as the transferred angular momentum is only $6\hbar$. The β decay of the low-spin isomer then populates the low-spin states in ^{94}Mo. The γ rays after β decay were measured out of beam which allowed the accumulation of high statistics on a low background so that weak decay branches could be observed (see Fig. 4.5). The key feature for the data analysis is that both reactions populate the 2_3^+ state at 2,067 keV and the 1_1^+ state at 3,129 keV. From the excitation cross-sections of the NRF measurement and by use of the branching and mixing ratios obtained from the γ–γ coincidences and correlations in the β-decay experiment, absolute transition rates can be derived, establishing that both states are of MS character [248]. The observation of the 2^+ MS state at 2,067 keV in NRF is possible through the weakly collective E2 decay [about 10% of the B(E2) value to the first-excited state] as predicted in the F-spin symmetric SO(6) limit. In contrast, the first 2^+ MS state in deformed nuclei

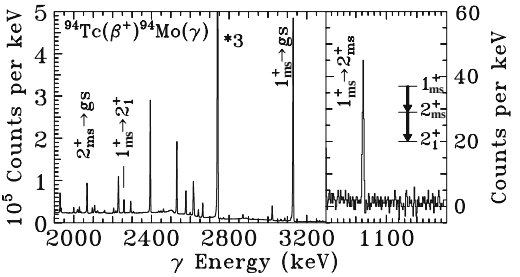

Fig. 4.5. Part of the observed γ-ray spectrum after β decay of the $J^\pi = (2)^+$ low-spin isomer in ^{94}Tc. The *left* part shows the de-exciting transitions out of the MS states and the *right* part the coincidence spectrum gated on the decay of the 2^+_3 MS state to 2^+_1. This establishes the 1^+ MS state as an excitation built on the lowest MS state. (Adapted from [248].)

is part of a rotational band built on the 1^+ MS state and its decay to the ground state is about three times weaker. To establish the MS character of both states, the essential signature is their collective M1 decay via the transitions $1^+_1 \rightarrow 0^+_1$ (0.16 μ_N^2) and $2^+_3 \rightarrow 2^+_1$ (0.48 μ_N^2). An additional proof of the MS character of the 1^+_1 state is the observation of a very weak $1^+_1 \rightarrow 2^+_1$ (0.007 μ_N^2) and a strong $1^+_1 \rightarrow 2^+_2$ (0.43 μ_N^2) M1 transition.

To understand the importance of the very small $B(\mathrm{M1}; 1^+_1 \rightarrow 2^+_1)$ value as far as symmetry is concerned, we recall that both U(5) and SO(6) share an SO(5) subalgebra. As discussed in Sect. 2.2, states with SO(5) symmetry can be expanded in a basis with either even or odd numbers of d bosons. In U(5) a single d-boson number value occurs; in SO(6) different values occur but they are always all even or all odd. This argument can be generalized to IBM-2. The M1 operator is, in lowest order, a d-boson number conserving operator. To construct the lowest 1^+ MS state with SO(5) symmetry, one needs an even number of d bosons, e.g., one neutron and one proton boson in U(5). On the other hand, the first-excited 2^+_1 state requires a one-d-boson state in U(5) and only odd-d-boson numbers in SO(6). Therefore, the $B(\mathrm{M1}; 1^+_1 \rightarrow 2^+_1)$ value vanishes as long as SO(5) is a conserved symmetry. A similar reasoning explains the vanishing $B(\mathrm{M1}; 1^+_1 \rightarrow 2^+_3)$ value, which is observed with an experimental upper limit of 0.05 μ_N^2 [248]. Finally, in the U(5) limit the d-boson number is fixed such that much more stringent selection rules follow; notably, the $1^+_1 \rightarrow 0^+_1$ M1 transition is forbidden. Figure 4.6 schematically illustrates the typical decay patterns.

The first observation of two MS states and the measurement of their absolute decay probabilities forms the first detailed test of predictions concerning *excited* MS states. An excellent agreement with the predictions in the F-spin symmetric SO(6) of IBM-2 was obtained. Some of the results concerning the E2 transition rates show that the 1^+ MS state can be interpreted in the Q-phonon scheme [249] as a symmetric quadrupole excitation on top of the asymmetric quadrupole excitation which corresponds to the 2^+ MS state. If

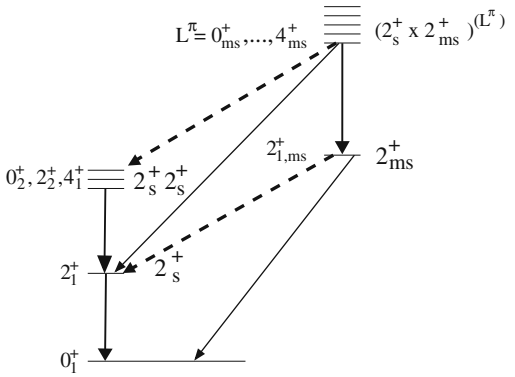

Fig. 4.6. Schematic overview of the electromagnetic decays of the normal and mixed-symmetry states. *Dashed* (*solid*) *lines* represent M1 (E2) transitions and the line thickness illustrates the relative strengths

this is so, one expects nearly the same $B(\mathrm{E2}; 2^+_1 \rightarrow 1^+_1)$ and $B(\mathrm{E2}; 2^+_3 \rightarrow 0^+_1)$ values where the symmetric quadrupole phonon plays the role of spectator and the spin sequence is chosen such that statistical factors entering the $B(\mathrm{E2})$ values are the same. The experimental ratio was found to be 0.39 (18) showing only a deviation by a factor of two. Likewise, the $B(\mathrm{E2}; 2^+_3 \rightarrow 1^+_1)$ and $B(\mathrm{E2}; 2^+_1 \rightarrow 0^+_1)$ values should be equal. Experimentally a ratio of 1.02 was determined but only under the assumption of a pure E2 decay between both MS states. [The E2/M1 mixing ratio could not be uniquely determined in the experiment. Two solutions were found, one with $\delta = -7^{+3}_{-20}$ compatible with a fairly pure collective E2 transition and one with $\delta = -0.57(16)$ indicating only a weakly collective E2 transition].

In a second experiment, the ^{91}Zr(α,n) reaction was used with the specific aim of maximizing the population of medium-spin states [250]. Indeed, light-ion fusion–evaporation reactions were shown to be able to populate states with $J \geq 2$ in a very complete way [151]. The energy of the α particles was 15 MeV leading to a population of states with spins between $J = 2$ and $J = 8$ at a maximal excitation energy of 9 MeV. The experiment was performed at the FN tandem accelerator of the University of Cologne using the Osiris spectrometer equipped with 10 high-purity Ge γ detectors. The data allowed the identification of a level at 2,965.4 keV as being the 3^+ MS state. The spin and parity of the state were obtained from the γ–γ angular correlations and its strong population in the β decay of the $J^\pi = (2)^+$ low-spin isomer in ^{94}Tc. It was found that the 3^+ MS state decays with nearly pure M1 transitions to the symmetric 2^+_2 and 4^+_1 two-phonon states and with mixed E2/M1 transitions to the 2^+_1 and 2^+_3 states. To judge the collective character of these transitions, the lifetime of the 3^+ MS state was determined using the Doppler shift attenuation (DSA) method. In this method the slowing-down time of the recoiling ^{94}Mo atom (moving at 0.38% of c) is compared to the lifetime of the 3^+ MS state via the measured Doppler shifts of de-exciting

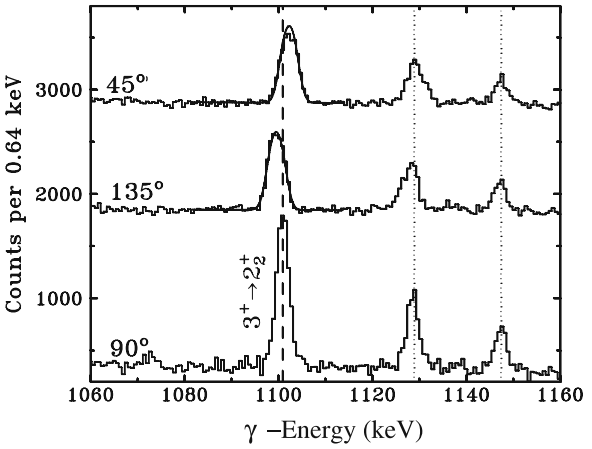

Fig. 4.7. The $3^+ \rightarrow 2_2^+$ transition at 1,101 keV as observed under 45, 135 and 90°. One clearly notices the Doppler shifts at forward and backward angles allowing the determination of the lifetime of the 3^+ MS state in ^{94}Mo.(Reprinted from N. Pietralla et al., Phys. Rev. Lett. 84 (1999) 3775 ©1999 by the American Physical Society, with kind permission.)

transitions. Figure 4.7 illustrates the data. After taking care of time delays due to the lifetimes of higher-lying states populating the 3^+ MS state, causing additional delays called side-feeding effects, a lifetime of 80(30) fs could be extracted [250]. With this information the MS character of the 3^+ state at 2,965 keV could be established by the M1 reduced matrix elements of about 1 μ_N to the 2_2^+ and 4_1^+ states and the collective E2 transition of tens of Weisskopf units (W.u.) to the 2_3^+ MS state.

In addition, with the same data set the level at 2,870 keV could be identified as the second 2^+ MS state [251]. As for the 3^+ state, the branching ratios and multipolarities of the de-exciting transitions allowed the determination of a lifetime of 100(20) fs. In contrast to the 1^+ and 3^+ MS states, which both are the second-excited state of that spin, at an energy of 3 MeV the excited 2^+ MS state is already the sixth 2^+ state. Therefore, one needs a clear signature for its identification. This signature was the collective $B(\mathrm{M1}; 2_6^+ \rightarrow 2_2^+)$ value of 0.35(11) μ_N^2, which is well above the corresponding values for the other excited 2^+ states as shown in Fig. 4.8. Moreover, the identification was not contradicted by the observed $B(\mathrm{E2}; 2_6^+ \rightarrow 2_3^+)$ value of 16^{+88}_{-15} W.u., although the experimental error did not allow a definite conclusion.

The final experiment on ^{94}Mo was performed at the 7 MV electrostatic accelerator of the University of Kentucky using inelastic neutron scattering. In the ^{94}Mo experiment 36.6 g of metallic Mo enriched to 91.6% in ^{94}Mo was used. Fransen et al. [252] used neutron beams with energies between 2.4 and 3.9 MeV. The excitation functions were measured in steps of 100 keV and the angular distributions were measured at 2.4, 3.3 and 3.6 MeV. Figure 4.9

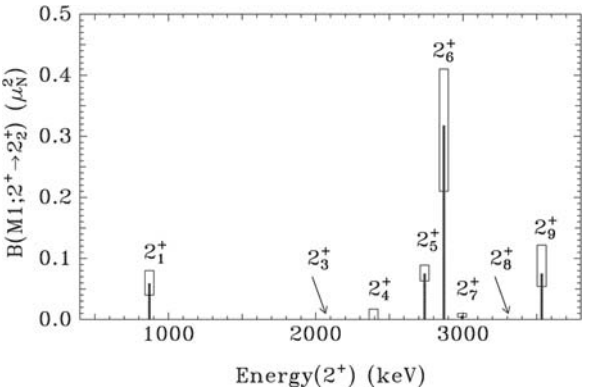

Fig. 4.8. Observed $B(\mathrm{M1}; 2_i^+ \rightarrow 2_2^+)$ values in ^{94}Mo. For the 2_3^+ and 2_8^+ states no M1 transition was observed. (Adapted from [251].)

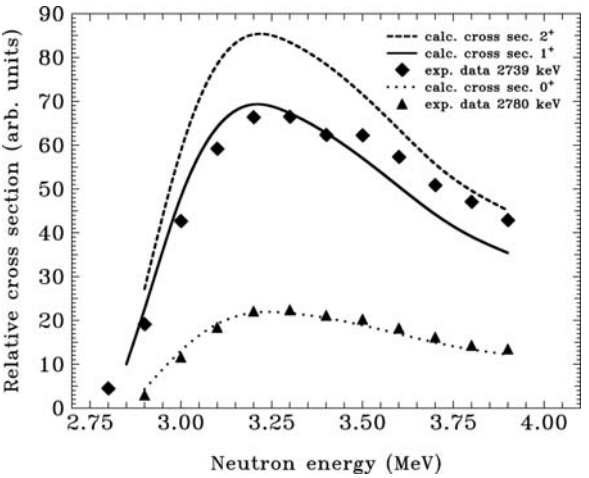

Fig. 4.9. Excitation functions for states at 2,739.9 and 2,780.5 keV observed in ^{94}Mo by inelastic neutron scattering. The *dots* represent the experimental points and the *lines* the results of calculations for excitation of states with $J = 0$ (*dots*), $J = 1$ (*full*) and $J = 2$ (*dashed line*). (Reprinted from Ch. Fransen et al., Phys. Rev. C67 (2003) 024307 ©2003 by the American Physical Society, with kind permission.)

shows the excitation functions for states at 2,739.9 and 2,780.5 keV. One clearly observes that the higher state has spin $J = 0$ and the lower spin $J = 1$. Positive parity was assigned to both states. The kink in the excitation of the latter observed at 3.4 MeV should be attributed to the occurrence of a level at this energy feeding the state of interest. The 2,780.5 keV state was not observed before and could be assigned a spin of zero. The measured excitation function contradicts the earlier association of the 2,739.9 keV level with the 2_5^+ state and indicates a new 1_1^+ state. The elimination of the feeding

problem in inelastic neutron scattering allowed to measure the lifetimes with about 10% error. As an example, the lifetime of the 3_2^+ and the now 2_5^+ excited MS state were found to be 131(14) fs and 79(8) fs, in good agreement with the previous results of 100(20) fs and 80(30) fs from the (α,n) reaction.

One aim of the experiment was the identification of the missing excited 0^+ and 4^+ MS states. No candidate for the 0^+ MS state could be identified. It should be noted that 0^+ states are very difficult to observe and only two excited 0^+ states were found in ^{94}Mo, both of normal multi-phonon character. A possible candidate for the 4^+ MS state was found to be the 4_3^+ state at 2,564.9 keV which decays with a B(M1) of 0.23 μ_N^2 and a B(E2) of $\leq$ 15 W.u. to the 4_1^+ state. However, a transition to the 2_3^+ MS state could not be observed and only an upper limit for this B(E2) of 50 W.u. was obtained. Neither was a transition to the 2_2^+ state observed. Therefore a unique identification was not possible.

While the excitation energies of the MS states resembles more the F-spin symmetric U(5) limit of IBM-2, the observation of the strong $1_2^+ \rightarrow 0_1^+$ M1 transition favors the SO(6) limit. With ^{100}Sn taken as the core, Table 4.4 compares the data to the analytic predictions for this limit given in [225]. For the M1 transitions, the standard values for the boson gyromagnetic ratios are used, $g_\nu = 0$ and $g_\pi = 1\ \mu_N$. The E2 transitions are calculated with the boson effective charges $e_\nu = 0$ and $e_\pi = 0.090\ e$b. An excellent agreement between

Table 4.4. Observed M1 and E2 transitions rates involving the 1_2^+, 2_3^+, 2_5^+ and 3_2^+ MS states in ^{94}Mo compared to different theoretical predictions

		$B(\mathrm{M1}; J_i \rightarrow J_f)^a$						$B(\mathrm{E2}; J_i \rightarrow J_f)^b$			
J_i^π	J_f^π	Expt	IBM-2	SM	QPM	J_i^π	J_f^π	Expt	IBM-2	SM	QPM
2_3^+	2_1^+	0.56(5)	0.30	0.51	0.20	0_1^+	2_1^+	203(3)	233	210	207
1_2^+	0_1^+	0.160^{+11}_{-10}	0.16	0.26	0.08	0_1^+	2_3^+	27.9(25)	15.0	21.0	10.0
1_2^+	2_1^+	0.012(3)	0	0.002	0.003	0_1^+	2_5^+	1.78^{+23}_{-20}	0	3.7	4.3
1_2^+	2_2^+	0.44(3)	0.36	0.46	0.42	2_3^+	2_1^+	12.4^{+76}_{-58}	0	0.003	0.99
1_2^+	2_3^+	< 0.05	0	0.08	0.003	1_2^+	2_1^+	1.83^{+69}_{-61}	4.8	1.3	7.6
2_5^+	2_1^+	0.0017^{+10}_{-12}	0	0.004	0.008	1_2^+	2_2^+	2.5^{+23}_{-16}	0	0.14	0.89
2_5^+	2_2^+	0.27(3)	0.100	0.17	0.56	1_2^+	2_3^+	< 69	55.6	22.8	73.9
2_5^+	2_3^+	< 0.16	0	0.06		2_5^+	2_1^+	1.02^{+48}_{-36}	1.6	4.6	8.4
3_2^+	2_1^+	0.006^{+3}_{-4}	0	0.10	0.004	2_5^+	2_2^+	1.02^{+23}_{-10}	0	3.0	
3_2^+	4_1^+	0.075(10)	0.13	0.058	0.12	2_5^+	2_3^+	< 355	42.9	14.0	57.1
3_2^+	2_2^+	0.24(3)	0.18	0.09	0.17	3_2^+	2_1^+	2.3^{+12}_{-10}	4.8	4.3	7.0
3_2^+	2_3^+	0.021^{+16}_{-12}	0	0.003	0.02	3_2^+	4_1^+	0.36^{+76}_{-33}	0	2.3	0.02
		0.09(2)				3_2^+	2_2^+	2.3^{+46}_{-20}	0	17.0	0.89
						3_2^+	2_3^+	24^{+32}_{-21}	37.1	19.8	64.5
								147(36)			

[a] In units of μ_N^2.
[b] In units of $10^{-3}\ e^2\mathrm{b}^2$.

experiment and IBM-2 is obtained which clearly establishes the proposed MS states. The data were also analyzed with the spherical shell model [253] and with the quasi-particle–phonon model [254]. These results are also shown in Table 4.4.

In conclusion, the use of a combination of different techniques of γ-ray spectroscopy allowed the first observation of excited MS states in atomic nuclei. A remarkable property is that these collective excitations survive up to an excitation energy of 3 MeV. These techniques have also led to a systematic study of other $N = 52$ nuclei where more MS states were found, notably in ^{96}Ru [255, 256]. Presently, radioactive-beam experiments are being performed to extend the studies to lighter $N = 52$ nuclei.

5 Supersymmetries with Neutrons and Protons

In this chapter we present the logical combination of ideas introduced previously. In Chap. 3 fermion degrees of freedom were introduced in the interacting boson model (IBM), leading to a description of odd-mass nuclei in the context of the interacting boson–fermion model (IBFM) and, after due consideration of the appropriate superalgebras, to a simultaneous description of even–even and odd-mass nuclei. The purpose of Chap. 4, on the other hand, was the introduction of the F-spin degree of freedom in the IBM to distinguish between neutron and proton bosons, with several consequences such as a better microscopic foundation of the IBM, the existence of F-spin multiplets of nuclei and the occurrence of states with a mixed-symmetry character in neutrons and protons.

In this chapter we combine these two extensions of the IBM and describe nuclei with bosons and fermions that can be of neutron or proton character. In the context of a supersymmetric description, this formalism allows a clear distinction—previously lacking—between odd-mass nuclei that have an odd number of neutrons and those that have an odd number of protons. In addition, it leads in a natural way to a description of odd–odd nuclei where both neutrons and protons are odd in number. The essential features of neutron–proton (or extended) supersymmetry are explained in Sect. 5.1, while a brief overview of several classifications is given in Sect. 5.2. Neutron–proton supersymmetry is particularly relevant for transfer reactions if a supersymmetric operator is used and Sect. 5.3 is devoted to this topic. We conclude the chapter with a detailed analysis of ^{196}Au as an illustration of the application of extended supersymmetry.

5.1 Combination of F Spin and Supersymmetry

The first question to be addressed concerns the choice of the dynamical algebra containing the degrees of freedom that we wish to include. As explained in Sect. 3.4, the simultaneous description of even–even and odd-mass nuclei requires the superalgebra $\mathrm{U}(6/\Omega)$, where Ω denotes the single-particle space available to the odd nucleon. On the other hand, the separate handling of neutron and proton bosons leads to the dynamical algebra $\mathrm{U}_\nu(6) \otimes \mathrm{U}_\pi(6)$ of

A. Frank et al., *Symmetries in Atomic Nuclei*,
Springer Tracts in Modern Physics 230, DOI 10.1007/978-0-387-87495-1_5,

IBM-2 (see Sect. 4.3). It is, therefore, natural to propose as a generalization the dynamical algebra [257]

$$\mathrm{U}_\nu(6/\Omega_\nu) \otimes \mathrm{U}_\pi(6/\Omega_\pi), \tag{5.1}$$

where Ω_ν and Ω_π are the dimensions of the neutron and proton single-particle spaces, respectively. This algebra contains generators which transform bosons into fermions and vice versa, and furthermore are distinct for neutrons and protons. To understand the consequences of this choice of dynamical algebra, the action of its generators is illustrated in Fig. 5.1 with the particular $\mathrm{U}_\nu(6/12) \otimes \mathrm{U}_\pi(6/4)$ supermultiplet based on the even–even nucleus ^{194}Pt. It shows that the supermultiplet now contains a quartet of nuclei (even–even, even–odd, odd–even and odd–odd) which are to be described simultaneously with a single hamiltonian. As indicated in the figure, further action of the operators leads to configurations with more than a single neutron and a single proton coupled to an even–even core. These correspond to excitations at higher energies, with a quasi-particle nature and not normally included in the analysis. The dynamical superalgebra (5.1) thus leads to correlations between the properties of a quartet of nuclei.

Inspired by the example of IBM-2, where the dynamical algebra $\mathrm{U}_\nu(6) \otimes \mathrm{U}_\pi(6)$ can be enlarged to U(12), leading to the notion of F-spin multiplets, it is possible to propose a similar enlargement here. The resulting dynamical algebra then becomes $\mathrm{U}(12/\Omega_\nu + \Omega_\pi)$ which contains a large number of different nuclei in a single of its representations [258]. This represents a merger of the concepts of F-spin and supermultiplets which is of interest conceptually. It is, however, problematic to find a single hamiltonian for a simultaneous

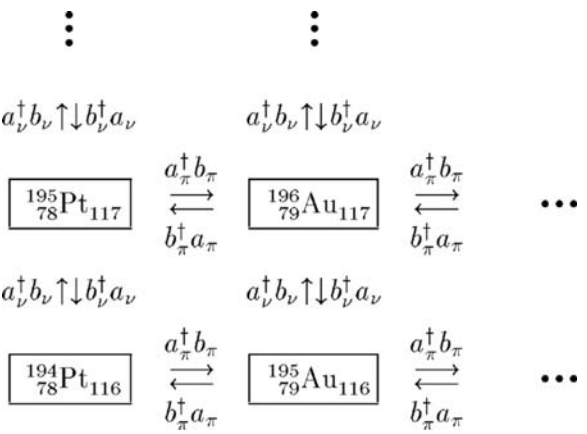

Fig. 5.1. Schematic illustration of part of a $\mathrm{U}_\nu(6/12) \otimes \mathrm{U}_\pi(6/4)$ supermultiplet in the Pt–Au region. The supermultiplet is characterized by the product of supersymmetric representations $[\mathcal{N}_\nu\} \otimes [\mathcal{N}_\pi\}$ with $\mathcal{N}_\nu = 5$ and $\mathcal{N}_\pi = 2$. Both the neutron and the proton bosons are hole like

description of all nuclei in the multiplet and this reduces the applicability of $\mathrm{U}(12/\Omega_\nu + \Omega_\pi)$ which therefore shall not be further explored here.

Next, one should define the breaking of the dynamical algebra $\mathrm{U}_\nu(6/\Omega_\nu) \otimes \mathrm{U}_\pi(6/\Omega_\pi)$, the details of which obviously will depend on the specific application at hand. Based on the analogy with IBFM and IBM-2, the extended supersymmetry classification starts with

$$\begin{array}{ccccccccccc}
\mathrm{U}_\nu(6/\Omega_\nu) & \otimes & \mathrm{U}_\pi(6/\Omega_\pi) & \supset & \mathrm{U}^{\mathrm{B}}_\nu(6) & \otimes & \mathrm{U}^{\mathrm{F}}_\nu(\Omega_\nu) & \otimes & \mathrm{U}^{\mathrm{B}}_\pi(6) & \otimes & \mathrm{U}^{\mathrm{F}}_\pi(\Omega_\pi) & \supset \\
\downarrow & & \downarrow & & \downarrow & & \downarrow & & \downarrow & & \downarrow & \\
[\mathcal{N}_\nu\} & & [\mathcal{N}_\pi\} & & [N_\nu] & & [1^{M_\nu}] & & [N_\pi] & & [1^{M_\pi}] &
\end{array}$$

$$\begin{array}{ccccc}
\mathrm{U}^{\mathrm{B}}_{\nu+\pi}(6) & \otimes & \mathrm{U}^{\mathrm{F}}_\nu(\Omega_\nu) & \otimes & \mathrm{U}^{\mathrm{F}}_\pi(\Omega_\pi) \\
\downarrow & & \downarrow & & \downarrow \\
[N_1, N_2] & & [1^{M_\nu}] & & [1^{M_\pi}]
\end{array} . \tag{5.2}$$

Generally, the neutron–proton degree of freedom is not explicitly used for the bosons since the mixed-symmetry states, with $N_2 \neq 0$, occur at high energy ($E_{\mathrm{x}} > 2$ MeV) which renders their detection in odd-mass nuclei difficult and precludes it in odd–odd nuclei. Therefore, one may restrict oneself (as will be done in the following) to the symmetric states at low energy, with $[N_1, N_2] = [N, 0]$, which can be described as $N = N_\nu + N_\pi$ identical s and d bosons.

A hamiltonian of the extended supersymmetry model is of the form

$$H = \sum_{r=1}^{s} \sum_{m} \kappa_{rm} C_m[\mathcal{G}_r], \tag{5.3}$$

where κ_{rm} are coefficients and $\mathcal{G}_r$ are subalgebras of the product of superalgebras $\mathrm{U}_\nu(6/\Omega_\nu) \otimes \mathrm{U}_\pi(6/\Omega_\pi)$. Usually only linear and quadratic Casimir operators $C_m[\mathcal{G}_r]$ are considered, $m = 1, 2$, which corresponds to a restriction to one- and two-body interactions. Depending on the realization of the generators of the various algebras, the Casimir operators generate, besides the boson interactions, also boson–fermion and fermion–fermion interactions with the fermion either a neutron or a proton. Finally, as discussed in Sect. 1.2.2, the algebras $\mathcal{G}_r$ may form a chain of nested subalgebras. Although this is not a necessary condition for supersymmetry to hold (see Sect. 3.6), it allows an analytic solution of the form

$$E(\Gamma_1, \ldots, \Gamma_s) = \sum_{r=1}^{s} \sum_{m} \kappa_{rm} E_m(\Gamma_r), \tag{5.4}$$

where $E_m(\Gamma_r)$ are known functions of the irreducible representation Γ_r of the algebra $\mathcal{G}_r$, as introduced in Sect. 1.1.4.

The properties of the even–even, even–odd, odd–even and odd–odd nuclei with the same total number of bosons and fermions $\mathcal{N} = N + M_\nu + M_\pi$ are then related through a constant parameter set $\{\kappa_{rm}\}$. In the even–even

and odd-mass members of the quartet, the representations Γ of two different subalgebras of $\mathrm{U}_\nu(6/\Omega_\nu) \otimes \mathrm{U}_\pi(6/\Omega_\pi)$ may become identical ($\Gamma_r = \Gamma_s$ for all levels) and therefore only the sum of parameters $\kappa_{rm} + \kappa_{sm}$ can be deduced from the experiment. Nevertheless, if a sufficient number of levels is known in the even–even and odd-mass nuclei, one is able to determine all parameters κ_{rm} and hence to *predict* unambiguously the structure of the odd–odd nucleus. This situation should be contrasted with supersymmetry between doublets of nuclei as discussed in Chap. 3. In that case, the even–even spectrum necessarily depends on certain sums $\kappa_{rm} + \kappa_{sm}$ only, which precludes an unambiguous prediction of the odd-mass spectrum. In extended supersymmetry between quartets of nuclei, the boson–boson and boson–fermion interactions deduced for the even–even and odd-mass members, uniquely determine the interaction between the neutron and the proton fermion. This leads to the most clear-cut experimental test of supersymmetry in atomic nuclei, of importance not only for nuclear physics but also for other conceivable applications of supersymmetry in physics where experimental verification so far is unavailable. In addition, extended supersymmetry concerns odd–odd nuclei which are highly complex and for which other theoretical approaches are often difficult to apply.

We emphasize once more that the concept of supersymmetry does not require the existence of a dynamical symmetry. In the context of the neutron–proton IBM, supersymmetry adopts the direct product (5.1) as the dynamical algebra for a quartet consisting of an even–even, even–odd, odd–even and odd–odd nucleus. Nevertheless, *dynamical* supersymmetry has the distinct advantage of immediately suggesting the form of the quartet's hamiltonian and operators, while the weaker form of *generalized* supersymmetry does not provide such a recipe for these operators. Also, wave functions are independent of the parameters of a hamiltonian with dynamical (super)symmetry and this property is not valid any longer for the generalized case.

5.2 Examples of Extended Supersymmetries

The SO(6) limit of $\mathrm{U}_\nu(6/12) \otimes \mathrm{U}_\pi(6/4)$ was the first proposed example of a dynamical-symmetry limit in an extended supersymmetry [257]. It combines the U(6/12) scheme [175] for the neutrons, with that of U(6/4) [183] for the protons, both described in Chap. 3. These classifications can be combined at the SO(6) level, using the isomorphism between $\mathrm{SO}_\nu^{\mathrm{B+F}}(6)$ and $\mathrm{SU}_\pi^{\mathrm{B+F}}(4)$. The neutron and proton single-particle spaces are such that the scheme is applicable to the Pt–Au region where the odd neutron predominantly occupies the $\nu 3p_{1/2}$, $\nu 3p_{3/2}$ and $\nu 2f_{5/2}$ orbits of the 82–126 shell, while the odd proton is mostly in the $\pi 2d_{3/2}$ orbit of the 50–82 shell.

The four nuclei in the supermultiplet shown in Fig. 5.1 are described by a single hamiltonian which reads

$$H = \kappa_0 C_2[\mathrm{U}_\nu^{\mathrm{B+F}}(6)] + \kappa_3 C_2[\mathrm{SO}_\nu^{\mathrm{B+F}}(6)] + \kappa_3' C_2[\mathrm{SO}_{\nu+\pi}^{\mathrm{B+F}}(6)] + \kappa_4 C_2[\mathrm{SO}_{\nu+\pi}^{\mathrm{B+F}}(5)] + \kappa_5 C_2[\mathrm{SO}_{\nu+\pi}^{\mathrm{B+F}}(3)] + \kappa_5' C_2[\mathrm{SU}(2)]. \quad (5.5)$$

The indices ν, π refer to the neutron or proton character of the fermion generators which are combined with the boson generators to form the boson–fermion algebra $\mathcal{G}^{\mathrm{B+F}}$. Associated with the hamiltonian (5.5) is a complete basis labeled by the irreducible representations of the different algebras,

$$\begin{array}{cccccc} \mathrm{U}_\nu^{\mathrm{B+F}}(6) & \mathrm{SO}_\nu^{\mathrm{B+F}}(6) & \mathrm{SO}_{\nu+\pi}^{\mathrm{B+F}}(6) & \mathrm{SO}_{\nu+\pi}^{\mathrm{B+F}}(5) & \mathrm{SO}_{\nu+\pi}^{\mathrm{B+F}}(3) & \mathrm{SU}(2) \\ \downarrow & \downarrow & \downarrow & \downarrow & \downarrow & \downarrow \\ [N_1, N_2] & \langle \Sigma_1, \Sigma_2 \rangle & \langle \sigma_1, \sigma_2, \sigma_3 \rangle & (\tau_1, \tau_2) & \tilde{L} & J \end{array}, \quad (5.6)$$

where J is the total angular momentum which only in the presence of a neutron fermion is different from $\tilde{L}$ with $J = \tilde{L} \pm 1/2$. The labels given in (5.6) are valid under the restriction to F-spin symmetric states for the even–even core. In the case of the odd–odd nucleus, the labels $[N_1, N_2]$ can be either $[N+1] \equiv [N+1, 0]$ or $[N, 1]$ with $N = N_\nu + N_\pi$ the total boson number. The allowed values of Σ_i for these representations are given by the following rules: $[N+1]$ contains $\Sigma_1 = N+1, N-1, \ldots, 1$ or 0 with $\Sigma_2 = 0$, $[N, 1]$ contains $\Sigma_1 = N, N-2, \ldots, 2$ or 1 with $\Sigma_2 = 1$ and $\Sigma_1 = N-1, N-3, \ldots, 2$ or 1 with $\Sigma_2 = 0$. The coupling of the proton leads to the following $\mathrm{SO}_{\nu+\pi}^{\mathrm{B+F}}(6)$ representations: $\langle \Sigma_1 \rangle$ contains $\sigma_1 = \Sigma_1 + 1/2$ or $\Sigma_1 - 1/2$ with $\sigma_2 = \sigma_3 = 1/2$ and $\langle \Sigma_1, 1 \rangle$ contains $\sigma_1 = \Sigma_1 + 1/2$ or $\Sigma_1 - 1/2$ with $\sigma_2 = 1/2$ or $3/2$ and $\sigma_3 = 1/2$, with the limitation that $\sigma_1 \geq \sigma_2$. The subsequent reduction to $\mathrm{SO}_{\nu+\pi}^{\mathrm{B+F}}(5)$ leads to the following result: $\langle \sigma_1, 1/2, 1/2 \rangle$ contains $\tau_1 = \sigma_1, \sigma_1 - 1, \ldots, 1/2$ with $\tau_2 = 1/2$ and $\langle \sigma_1, 3/2, 1/2 \rangle$ contains $\tau_1 = \sigma_1, \sigma_1 - 1, \ldots, 1/2$ with $\tau_2 = 1/2$ and $\tau_1 = \sigma_1, \sigma_1 - 1, \ldots, 3/2$ with $\tau_2 = 3/2$. The reduction from $\mathrm{SO}_{\nu+\pi}^{\mathrm{B+F}}(5)$ to $\mathrm{SO}_{\nu+\pi}^{\mathrm{B+F}}(3)$ is given in Table 5.1 for the lowest Spin(5) representations. Finally, the values of J are obtained by coupling $\tilde{L}$ with pseudo-spin 1/2.

The hamiltonian (5.5) is diagonal in the basis (5.6) and its eigenvalues can be expressed as a function of the quantum numbers given in (5.6), resulting in the energy expression

Table 5.1. Angular momentum content of some Spin(5) representations

(τ_1, τ_2)	J
(1/2,1/2)	3/2
(3/2,1/2)	1/2, 5/2, 7/2
(5/2,1/2)	3/2, 5/2, 7/2, 9/2, 11/2
(7/2,1/2)	3/2, 5/2, 7/2, 9/2, 9/2, 11/2, 13/2, 15/2
(3/2,3/2)	3/2, 5/2, 9/2
(5/2,3/2)	1/2, 3/2, 5/2, 7/2, 7/2, 9/2, 11/2, 13/2

$$
\begin{aligned}
&E(N_i, \Sigma_i, \sigma_i, \tau_i, \tilde{L}, J) \\
&\quad = \kappa_0[N_1(N_1+5) + N_2(N_2+3)] + \kappa_3[\Sigma_1(\Sigma_1+4) + \Sigma_2(\Sigma_2+2)] \\
&\qquad +\kappa_3'[\sigma_1(\sigma_1+4) + \sigma_2(\sigma_2+2) + \sigma_3^2] + \kappa_4[\tau_1(\tau_1+3) + \tau_2(\tau_2+1)] \\
&\qquad +\kappa_5\tilde{L}(\tilde{L}+1) + \kappa_5' J(J+1). \qquad (5.7)
\end{aligned}
$$

This expression is valid for all four members of the supermultiplet. In addition, supersymmetry requires that the parameters are the same for the four nuclei.

Another example of an extended supersymmetry is the $\mathrm{U}_\nu(6/12) \otimes \mathrm{U}_\pi(6/12)$ scheme in which both neutrons and protons occupy single-particle orbits with $j = 1/2$, $3/2$ and $5/2$ [259]. The advantage of this scheme is that it contains the three limits of the IBM. The scheme was worked out for the vibrational U(5) limit and applied to the nearly stable isotopes around mass $A = 75$ [259, 260, 261]. The most detailed study concerned ^{76}As where good agreement was found [260].

5.3 One-Nucleon Transfer in Extended Supersymmetry

One of the possible tests of supersymmetry is with one- or two-nucleon transfer reactions and we begin this section with a discussion of the first of these. The single-particle-transfer operator commonly used in the IBFM has a microscopic foundation in the shell model and, specifically, one based on the seniority scheme [262]. Although this derivation in principle is valid in vibrational nuclei only, it has been used for deformed nuclei as well. An alternative method to arrive at the structure of the transfer operator and at predictions concerning transfer intensities, is based on symmetry considerations. It consists in expressing the single-particle-transfer operator in terms of tensor operators under the subalgebras that appear in the subalgebra chain of a dynamical (super)algebra [173, 179]. The use of tensor operators has the advantage of giving rise to selection rules and closed expressions for the spectroscopic strengths. If the single-particle transfer is between different members of a single supermultiplet, it provides an important test of supersymmetry since it involves the transformation of a boson into a fermion or vice versa but conserves the total number of bosons plus fermions.

The operators that describe one-proton-transfer reactions between the members of the $\mathrm{U}_\nu(6/12) \otimes \mathrm{U}_\pi(6/4)$ multiplet are [263]

$$
\begin{aligned}
T_{1,m}^{\langle 1/2,1/2,1/2\rangle(1/2,1/2)3/2} &= -\sqrt{\frac{1}{6}}\left(\tilde{s}_\pi \times a_\pi^\dagger\right)_m^{(3/2)} + \sqrt{\frac{5}{6}}\left(\tilde{d}_\pi \times a_\pi^\dagger\right)_m^{(3/2)}, \\
T_{2,m}^{\langle 3/2,1/2,1/2\rangle(1/2,1/2)3/2} &= \sqrt{\frac{5}{6}}\left(\tilde{s}_\pi \times a_\pi^\dagger\right)_m^{(3/2)} + \sqrt{\frac{1}{6}}\left(\tilde{d}_\pi \times a_\pi^\dagger\right)_m^{(3/2)}, \qquad (5.8)
\end{aligned}
$$

where $a_\pi^\dagger$ creates a proton in an orbit with $j = 3/2$. The operators T_1 and T_2 are, by construction, tensor operators under $\mathrm{SO}_{\nu+\pi}^{\mathrm{B+F}}(6)$, $\mathrm{SO}_{\nu+\pi}^{\mathrm{B+F}}(5)$ and

$\mathrm{SO}^{\mathrm{B+F}}_{\nu+\pi}(3)$ [or SU(2)] and the upper indices $\langle\sigma_1,\sigma_2,\sigma_3\rangle$, (τ_1,τ_2) and J specify the tensor properties under these algebras.

Figure 5.2 shows the allowed transitions induced by the operators (5.8) for the transfer of one proton from the ground state of the even–even nucleus ^{194}Pt to states in the odd-proton nucleus ^{195}Au. By convention, N is the number of bosons in the odd–odd nucleus ^{196}Au, $N = N_\nu + N_\pi = 5$. The operators T_1 and T_2 have the same transformation character under SO(5) and SO(3) and can only excite states with $(\tau_1,\tau_2) = (1/2,1/2)$ and $\tilde{L} = 3/2$. They have different transformation properties under SO(6), however, leading to different selection rules in the associated quantum number. Whereas T_1, acting on an even–even nucleus with $N+2$ bosons, can only excite the ground state of the odd-mass nucleus with $\langle\sigma_1,\sigma_2,\sigma_3\rangle = \langle N+3/2,1/2,1/2\rangle$, the operator T_2 also allows the transfer to an excited state with $\langle N+1/2,1/2,1/2\rangle$. The ratio of the intensities is given by

$$R_1(^{194}\mathrm{Pt} \rightarrow {}^{195}\mathrm{Au}) \equiv \frac{I(T_1;\mathrm{gs}\rightarrow\mathrm{exc})}{I(T_1;\mathrm{gs}\rightarrow\mathrm{gs})} = 0,$$
$$R_2(^{194}\mathrm{Pt} \rightarrow {}^{195}\mathrm{Au}) \equiv \frac{I(T_2;\mathrm{gs}\rightarrow\mathrm{exc})}{I(T_2;\mathrm{gs}\rightarrow\mathrm{gs})} = \frac{9(N+1)(N+5)}{4(N+6)^2}, \qquad (5.9)$$

for T_1 and T_2, respectively. For $^{194}\mathrm{Pt} \rightarrow {}^{195}\mathrm{Au}$, the second ratio is $R_2 = 1.12$ $(N = 5)$.

The available experimental data [264] from the proton stripping reactions ^{194}Pt(α,t)^{195}Au and ^{194}Pt(^{3}He,d)^{195}Au show that the $J = 3/2$ ground state of ^{195}Au is excited strongly with spectroscopic strength $C^2S = 0.175$, whereas the second $J = 3/2$ state is excited weakly with $C^2S = 0.019$. In the supersymmetry scheme, the latter state is assigned as a member of the ground-state band with $(\tau_1,\tau_2) = (5/2,1/2)$. Therefore, the one-proton

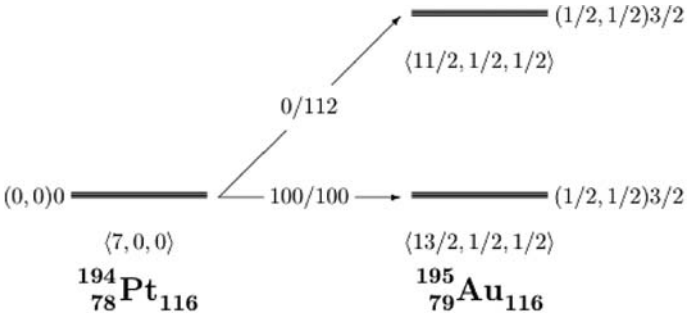

Fig. 5.2. Allowed one-proton transfer in the reaction $^{194}\mathrm{Pt} \rightarrow {}^{195}\mathrm{Au}$. The transfer intensities are normalized to 100 for the ground-to-ground transition. The quoted intensities I_1/I_2 apply to the operators T_1/T_2. The $\mathrm{SO}^{\mathrm{B+F}}_{\nu+\pi}(6)$ labels $\langle\sigma_1,\sigma_2,\sigma_3\rangle$ are given below each level; the $\mathrm{SO}^{\mathrm{B+F}}_{\nu+\pi}(5)$ and $\mathrm{SO}^{\mathrm{B+F}}_{\nu+\pi}(3)$ [or SU(2)] labels $(\tau_1,\tau_2)\tilde{L} = J$ are given next to each level

transfer to this state is forbidden by the SO(5) selection rule of the tensor operators (5.8). The observed strength to excited $J = 3/2$ states is small which suggests that the operator T_1 in (5.8) can be used to describe the data.

In Fig. 5.3 we show the allowed transitions in the one-proton transfer from the ground state of the odd-neutron nucleus ^{195}Pt to states in the odd–odd nucleus ^{196}Au. Also in this case the operator T_1 only excites the ground-state doublet of ^{196}Au with $\langle\sigma_1, \sigma_2, \sigma_3\rangle = \langle N+3/2, 1/2, 1/2\rangle$, $(\tau_1, \tau_2) = (1/2, 1/2)$, $\tilde{L} = 3/2$ and $J = \tilde{L} \pm 1/2$ whereas T_2 also populates the excited state with $\langle N + 1/2, 1/2, 1/2\rangle$. The ratio of the intensities is the same as for the $^{194}\text{Pt} \rightarrow {}^{195}$Au transfer reaction,

$$
\begin{aligned}
R_1(^{195}\text{Pt} \rightarrow {}^{196}\text{Au}) &= R_1(^{194}\text{Pt} \rightarrow {}^{195}\text{Au}), \\
R_2(^{195}\text{Pt} \rightarrow {}^{196}\text{Au}) &= R_2(^{194}\text{Pt} \rightarrow {}^{195}\text{Au}).
\end{aligned}
\tag{5.10}
$$

These relations are a direct consequence of supersymmetry. Just as energies and electromagnetic transition rates of nuclei in the supersymmetric quartet are connected because they are calculated with the same hamiltonian or transition operator, one-proton-transfer intensities can be related in a similar fashion. As a result, we find definite predictions for the spectroscopic strengths in the $^{195}\text{Pt} \rightarrow {}^{196}$Au transfer and these can be tested experimentally.

One-neutron-transfer reactions can be treated in a similar way. The available data from the neutron stripping reaction ^{194}Pt(d,p)^{195}Pt [265] can be used to determine the appropriate form of the one-neutron-transfer operator [187, 188], with which spectroscopic strengths can be predicted for the transfer reaction $^{195}\text{Au} \rightarrow {}^{196}$Au. Unfortunately, ^{195}Au is unstable and only radioactive-beam experiments in inverse kinematics conceivably might allow a test of this kind.

In summary, as a consequence of supersymmetry, a number of correlations exist for transfer reactions between different pairs of nuclei. Such relations

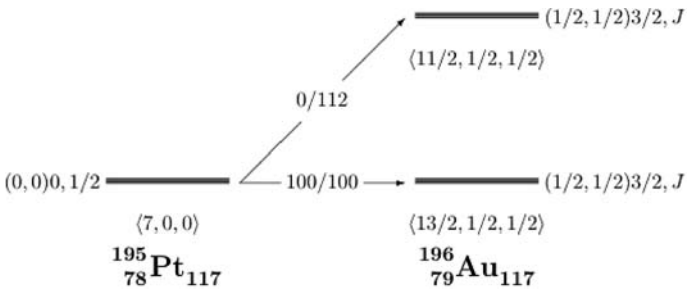

Fig. 5.3. Allowed one-proton transfer in the reaction $^{195}\text{Pt} \rightarrow {}^{196}$Au. The transfer intensities are normalized to 100 for the ground-to-ground transition. The quoted intensities I_1/I_2 apply to the operators T_1/T_2. The $\text{SO}^{\text{B+F}}_{\nu+\pi}(6)$ labels $\langle\sigma_1, \sigma_2, \sigma_3\rangle$ are given below each level; the $\text{SO}^{\text{B+F}}_{\nu+\pi}(5)$, $\text{SO}^{\text{B+F}}_{\nu+\pi}(3)$ and SU(2) labels $(\tau_1, \tau_2)\tilde{L}, J$ are given next to each level

may provide a challenge and motivation for future detailed experiments of the kind described in the next section.

5.4 A Case Study: Structure of ^{196}Au

5.4.1 First Transfer Reaction Experiments

A first investigation of the structure of ^{196}Au to test predictions of the $U_\nu(6/12) \otimes U_\pi(6/4)$ extended supersymmetry was performed in the late 1980s [266]. From the known experimental level schemes of the even–even and odd-mass members of the quartet, the level scheme of ^{196}Au was predicted and subsequently the single-particle-transfer amplitudes for the ^{197}Au(d,t)^{196}Au reaction were calculated. All these results were derived in the SO(6) limit of the $U_\nu(6/12) \otimes U_\pi(6/4)$ scheme, for which, as always in the presence of a dynamical symmetry, the wave functions do not depend on the hamiltonian parameters. Therefore, quantities such as the spectroscopic strengths are fingerprints of the underlying symmetries. At the Accelerator Laboratory in Munchen the transfer reaction was performed by the group headed by von Egidy. As the ground state of ^{197}Au has $J^\pi = 3/2^+$, transfer with $l = 1, 3$ leads to the negative-parity states described by the model but also to states based on $\nu 2f_{7/2}$ excitations which are outside the model. Other negative-parity states, arising from the unique-parity orbitals $\nu 1i_{13/2} \times \pi 1h_{11/2}$ occur at higher energies, above the known isomeric $J^\pi = 12^-$ state at 595.66 keV. To distinguish them unambiguously and also the positive-parity states populated by $\nu 1i_{13/2}$ transfer, the ^{197}Au(^{3}He,α)^{196}Au reaction can be used which is dominated by $l = 6$ transfer.

Because the spin and parity of the excited states were unknown, the only test possible was a comparison of the measured strength function with the one predicted from the supersymmetry scheme. Theory predicts the excitation of 22 states and a negligible strength distribution above 500 keV. Figure 5.4 shows the results obtained in Ref. [266]. In accordance with the theoretical predictions, about 20 states share the transfer strength below 500 keV. However, a clear discrepancy occurs at low energy where theory predicts strength to two states while the only strength observed at that time was to the ground state. Also, a huge peak was observed at an excitation energy of 165 keV, whereas the theoretical prediction showed much more fragmentation. The running sums of the strength did, however, agree very well as can be seen from the inset of Fig. 5.4.

Although the transfer experiment sensitively probed states predicted by the model, one of its drawbacks was that it could not distinguish between $l = 1$ and $l = 3$ transfer. Therefore, no information could be deduced about spins. A few years later Vergnes and collaborators performed additional transfer experiments at the Institut de Physique Nucléaire in Orsay using the reaction ^{197}Au(p,d)^{196}Au. The resolution in this experiment was 11 keV full width

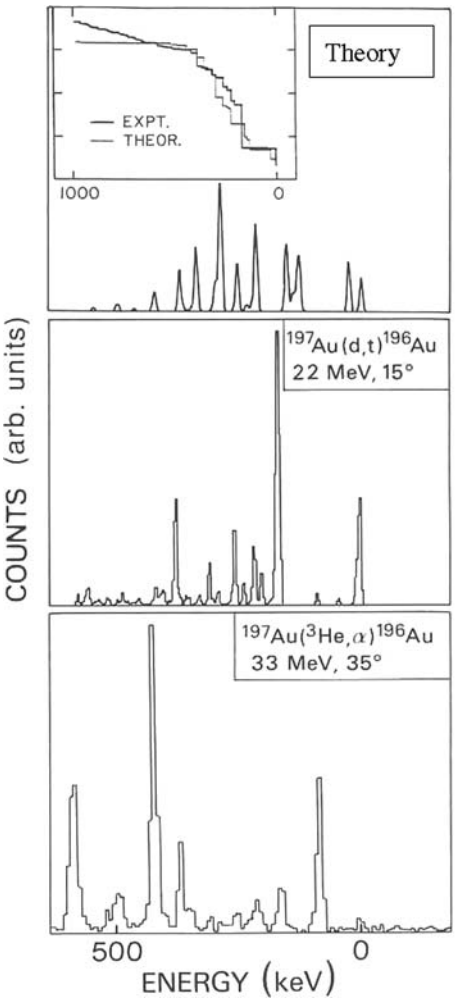

Fig. 5.4. Observed transfer strength at 15° for the reaction ^{197}Au(d,t)^{196}Au (*middle*), compared to the predictions of the $U_\nu(6/12) \otimes U_\pi(6/4)$ extended supersymmetry (*top*). The inset compares the summed $l = 1, 3$ strength. The character of the states populated with $l = 6$ can be deduced from ^{197}Au(^{3}He,α)^{196}Au (*bottom*). (Reprinted from J. Jolie et al., Phys. Rev. C43. (1991) R16 ©1991 by the American Physical Society, with kind permission.)

at half maximum (FWHM). The measured angular distributions allowed to distinguish between the $l = 1$ and the $l = 3$ transfer and the corresponding strengths could now be compared separately to the theoretical results. The experiment essentially confirmed the discrepancies already mentioned but also that the summed $l = 1$ and $l = 3$ strengths agree with the predictions. Because of the considerable observed strength in the ground state and in the

level at 165 keV, breaking of the dynamical supersymmetry was envisaged to explain the observed strength distribution [267]. The main problem, shared by all these experiments, is that the ground-state spin 3/2 of ^{197}Au did not allow one to determine the spin values of the excited states in ^{196}Au nor did it allow one to distinguish between the transfer of a $3p_{1/2}$ or $3p_{3/2}$ neutron.

5.4.2 New Experiments at the PSI, the Bonn Cyclotron and the Munchen Q3D Spectrometer

At that moment of despair during the mid-1990s, a new collaboration was established involving the University of Fribourg, the University of Bonn and the Ludwig–Maximillian University of Munich. In an ultimate attempt to determine the structure of ^{196}Au, in-beam spectroscopy, in which radiation emitted by ^{196}Au is measured, was performed at the Philips cyclotron of the Paul Scherrer Institute (PSI) in Switzerland and at the Bonn cyclotron. In-beam studies are needed because the unstable ^{196}Au isotope must be created by continuously bombarding stable isotopes, such as ^{196}Pt or ^{197}Au, with accelerated protons or deuterons. Under these circumstances the observed radiation is extremely complex since many states are excited by the different nuclear reactions and are populated in the de-excitation of these states. In parallel with the in-beam experiments, several sophisticated transfer experiments were performed at the Tandem accelerator in Garching.

The first in-beam experiments were performed at the Philips cyclotron of the PSI with the ^{196}Pt(d,2n)^{196}Au reaction at 12.5 MeV. The very complex spectra were then analyzed with γ–γ coincidences obtained with a spectrometer consisting of five BGO shielded Ge detectors [268]. From the coincidence conditions several γ rays could be interrelated leading to the identification of several structures of connected excited states. Of importance were also the coincidences between the γ rays associated with these structures and the x-rays which allowed to identify whether they belonged to Au or Pt isotopes. The observation of structures associated with ^{195}Pt showed that beside the (d,2n) reaction also ^{196}Pt(d,p)^{195}Pt contributed. Therefore, complementary in-beam γ–γ coincidence experiments were performed at the Cyclotron in Bonn with use of the ^{196}Pt(p,n)^{196}Au reaction at 9.12 MeV. This very low energy, well below the Coulomb barrier of 13 MeV, ensured that all other reaction channels essentially were closed. The cross-section was estimated to be 30 mb only. To assign spins, an excitation function was measured with protons at three higher energies.

Internal conversion, in which atomic electrons instead of γ rays carry away the energy of a nuclear de-excitation, is a strong competitor to γ-ray emission in heavy odd–odd nuclei. The K-to-L conversion intensity ratio is strongly dependent on the multipolarity and this mechanism can be used to determine the latter. Therefore, in addition to the in-beam γ-ray experiments, conversion electrons were measured with the Orange spectrometers in Bonn

in both the (d,2n) and the (p,n) reactions. These experiments included the determination of e–γ and e–e coincidences.

The analysis of the in-beam data quickly revealed that the peak observed at 165 keV was in fact a closely spaced triplet of levels, decaying to the 2^- ground state with an M1 transition [269]. The multipolarity of the transition was determined from the conversion electron spectra using e–γ coincidences to clean up the spectrum. All three states turned out to have low spin and negative parity and as such belonged to the supersymmetric model space.

To study the very dense odd–odd nucleus ^{196}Au, state-of-the-art instrumentation provided at the magnetic Q3D spectrometer is needed for transfer reaction studies. Improvements to the detector and the polarized source made new transfer experiments worthwhile. The detector measures the energy of the outgoing particle and as such the excitation energy of the newly formed excited nucleus which appears as missing energy. As discussed in Sect. 3.5, the detector developed by Graw and collaborators attained an energy resolution of 3 keV FWHM for the (p,d) reaction, representing an improvement with a factor of about four compared to the Orsay experiment.

The high-resolution data of the ^{197}Au(p, d)^{196}Au transfer showed for the first time [270] that the strength previously associated with the ground state of ^{196}Au was in fact split into a closely spaced doublet—a crucial ingredient for the solution of the problems encountered before (see Fig. 5.5). In total 47 states were resolved in the energy interval 0–1,350 keV. With knowledge of the energies of the excited states the ^{197}Au(**d**,t)^{196}Au reaction was then used to determine the nature of the transferred particle. This allows to compare the spectroscopic strengths with the theoretical predictions, as discussed in Sect. 3.5. However, as the initial state (ground state of ^{197}Au) has $J = 3/2^+$, several orbits can contribute to the strength to an excited state in ^{196}Au, and these contributions may add incoherently. This feature was incorporated in the data analysis which allowed for several contributions to the angular distributions and analyzing powers. Figure 5.6 illustrates the quality of such fits. Due to this possibility of transferring nucleons in different single-particle states, the spin of the final state cannot be determined unambiguously as was the case for ^{195}Pt. Nevertheless, the possible spins can be limited as follows. Observation of a $3p_{3/2}$ transfer leads to possible spin–parities in the range from 0^- to 3^-; a $2f_{5/2}$ transfer gives 1^- to 4^-. When both are observed, only 1^-, 2^- and 3^- are possible. The high-quality data of the (**d**,t) reaction allow the observation of extremely weak contributions to the strengths and this can be used in the spin determination. The starting hypothesis is that any state that can be reached by a given transfer will show some small components of this transfer. Due to the high level density, the non-observation of a given transfer can be used to restrict the range of possible spins. For example, if only $3p_{3/2}$ and $2f_{5/2}$ but no $3p_{1/2}$ transfer is observed, the state is assumed to be 3^-. The observation of only $3p_{3/2}$ transfer indicates a possible 0^- state.

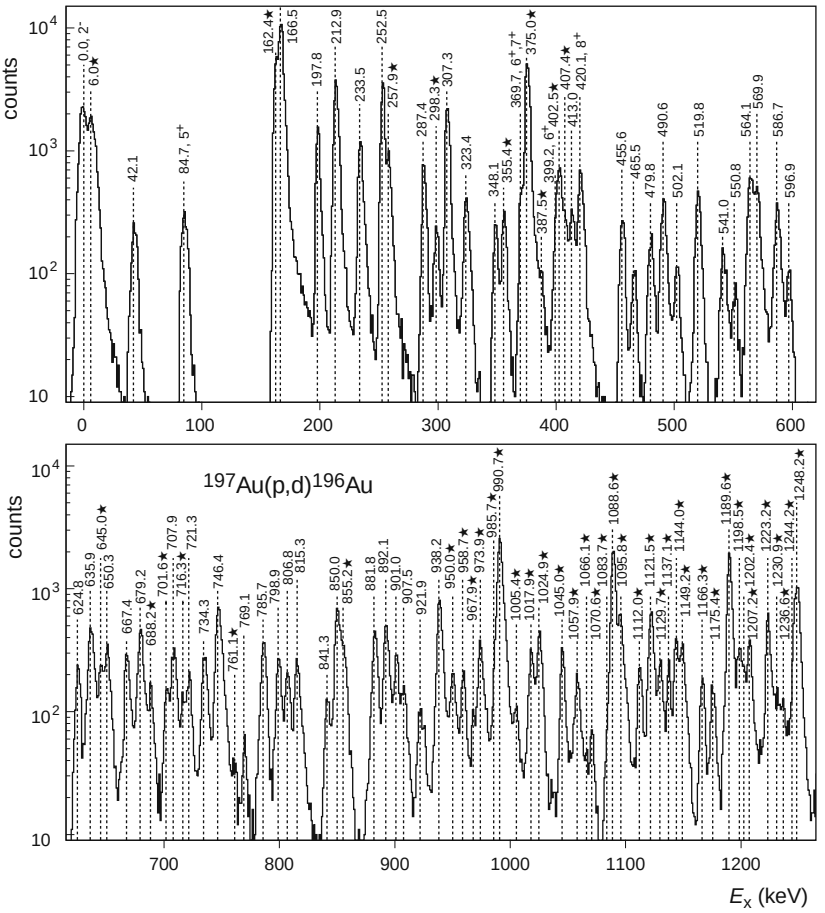

Fig. 5.5. Spectra measured in the (p,d) reaction from ^{197}Au to the low-energy states in ^{196}Au. Multiplets of levels that were previously unresolved are indicated by an asterisk. (Reprinted from H.F. Wirth et al., Phys. Rev. C70 (2004) 014610 ©2004 by the American Physical Society, with kind permission.)

To test this method, a third transfer experiment with 18 MeV polarized deuterons was performed using the ^{198}Hg$(\mathbf{d},\alpha)^{196}$Au reaction. This type of experiment is very difficult due to an increased energy loss of the α particles in target and detectors. With use of very thin targets (34 μg/cm^2 of enriched mercury-sulphid on 7 μg/cm^2 of carbon) an energy resolution of 7 keV could be reached which is excellent for this reaction. The low cross-section combined with the small amount of target atoms led to low statistics which allowed the observation of 17 states only. The main advantage of the $(\mathbf{d},\alpha)$ reaction is that it yields firm spin values because the transfer starts from an even–even Hg isotope with a 0^+ ground state and produces as ejectile an α-particle

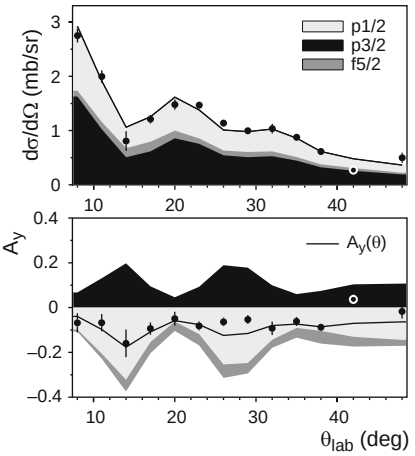

Fig. 5.6. Fits of angular distributions and analyzing powers observed in the (**d**,t) reaction on ^{197}Au to the low-energy states in ^{196}Au. Also indicated are the different contributions of transferred orbits. (Reprinted from H.F. Wirth et al., Phys. Rev. C70 (2004) 014610 ©2004 by the American Physical Society, with kind permission.)

with spin $J = 0$. As the transfer involves a deuteron with spin $S = 1$, the knowledge of the transferred orbital angular momentum L (obtained from angular distributions) is insufficient to determine the J^π value of the final state. The solution of this problem is to have vector-polarized deuterons which are in a magnetic substate with either $M_S = -1$ or $M_S = +1$. The tensor analyzing powers then determine the favored relative orientation of L and S and as such the J^π value of the state excited in the reaction. In all 17 cases the result agreed with the spin assignment obtained from the (**d**,t) reaction [270].

The results of the transfer reaction analyzed under the weaker spin assignment assumption showed a very good agreement with the predictions of the $\mathrm{U}_\nu(6/12) \otimes \mathrm{U}_\pi(6/4)$ extended supersymmetry [270]. The predictions for the odd–odd nucleus were partially based on the new quantum number assignments for negative-parity states in ^{195}Pt which were obtained in parallel (see Table 3.2). The most important result of the entire analysis was the existence of a ground-state doublet with spins 2^- and 1^- in agreement with the supersymmetry prediction, although the order of the two levels was reversed. Also the resolution of the structures at 165 keV was a success. The observation of almost all predicted states in the very complex level scheme of a transitional odd–odd nucleus was particularly spectacular [271].

Following these encouraging results, a collaboration with the group at Yale University, headed by Casten, was set up to get high-statistics γ data. While the Bonn and PSI experiments used only five Compton-shielded detectors, the third in-beam experiment was performed at the ESTU Tandem accelerator in Yale with the YRAST ball, equipped with four fourfold-segmented clover detectors, 17 single Ge detectors and two low-energy photon detectors.

In 3 days of data taking about 6×10^8 coincidences were accumulated. The combination of all in-beam data led to the identification of 53 states below 800 keV of which 10 new in comparison with the transfer reaction work. In total, 300 transitions between these levels could be placed. The range of possible spins and parities of these levels could be limited via the multipolarities. A detailed account of the analysis of all in-beam data is given in Ref. [272].

5.4.3 Recent High-Resolution and Polarized-Transfer Experiments

In recent years more transfer reactions leading to ^{196}Au were performed, with the aim of limiting the possible spins of the observed states. These efforts are presented in Ref. [273] and rely on higher statistics for ^{198}Hg($\mathbf{d}, \alpha$)^{196}Au, and the new reactions ^{194}Pt(α,d)^{196}Au and ^{195}Pt(^{3}He,d)^{196}Au. The latter two reactions are theoretically interesting as they involve only nuclei that belong to one supermultiplet. The proton-transfer reaction ^{195}Pt(^{3}He,d)^{196}Au did provide important clues. Specifically, the importance of the $\pi 3s_{1/2}$ orbit, which is neglected in the supersymmetric scheme, could be established. Its influence can be deduced from the running sums of the $\pi 3d_{3/2}$ and $\pi 3s_{1/2}$ strengths, shown in Fig. 5.7. One observes that $\pi 3d_{3/2}$ is dominant at low energies and $\pi 3s_{1/2}$, which might give rise to additional states, becomes important above 900 keV only. The observation of the weaker $\pi 3s_{1/2}$-transfer contributions was nevertheless important to limit the possible spin assignments because it reduced the possible spins of the final state in ^{196}Au to $J^\pi = 0^-, 1^-$. The

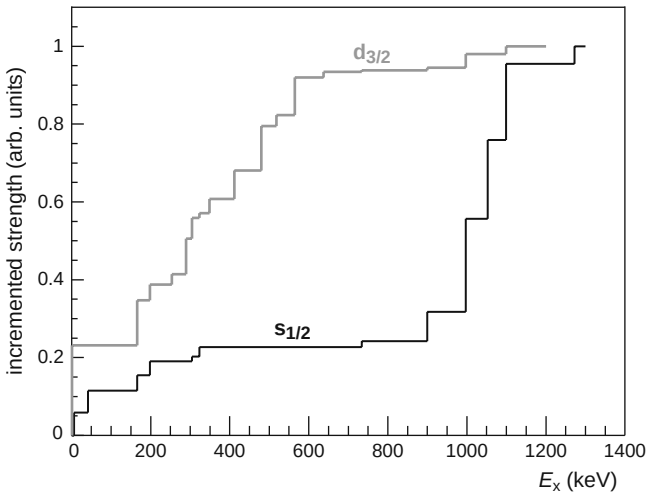

Fig. 5.7. Incremental plot of the observed $\pi 3d_{3/2}$ and $\pi 3s_{1/2}$ strengths obtained from the ^{195}Pt(^{3}He,d)^{196}Au reaction. (Reprinted from H.F. Wirth et al., Phys. Rev. C70 (2004) 014610 ©2004 by the American Physical Society, with kind permission.)

other reaction ^{194}Pt(α,d)^{196}Au had an extremely small cross-section of only 5 μb/sr and needed a very thin target. From these new data many uncertain spin assignments could be confirmed and this has been an important element in the clarification of the comparison with theory to which we now turn.

5.4.4 Comparison with Theory

By combining the information obtained from the different experiments described in the previous subsections, 27 negative-parity states are now known below 500 keV, of which 21 have firm spin values and 6 restricted ones [273]. Figure 5.8 summarizes the present experimental status and displays a comparison with theory [273]. One notices that the energies and spins of most excited states agree well with the prediction, considering that the level density is very high (compare with Fig. 3.6). Table 5.2 lists two parameter sets which are obtained either by fitting all four nuclei of the supermultiplet (including the 27 levels in ^{196}Au) or only to the even–even and odd-mass nuclei. In both fits the six-parameter hamiltonian (5.5) involves 8 levels in ^{196}Pt, 32 in ^{195}Pt and 11 in ^{195}Au. Significant changes are seen to occur only in the values of κ_5 and κ_5' which govern the fine splitting of the levels. Other parameters remain essentially the same which supports the validity of extended supersymmetry for this particular quartet of nuclei.

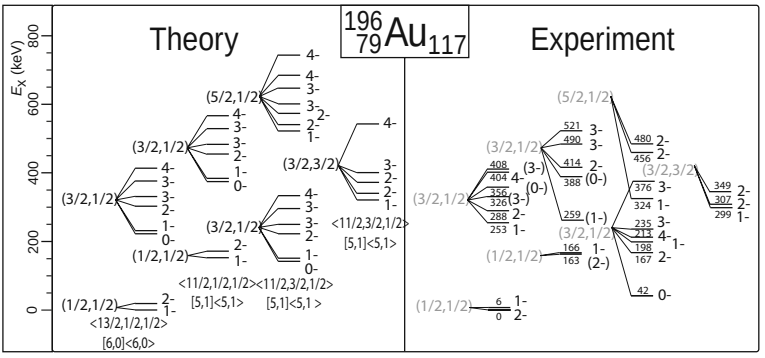

Fig. 5.8. Observed and calculated negative-parity spectrum of ^{196}Au. Levels are labeled by their angular momentum and parity J^π (to the *right* of each level) and by the other quantum numbers in the classification (5.6). (Reprinted from H.F. Wirth et al., Phys. Rev. C70 (2004) 014610 ©2004 by the American Physical Society, with kind permission.)

Table 5.2. Parameters (in keV) for the quartet with and without ^{196}Au

	κ_0	κ_3	κ_3'	κ_4	κ_5	κ_5'
With ^{196}Au	52.5	8.7	−53.9	48.8	8.8	4.5
Without ^{196}Au	51.2	7.9	−52.6	49.0	6.9	6.2

In Table 5.3 the observed and calculated spectroscopic strengths are summarized. The theoretical values for the strengths G_{lj} are obtained with the transfer operator (3.26) with coefficients v_j as determined in the study of ^{195}Pt (see Sect. 3.5). The agreement is reasonable although one might hope to reach a better fragmentation of strength if more realistic transfer operators are used. The overall strength for the $\nu 3p_{3/2}$ orbit is observed to be much weaker than in ^{195}Pt and a better agreement can be obtained by lowering the value of $v^2_{3/2}$.

Table 5.3. Observed (d,t) transfer strength to negative-parity states in ^{196}Au compared with the predictions of $\mathrm{U}_\nu(6/12) \otimes \mathrm{U}_\pi(6/4)$

Experiment					Theory		
E^a	$J^{\pi\,b}$	$G_{p1/2}{}^c$	$G_{p3/2}{}^c$	$G_{f5/2}{}^c$	$G_{p1/2}{}^c$	$G_{p3/2}{}^c$	$G_{f5/2}{}^c$
0.0	2^-	24.3(3)		15.0(10)	43.	1.1	6.5
6.48(4)	1^-	1.2(7)	6.3(7)	2.6(15)	26.	3.4	0.9
41.86(6)	0^-		1.68(4)		0	7.6	0
162.56(4)	$\mathbf{2}^-, 3^-$		5.2(9)	59.3(21)	1.1	6.7	40.2
166.40(4)	1^-	23.8(13)^d	27.0(9)^d	16.4(27)^d	0.66	20.	5.7
167.43(4)	2^-	23.8(13)^d	27.0(9)^d	16.4(27)^d	0	32.	6.9
197.97(4)	$\mathbf{1}^-, 2^-$	2.84(28)	3.16(24)	4.98(6)	0	4.5	21.
212.80(4)	4^-			56.2(3)	0	0	77.
234.53(4)	3^-		[0.12(12)]	16.6(6)	0	49.	5.2
252.58(4)	1^-	3.1(7)	3.6(5)	2.34(14)	0	1.5	6.9
258.61(5)	$\mathbf{1}^-, 2^-$			1.21(12)	0	0.28	1.25
288.06(4)	2^-		1.64(12)	0.84(3)	0	10.5	2.3
298.56(5)	$\mathbf{1}^-, 2^-$	[0.4(3)]	0.72(28)		0	0	0
307.22(4)	2^-	1.7(6)	3.1(6)	11.6(12)	0	0	0
323.83(4)	1^-		1.48(20)^d	2.0(5)^d	0	0	0
326.09(5)	$1^-, 2^-, \mathbf{3}^-$		1.48(20)^d	2.0(5)^d	0	1.53	18.3
349.17(4)	2^-	0.28(7)	0.30(5)	1.19(12)	0	0	0
355.91(11)	0^-		1.40(12)		0	2.5	0
375.61(4)	3^-		19.2(3)	12.7(7)	0	4.5	55.
387.5(7)	$\mathbf{0}^-$ to 3^-		0.32(4)		0	0.45	0
403.79(4)	4^-			7.3(5)	0	0	26.
408.36(5)	$2^-, \mathbf{3}^-$		0.91(10)	1.1(3)	0	16.	1.75
413.74(5)	2^-	0.33(9)		3.5(3)	0	2.0	0.42
456.44(5)	2^-	0.34(6)	0.76(8)		0	0	0
465.5(7)	2^-	0.12(4)	0.08(4)		—	—	—
480.29(4)	2^-	0.22(6)	0.08(4)		0	0	0
490.19(4)	3^-		1.12(4)	2.40(12)	0	0.29	3.4

[a] Energy from in-beam studies, in units of keV.
[b] Bold value is the one used to compare with theory.
[c] Spectroscopic strength in units of 10^{-2}.
[d] Unresolved doublet.

5.4.5 Two-Nucleon-Transfer Reactions

The one-nucleon-transfer reactions discussed so far, ^{197}Au(**d**,t)^{196}Au and ^{196}Pt(**d**,t)^{195}Pt, are interpreted, in first approximation, with a transfer operator of the form $a^\dagger_\nu$. As already argued, these reactions are useful for measuring energies, spins and parities of states in the residual nucleus. However, they do not test correlations present in the quartet's wave functions as is the case for one-nucleon-transfer reactions *inside* the supermultiplet. The latter reactions do provide a direct test of the fermionic sector of the graded Lie algebras $\mathrm{U}_\nu(6/12)$ and $\mathrm{U}_\pi(6/4)$ (operators $a^\dagger b$ and $b^\dagger a$ of Sect. 1.2.4).

In contrast to one-nucleon-transfer reactions where the single-particle content of the states of the final nucleus is scrutinized, *two*-nucleon-transfer reactions probe the structure of these states in a more subtle way, through the exploration of possible two-nucleon correlations [274]. The spectroscopic strength of the two-nucleon-transfer reaction depends on two factors: the similarity between the states in the initial and final nucleus which differ by two nucleons and the correlation of the transferred pair of nucleons. The information extracted through these reactions supply a challenging test of the wave functions of any nuclear structure model.

As an illustration of such a test, we present results for the reaction $^{198}\mathrm{Hg}(\mathbf{d},\alpha)^{196}\mathrm{Au}$ [273] and compare them with predictions of $\mathrm{U}_\nu(6/12) \otimes \mathrm{U}_\pi(6/4)$ [275]. The initial nucleus ^{198}Hg is assumed to have an SO(6) ground state, while the states of the final nucleus ^{196}Au are characterized by the labels (6.6) of the $\mathrm{U}_\nu(6/12)\otimes\mathrm{U}_\pi(6/4)$ scheme. In first order, the two-nucleon-transfer operator for the $(\mathbf{d},\alpha)$ reaction is

$$(a^\dagger_{j_\nu} \times a^\dagger_{j_\pi})^{(\lambda)}. \tag{5.11}$$

As in Sect. 5.3, two-nucleon-transfer operators of this type can be constructed which transform as a given tensor under the various (dynamical) symmetry algebras of the classifications. As a result, the transfer operator (5.11) can be expanded in terms of the following three tensor operators:

$$\begin{aligned} &T^{\langle 1/2,1/2,1/2\rangle (1/2,1/2)\tilde{L}J}_{1,m}, \\ &T^{\langle 3/2,1/2,1/2\rangle (1/2,1/2)\tilde{L}J}_{2,m}, \\ &T^{\langle 3/2,1/2,1/2\rangle (3/2,1/2)\tilde{L}J}_{3,m}. \end{aligned} \tag{5.12}$$

These are the analogs of the one-proton-transfer operators (5.8) except that now $\tilde{L}$ and J may be different because the transfer involves a neutron as well. Each of the operators (5.12) has well-defined selection rules for the deuteron transfer which are given in Table 5.4. Furthermore, closed expressions for their matrix elements can be derived [275].

The $^{198}\mathrm{Hg}(\mathbf{d},\alpha)^{196}\mathrm{Au}$ reaction is characterized by the transfer of a correlated neutron–proton pair with spin $S = 1$. Since the angular momentum

Table 5.4. Selection rules for deuteron transfer operators

$\langle\sigma_1,\sigma_2,\sigma_3\rangle$	(τ_1,τ_2)	T_1	T_2	T_3
$\langle N\pm 3/2,1/2,1/2\rangle$	(1/2,1/2)		$\surd$	
	(3/2,1/2)			$\surd$
$\langle N\pm 1/2,1/2,1/2\rangle$	(1/2,1/2)	$\surd$	$\surd$	
	(3/2,1/2)			$\surd$
$\langle N\pm 1/2,3/2,1/2\rangle$	(3/2,1/2)			$\surd$

of the ground state of ^{198}Hg is zero, the transferred angular momentum λ is equal to the J of the final state in ^{196}Au. Thus for each value of $\lambda = J$ there are three different transfers possible corresponding to $L = J-1$, J and $J+1$. Since the initial and final states have opposite parity, parity conservation requires the allowed values of L to be odd. The transferred angular momentum and parity of the two-nucleon-transfer operator (5.11) can be $J^\pi = 0^-$, 1^-, 2^-, 3^- and 4^-. This leads to seven possible combinations of L transfer with total angular momentum J (denoted as L_J): P_0, P_1, P_2, F_2, F_3, F_4 and H_4.

The spectroscopic strengths G_{LJ} for the transfer of a neutron–proton pair were determined from the measured angular distributions of the differential cross-section and from the analyzing powers of the $^{198}\mathrm{Hg}(\mathbf{d},\alpha)^{196}\mathrm{Au}$ reaction [273]. The calculated spectroscopic strengths can be written as

$$G_{LJ} = \left| \sum_{j_\nu j_\pi} g^{LJ}_{j_\nu j_\pi} \left\langle {}^{196}\mathrm{Au} \middle\| \left(a^\dagger_{j_\nu} \times a^\dagger_{j_\pi}\right)^{(\lambda)} \middle\| {}^{198}\mathrm{Hg} \right\rangle \right|^2 , \tag{5.13}$$

where the coefficients $g^{LJ}_{j_\nu j_\pi}$ contain factors that arise from the reaction mechanism for two-nucleon transfer, such as a $9j$ symbol for the change from jj to LS coupling and a Talmi–Moshinksy bracket for the transformation to relative and center-of-mass coordinates of the transferred nucleons [274]. The nuclear structure part is contained in the reduced matrix elements in (5.13).

To compare with data, we show for each combination L_J the relative strength $R_{LJ} = G_{LJ}/G^{\mathrm{ref}}_{LJ}$, where G^{ref}_{LJ} is the spectroscopic strength of a given reference state with that L_J transfer.

Because of the tensor character of the transfer operator (5.11), only states in ^{196}Au with $(\tau_1,\tau_2) = (3/2,1/2)$ or $(1/2,1/2)$ can be excited. The $(3/2,1/2)$ multiplet contains $J' = 1/2$, $5/2$ and $7/2$ (see Table 5.1) from where the total angular momenta are obtained through $J = J' \pm 1/2$. Table 5.4 shows that these states can only be excited by the tensor operator T_3. Therefore, the ratios of spectroscopic strengths to these states provide a direct test of the nuclear wave functions, since they do not depend on the coefficients $g_{j_\nu j_\pi}$ but only on the nuclear structure part, the reduced matrix elements of T_3. The states belonging to $(\tau_1,\tau_2) = (1/2,1/2)$ have $J' = 3/2$ and $J = J' \pm 1/2$. Table 5.4 shows that they can be excited by the tensor operators T_1 and

T_2. For these states the ratios R_{LJ} depend both on the reaction and on the structure part.

In Fig. 5.9 the experimental and calculated ratios R_{LJ} are shown [275]. The reference states are identified since they are normalized to one. One observes a good overall agreement, taking into account the simple form of the transfer operator. Large ratios generally are well reproduced except in one case related to a 4^- state; all small ratios are consistent with the data.

These results have led Barea et al. [275] to interchange the assignment of the 2^- states at 162.56 and 167.43 keV. Note that this interchange is not without consequences for the comparison in Table 5.3 where good agreement for the (d,t) transfer strength is obtained for the 162.56 keV state with its original assignment. This, however, would lead to worse results for the (d,α) reaction since it would correspond to interchanging the two gray bars in the two right-hand panels of Fig. 5.9. So, at the moment the correct assignment for the two states is not yet clear.

From this analysis we conclude that it is possible to describe the excited states in four nuclei with a single hamiltonian with only six parameters and this constitutes strong evidence for the existence of nuclear dynamical supersymmetry. Nucleon-transfer-reactions not only offer a powerful tool to

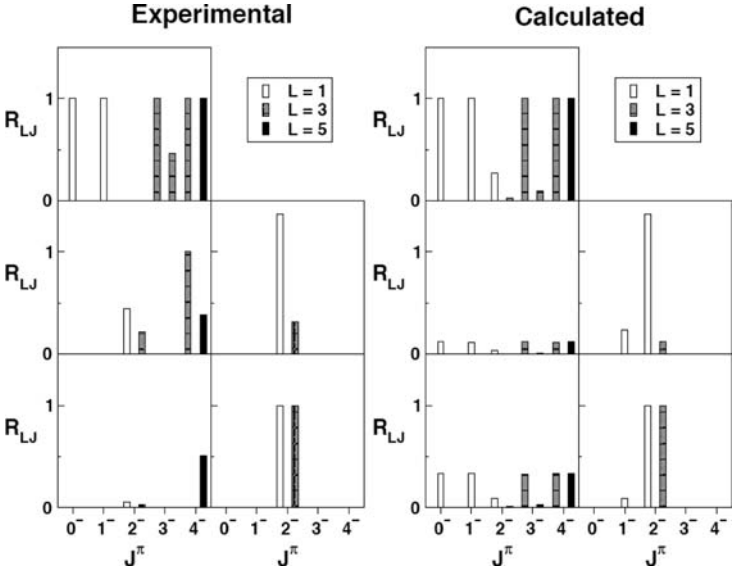

Fig. 5.9. Observed and calculated ratios of spectroscopic strengths. The two columns in each frame correspond to states with the labels $(\tau_1, \tau_2) = (3/2, 1/2)$ and $(1/2, 1/2)$, respectively. The rows are characterized by the labels $[N_1, N_2]$, $\langle \Sigma_1, \Sigma_2, 0 \rangle$, $\langle \sigma_1, \sigma_2, \sigma_3 \rangle$. From bottom to top we have (i) $[6, 0]$, $\langle 6, 0, 0 \rangle$, $\langle 13/2, 1/2, 1/2 \rangle$, (ii) $[5, 1]$, $\langle 5, 1, 0 \rangle$, $\langle 11/2, 1/2, 1/2 \rangle$ and (iii) $[5, 1]$, $\langle 5, 1, 0 \rangle$, $\langle 11/2, 3/2, 1/2 \rangle$. (Reprinted from J. Barea et al., Phys. Rev. Lett. 94 (2005) 01525010)

establish the spin and parity assignments in odd–odd nuclei but also provide sensitive tests of the wave functions via ratios of spectroscopic strengths. In one- as well as two-nucleon-transfer reactions it is possible to identify several ratios which only depend on the nuclear structure part, and not on factors that arise from the kinematical part. Comparisons with measured spectroscopic strength show a good overall agreement with the predictions of extended supersymmetry and, in this way, lend further support to the validity of this scheme in atomic nuclei, especially in the Pt–Au region. Of interest, for the future, will be even more detailed comparisons between theoretical and experimental transfer strengths.

Besides its application to ^{196}Au, the $\mathrm{U}_\nu(6/12) \otimes \mathrm{U}_\pi(6/4)$ scheme was also tested in ^{198}Au [276, 277] and in ^{194}Ir [278]. Especially in the latter study, a good description of the odd–odd nucleus was obtained although a slight breaking of supersymmetry was needed.

6 Supersymmetry and Supersymmetric Quantum Mechanics

In this chapter we describe briefly, for the sake of completeness, some of the ideas and applications of supersymmetry, as defined and understood in other fields of physics. Supersymmetry was originally introduced in particle physics, more accurately, in relativistic quantum field theory where it was introduced in an attempt to obtain a unified description of the full range of fundamental interactions in nature.

As discussed in previous chapters, supersymmetry generates transformations between bosons and fermions. For normal symmetries the corresponding algebra involves only commutators, while supersymmetric algebras also include anti-commutators. The elements of a superalgebra can be interpreted as infinitesimal generators of a (super)symmetry, similar to the usual Lie algebra generators. In the simplest situation the supersymmetry generators commute with the hamiltonian, implying that boson and fermion states should be degenerate in energy.

In quantum field theory the degrees of freedom correspond to relativistic fields which in turn correspond to elementary particles. Supersymmetry is particularly appealing in this case since it can eliminate divergences that are endemic in quantum theories and can often avoid the instabilities of the standard model of elementary particles. In addition, it represents a step forward toward unification of the gauge forces. Only the force of gravity is not included in its framework; this requires the introduction of (super)string theory but also the addition of seven extra (and 'compactified') dimensions [279]. It is generally believed that supersymmetry in quantum field theory might be a low-energy 'remnant' of superstring theory.

6.1 The Supersymmetric Standard Model

To incorporate supersymmetry into particle physics, the standard model must be extended to describe twice as many particles. In some super*symmetric* models this is achieved via the introduction of very heavy stable particles called weakly interacting massive particles or WIMPs, such as the sneutrino and the photino (supersymmetric partners to the neutrino and the photon, respectively). These would interact very weakly with normal matter and thus

A. Frank et al., *Symmetries in Atomic Nuclei*,
Springer Tracts in Modern Physics 230, DOI 10.1007/978-0-387-87495-1_6,

could be candidates for dark matter. In supersymmetric theories every fundamental fermion has a boson superpartner and vice versa. But, are there solid arguments for the existence of supersymmetric particles at the weak scale, with masses comparable to those of the heaviest known elementary particles, the W and Z bosons and the top quark? Not quite, except for the mathematical beauty and consistence of the theory. In the past decades thousands of papers dealing with supersymmetric field theories have been published. This is rather unusual since there is as yet no direct experimental evidence for the existence of any of the new particles predicted by supersymmetry.

As has been pointed out throughout this book, supersymmetry is an unconventional symmetry since fermions and bosons display very different physical properties. While identical bosons may condense—a phenomenon known as Bose–Einstein condensation—in view of the Pauli exclusion principle no two identical fermions can populate the same state. Thus it would be remarkable if a link between these seemingly distinct and dissimilar particles exists. We have analyzed in previous chapters the kind of algebras associated to supersymmetry (i.e., graded Lie algebras) which close under a combination of commutation and anti-commutation relations. In the context of particle physics, supersymmetry predicts that corresponding to every basic constituent of nature, there should be a supersymmetric partner with spin differing by a half-integral unit. It further predicts that the two supersymmetric partners must have identical mass in case supersymmetry is an exact symmetry. In the context of a unified theory of the basic interactions of nature, supersymmetry thus predicts the existence of partners to all the basic constituents of nature, i.e., partners to the six leptons, the six quarks and the corresponding gauge quanta (the photon, three weak bosons, W_+, W_- and Z_0, and eight gluons). The fact that no scalar electron (the spinless 'selectron') has been observed with a mass of less than about 100 GeV (while the electron mass is only 0.5 MeV) suggests that supersymmetry, if present in nature, must be a broken symmetry. It is evident that if any such 'particle' exists, supersymmetry must be strongly broken since large mass differences must occur among superpartners or otherwise at least some of them would have already been detected. Unfortunately, competing supersymmetry models give rise to diverse mass predictions. Supersymmetry, proposed more than three decades ago, has become the dominant framework to formulate physics beyond the standard model despite of the lack of direct experimental evidence.

6.2 Strings and Superstrings

The fundamental assumption of string theory is that elementary particles are not point like but arise as elementary excitations of an extended object of dimension one, a string. The time evolution of the string spans a two-dimensional surface embedded in space–time (see Fig. 6.1). In the

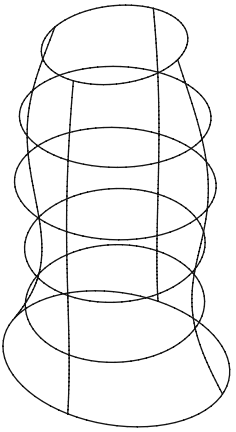

Fig. 6.1. Worldsheet of a string

supersymmetric version of string theory, the gauge forces and gravity become unified while the world acquires new dimensions. Most of the major developments in physics in the past century arose when contradictions were found in the ideas and models of the world. For example, the incompatibility of Maxwell's equations and Galilean invariance led Einstein to propose the special theory of relativity. Similarly, the inconsistency of special relativity with Newtonian gravity led him to develop the general theory of relativity. More recently, the reconciliation of special relativity with quantum mechanics led to the development of quantum field theory. Today, general relativity appears to be incompatible with quantum field theory. Any straightforward attempt to 'quantize' general relativity leads to a non-renormalizable theory. This means that the theory is inconsistent and needs to be modified at short distances or high energies. String theory achieves internal consistency by giving up one of the basic assumptions of quantum field theory, namely that elementary particles are mathematical points, and instead develops a quantum field theory of one-dimensional strings. There are very few consistent theories of this type. Superstring theory and its extensions are the only ones capable of a unified quantum theory of all fundamental forces including gravity. There is still no realistic string theory of elementary particles that could serve as a new standard model since much is not yet understood. But that, together with a better understanding of cosmology, is the basic goal of many of today's physicists.

Even though string theory is not yet fully formulated and not yet capable to give a detailed description of how the standard model of elementary particles emerges at low energies, there are some general features of the theory that are quite remarkable. The first is that general relativity appears in the theory. At very short distances or at high energies the theory is modified but at ordinary ranges it is present in the classical form proposed by

Einstein. This is impressive since gravity arises spontaneously within a consistent quantum theory. In ordinary quantum field theory gravity does not appear or is inconsistent, while string theory requires it. A second characteristic is that Yang–Mills gauge theories appear naturally in string theory. While it is not known precisely why the $SU(3) \otimes SU(2) \otimes U(1)$ gauge theory of the standard model originates, symmetries of this general type do arise naturally at ordinary energies. The third and most remarkable general feature of string theory is supersymmetry. The mathematical consistency of string theory depends on supersymmetry in an essential way, and it is nearly impossible to find consistent solutions that do not preserve supersymmetry, at least in a partial way. This feature of string theory differs from the other two (general relativity and gauge theories) in that it is a real prediction. It is a generic feature of string theory that has not yet been confirmed experimentally. Some books that could help the reader to understand better these aspects of supersymmetry are Refs. [280, 281, 36], while the phenomenology of supersymmetric models is discussed in Refs. [282, 283, 284]. Strings and superstrings are introduced at a more elementary level in Refs. [285, 286].

Rather than attempting to present here a necessarily shallow account of these theories, we shall turn our attention to a different aspect of supersymmetry. Given its pedagogic value, we discuss in the following a one-dimensional version of supersymmetry which has become an interesting subject on its own, that of supersymmetric quantum mechanics.

6.3 Supersymmetric Quantum Mechanics

Supersymmetric quantum mechanics (SQM) arose several years ago when the ideas of supersymmetry in quantum field theory were applied to the simpler case of quantum mechanics and, in particular, with the suggestion in 1981 by Witten [287] that it should be easier to understand the breaking of supersymmetry for the simpler case of non-relativistic quantum mechanics. The framework of SQM has been very fruitful in the study of potential problems in quantum mechanics, not only to understand the connections between analytically solvable problems but also to discover new solutions.

The language and methods of SQM are similar to those developed in this book. Nuclear supersymmetry has similarities to SQM but there are some significant differences too. While both frameworks treat bosonic and fermionic systems on an equal footing, in the traditional SQM approach the hamiltonian H is factorized in terms of so-called supercharges (as we shall see, H is a combination of anti-commutators of the supercharges) whereas in nuclear supersymmetry the hamiltonian is more general and can be written in terms of the bosonic generators of the graded Lie algebra which governs the algebraic structure of the problem. In SQM the fermionic generators of the graded Lie algebra play the role of supercharges. In nuclear supersymmetry the fermionic generators of the graded Lie algebra are associated with nucleon

transfer operators which connect the states of the bosonic and fermionic systems; in general, these 'supercharges' do not commute with the hamiltonian. As a consequence, the spectra of the systems under study are not identical, as they are in SQM. In other words, whereas in SQM H is a generator of the superalgebra, this is not the case in nuclear supersymmetry where a more complicated structure is used. This is of course an unavoidable characteristic because in nuclear supersymmetry the bosonic states are associated with the spectroscopic properties of even–even nuclei, while the fermionic ones with those of the neighboring odd-mass nuclei, and we know these properties are quite different. As discussed in the previous chapters, in contrast to the case of fundamental supersymmetry, a precise correlation between measurable observables in these neighboring nuclei is predicted by nuclear supersymmetry and over two decades has been verified to be valid to a good approximation in particular examples. Another application of supersymmetry is SQM. Once researchers started studying various aspects of SQM, other evidences of low-energy phenomena were found which involve hidden symmetries of this sort and are not just a model for testing concepts of supersymmetric field theories. In this way and during the past years, SQM has provided new insights into many aspects of standard non-relativistic quantum mechanics. For example, it was found that SQM has a direct relation with the factorization method of Infeld and Hull [288], who were the first to classify the analytically solvable potential problems. We shall present here a short discussion of this method. The ideas of supersymmetry have stimulated new approaches to other branches of physics [289]. Besides the evidence for dynamical supersymmetries, relating doublets and quartets of nuclei and extensively discussed in this book, there are also applications in atomic [290, 291, 292, 293], condensed-matter [294, 295] and fundamental nuclear physics [296], together with the method of stochastic quantization which has a path integral formulation directly associated to SQM [297]. A few selected examples are discussed in this chapter.

6.3.1 Potentials Related by Supersymmetry

If the wave function of the ground state of a particular one-dimensional potential is known, one can establish, up to a constant, the corresponding potential. To see this property, we choose, without any loss in generality, the ground-state energy to be zero. The ground-state wave function then satisfies

$$H_1\phi_0(x) \equiv -\frac{\hbar^2}{2m}\frac{d^2\phi_0}{dx^2} + V_1(x)\phi_0(x) = 0, \tag{6.1}$$

so that

$$V_1(x) = \frac{\hbar^2}{2m}\frac{\phi_0''(x)}{\phi_0(x)}. \tag{6.2}$$

The potential can thus be determined from the nodeless ground-state wave function $\phi_0(x)$. We now factorize the hamiltonian as follows:

$$H_1 = A^\dagger A, \tag{6.3}$$

where

$$A = \frac{\hbar}{\sqrt{2m}}\frac{d}{dx} + W(x), \qquad A^\dagger = -\frac{\hbar}{\sqrt{2m}}\frac{d}{dx} + W(x). \tag{6.4}$$

This leads to the relation

$$V_1(x) = W^2(x) - \frac{\hbar}{\sqrt{2m}}W'(x), \tag{6.5}$$

which has the form of a Riccati equation [298]. The function $W(x)$ is usually referred to as the 'superpotential' of the problem. It can be written in terms of the ground-state wave function as

$$W(x) = -\frac{\hbar}{\sqrt{2m}}\frac{\phi_0'(x)}{\phi_0(x)}, \tag{6.6}$$

since substitution of this expression for $W(x)$ in the relation (6.5) leads to the original Schrödinger equation (6.1) for $\phi_0(x)$. We can now define a new hamiltonian

$$H_2 = AA^\dagger, \tag{6.7}$$

which corresponds to a new potential $V_2(x)$,

$$H_2 = -\frac{\hbar^2}{2m}\frac{d^2}{dx^2} + V_2(x), \qquad V_2(x) = W^2(x) + \frac{\hbar}{\sqrt{2m}}W'(x). \tag{6.8}$$

The potentials $V_1(x)$ and $V_2(x)$ are called supersymmetric partners. One can show that the energy eigenvalues of H_1 and H_2 are positive semi-definite, that is, $E_n^{(1,2)} \geq 0$. For $n > 0$ the Schrödinger equation

$$H_1\phi_n^{(1)} = A^\dagger A\phi_n^{(1)} = E_n^{(1)}\phi_n^{(1)}, \tag{6.9}$$

leads to

$$H_2\left(A\phi_n^{(1)}\right) = AA^\dagger A\phi_n^{(1)} = AH_1\phi_n^{(1)} = E_n^{(1)}\left(A\phi_n^{(1)}\right), \tag{6.10}$$

while the equation for H_2,

$$H_2\phi_n^{(2)} = AA^\dagger\phi_n^{(2)} = E_n^{(2)}\phi_n^{(2)}, \tag{6.11}$$

implies that

$$H_1\left(A^\dagger\phi_n^{(2)}\right) = A^\dagger AA^\dagger\phi_n^{(2)} = A^\dagger H_2\phi_n^{(2)} = E_n^{(2)}\left(A^\dagger\phi_n^{(2)}\right). \tag{6.12}$$

Since $E_0^{(1)} = 0$, we find from Eqs. (6.9, 6.10, 6.11, 6.12), that the eigenvalues and eigenfunctions of the two hamiltonians H_1 and H_2 are related by

$$E_n^{(2)} = E_{n+1}^{(1)}, \qquad E_0^{(1)} = 0, \tag{6.13}$$

and

$$\phi_n^{(2)}(x) = \left(\sqrt{E_{n+1}^{(1)}}\right)^{-1} A\phi_{n+1}^{(1)}(x), \tag{6.14}$$

$$\phi_{n+1}^{(1)}(x) = \left(\sqrt{E_n^{(2)}}\right)^{-1} A^\dagger \phi_n^{(2)}(x). \tag{6.15}$$

From these equations we see that, if $\phi_{n+1}^{(1)}(x)$ and $\phi_n^{(2)}(x)$ are normalized, so are $\phi_n^{(2)}(x)$ and $\phi_{n+1}^{(1)}(x)$ on the left-hand side of Eqs. (6.14) and (6.15). Furthermore, A ($A^\dagger$) transforms the eigenfunctions of H_1 (H_2) into eigenfunctions of H_2 (H_1) with the same energy while annihilating (creating) a node in the corresponding eigenfunction. This is so except for the ground-state wave function of H_1 since it is annihilated by the operator A, implying that it has no supersymmetric partner (see Fig. 6.2).

We now consider a simple example of SQM which already displays most of its interesting features.

6.3.2 The Infinite Square-Well Potential

Let us look at the problem of the infinite square well and determine its supersymmetric partner potential. Consider a particle of mass m in an infinite square-well potential of width L,

$$V(x) = \begin{cases} 0, & 0 \le x \le L, \\ +\infty, & -\infty < x < 0, \quad L < x. \end{cases} \tag{6.16}$$

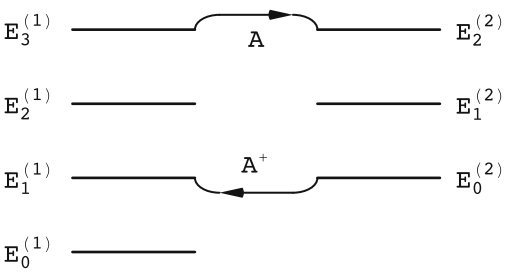

Fig. 6.2. Energy levels of two supersymmetric partner potentials. The action of the operators A and $A^\dagger$ is displayed. The spectra are identical except that one potential has an extra eigenstate at zero energy

The normalized ground-state wave function is given by

$$\phi_0^{(1)}(x) = \sqrt{\frac{2}{L}} \sin \frac{\pi x}{L}, \qquad 0 \le x \le L, \tag{6.17}$$

while the ground-state energy is $E_0 = \hbar^2\pi^2/2mL^2$. Subtracting the ground-state energy in order to factorize the hamiltonian, we have that for $H_1 \equiv H - E_0$ the energy eigenvalues are

$$E_n^{(1)} = \frac{n(n+2)\hbar^2\pi^2}{2mL^2}, \tag{6.18}$$

while the eigenfunctions are

$$\phi_n^{(1)}(x) = \sqrt{\frac{2}{L}} \sin \frac{(n+1)\pi x}{L}, \qquad 0 \le x \le L, \tag{6.19}$$

which reduce to the expression (6.17) for $n = 0$. The superpotential for this problem is readily obtained from Eq. (6.6),

$$W(x) = -\frac{\hbar\pi}{\sqrt{2m}L} \cot \frac{\pi x}{L}, \qquad 0 \le x \le L, \tag{6.20}$$

and thus the supersymmetric partner potential $V_2(x)$ is

$$V_2(x) = \frac{\hbar^2\pi^2}{2mL^2} \left(2 \csc^2 \frac{\pi x}{L} - 1\right), \tag{6.21}$$

with $\csc x = 1/\sin x$. The eigenfunctions of H_2 are obtained by applying the operator A to the eigenfunctions of H_1. We find that

$$\phi_0^{(2)}(x) = \sqrt{\frac{8}{3L}} \sin^2 \frac{\pi x}{L}, \qquad \phi_n^{(2)}(x) = \sqrt{\frac{4}{L}} \sin \frac{\pi x}{L} \sin \frac{(n+1)\pi x}{L}. \tag{6.22}$$

We have thus demonstrated that two different potentials $V_1(x)$ and $V_2(x)$ have exactly the same spectra except for the fact that $V_2(x)$ has one less bound state. In Fig. 6.3 are shown the supersymmetric partner potentials $V_1(x)$ and $V_2(x)$, and the first few eigenfunctions, in the convention $L = \pi$ and $\hbar = 2m = 1$.

6.3.3 Scattering Off Supersymmetric Partner Potentials

The techniques of supersymmetry also allow one to relate reflection and transmission coefficients in situations where the two partner potentials have continuum spectra [299]. For scattering to take place for both of the partner potentials, it is necessary that they are finite as $x \to -\infty$ or as $x \to +\infty$, or both. Imposing the condition

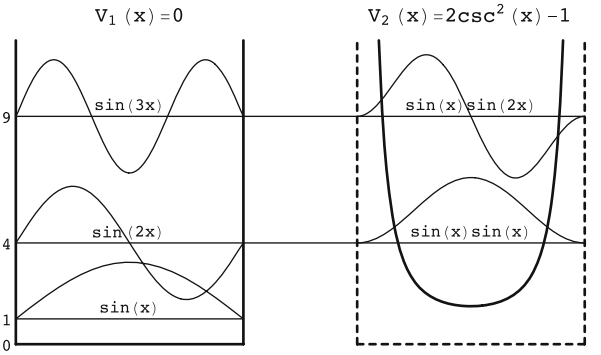

Fig. 6.3. The infinite square-well potential of width $L = \pi$ and its supersymmetric partner potential in units $\hbar = 2m = 1$

$$W(x \to \pm\infty) \to \frac{\hbar}{\sqrt{2m}} W_{\pm} \equiv \tilde{W}_{\pm}, \tag{6.23}$$

we find the following asymptotic properties for the potentials:

$$V_{1,2}(x \to \pm\infty) \to \frac{\hbar^2}{2m} W_{\pm}^2 \equiv \tilde{W}_{\pm}^2. \tag{6.24}$$

Consider an incident plane wave e^{ikx} of energy E coming from $-\infty$. As a result of scattering off the potentials $V_{1,2}(x)$ one obtains transmitted and reflected waves $T_{1,2}e^{ik'x}$ and $R_{1,2}e^{-ikx}$, respectively. It follows that

$$\begin{aligned} \phi^{(1,2)}(k, x \to -\infty) &\to e^{ikx} + R_{1,2}e^{-ikx}, \\ \phi^{(1,2)}(k', x \to +\infty) &\to T_{1,2}e^{ik'x}. \end{aligned} \tag{6.25}$$

The continuum eigenfunctions of H_1 and H_2 with the same energy are connected by supersymmetry in the same way as the discrete states. We thus find the relationships

$$\begin{aligned} e^{ikx} + R_1 e^{-ikx} &= N\left[(-ik + W_-)e^{ikx} + (ik + W_-)R_2 e^{-ikx}\right], \\ T_1 e^{ik'x} &= N\left[(-ik' + W_+)T_2 e^{ik'x}\right], \end{aligned} \tag{6.26}$$

where N is an overall normalization constant. Equating terms with the same exponent and eliminating N, we find

$$R_1 = \left(\frac{W_- + ik}{W_- - ik}\right) R_2, \qquad T_1 = \left(\frac{W_+ - ik'}{W_- - ik}\right) T_2, \tag{6.27}$$

where k and k' are given by

$$k = \sqrt{E - \tilde{W}_-^2}, \qquad k' = \sqrt{E - \tilde{W}_+^2}. \tag{6.28}$$

We see that the following properties are satisfied:

- The partner potentials have identical transmission and reflection and probabilities since $|T_1|^2 = |T_2|^2$ and $|R_1|^2 = |R_2|^2$.
- The transmission coefficients T_1 and T_2 as well as the reflection coefficients R_1 and R_2 have the same poles in the complex plane except that T_1 and R_1 have an extra pole at $k = -iW_-$. This pole is on the positive imaginary axis only if $W_- < 0$ in which case it corresponds to a zero-energy bound state.
- In the particular case with $W_- = W_+$, we find that $T_1 = T_2$.
- If $W_- = 0$ then $R_1 = -R_2$.

From this analysis it is clear that, if one of the potentials is constant (i.e., a free particle), then its partner will be reflectionless. Consider as an example the superpotential $W(x) = \beta \tanh \alpha x$ in which case the partner potentials are

$$V_1(x) = \beta^2 - \beta \left(\beta + \frac{\alpha\hbar}{\sqrt{2m}} \right) \frac{1}{\cosh^2 \alpha x},$$
$$V_2(x) = \beta^2 - \beta \left(\beta - \frac{\alpha\hbar}{\sqrt{2m}} \right) \frac{1}{\cosh^2 \alpha x}. \tag{6.29}$$

If $\beta = \alpha\hbar/\sqrt{2m}$, $V_2(x)$ is a constant potential so that the partner potential must be reflectionless. On the basis of SQM one can thus understand the property of total absence of reflection which occurs for certain depths β of the potential $V(x) = \beta/\cosh^2 \alpha x$ and which plays an important role in the soliton solutions of the Kortewijk–de Vries equations [299]. In addition, this property might have technical applications.

6.3.4 Long-Range Nucleon–Nucleon Forces and Supersymmetry

Although the previous examples are very illustrative and exhibit the power and elegance of SQM, they do not relate directly to a realistic physical system. We now consider a nuclear physics example associated in a very surprising way to the problem of the nucleon–nucleon interaction [296].

The essential idea underlying an exactly supersymmetric model is that the corresponding hamiltonian can be written as

$$H = \frac{1}{2}\{Q, Q^\dagger\} \equiv \frac{1}{2}(QQ^\dagger + Q^\dagger Q), \tag{6.30}$$

where Q and $Q^\dagger$ are anti-commuting operators which generate the supersymmetry transformations. Consider now three hermitean operators x_k $(k = 1, 2, 3)$, together with their associated momenta p_k, which satisfy the usual commutation relations and correspond to the bosonic variables of the model. The (non-hermitean) fermionic degrees of freedom are given by the Clifford operators ξ_k and $\xi_k^\dagger$ which satisfy

$$\{\xi_k, \xi_l\} = \{\xi_k^\dagger, \xi_l^\dagger\} = 0, \qquad \{\xi_k, \xi_l^\dagger\} = \delta_{kl}. \tag{6.31}$$

Bosons and fermions commute. In terms of these variables we now construct the (super)generators

$$Q = [p_k - ix_k V(r)]\xi_k, \qquad Q^\dagger = [p_k + ix_k V(r)]\xi_k^\dagger, \tag{6.32}$$

where a summation over k is implied. The real function $V(r)$ is the 'superpotential' and depends only on the radius r with $r^2 = \sum_k x_k x_k$. One can then show that $(Q)^2 = (Q^\dagger)^2 = 0$ which together with (6.30) implies

$$[Q, H] = [Q^\dagger, H] = 0. \tag{6.33}$$

The explicit form of the hamiltonian is then given by

$$H = \frac{1}{2}\left(p^2 + r^2[V(r)]^2 + [\xi_k, \xi_k^\dagger]V(r) + \frac{x_k x_l}{r}[\xi_k, \xi_l^\dagger]\frac{dV}{dr}\right). \tag{6.34}$$

To interpret this result, it is necessary to find an appropriate realization for the fermionic operators. The ξ_k and $\xi_k^\dagger$ operators can be first expressed in terms of hermitean variables $\boldsymbol{a}$ and $\boldsymbol{b}$ through $\xi_k = (a_k + ib_k)/\sqrt{2}$ and $\xi_k^\dagger = (a_k - ib_k)/\sqrt{2}$. The vectors $\boldsymbol{a}$ and $\boldsymbol{b}$ then satisfy

$$\{a_k, a_l\} = \{b_k, b_l\} = \delta_{kl}, \qquad \{a_k, b_l\} = 0, \tag{6.35}$$

which in turn suggests the following realization for $\boldsymbol{a}$ and $\boldsymbol{b}$ in terms of the Pauli spin matrices

$$\boldsymbol{a} = \sqrt{\frac{1}{2}}\left(A \times \boldsymbol{\sigma}^{(1)}\right), \qquad \boldsymbol{b} = \sqrt{\frac{1}{2}}\left(B \times \boldsymbol{\sigma}^{(2)}\right), \tag{6.36}$$

where $\boldsymbol{\sigma}^{(1)}$ and $\boldsymbol{\sigma}^{(2)}$ are a pair of independent (commuting) Pauli matrices and A and B are hermitean and satisfy

$$A^2 = B^2 = 1, \qquad \{A, B\} = 0. \tag{6.37}$$

These conditions are required in order for (6.35) to hold. Up to this point the model hamiltonian (6.34) describes a supersymmetric interaction of two spin-1/2 particles with spin operators $\boldsymbol{\sigma}^{(i)}/2$ and with relative coordinates x_k and p_k. In addition, these particles possess an 'internal quantum number' space related to the operators A and B and which we shall later identify. To understand the meaning of these quantum numbers, we first require a physical representation for them.

Since we are dealing with a two-particle system, the following realization can be constructed

$$A = \rho_1^{(1)} \times \rho_3^{(2)}, \qquad B = \rho_2^{(1)} \times I^{(2)}, \tag{6.38}$$

where the $\boldsymbol{\rho}^{(i)}$ are independent sets of Pauli matrices that operate in the internal spaces of particle $i = 1$ and $i = 2$. The definition (6.38) ensures that the relations (6.37) are satisfied. We now claim that each particle has an additional internal quantum number $C^{(i)}$ which we choose to be the eigenvalues ± 1 of $\rho_3^{(i)}$. In terms of this explicit realization the hamiltonian (6.34) can be written in the form

$$H = \frac{1}{2}\left(p^2 + r^2[V(r)]^2 + C\left[\boldsymbol{\sigma}^{(1)}\cdot\boldsymbol{\sigma}^{(2)}V(r) + (\boldsymbol{\sigma}^{(1)}\cdot\hat{\boldsymbol{r}})(\boldsymbol{\sigma}^{(2)}\cdot\hat{\boldsymbol{r}})r\frac{dV}{dr}\right]\right), \tag{6.39}$$

where $\hat{\boldsymbol{r}} \equiv \boldsymbol{r}/r$. The only remnant of the internal $\boldsymbol{\rho}$ spaces is the operator C which is given by $C = -iAB = C_1C_2 = \rho_3^{(1)} \times \rho_3^{(2)}$, i.e., product of the 'internal charges'. This hamiltonian includes central, spin–spin and tensor interactions with coefficients that are strongly correlated in terms of the superpotential $V(r)$, as a consequence of the underlying supersymmetry of the system. The hamiltonian conserves total spin, total angular momentum and its projection, as well as parity and the product of the individual internal charges. The action of the supersymmetric generators Q and $Q^\dagger$, on the other hand, can be seen to transform $\boldsymbol{p}$ into $-\boldsymbol{p}$ and C into $-C$. They also act as shift operators for the angular momentum.

It is possible to show at this point that the long-range, so-called one-pion exchange potential (OPEP) is a particular example of the supersymmetric potential (6.39). While at short range the nucleon–nucleon OPEP has a complicated form due to a complex exchange of mesons, for $r \leq 3$ fm it has a well-defined form, given by

$$V_\pi = \boldsymbol{\tau}^{(1)}\cdot\boldsymbol{\tau}^{(2)}\left\{\boldsymbol{\sigma}^{(1)}\cdot\boldsymbol{\sigma}^{(2)}V_{\rm s}(r) + \left[3(\boldsymbol{\sigma}^{(1)}\cdot\hat{\boldsymbol{r}})(\boldsymbol{\sigma}^{(2)}\cdot\hat{\boldsymbol{r}}) - \boldsymbol{\sigma}^{(1)}\cdot\boldsymbol{\sigma}^{(2)}\right]V_{\rm t}(r)\right\}, \tag{6.40}$$

where $\boldsymbol{\tau}^{(1)}$ and $\boldsymbol{\tau}^{(2)}$ refer to the isospin of each nucleon, while the functions $V_{\rm s}(r)$ and $V_{\rm t}(r)$ are the scalar and tensor potentials,

$$V_{\rm s}(r) = \frac{\mu}{3}\left(\frac{g^2}{4\pi}\right)\frac{e^{-x}}{x}, \qquad V_{\rm t}(r) = \frac{\mu}{3}\left(\frac{g^2}{4\pi}\right)\left(1 + \frac{3}{x} + \frac{3}{x^2}\right)\frac{e^{-x}}{x}. \tag{6.41}$$

In these formulae $x \equiv \mu r$, μ is the pion mass and g is the pion–nucleon coupling constant. It is now possible to compare the hamiltonians (6.34) and (6.40) for each individual isospin channel: $\xi \equiv \boldsymbol{\tau}^{(1)}\cdot\boldsymbol{\tau}^{(2)} = -3/4$ and $1/4$. (These values are obtained from the simple relation for two spin operators $\boldsymbol{s}_1\cdot\boldsymbol{s}_2 = [(\boldsymbol{s}_1+\boldsymbol{s}_2)^2 - \boldsymbol{s}_1^2 - \boldsymbol{s}_2^2]/2$ for $s_1 = s_2 = 1/2$.) By comparing the coefficients in (6.34) and (6.40) we find that

$$\frac{1}{2}V(r) = \xi[V_{\rm s}(r) - V_{\rm t}(r)], \qquad \frac{1}{2}r\frac{dV}{dr} = 3\xi V_{\rm t}(r). \tag{6.42}$$

Combining these equations, we find the differential condition

$$r\frac{d(V_{\rm s}-V_{\rm t})}{dr}=3V_{\rm t}. \tag{6.43}$$

Using the explicit expressions (6.41), we find that this relation between the scalar and the tensor components is satisfied *exactly*. The term $r^2V^2/2$ in Eq. (6.34) has no counterpart in the potential (6.40) but this term can be seen to be proportional to e^{-2x} and is negligible in the long-range approximation (where the dominant term goes like e^{-x}) as it involves the onset of the two-pion exchange processes. The fact that the relation (6.43) is satisfied by the scalar and tensor components of the one-pion exchange interaction exerted between nucleons at long range is remarkable indeed.

6.3.5 Matrix Approach to Supersymmetric Quantum Mechanics

We now make a short mathematical detour to introduce a different and widespread representation of SQM. As has been discussed in the examples above, SQM is characterized by the existence of charge operators Q that obey the relations

$$\{Q_i,Q_j\}=\delta_{ij},\qquad [Q_i,H]=0,\qquad i,j=1,2,\ldots,N, \tag{6.44}$$

where H is the supersymmetric hamiltonian and N is the number of generators. Note that this definition has a conventional factor $1/2$ difference with the one used in previous examples. We consider the simplest of such systems with two operators Q_1 and Q_2. In terms of $Q=(Q_1+iQ_2)/\sqrt{2}$ and its hermitian adjoint $Q^\dagger=(Q_1-iQ_2)/\sqrt{2}$, the algebra governing this supersymmetric system is characterized by

$$H=\{Q,Q^\dagger\},\qquad (Q)^2=(Q^\dagger)^2=0. \tag{6.45}$$

From these equations we readily find

$$[Q,H]=[Q^\dagger,H]=0, \tag{6.46}$$

that is, the charge operator Q is nilpotent and commutes with the hamiltonian H. A simple realization of the algebra defined above is

$$Q=\begin{bmatrix}0&0\\A&0\end{bmatrix},\qquad H=\begin{bmatrix}h_+&0\\0&h_-\end{bmatrix}, \tag{6.47}$$

where

$$A=-\frac{\partial}{\partial x}-\frac{i}{2}\frac{dU}{dx}, \tag{6.48}$$

for some function $U=U(x)$. In this representation the supersymmetric hamiltonian H contains two components h_+ and h_-, referred to as the bosonic and fermionic hamiltonians, respectively. These satisfy the equations

$$h_{\pm}\Phi_{\pm n}(x) \equiv \left[-\frac{d^2}{dx^2} + V_{\pm}(x)\right]\Phi_{\pm n}(x) = \epsilon_n \Phi_{\pm n}(x),$$
$$V_{\pm}(x) = \left(\frac{1}{2}\frac{dU}{dx}\right)^2 \mp \frac{d^2U}{dx^2}, \tag{6.49}$$

which correspond to the supersymmetry partners V_1 and V_2 defined earlier while $U(x)$ is the superpotential. Again we see that the operators Q and $Q^\dagger$ induce transformations between the bosonic sector represented by α and the fermionic one represented by β. We may also interpret H in the same way as before: The scalar hamiltonian $H = AA^\dagger$ has a partner $\tilde{H} = A^\dagger A$ such that H and $\tilde{H}$ are the diagonal elements of a supersymmetric hamiltonian. Having demonstrated that Q and H can be constructed in a matrix form, we switch back to the operator language of quantum mechanics to discuss a three-dimensional example.

6.3.6 Three-Dimensional Supersymmetric Quantum Mechanics in Atoms

In a series of papers Kostelecky et al. [290, 291, 292, 293] have discussed the relationship between the spectra of atoms and ions using SQM. In particular, they have suggested that the lithium and hydrogen spectra come from supersymmetric partner potentials.

Consider the Schrödinger equation for the hydrogen atom. In spherical polar coordinates the equation separates into angular and radial parts. While the angular part is solved by the spherical harmonics, the radial part can be written as

$$\left[-\frac{d^2}{dy^2} - \frac{1}{y} + \frac{l(l+1)}{y^2} - \frac{1}{2}E_n\right] R_{nl}(y) = 0. \tag{6.50}$$

We adopt atomic units and use the definitions $y = 2r$ and $E_n = -1/2n^2$. The radial wave functions can be written as

$$R_{nl}(r) = \frac{2}{n^2}\left[\frac{\Gamma(n-l)}{\Gamma(n+l+1}\right]^{1/2}\left(\frac{2r}{n}\right)^l \exp\left(\frac{-r}{n}\right) L_{n-l-1}^{2l+1}\left(\frac{2r}{n}\right). \tag{6.51}$$

The $L_n^\alpha(x)$ are the associated Laguerre polynomials for which α is not restricted to be an integer, defined as

$$L_n^\alpha(x) = \sum_{p=0}^{n}(-x)^p \frac{\Gamma(n+\alpha+1)}{p!(n-p)!\Gamma(p+\alpha+1)}. \tag{6.52}$$

The symbols in brackets in Eq. (6.49) can be interpreted, for fixed l, in terms of the hamiltonian h_+ of Eq. (6.47) as $h_+ - \epsilon_n$. Since the ground-state energy is chosen to be zero, this allows the separation of h_- and ϵ_n, so that it is possible to find the supersymmetry generator Q and the supersymmetric partner hamiltonian [291], once we define the function $U(x)$ of Eq. (6.48)

$$U(y) = \frac{y}{l+1} - 2(l+1)\ln y. \tag{6.53}$$

In this realization the hamiltonian h_- is identical in form to h_+ but with the constant $l(l+1)$ replaced with $(l+1)(l+2)$, so that

$$h_- - h_+ = \frac{2(l+1)}{y^2}. \tag{6.54}$$

This implies that for each l the eigenstates of h_- are $R_{n,l+1}(y)$ where in this case $n \geq 2$.

We now consider a possible physical interpretation for these equations. For $l = 0$ the boson sector describes the s orbitals of a hydrogen atom. Since the spectrum of h_- is degenerate with that of h_+ except for the ground state and since the supersymmetry generator Q acts on the radial part of the hydrogen wavefunctions but leaves the spherical harmonics untouched, h_- describes a physical system that appears hydrogenic but that has the $1s$ orbitals absent or unavailable. This situation is attained by considering that the $1s$ orbital is full, thereby placing the valence electron in the $2s$ and $2p$ states. The element with a filled $1s$ orbital and one valence electron is lithium. This suggests that h_- can be interpreted as an effective one-body hamiltonian describing the valence electron of lithium when it occupies the s orbitals. This description can only be approximate since the electron–electron interactions are ignored. These can be introduced as supersymmetry-breaking terms. Even in the absence of such terms, one can claim some experimental support for this atomic supersymmetry as discussed in Ref. [291].

By repeating the argument defining the energy of the $2s$ orbital in lithium to be zero, the hamiltonian h_- becomes a suitable choice for a bosonic hamiltonian to apply a second supersymmetric transformation. The fermionic partner can be constructed and an analogous interpretation to the one above can be made. This suggests that the s orbitals of lithium and sodium should also be viewed as supersymmetric partners. The process can be repeated for s orbitals and can also be applied for other values of the orbital angular momentum quantum number l, leading to supersymmetric connections among atoms and ions across the periodic table. In the exact-symmetry limit these connections all involve integer shifts in l and are linked to the Pauli principle. We shall not further pursue this example in detail but rather refer the reader to the original references [290, 291, 292, 293].

The formalism of SQM has also been applied in the fields of condensed-matter [294, 295] and statistical physics [300, 301] as well as in problems associated with random magnetic fields in Ising-like models, polymers, electron localization in disordered media and ferromagnets [302, 303]. We also mention the relationship between SQM and stochastic differential equations such as the Langevin equation [304], the path integral formulation of SQM first given in Ref. [305] and the SQM analysis of the tunneling rate through double-well barriers which is of much interest in molecular physics [306, 307, 308].

In terms of the formalism itself and other developments, it should be noted that the ideas of SQM have been extended to higher-dimensional systems as well as to systems with large numbers of particles. Inverse-scattering methods are related to supersymmetry in Ref. [309]. Finally, we would like to point out the extensive work related to shape-invariant potentials [310, 311] and self-similar potentials [312], a set of ideas explored by many researchers. Recent applications to possible deviations from Lorentz symmetry are discussed in Ref. [313]. A connection of supersymmetry to the prime number Riemann hypothesis is proposed in Ref. [314]. The list of applications is very long and a review can be found in Ref. [291].

7 Conclusion

As has become increasingly clear, symmetries in physics, particularly in the microscopic domain, are intimately related to the dynamics of the systems being studied. Symmetry methods and concepts have become essential tools to study the phenomena observed in the nuclear- and particle-physics realm. Since in these areas of nature the basic forces are not known in detail and observations are very difficult to carry out, building a coherent picture is hard. Fortunately, the discovery of conserved quantities, patterns in the data and selection rules often lead to the identification of (manifest or hidden) symmetries in theories and models. Group theory thus becomes the natural language of the physics of the microworld.

Even when symmetries are not exactly satisfied, symmetry breaking, particularly when the successive splittings leave a subgroup of the symmetry transformations intact (in which case we refer to the symmetry as dynamical symmetry), provides a valuable ordering scheme and often leads to additional insights into the nature of the physical system under consideration. Particularly interesting are cases when hamiltonians (or lagrangians) of seemingly distinct systems are unified by the inclusion of additional transformations among the constituent physical objects.

Supersymmetry is one such theoretical generalization, where matter and forces, i.e., fermions and bosons, become part of a single entity, in similar fashion as, e.g., the unification of space and time into 'space–time', achieved by the theory of special relativity. Supersymmetry has wide-ranging consequences and is the precursor of superstring theory and its generalizations, thought by many physicists to be the appropriate road for including gravity into a common framework with the other (gauge) forces. Unfortunately, the problem with supersymmetry and superstring theory is that experimental evidence for them is yet to be found.

In this general context, it is gratifying that many of the same symmetry-based concepts and methods—albeit in a non-relativistic framework—can be found in the low-energy realm of nuclear structure physics, with the added advantage that ideas and models can be subject to experimental verification.

In this book we discussed different aspects of symmetry and supersymmetry in nuclear physics. We attempted to give a general overview of the subject, starting from the fundamental concepts in the theory of Lie algebras, which

A. Frank et al., *Symmetries in Atomic Nuclei*,
Springer Tracts in Modern Physics 230, DOI 10.1007/978-0-387-87495-1_7,

is the necessary mathematical framework for these phenomena. We analyzed the role of symmetry in the general area of nuclear structure physics, starting with a review of the historical roles of Heisenberg's isospin SU(2) symmetry and Wigner's spin–isospin SU(4) symmetry, Racah's pairing SU(2) and Elliott's rotational SU(3) model, and then focusing attention on the interacting boson model and its extensions. We discussed dynamical symmetry and dynamical-symmetry breaking, both for identical particles and for neutron–proton systems. We then analyzed boson–fermion symmetries and supersymmetries and showed their role in the unified description of multiplets of neighboring nuclei. Throughout we illustrated ideas and concepts with experimental examples.

In conclusion, we have analyzed the important role and current status of symmetry and supersymmetry in nuclear structure physics and considered diverse extensions that could encompass a large number of nuclei. The Lie-algebraic methods described in this book are useful in various fields of physics and will continue to prove a powerful tool in the description of nuclear-structure phenomenology. We have emphasized how the experimental verification of symmetry concepts is often possible when taking advantage of new experimental capabilities and that symmetries lead to crystal clear predictions to be verified.

We hope to have convinced the reader that symmetry concepts form a particularly striking example of the combination of the Platonic ideal of symmetry with the down-to-earth Aristotelean ability to recognize complex patterns in Nature.

References

1. M. Hamermesh: *Group Theory and Its Application to Physical Problems* (Addison–Wesley, Reading MA 1962) VII, 43, 44
2. H.J. Lipkin: *Lie Groups for Pedestrians* (North-Holland, Amsterdam 1966) VII
3. M. Moshinsky: *Group Theory and the Many-Body Problem* (Gordon & Breach, New York 1968) VII
4. B.G. Wybourne: *Classical Groups for Physicists* (Wiley-Interscience, New York 1974) VII, 3, 5, 7, 12
5. R. Gilmore: *Lie Groups, Lie Algebras, and Some of Their Applications* (Wiley-Interscience, New York 1974) VII
6. J.P. Elliott, P.G. Dawber: *Symmetry in Physics*, vols 1 & 2 (Oxford University Press, Oxford 1979) VII
7. A. Frank, P. Van Isacker: *Algebraic Methods in Molecular and Nuclear Structure Physics* (Wiley-Interscience, New York 1994) VII, 1, 12
8. F. Iachello: *Lie Algebras and Applications* (Springer-Verlag, Berlin 2006) VII, 3, 4
9. J.-P. Blaizot, J.-C. Tolédano: *Symétries et Physique Microscopique* (Ellipses, Paris 1997) 2, 6, 7
10. M.E. Rose: *Elementary Theory of Angular Momentum* (Wiley, New York 1957) 3, 12, 40
11. V.I. Man'ko: In: *Symmetries in Science V*, ed by B. Gruber, L.C. Biedenharn, H.D. Doebner (Plenum, New York 1991) p 453 4
12. A. Messiah: *Quantum Mechanics* (Wiley, New York 1968) 4
13. O. Castaños, A. Frank, R. Lopez–Peña: J. Phys. A: Mathematical and Theoretical **23**, 5141 (1990) 5
14. W. Heisenberg: Z. Phys. **77**, 1 (1932) 8
15. W.-M. Yao et al.: J. Phys. G: Nuclear and Particle Physics **33**, 1 (2006) 9
16. E.P. Wigner: Phys. Rev. **51**, 106 (1937) 9, 41, 109
17. W.M. MacDonald: Phys. Rev. **98**, **100**, 51 (1955) & **101**, 271 (1956) 11
18. E.P. Wigner: In: *Proceedings of the Robert A Welch Foundation Conferences on Chemical Research. I The Structure of the Nucleus*, ed by W.O. Millikan (Welch Foundation, Houston 1957) p 86 13
19. S. Weinberg, S.B. Treiman: Phys. Rev. **116**, 465 (1959) 13
20. D.H. Wilkinson: Phys. Lett. **11**, 243 (1964) & **12**, 348 (1964) 13
21. J. Britz, A. Pape, M.S. Antony: At. Data Nucl. Data Tables **69**, 125 (1998) 13, 15, 121
22. K. Blaum: Phys. Reports **425**, 1 (2006) 14
23. K. Blaum, G. Audi, D. Beck, G. Bollen, F. Herfurth, A. Kellerbauer, H.-J. Kluge, E. Sauvan, S. Schwartz: Phys. Rev. Lett. **91**, 260801 (2003) 14
24. M.C. Pyle, A. García, E. Tatar, J. Cox, S. Triambak, B. Laughman, A. Komives, L.O. Lamm, J.E. Rolon, T. Finnesey, L.D. Knutson, P.A.Voytas: Phys. Rev. Lett. **88**, 122501 (2002) 14

25. L.E.H. Trainor: Phys. Rev. **85**, 962 (1952) 16
26. L.A. Radicati: Phys. Rev. **87**, 521 (1952) 16
27. J.M. Freeman, J.G. Jenkin, G. Murray, W.E. Burcham: Phys. Rev. Lett. **16**, 959 (1966) 17
28. A. Bohr, B.R. Mottelson: *Nuclear Structure. I Single-Particle Motion* (Benjamin, New York 1969) 17, 30
29. E. Farnea et al.: Phys. Lett. B **551**, 56 (2003) 17
30. M. Gell-Mann: Phys. Rev. **125**, 1067 (1962) 22
31. S. Okubo: Progr. Theor. Phys. **27**, 949 (1962) 22
32. M. Gell-Mann, Y. Ne'eman: *The Eightfold Way* (Benjamin, New York 1964) 22
33. J. Wess, B. Zumino: Nucl. Phys. B **70**, 39 (1974) 25
34. P. Fayet, S. Ferrara: Phys. Reports **32**, 249 (1977) 25
35. P. van Nieuwenhuizen: Phys. Reports **68**, 189 (1981) 25
36. S. Weinberg: *The Quantum Theory of Fields: Supersymmetry* (Cambridge University Press, Cambridge 2000) 25, 87, 158
37. F. Iachello: Phys. Rev. Lett. **44**, 772 (1980) 25, 84, 87
38. I. Bars: In: *Introduction to Supersymmetry in Particle and Nuclear Physics*, ed by O. Castaños, A. Frank, L. Urrutia (Plenum, New York 1983) p 107 26
39. M.G. Mayer: Phys. Rev. **75**, 1969 (1949) 30
40. J.H.D. Jensen, H. Suess, O. Haxel: Die Naturwissenschaften **36**, 155 (1949) 30
41. D.R. Inglis: Rev. Mod. Phys. **25**, 390 (1953) 31
42. D.H. Wilkinson: Annu. Rev. Nucl. Part. Sci. **45**, 1 (1995) 31
43. R.F. Casten: Nucl. Phys. A **443**, 1 (1985) 31
44. National Nuclear Data Center: http://www.nndc.bnl.gov 32, 48, 51, 70, 96, 101, 102, 120
45. A.K. Kerman: Ann. Phys. (NY) **12**, 300 (1961) 32
46. G. Racah: Phys. Rev. **63**, 367 (1943) 33, 106
47. I. Talmi: *Simple Models of Complex Nuclei. The Shell Model and Interacting Boson Model* (Harwood, Chur 1993) 33, 37, 46
48. I. Talmi: Nucl. Phys. A **172**, 1 (1971) 33
49. J. Bardeen, L.N. Cooper, J.R. Schrieffer: Phys. Rev. **106**, 162 (1957) & **108**, 1175 (1957) 34
50. A. Bohr, B.R. Mottelson, D. Pines: Phys. Rev. **110**, 936 (1958) 34
51. R.W. Richardson: Phys. Lett. **3**, 277 (1963) 34, 37
52. M. Gaudin: *La Fonction d'Onde de Bethe* (Masson, Paris 1983) 34, 36
53. J. Dukelsky, C. Esebbag, P. Schuck: Phys. Rev. Lett. **87**, 066403 (2001) 34
54. J. Dukelsky, S. Pittel, G.Sierra: Rev. Mod. Phys. **76**, 1 (2004) 37
55. G. Audi, A.H. Wapstra, C. Thibault: Nucl. Phys. A **729**, 337 (2003) 38, 45, 120
56. H.J. Lipkin, N. Meshkov, A.J. Glick: Nucl. Phys. **62**, 188 & 199 & 211 (1965) 38
57. A. Bohr, B.R. Mottelson: Mat. Fys. Medd. Dan. Vid. Selsk. **27**, No 16 (1953) 39, 52, 58, 71
58. S.G. Nilsson: Mat. Fys. Medd. Dan. Vid. Selsk. **29**, No 16 (1955) 39
59. J.P. Elliott: Proc. Roy. Soc. (London) A **245**, 128 & 562 (1958) 39, 46, 48
60. N. Bohr, J.A. Wheeler: Phys. Rev. C**56**, 426 (1939) 39
61. J.M. Eisenberg, W. Greiner: *Nuclear Models* (North-Holland, Amsterdam 1970) 39
62. A. Bohr, B.R. Mottelson: *Nuclear Structure. II Nuclear Deformations* (Benjamin, New York 1975) 39, 58, 79
63. E. Chacón, M. Moshinsky, R.T. Sharp: J. Math. Phys. **17**, 668 (1976) 40
64. E. Chacón, M. Moshinsky: J. Math. Phys. **18**, 870 (1977) 40

65. G. Gneuss, W. Greiner: Nucl. Phys. A **171**, 449 (1971) 40
66. F. Iachello: Phys. Rev. Lett. **85**, 3580 (2000) 41
67. F. Iachello: Phys. Rev. Lett. **87**, 052502 (2001) 41
68. L. Fortunato: Eur. Phys. J. A **26**, 1 (2005) 41
69. P.O. Lipas: In: *Algebraic Approaches to Nuclear Structure. Interacting Boson and Fermion Models*, ed by R.F. Casten (Harwood, Chur 1993) p 47 43
70. P. Halse, B.R. Barrett: Ann. Phys. (NY) **192**, 204 (1989) 44
71. P. Van Isacker, D.D. Warner, D.S. Brenner: Phys. Rev. Lett. **74**, 4607 (1995) 44
72. J.-Y. Zhang, R.F. Casten, D.S. Brenner: Phys. Lett. B **227**, 1 (1989) 45
73. J.-Y. Zhang, J.D. Garrett, R.F. Casten, D.S. Brenner, C. Wesselborg, R.F. Casten, C.-H. Yu, M. Carpenter: Nucl. Phys. A **520**, 251c (1990) 45
74. B. Cakirli, R.F. Casten: Phys. Rev. Lett. **96**, 132501 (2006) 45
75. D.S. Brenner, C. Wesselborg, R.F. Casten, D.D. Warner, J.-Y. Zhang: Phys. Lett. B **243**, 1 (1990) 45
76. P. Franzini, L.A. Radicati: Phys. Lett. **6**, 322 (1963) 45
77. K.T. Hecht, A. Adler: Nucl. Phys. A **137**, 129 (1969) 49
78. A. Arima, M. Harvey, K. Shimizu: Phys. Lett. B **30**, 517 (1969) 49
79. R.D. Ratna Raju, J.P. Draayer, K.T. Hecht: Nucl. Phys. A **202**, 433 (1973) 49
80. A. Bohr, I. Hamamoto, B.R. Mottelson: Phys. Scr. **26**, 267 (1982) 49
81. O. Castaños, M. Moshinsky, C. Quesne: Phys. Lett. B **277**, 238 (1992) 49
82. J.N. Ginocchio: Phys. Rev. Lett. **78**, 436 (1997) 50
83. G. Rosensteel, D.J. Rowe: Phys. Rev. Lett. **38**, 10 (1977) 50
84. J.N. Ginocchio: Ann. Phys. (NY) **126**, 234 (1980) 51, 83
85. C.L. Wu, D.H. Feng, X.G. Chen, J.Q. Chen, M.W. Guidry: Phys. Rev. C **36**, 1157 (1987) 51
86. N.V. Zamfir, R.F. Casten, D.S. Brenner: Phys. Rev. Lett. **72**, 3480 (1994) 51
87. A. Arima, F. Iachello: Phys. Rev. Lett. **35**, 1069 (1975) 52
88. F. Iachello, A. Arima: *The Interacting Boson Model* (Cambridge University Press, Cambridge 1987) 52, 54
89. T. Otsuka, A. Arima, F. Iachello: Nucl. Phys. A **309**, 1 (1978) 52, 114, 118
90. O. Castaños, E. Chacón, A. Frank, M. Moshinsky: J. Math. Phys. **20**, 35 (1979) 54
91. A. Arima, F. Iachello: Ann. Phys. (NY) **99**, 253 (1976) 54
92. A. Arima, F. Iachello: Ann. Phys. (NY) **111**, 201 (1978) 54, 57
93. A. Arima, F. Iachello: Ann. Phys. (NY) **123**, 468 (1979) 54, 56
94. A. Arima, F. Iachello: Phys. Rev. Lett. **40**, 385 (1978) 55
95. J.A. Cizewski, R.F. Casten, G.J. Smith, M.L. Stelts, W.R. Kane, H.G. Börner, W.F. Davidson: Phys. Rev. Lett. **40**, 167 (1978) 55
96. R.F. Casten, J.A. Cizewski: Phys. Lett. B **79**, 5 (1978) 55
97. R.F. Casten: In: *Interacting Bose–Fermi Systems in Nuclei*, ed by F. Iachello (Plenum, New York 1981) p 3 55
98. A. Leviatan, A. Novoselsky, I. Talmi: Phys. Lett. B **172**, 144 (1986) 56, 64
99. J. Jolie, H. Lehmann: Phys. Lett. B **342**, 1 (1995) 56, 74
100. D.D. Warner, R.F. Casten: Phys. Rev. Lett. **48**, 1385 (1982) 56, 103
101. H.G. Börner, J. Jolie, S.J. Robinson, R.F. Casten, J.A. Cizewski: Phys. Rev. C **42**, R2271 (1990) 56
102. C.S. Lim, R.H. Spear, M.P. Fewell, G.J. Gyapong: Nucl. Phys. A **548**, 308 (1992) 56
103. J. Jolie, A. Linnemann: Phys. Rev. C **68**, 031301(R) (2003) 56, 63, 64, 103

104. A.M. Shirokov, N.A. Smirnova, Yu.F. Smirnov: Phys. Lett. B **434**, 237 (1998) 57
105. D. Kusnezov: Phys. Rev. Lett. **79**, 537 (1997) 57
106. P. Cejnar, J. Jolie: Phys. Lett. B **420**, 241 (1998) 57
107. F. Pan, J.P. Draayer: Nucl. Phys. A **636**, 156 (1998) 57
108. O. Scholten, F. Iachello, A. Arima: Ann. Phys. (NY) **115**, 324 (1978) 57, 63, 64
109. R.F. Casten, J.A. Cizewski: Nucl. Phys. A **309**, 477 (1978) 57
110. J. Stachel, P. Van Isacker, K. Heyde: Phys. Rev. C **25**, 650 (1982) 57, 99
111. D. Bonatsos: *Interacting Boson Models of Nuclear Structure* (Clarendon, Oxford, 1988) 57
112. Y.D. Devi, V.K.B. Kota: Pramana J. Phys. **39**, 413 (1992) 57
113. J. Engel, F. Iachello: Phys. Rev. Lett. **54**, 1126 (1985) 57
114. J.N. Ginocchio, M.W. Kirson: Phys. Rev. Lett. **44**, 1744 (1980) 57
115. A.E.L. Dieperink, O. Scholten, F. Iachello: Phys. Rev. Lett. **44**, 1747 (1980) 57
116. A. Bohr, B.R. Mottelson: Phys. Scripta **22**, 468 (1980) 57
117. D.M. Brink, A.F.R. De Toledo Piza, A.K. Kerman: Phys. Lett. **19**, 413 (1965) 58
118. L. Wilets, M. Jean: Phys. Rev. C **102**, 788 (1956) 58
119. J.P. Elliott, J.A. Evans, P. Park: Phys. Lett. B **169**, 309 (1986) 58
120. R. Gilmore: *Catastrophe Theory for Scientists and Engineers* (Wiley, New York 1981) 58, 60
121. E. López-Moreno, O. Castaños: Phys. Rev. C **54**, 2374 (1996) 58, 60
122. J. Jolie, R.F. Casten, P. von Brentano, V. Werner: Phys. Rev. Lett. **87**, 162501 (2001) 58
123. F. Iachello, N.V. Zamfir, R.F. Casten: Phys. Rev. Lett. **81**, 1191 (1998) 60
124. J. Jolie, P. Cejnar, R.F. Casten, S. Heinze, A. Linnemann, V. Werner: Phys. Rev. Lett. **89**, 182502 (2002) 61
125. P. Cejnar, S. Heinze, J. Jolie: Phys. Rev. C **68**, 034326 (2003) 61, 63
126. L. Landau: Phys. Z. Sowjet. **11**, 26 & 545 (1937); reprinted in *Collected Papers of L.D. Landau* (Pergamon, Oxford, 1965) p 193 61
127. R.F. Casten: Nature Physics **2**, 811 (2006) 61, 62
128. P. Cejnar, J. Jolie: Phys. Rev. E **6**, 6237 (2000) 63
129. V. Werner, P. von Brentano, R.F. Casten, J. Jolie: Phys. Lett. B **527**, 55 (2002) 63
130. Y. Alhassid, A. Leviatan: J. Phys. A: Mathematical and Theoretical **25**, L1265 (1992) 64
131. A. Leviatan: Phys. Rev. Lett. **77**, 818 (1996) 64, 66
132. P. Van Isacker: Phys. Rev. Lett. **83**, 4269 (1999) 64
133. A. Leviatan, P. Van Isacker: Phys. Rev. Lett. **89**, 222501 (2002) 65
134. E. Tavukcu et al.: Phys. Rev. C **65**, 064309 (2002) 68
135. R.F. Casten, P. von Brentano, K. Heyde, P. Van Isacker, J. Jolie: Nucl. Phys. A **439**, 289 (1985) 69
136. J.E. García–Ramos, A. Leviatan, P. Van Isacker: unpublished 69
137. J.L. Wood, K. Heyde, W. Nazarewicz, M. Huyse, P. Van Duppen: Phys. Reports **215**, 101 (1992) 69
138. A. Bäcklin, N.G. Jonsson, R. Julin, J. Kantele, M. Luontama, A. Passoja, T. Poikolainen: Nucl. Phys. A **351**, 490 (1981) 70
139. P.D. Duval, B.R. Barrett: Phys. Lett. B **100**, 223 (1981) 70
140. K. Heyde, C. De Coster, J. Jolie, J.L. Wood: Phys. Rev. C **46**, 541 (1992) 70
141. G. Schraff-Goldhaber, J. Wesener: Phys. Rev. **98**, 212 (1955) 71
142. B.L. Cohen, R.E. Price: Phys. Rev. **121**, 1441 (1961) 71

143. D.R. Bes, G.G. Dussel: Nucl. Phys. A **135**, 327 (1969) 71
144. R.E. Anderson et al.: Nucl. Phys. A **281**, 389 (1977) 71
145. J. Kumpulainen et al.: Phys. Rev. C **45**, 640 (1992) 71
146. K. Heyde et al.: Nucl. Phys. A **466**, 189 (1987) 71
147. P. Twin et al.: Phys. Rev. Lett. **57**, 811 (1986) 72
148. D. Darquennes et al.: Phys. Rev. C **42**, R804 (1990) 72
149. M. Délèze, S. Drissi, J. Jolie, J. Kern, J.P. Vorlet: Nucl. Phys. A **554**, 1 (1993) 72, 73, 76, 77
150. M. Délèze, S. Drissi, J. Kern, P.A. Tercier, J.P. Vorlet, J. Rikovska, T. Otsuka, S. Judge, A. Williams: Nucl. Phys. A **551**, 269 (1993) 72
151. J. Kern: Phys. Lett. B **320**, 7 (1994) 72, 127
152. D. Kusnezov: *OCTUPOLE*, Computer Code, Yale University (1987) 73
153. R. Hertenberger et al.: Nucl. Phys. A **574**, 414 (1994) 74
154. T. Belgya, G. Molnar, S.W. Yates: Nucl. Phys. A **607**, 43 (1996) 75
155. P.E. Garrett, H. Lehmann, C.A. McGrath, Minfang Yeh, S.W. Yates: Phys. Rev. C **54**, 2259 (1996) 76, 125
156. H. Lehmann, J. Jolie, C. De Coster, B. Decroix, K. Heyde, J.L. Wood: Nucl. Phys. A **621**, 767 (1997) 76
157. C. De Coster, K. Heyde, B. Decroix, P. Van Isacker, J. Jolie, H. Lehmann, J.L. Wood: Nucl. Phys. A **600**, 251 (1996) 76
158. P.E. Garrett, H. Lehmann, J. Jolie, C.A. McGrath, Minfang Yeh, S.W. Yates: Phys. Rev. C **59**, 2455 (1999) 77
159. P.E. Garrett, H. Lehmann, J. Jolie, C.A. McGrath, Minfang Yeh, W. Younes, S.W. Yates: Phys. Rev. C **64**, 024316 (2001) 77, 78
160. P.E. Garrett, K.L. Green, H. Lehmann, J. Jolie, C.A. McGrath, M. Yeh, S.W. Yates: Phys. Rev. C **75**, 054310 (2007) 77
161. F. Iachello, P. Van Isacker: *The Interacting Boson–Fermion Model* (Cambridge University Press, Cambridge 1991) 79, 84
162. F. Iachello, O. Scholten: Phys. Rev. Lett. **43**, 679 (1979) 80, 81
163. V. Paar, S. Brant: Phys. Lett. B **105**, 81 (1981) 80
164. A. Gelberg, A. Zemel: Phys. Rev. C **22**, 937 (1980) 81
165. I. Morrison, A. Faessler, C. Lima: Nucl. Phys. A **372**, 13 (1981) 81
166. N. Yoshida, A. Arima, T. Otsuka: Phys. Lett. B **114**, 86 (1982) 81
167. D. Vretenar, V. Paar, G. Bonsignori, M. Savoia: Phys. Rev. C **42**, 993 (1990) 81
168. F. Iachello, D. Vretenar: Phys. Rev. C **43**, R945 (1991) 81
169. I. Talmi: In: *Interacting Bose–Fermi Systems in Nuclei*, ed by F. Iachello (Plenum, New York 1981) p 329 82
170. O. Scholten, A.E.L. Dieperink: In: *Interacting Bose–Fermi Systems in Nuclei*, ed by F. Iachello (Plenum, New York 1981) p 343 82
171. T. Otsuka, N. Yoshida, P. Van Isacker, A. Arima, O. Scholten: Phys. Rev. C **35**, 328 (1987) 82
172. J. Vervier: Riv. Nuovo Cim. **10** No 9, 1 (1987) 84, 85
173. F. Iachello, S. Kuyucak: Ann. Phys. (NY) **136**, 19 (1981) 84, 85, 138
174. S. Kuyucak: *Study of Spinor Symmetries in Nuclear Structure*, Ph.D. Thesis, Yale University (1982) 84, 85
175. A.B. Balantekin, I. Bars, R. Bijker, F. Iachello: Phys. Rev. C **27**, 1761 (1983) 85, 136
176. A.B. Balantekin: *A Study of Dynamical Supersymmetries in Nuclear Physics*, Ph.D. Thesis, Yale University (1982) 85
177. R. Bijker: *Dynamical Boson–Fermion Symmetries in Nuclei*, Ph.D. Thesis, University of Groningen (1984) 85

178. P. Van Isacker, A. Frank, H.Z. Sun: Ann. Phys. (NY) **157**, 183 (1984) 85, 86
179. R. Bijker, F. Iachello: Ann. Phys. (NY) **161**, 360 (1985) 85, 86, 138
180. R. Bijker, V.K.B. Kota: Ann. Phys. (NY) **156**, 110 (1984) 85
181. R. Bijker, V.K.B. Kota: Ann. Phys. (NY) **187**, 148 (1988) 85
182. *Supersymmetry in Physics*, ed by A. Kostelecký, D.K. Campbell (North Holland, Amsterdam 1984) 87
183. A.B. Balantekin, I. Bars, F. Iachello: Phys. Rev. Lett. **47**, 19 (1981); Nucl. Phys. A **370**, 284 (1981) 87, 88, 136
184. A.M. Bruce, W. Gelletly, J. Łukasiak, W.R. Phillips, D.D. Warner: Phys. Lett. B **165**, 43 (1985) 90
185. A. Mauthofer, K. Stelzer, J. Gerl, Th.W. Elze, Th. Happ, G. Eckert, T. Faestermann, A. Frank, P. Van Isacker: Phys. Rev. C **34**, 1958 (1986) 90
186. S. Kuyucak, A.E. Stuchberry: Phys. Rev. C **48**, R13 (1993) 91
187. M. Vergnes, G. Berrier-Ronsin, R. Bijker: Phys. Rev. C **28**, 360 (1983) 91, 140
188. M. Vergnes, G. Berrier-Ronsin, G. Rotbard: Phys. Rev. C **36**, 1218 (1987) 91, 93, 140
189. A. Mauthofer, K. Stelzer, Th.W. Elze, Th. Happ, J. Gerl, A. Frank, P. Van Isacker: Phys. Rev. C **39**, 1111 (1989) 91, 92
190. A. Metz, Y. Eisermann, A. Gollwitzer, R. Hertenberger, B.D. Valnion, G. Graw, J. Jolie: Phys. Rev. C **61**, 064313 (2000); **67**, 049901 (2003) 92, 93, 94, 96
191. W. Assmann et al.: Nucl. Instr. Meth. **122**, 191 (1974) 93
192. E. Zanotti, M. Bisenberger, R. Hertenberger, H. Kader, G. Graw: Nucl. Instr. Meth. A **310**, 706 (1991) 93
193. J. Barea, C. Alonso, J. Arias, J. Jolie: Phys. Rev. C **71**, 014314 (2005) 96
194. A. Frank, P. Van Isacker, D.D. Warner: Phys. Lett. B **197**, 474 (1987) 99
195. M. Sakai: At. Data Nucl. Data Tables **31**, 399 (1984) 99
196. O. Castaños, P. Federman, A. Frank, S. Pittel: Nucl. Phys. A **379**, 61 (1982) 100
197. J. Jolie, S. Heinze, P. Van Isacker, R.F. Casten: Phys. Rev. C **70**, 011305(R) (2004) 103
198. D.D. Warner, P. Van Isacker, J. Jolie, A.M. Bruce: Phys. Rev. Lett. **54**, 1365 (1985) 103
199. B.H. Flowers: Proc. Roy. Soc. (London) A **212**, 248 (1952) 107
200. K.T. Hecht: Phys. Rev. **139**, 794 (1965); Nucl. Phys. A **102**, 11 (1967) & **493**, 29 (1989) 107, 109
201. J.N. Ginocchio: Nucl. Phys. **74**, 321 (1965) 107
202. B.H. Flowers, S. Szpikowski: Proc. Phys. Soc. **84**, 673 (1964) 108
203. S.C. Pang: Nucl. Phys. A **128**, 497 (1969) 108, 109
204. J.A. Evans, G.G. Dussel, E.E. Maqueda, R.P.J. Perazzo: Nucl. Phys. A **367**, 77 (1981) 108
205. P. Van Isacker: C. R. Physique **4**, 529 (2003) 110
206. M. Dufour, A.P. Zuker: Phys. Rev. C **54**, 1641 (1996) 110
207. J. Dobeš, S. Pittel: Phys. Rev. C **57**, 688 (1998) 110, 114
208. A. Arima, T. Otsuka, F. Iachello, I. Talmi: Phys. Lett. B **66**, 205 (1977) 111
209. K.L.G. Heyde: *The Nuclear Shell Model* (Springer–Verlag, Berlin 1990) 111
210. J.P. Elliott, A.P. White: Phys. Lett. B **97**, 169 (1980) 111
211. J.P. Elliott, J.A. Evans: Phys. Lett. B **101**, 216 (1981) 111
212. P. Van Isacker, A. Frank, J. Dukelsky: Phys. Rev. C **31**, 671 (1985) 112
213. P. Van Isacker, J. Dukelsky, S. Pittel, O. Juillet: J. Phys. G: Nuclear and Particle Physics **24**, 1261 (1998) 112, 114
214. P. Van Isacker, D.D.Warner: Phys. Rev. Lett. **78**, 3266 (1997) 113

215. A. Klein, E.R. Marshalek: Rev. Mod. Phys. **63**, 375 (1991) 114
216. P. Halse, J.P. Elliott, J.A. Evans: Nucl. Phys. A **417**, 301 (1984) 115
217. P. Halse: Nucl. Phys. A **445**, 93 (1985) 115
218. J.E. Garcia–Ramos, P. Van Isacker: Ann. Phys. (NY) **274**, 45 (1999) 116
219. J.N. Ginocchio: Phys. Rev. Lett. **77**, 28 (1996) 116
220. V.K.B. Kota: Ann. Phys. (NY) **265**, 101 (1998) 116
221. M.J. Thompson, J.P. Elliott, J.A. Evans: Phys. Lett. B **195**, 511 (1987) 117
222. J.P. Elliott, J.A. Evans: Phys. Lett. B **195**, 1 (1987) 117, 118
223. J.P. Elliott: Rep. Prog. Phys. **48**, 171 (1985) 117
224. P.O. Lipas, P. von Brentano, A. Gelberg: Rep. Progr. Phys. **53**, 1355 (1990) 117
225. P. Van Isacker, K. Heyde, J. Jolie, A. Sevrin: Ann. Phys. (NY) **171**, 253 (1986) 117, 122, 124, 130
226. P. von Brentano, A. Gelberg, H. Harter, P. Sala: J. Phys. G: Nuclear and Particle Physics **11**, L85 (1985) 118, 120
227. E.D. Davis, A.F. Diallo, B.R. Barrett, A.B. Balantekin: Phys. Rev. C **44**, 1655 (1991) 120
228. F. Iachello: Phys. Rev. Lett. **53**, 1427 (1984) 121
229. J.N. Ginocchio, A. Leviatan: Ann. Phys. (NY) **216**, 152 (1992) 123
230. A. Faessler: Nucl. Phys. A **85**, 653 (1966) 123
231. N. Lo Iudice, F. Palumbo: Phys. Rev. Lett. **41**, 1532 (1978) 123
232. D. Bohle, A. Richter, W. Steffen, A.E.L. Dieperink, N. Lo Iudice, F. Palumbo, O. Scholten: Phys. Lett. B **137**, 27 (1984) 123, 124
233. U.E.P. Berg, K. Ackermann, K. Bangert, C. Bläsing, W. Naatz, R. Stock, K. Wienhard, M.K. Brussel, T.E. Chapuran, B.H. Wildenthal: Phys. Lett. B **140**, 191 (1984) 124
234. A. Richter: Prog. Part. Nucl. Phys. **34**, 261 (1995) 124
235. U. Kneissl, H.H. Pitz, A. Zilges: Prog. Part. Nucl. Phys. **37**, 349 (1996) 124
236. K.L.G. Heyde, P. von Neumann-Cosel, A. Richter: to be published in Rev. Mod. Phys. 124
237. D. Bohle, A. Richter, K. Heyde, P. Van Isacker, J. Moreau, A. Sevrin: Phys. Rev. Lett. **55**, 1661 (1985) 124
238. O.M. Maragò, S.A. Hopkins, J. Arlt, E. Hodby, G. Hechenblaikner, C.J. Foot: Phys. Rev. Lett. **84**, 2056 (2000) 124
239. W.D. Hamilton, A. Irbäck, J.P. Elliott, Phys. Rev. Lett. **53**, 2469 (1984) 125
240. S.A.A. Eid, W.D. Hamilton, J.P. Elliott: Phys. Lett. B **166**, 267 (1986) 125
241. H.G. Börner, J. Jolie: J. Phys. G: Nuclear and Particle Physics **19**, 217 (1993) 125
242. K.P. Lieb, H.G. Börner, M.S. Dewey, J. Jolie, S.J. Robinson, S. Ulbig, Ch. Winter, Phys. Lett. B **215**, 50 (1988) 125
243. S.J. Robinson, J. Jolie, J. Copnell: A.I.P. Conf. Proc. **238**, 210 (1991) 125
244. H. Nakada, T. Otsuka, T. Sebe: Phys. Rev. Lett. **67**, 1086 (1991) 125
245. R. De Leo et al.: Phys. Rev. C **53**, 2718 (1996) 125
246. P. von Brentano et al.: Phys. Rev. Lett. **76**, 2029 (1996) 125
247. H. Maser, N. Pietralla, P. von Brentano, R.-D. Herzberg, U. Kneissl, J. Margraf, H. H. Pitz, A. Zilges: Phys. Rev. C **54**, R2129 (1996) 125
248. N. Pietralla et al.: Phys. Rev. Lett. **83**, 1303 (1999) 125, 126
249. T. Otsuka, K.-H. Kim: Phys. Rev. C **52**, 2792 (1995) 126
250. N. Pietralla, C. Fransen, P. von Brentano, A. Dewald, A. Fitzler, C. Friessner, J. Gableske: Phys. Rev. Lett. **84**, 3775 (2000) 127, 128
251. C. Fransen, N. Pietralla, P. von Brentano, A. Dewald, J. Gableske, A. Gade, A. Lisetskiy, V. Werner: Phys. Lett. B **508**, 219 (2001) 128, 129

252. C. Fransen et al.: Phys. Rev. C **67**, 024307 (2003) 128
253. A. Lisetskiy, N. Pietralla, C. Fransen, R.V. Jolos, P. von Brentano: Nucl. Phys. A **677**, 100 (2000) 131
254. N. Lo Iudice, Ch. Stoyanov: Phys. Rev. C **65**, 064304 (2002) 131
255. N. Pietralla et al.: Phys. Rev. C **64**, 031301 (2001) 131
256. H. Klein, A.F. Lisetskiy, N. Pietralla, C. Fransen, A. Gade, P. von Brentano: Phys. Rev. C **65**, 044315 (2002) 131
257. P. Van Isacker, J. Jolie, K. Heyde, A. Frank: Phys. Rev. Lett. **54**, 653 (1985) 134, 136
258. J. Jolie, P. Van Isacker, K. Heyde, A. Frank: Phys. Rev. Lett. **55**, 1457 (1985) 134
259. P. Van Isacker, J. Jolie: Nucl. Phys. A **503**, 429 (1989) 138
260. F. Hoyler et al.: Nucl. Phys. A **512**, 189 (1990) 138
261. A. Algora, T. Fenyes, Zs. Dombradi, J. Jolie: Z. Phys. A **352**, 25 (1995) 138
262. O. Scholten: Prog. Part. Nucl. Phys. **14**, 189 (1985) 138
263. J. Barea, R. Bijker, A. Frank, G. Loyola: Phys. Rev. C **64**, 064313 (2001) 138
264. M.L. Munger, R.J. Peterson: Nucl. Phys. A **303**, 199 (1978) 139
265. Y. Yamazaki, R.K. Sheline: Phys. Rev. C **14**, 531 (1976) 140
266. J. Jolie, U. Mayerhofer, T. von Egidy, H. Hiller, J. Klora, H. Lindner, H.Trieb: Phys. Rev. C **43**, R16 (1991) 141
267. G. Rotbard, G. Berrier, M. Vergnes, S. Fortier, J. Kalifa, J.M. Maison, L. Rosier, J. Vernotte, P. Van Isacker, J. Jolie: Phys. Rev. C **47**, 1921 (1993) 143
268. N. Warr, S. Drissi, P.E. Garrett, J. Jolie, J. Kern, S.J. Mannanal, J.-L. Schenker, J.-P. Vorlet: Nucl. Phys. A **620**, 127 (1997) 143
269. J. Gröger: *Spektroskopie an 196-Au und 190-Ir mit dem Bonner Orangenspektrometer*, Diplomarbeit, Universität Bonn (1996) 144
270. A. Metz, J. Jolie, G. Graw , R. Hertenberger, J. Gröger, C. Günther, N. Warr, Y. Eisermann: Phys. Rev. Lett. **83**, 1542 (1999) 144, 146
271. J. Jolie, Scientific American **282**, 54 (July 2002) 146
272. J. Gröger et al.: Phys. Rev. C **62**, 064304 (2000) 147
273. H.F. Wirth et al.: Phys. Rev. C **70**, 014610 (2004) 147, 148, 150, 151
274. N.K. Glendenning: *Direct Nuclear Reactions* (Academic Press, New York 1983) 150, 151
275. J. Barea, R. Bijker, A. Frank: Phys. Rev. Lett. **94**, 152501 (2005) 150, 152
276. D.D. Warner, R.F. Casten, A. Frank: Phys. Lett. B **180**, 207 (1986) 153
277. G. Berrier-Ronsin, G. Rotbard, M. Vergnes, S. Fortier, J.M. Maison, L.-H. Rosier, J. Vernotte, P. Van Isacker, J. Jolie: Phys. Rev. C **55**, 1200 (1997) 153
278. J. Jolie, P.E. Garrett: Nucl. Phys. A **596**, 234 (1996) 153
279. J.H. Schwarz, N. Seiberg: Rev. Mod. Phys. **71**, S112 (1999) 155
280. J. Wess, J. Bagger: *Supersymmetry and Supergravity* (Princeton University Press, Princeton 1992) 158
281. P.C. West: *Introduction to Supersymmetry and Supergravity* (World Scientific, Singapore 1990) 158
282. H.P. Nilles: Phys. Reports **110**, 1 (1984) 158
283. H.E. Haber, G.L. Kane: Scientific American **254**, 42 (1986) 158
284. S.P. Martin: http://arxiv.org/list/hep-ph/9709356 158
285. F. Cooper, A. Khare, U. Sukhatme: Phys. Reports **251**, 267 (1995) 158
286. H.E. Haber: In: *Recent Directions in Particle Theory*, ed by J. Harvey, J. Polchinski (World Scientific, Singapore 1993) p 589 158
287. E. Witten: Nucl. Phys. B **188**, 513 (1981) 158
288. L. Infeld, T.E. Hull: Rev. Mod. Phys. **23**, 21 (1951) 159

289. *Supersymmetry and its Application in Physics*, ed by R. Bijker et al., AIP Conference Proceedings **744** (2005) 159
290. V.A. Kostelecký, M.M. Nieto: Phys. Rev. Lett. **53**, 2285 (1984) 159, 168, 169
291. V.A. Kostelecký: *Supersymmetry in Physics* (Elsevier Science Ltd, 1985) 159, 168, 169
292. R. Bluhm, V.A. Kostelecký: Phys. Rev. A **49**, 4628 (1994) 159, 168, 169
293. V.A. Kostelecký: *Symmetries in Science VII*, ed by B. Gruber, T. Otsuka (Plenum, New York 1994) p 295 159, 168, 169
294. N. Sourlas: Physica D **15**, 115 (1985) 159, 169
295. L.H. Bennett, R.E. Watson: Phys. Rev. B **35**, 845 (1987) 159, 169
296. L.F. Urrutia, E. Hernández: Phys. Rev. Lett. **51**, 755 (1983) 159, 164
297. J.J.M. Verbaarschot, H.A. Weidenmüller, M.R. Zirnbauer: Phys. Reports **129**, 367 (1985) 159
298. D. Zwillinger: *Handbook of Differential Equations* (Academic Press, San Diego 1992) 160
299. A. Frank, K.B. Wolf: Phys. Rev. Lett. **52**, 1737 (1984) 162, 164
300. J.L. Cardy: Physica D **15**, 123 (1985) 169
301. Y. Shapir: Physica D **15**, 129 (1985) 169
302. B. Berche, F. Iglói: J. Phys. A: Mathematical and Theoretical **28**, 3579 (1995) 169
303. K.J. Wiese: J. Phys. : Condensed Matter **17**, S1889 (2005) 169
304. R. Filliger, M.-O. Hongler: Physica A **332**, 141 (2004) 169
305. K. Fujikawa: Phys. Rev. Lett. **44**,1733(1980) 169
306. P. Kumar, M. Ruiz-Altaba, B.S. Thomas: Phys. Rev. Lett. **57**, 2749 (1986) 169
307. W.Y. Keung, E. Kovacs, U.P. Sukhatme: Phys. Rev. Lett. **60**, 41 (1988) 169
308. A. Valence, H. Bergeron: Phys. Lett. A, **135**, 276 (1989) 169
309. J.-M. Sparenberg, D. Baye: Phys. Rev. C **55**, 2175 (1997) 170
310. A. Khare, U.P. Sukhatme: J. Phys. A: Mathematical and Theoretical **26**, L901 (1993) 170
311. C. Quesne, N. Vansteenkiste: Helv. Phys. Acta **72**, 71 (1999) 170
312. V.P. Spiridonov: In: *Special Functions 2000: Current Perspective and Future Directions* (Kluwer, Dordrecht 2001) p 335 170
313. M.S. Berger, V.A. Kostelecký: Phys. Rev. D **65**, 091701 (2002) 170
314. C. Castro, J. Mahecha: Int. J. Geom. Methods Mod. Phys. **1** no. 6 , 751 (2004) 170

Index